Study of structural changes and kernel properties in specialty maize subjected to dry heat: traditional and microwave toasting

(*Estudio de cambios estructurales y propiedades de grano en maíces de especialidad sometidos a calor seco: tostado tradicional y microondas*)

Escuela Politécnica Nacional

Nelly Violeta Lara Valdez

Quito, Ecuador

2022

Escuela Politécnica Nacional

Philosophy Doctor in Food Science and Technology

Study of structural changes and kernel properties in specialty maize subjected to dry heat: traditional and microwave toasting

Presented by: Nelly Violeta Lara Valdez

Supervised by: Jenny Cumandá Ruales Najera, Ph.D.

A dissertation submitted to Escuela Politécnica Nacional in partial fulfillment of the requirements for the degree of Doctor (Ph.D.) of the Department of Food Science and Biotechnology, Av. Ladrón de Guevara E11-253, Quito, Ecuador

Oral examination date
Examination committee:

Nombre, PhD.
Universidad, President
Nombre, PhD.
Universidad, Secretar, Reviewer 1
Nombre, PhD.
Universidad, Reviewer 2
Nombre, PhD.
Universidad, Reviewer 3
Nombre, PhD.
Universidad, Reviewer 4
Nombre, PhD.
Universidad, Reviewer 4

Study of structural changes and kernel properties in specialty maize subjected to dry heat: traditional and microwave toasting

Thesis

ISBN

Sponsor
DOCT-DI-2019-49 Project, Dirección de Investigaciones, Universidad Central del Ecuador.

Cooperation
Campo Académico Docente Experimental La Tola (CADET) in Tumbaco and Laboratorio de Nutrición Animal in Quito, Facultad de Ciencias Agrícolas, Universidad Central del Ecuador, Quito, Ecuador.
Laboratorio de Coloides, Facultad de Ciencias Químicas, Universidad Central Del Ecuador, Av. Universitaria, Quito, Ecuador.
Centro de Investigaciones Aplicadas a Polímeros, Escuela Politécnica Nacional, Quito, Ecuador.
Laboratorio de Nuevos Materiales, Escuela Politécnica Nacional, Quito, Ecuador.
Departamento de Ciencia de Alimentos y Biotecnología, Escuela Politécnica Nacional, Quito, Ecuador.
Centro de Nanociencia y Nanotecnología, Universidad de Las Fuerzas Armadas ESPE, Sangolquí, Rumiñahui, Ecuador.
Departamento de Nutrición y Calidad, Estación Experimental Santa Catalina, INIAP, Cutuglagua, Mejía, Ecuador.
Laboratorio de Reología, Departamento de Ciencia y Tecnología de Alimentos, Universidad de Santiago de Chile, Santiago, Chile

Dedication

I dedicate this thesis to my sister.

Thank you so much, dear sister, for your unconditional help.

Acknowledgment

I sincerely thank the Universidad Central del Ecuador and the Facultad de Ciencias Agrícolas for allowing me to dispose of my academic time for food science and technology doctoral studies with institutional support.

I am deeply grateful to the Food Science and Technology Doctoral Program of the Escuela Politécnica Nacional and Dra. Jenny Ruales, Program Director and my advisor, for her advice and the sisterly atmosphere she created to facilitate a friendly research working environment.

My special thanks to my co-authors, Karla Vizuete, Alexis Debut, Iván Chango, Orlando Campaña, Elena Villacrés, Pablo Bonilla, Arnulfo Portilla, Fernando Osorio, and Jenny Ruales, for their valuable cooperation in carrying out specialized aspects of this research.

My heartfelt thanks to Yolanda Lara, my sister, for patiently helping me during the study period.

I wish to express my sincere gratitude to the staff of the following institutions for the help they provided in the form of technical support and research facilities:

- Departamento de Ciencia de Alimentos y Biotecnología, Escuela Politécnica Nacional, Ecuador.
- Campo Académico Docente Experimental la Tola and Laboratorio de Nutrición Animal, Facultad de Ciencias Agrícolas, Universidad Central Del Ecuador, Ecuador
- Centro de Nanociencia y Nanotecnología, Universidad de Las Fuerzas Armadas ESPE, Ecuador.
- Centro de Investigaciones Aplicadas a Polímeros, Escuela Politécnica Nacional, Ecuador.
- Laboratorio de Nuevos Materiales, Facultad de Ingeniería Mecánica, Escuela Politécnica Nacional, Ecuador
- Departamento de Nutrición y Calidad, Estación Experimental Santa Catalina, INIAP, Ecuador.
- Laboratorio de Coloideoquímica, Facultad de Ciencias Químicas, Universidad Central del Ecuador. Ecuador.
- Laboratorio de Reología, Departamento de Ciencia y Tecnología de Alimentos, Universidad de Santiago de Chile, Chile.

This research had institutional support through the DOCT-DI-2019-49 Project of the Dirección de Investigaciones of the Universidad Central del Ecuador, Ecuador.

Table of contents

List of papers

Lara, N. Maize types from the Andean region with specialty kernels to make whole ready-to-eat maize by toasting and future frontiers. (Mayor revisión manuscript submitted to Journal)

Lara, N., Vizuete, K., Debut, A., Chango, I., Campaña, O., Villacrés, E., Bonilla, P., & Ruales, J. (2021). Underutilized maize kernels (*Zea mays* L. var. *amylacea* and var. *saccharata*) subjected to pan and microwave toasting: A comparative structure study in the whole kernel. *Journal Cereal Science*, *100*, 103249. https://doi.org/10.1016/j.jcs.2021.103249

Lara, N., & Ruales, J. (2021). Physical and hydration properties of specialty floury and sweet maize kernels subjected to pan and microwave toasting. *Journal of Cereal Science*, *101*, 103298. https://doi.org/10.1016/j.jcs.2021.103298

Lara, N., Osorio, F., & Ruales, J. (2022). Variables related to microwave heating-toasting time and water migration assessment with kernel size approaches of specialty maize types. *Journal of the Science of Food and Agriculture*. https://doi.org/10.1002/jsfa.11961

Lara, N., Portilla, A., Osorio, F., & Ruales, J. (2022). Modeling of the microwave heating-toasting time-related variables and characterization of non-isothermal rheological properties of floury and sweet specialty maize kernels. Accepted for publication in *Applied Food Research*. A sister of Journal of Food Engineering, Food Research International, and LWT – Food Science and Technology.

Summary of the thesis

Maize types (*Zea mays* L. var. *amylacea* and var. *saccharata*) from the Andean region currently appear promising, mainly because floury and sweet maize have specialty kernels to make unconventional ready-to-eat toasted maize. It consists in converting raw seeds into edible maize kernels using traditional toasting. Whole maize kernel toasting is an ancestral knowledge that can innovate toward raw microwave maize, but it has remained ignored by the Andean region's scientific community. Therefore, based on the lack of understanding of the science behind the maize kernel toasting, this study sought to 1) review the state-of-the-art of Andean maize with specialty floury and sweet kernel for toasting, 2) research the structural changes and kernel properties before and after traditional and microwave toasting, 3) explore the behavior of a broad scope of variables related to water migration in these maize types subjected to microwave heating-toasting from 0 to 390 s, 4) model the microwave heating-toasting time-related variables and, 5) characterize the non-isothermal rheological properties. The experimental units were kernel samples (150 g) of the three maize types with initial water contents of 14.06 ± 0.13 g/100 g on a wet basis (16 ± 1 g/100 g on a dry basis) for all tests performed. The experimental kernel units for microwave toasting (2450 MHz microwave oven, 492 W) were packed and sealed in paper envelopes. Thus, floury (a0 and a1) and sweet (a2) raw kernels (T0), respectively subjected to a pan (T1) and microwave (T2) toasting for 1500 s and 390 s, were evaluated using different techniques. After that, raw microwave maize was treated for six heating-toasting times (0, 78, 156, 234, 312, and 390 s.), measuring a wide scope of physical properties.

The comparative evaluation of maize types before and after toasting conditions revealed structural and conformational changes associated with variations in starch granule size, diffraction pattern, blue value (BV), number average of molecular weight ($\bar{M}_n$), the intrinsic viscosity [η], and Raman and ATR FTIR bands. Large kernel sizes, low hardness, and small average particle size explained the floury maize softness. High color differences, high water-soluble index, low density, large average particle size, and kernel hardness confirmed the sugary-vitreous fraction in sweet maize. The pan and microwave toasting effects differed in remaining moisture content, kernel density, expansion volume associated with the internal porosity created during toasting, water absorption capacity, and swelling power. Based on high Pearson's correlations, most kernel properties were time-related variables. The third-order polynomial regression curves calculated with the spatial $(S/V)^2$ and distance $(GMD/2)^2$ approaches described the water migration at each microwave heating-toasting time with a noticeable difference among maize types a0, a1, and a2. The maximum rates of water migration exchange profiles showed significant differences between maize types and water content compared to water loss. Likewise, the top rates displayed substantial differences between the spatial

surface area to volume $(S/V)^2$ and geometric mean diameter distance $(GMD/2)^2$ approaches, revealing a notable lack of consistency with the distance $(GMD/2)^2$ approach. Surface color difference (ΔE^*), internal porosity, milling average particle size, and flour hydration properties displayed curves adequately described by simple and nonlinear regression models. The milling particle size, hydration properties, and rheological parameters illustrated floury and sweet kernel differences ascribed to their proximal composition. The elastic/viscous modulus ratio increased in floury maize. It decreased in sweet maize, unveiling rheological differences associated with microwave heating-toasting time effect on the contrasting structure of floury and sweet specialty Andean maize kernels used for toasting. Floury and sweet maize types reflected unique properties toward the challenge of new frontiers for these specialty kernels. The basic information represents the first insight into more physical-based models of water diffusion during the raw microwave maize heating-toasting.

Resumen de la tesis

Actualmente, los tipos de maíz (*Zea mays* L. var. *amylacea* and var. *saccharata*) de la región andina, parecen promisorios, principalmente, porque maíz harinoso y dulce tienen granos de especialidad para hacer maíz tostado no convencional, listo para consumir. Consiste en convertir semillas crudas en granos comestibles mediante tostación tradicional. El conocimiento ancestral de tostado de grano entero puede innovar hacia maíz crudo para microondas, pero ha permanecido ignorado por la comunidad científica de la región andina. Por lo tanto, con base en la falta de información de la ciencia detrás del tostado del grano de maíz, este estudio buscó 1) revisar el estado del arte del maíz andino con grano de especialidad harinosa y dulce para tostación, 2) investigar los cambios estructurales y propiedades de grano, antes y después del tostado tradicional y por microondas, 3) explorar el comportamiento de una amplia gama de variables relacionadas con la migración de agua en estos tipos de maíz sometidos a calentamiento-tostado por microondas de 0 a 390 s, 4) modelar el calentamiento-tostación por microondas de las variables relacionadas con el tiempo y, 5) caracterizar las propiedades reológicas no isotérmicas. Las muestras de grano (150 g) de los tres tipos de maíz, con contenidos iniciales de agua de 14.06 ± 0.13 g/100 g en base húmeda (16 ± 1 g/100 g en base seca) fueron las unidades experimentales para todas las pruebas realizadas. Las unidades experimentales de grano crudo para tostado por microondas (horno de microondas de 2450 MHz, 492 W) fueron empacadas y selladas en sobres de papel. Así, granos harinosos (a0 y a1) y dulces (a2) crudos (T0), sometidos respectivamente a tostación en sartén (T1) y microondas (T2), durante 1500 y 390 s, fueron evaluados a través de diferentes técnicas. Después de eso, maíz crudo para microondas se trató durante seis tiempos de calentamiento-tostación (0, 78, 156, 234, 312 y 390 s) y se midió una amplia gama de propiedades físicas.

La evaluación comparativa de los tipos de maíz antes y después de las condiciones de tostado reveló cambios estructurales y conformacionales asociados con variaciones en el tamaño de los gránulos de almidón, el patrón de difracción, el valor azul (BV), el numérico promedio de peso molecular ($\overline{M}_n$), la viscosidad intrínseca [η], y las bandas Raman y ATR FTIR. El tamaño grande de los granos, la dureza baja y el tamaño promedio pequeño de las partículas explicaron la suavidad del maíz harinoso. Las diferencias altas de color, el índice alto de solubilidad en agua, la densidad bajo, el tamaño de partícula promedio grande y la dureza del grano corroboraron la presencia de una fracción vítrea azucarada en maíz dulce. Los efectos del tostado en sartén y microondas difirieron en el contenido de humedad remanente, la densidad del grano, el volumen de expansión asociado con la porosidad interna creada durante el tostado, la capacidad de absorción de agua y el poder de hinchamiento. Según las correlaciones altas de Pearson, la mayoría de las propiedades del grano fueron variables relacionadas con el tiempo. Las curvas de regresión polinomial de tercer orden, calculadas con los

enfoques espacial $(S/V)^2$ y de distancia $(GMD/2)^2$, describieron la migración de agua en cada tiempo de calentamiento-tostación por microondas con una diferencia notable entre los tipos de maíz a0, a1 y a2 . Las tasas máximas de los perfiles de cambio de migración de agua mostraron diferencias significativas entre los tipos de maíz y del mismo modo, el contenido de agua en comparación con la pérdida de agua. Igualmente, las tasas más altas mostraron diferencias significantes entre los enfoques de área de superficie espacial a volumen $(S/V)^2$ y distancia de diámetro medio geométrico $(GMD/2)^2$, las cuales revelaron una falta notoria de consistencia con el enfoque de distancia $(GMD/2)^2$. La diferencia de color de la superficie (ΔE*), la porosidad interna, el tamaño de partícula promedio de molienda y las propiedades de hidratación de la harina mostraron curvas adecuadamente descritas por modelos de regresión simple y no lineal. El tamaño de las partículas de molienda, las propiedades de hidratación y los parámetros reológicos ilustraron las diferencias entre granos harinosos y dulces atribuidos a sus composiciones proximales. La relación módulo elástico/viscoso aumentó en maíz harinoso. Disminuyó en el maíz dulce, revelando diferencias reológicas asociadas con el efecto del tiempo calentamiento-tostación por microondas en la estructura contrastante de los granos de maíz andino con especialidad harinosa y dulce, utilizados para tostar. Los tipos de maíz dulce y harinoso reflejaron propiedades únicas frente al desafío de nuevas fronteras para estos granos de especialidad. La información básica generada representa la primera visión hacia modelos fundamentales de la difusión del agua durante el calentamiento y la tostación del maíz crudo para microondas.

Research framework

Floury (*Zea mays* L. var. *amylacea*) and sweet maize types (*Zea mays* L. var. *saccharata*) highly contrasted in starch and endosperm structure have specialty kernels for toasting in a pan and making whole ready-to-eat maize. Although people from southern Colombia to northern Chile widely consume whole ready-to-eat maize, these products remain underutilized worldwide.

The effect of toasting (dry heating) initiated from a pan and microwave on the maize kernels remains unexplored. Information on kernel sizes, shapes, texture, and hydration properties associated with water losses and kernel expansions during toasting is unavailable for floury and sweet maize types. Furthermore, no earlier microwave toasting studies used the floury and sweet specialty maize types to predict the toasting kinetics associated with kernel size approaches. Therefore, it is of great interest to understand the toasting impact on floury and sweet maize kernels focused on scaling ready-to-eat maize to raw microwave maize.

This thesis presents the first investigations on floury (a0 and a1) and sweet (a2) maize with specialty raw kernels (T0) for toasting using microwaves (T2) as an innovative technique compared to toasting in a pan (T1) and advanced investigation on microwave heating-toasting time effect with six levels (0, 78, 156, 234, 312, and 390 s) on the main time-related variables colligated to toasting kinetics.

General objective

To study the structural changes in specialty maize kernels by dry heat application: pan and microwave toasting

Specific objectives

To investigate the structural changes in three primary specialty maize kernels (a0, a1, and a2) before (T0) and after being subjected to a pan (T1 antique way) and microwave (T2 innovative way) toasting by the size distribution of starch granules, diffraction patterns, average crystallite size, Raman and ATR-FTIR bands ascribed to functional groups, starch content, blue value, the number average molecular weight, and intrinsic viscosity

To characterize physical (kernel sizes, shapes, texture, and color) and hydration properties (water absorption capacity, swelling power, and water-soluble index) of specialty floury (a0 and a1) and sweet (a2) maize kernels before (T0) and after subjected to a pan (T1) and microwave (T2) toasting.

To study the correlation of time-related variables (water content, water ratio, water loss, kernel sizes, true density, kernel surface color, and average particle size after milling) obtained at six microwave heating-toasting times (0, 78, 156, 234, 312, and 390 s) and the toasting kinetics (water content, water ratio, water loss) with kernel size approaches by specialty maize type.

To establish the models of microwave heating-toasting time-related variables and characterize the non-isothermal rheological properties (onset and peak temperatures, elastic and viscous moduli, and complex and dynamic viscosities at peak temperatures) of floury (a0 and a1) and sweet (a2) specialty maize kernels treated at 0, 78, 156, 234, 312, and 390 s.

Chapter 1

Maize types from the Andean region with specialty kernels to make whole ready-to-eat maize by toasting and future frontiers

Nelly Lara[a,b*]

[a] Campo Académico Docente Experimental la Tola (CADET), Facultad de Ciencias Agrícolas, Universidad Central del Ecuador, Calle Universitaria s/n, Tumbaco, Ecuador

[b] Departamento de Ciencia de Alimentos y Biotecnología, Escuela Politécnica Nacional, Av. Ladrón de Guevara E11-253 Edificio 19, Quito, Ecuador

ABSTRACT

Maize types with unique endosperms, such as floury and sweet maize, create vast interest, mainly because floury and sweet maize have specialty kernels to consume as a non-conventional whole ready-to-eat maize. That consists in converting raw seeds into edible maize kernels using traditional toasting. Toasting conducted at low moisture content is a well-known step in breakfast cereal processing. In contrast, whole maize kernel toasting is an inherited ancestral knowledge that has remained without importance for the Andean region's scientific community. This review addresses the state-of-the-art Andean maize with specialty floury and sweet kernel for toasting and its characterization compared to normal maize; Andean traditional toasting and the current interest in the toasting process; the innovative raw microwave maize and future perspectives on unknown topics in whole ready-to-eat maize such as acrylamide formation, phytoglycogen in sweet maize, resistant starch, and the necessity of emergent technology in milling for floury maize types.

Keywords: specialty maize; soft endosperm; sugary-vitreous; toasting; microwave; microstructural changes

[*] Corresponding author: CADET, Facultad de Ciencias Agrícolas, Universidad Central del Ecuador, Calle Universitaria s/n, Tumbaco, Ecuador. E-mail: nvlara@uce.edu.ec (N. Lara)

1. Introduction

By natural segregation in Mesoamerica and subsequent domestication, maize or corn was the main staple food of pre-Columbian civilizations from North to South America (Boyer & Hannah, 2001; García-Lara & Serna-Saldivar, 2019). The primitive maize races were pod maize *Zea mays* var. *tunicata*, popcorn *Zea mays* var. *everta*, flint maize *Zea mays* var. *indurata*, floury maize *Zea mays* var. *amylacea*, dent maize *Zea mays* var. *identata*, sweet maize *Zea mays* var. *saccharata*, and waxy maize *Zea mays* var. *ceratina* Kul (Singh et al., 2019). Most of them are used as genetic background to produce new open-pollinated varieties and hybrids, transgenic, and select types such as popcorn, sweet, pigmented, and quality protein maize (Domínguez-Hernández et al., 2022; García-Lara & Serna-Saldivar, 2019). Therefore, maize kernel, with great genetic variability, is the leading cereal crop worldwide and is used to produce a diversity of human food, animal feeds, and other industrial products; being African and American people the main consumers of maize on the cob, as industrialized foods and ethnic products (Serna-Saldivar & Perez Carrillo, 2019). A complex mixture of starch granules and protein bodies is an endosperm characteristic inherent to maize types, and the proximal composition depends on the pericarp, endosperm, and germ percentages in each maize type (Narváez-González et al., 2006). It is consistent with the variations in maize kernel texture properties ascribed to differences in endosperm structure (Lara & Ruales, 2021). These articles agree with satisfactory results for segregating maize kernel samples by their geographical origin (Ukraine, USA, and Peru countries) using FTIR spectroscopy on milling samples, combined with multivariate classification (Achten et al., 2019).

The main types planted today are flint maize, dent maize, super sweet mutants, popcorn, waxy maize, high amylose maize, with color kernels ranging from white to yellow (Serna-Saldivar & Perez Carrillo, 2019; Singh et al., 2019), and Cuzco maize hybrid adapted to the US to make cornnut by the process of deep-frying kernels (Serna-Saldivar et al., 2001). The terms common, normal, or regular maize refer to dent and flint cultivars. In contrast, other maize types such as floury maize and native sweet maize with specialty kernels to make whole ready-to-eat maize by toasting remain underutilized worldwide. Consequently, scientific articles like those recently published on Andean maize kernel characterization (Salvador-Reyes & Clerici, 2020; Salvador-Reyes et al., 2021) and toasting (Lara & Ruales, 2021; Lara et al., 2021) are limited. Furthermore, a review that summarizes the existing literature on specialty Andean maize for toasting gives an overview compared to normal maize and discusses kernel properties in raw microwave maize is not available. However, the toasting process that employs dry heating has attracted the scientific community's attention with recent reviews related to up-to-date scientific literature regarding conventional and novel toasting techniques and their effect on the main properties in some foods (Sruthi et al., 2021) and toasting

appears as an efficient way to retain resistant starch in millets (Kaimal et al., 2021). In addition, several reviews aim to dry heating as a thermal technology to enhance hydration properties in starchy products (Chieregato Maniglia et al., 2021), new functionalities in native starch for industrial applications (Hamaker, 2021), and control digestibility in maize-based foods (Bello-Pérez et al., 2021). This review encompasses Andean maize cultivars with specialty kernels for toasting, kernel characterization, Andean traditional toasting, raw microwave maize, heating-toasting time effect on raw microwave maize and kernel properties, and future frontier for the Andean maize.

2. Andean maize cultivars

Archaeological studies evidence maize cultivation in seven localities from north to south of the Colombian Andean region (Aceituno & Loaiza, 2018; Santos Vecino et al., 2015), in Ecuadorian highlands, with significant maize archeological sites (Athens et al., 2017; McMichael et al., 2021; Pagán-Jiménez et al., 2016) and the Peruvian coastal sites around the middle and late preceramic and early ceramic periods (Grobman et al., 2012; Washburn et al., 2020). On the other hand, sampling locations in expansion routes to investigate how environmental factors from lowland to highland affect the adaptation of maize landraces provides a model to understand convergent evolution and adaptation across ecological gradients (Wang et al., 2021). Thus, in terms of calibrated years before present (cal yr BP), the maize adaptation routes might initiate in Mexican lowland at 9000 cal yr BP and highland at 6200 cal yr BP, archaeological sites in Panama at 7500 cal yr BP, South American lowland at 6600 cal yr BP and disperse to the Andean region at 6500 cal yr BP (Wang et al., 2021). However, it is still unclear when the Andean population includes maize as food in their diet (Alfonso-Durruty et al., 2017; Washburn et al., 2020).

In the Andean region, maize kernels maintain their characteristics developed during the adaptation process of ancient landraces, such as pod maize, popcorn, flint maize, dent maize, floury maize, and sweet maize. A current review provides an overview of *Zea mays* races cultivated in Peru according to their degree of evolution based on the kernel, pericarp, and endosperm variability attributed to genetic expressions of color and endosperm structure, discussing the morphological and agronomic characteristics of the main Peruvian maize (Salvador-Reyes & Clerici, 2020). On the other hand, according to more than 100 races collected in the Andean highland of Colombia, Ecuador, Peru, Bolivia, Chile, and Argentina, most of them are floury maize types, and others are native sweet maize types named *Chullpi* (Salvador-Reyes & Clerici, 2020). These facts infer that floury maize (*Zea mays* var. *amylacea*) is one of the oldest maize types created in South America during the ancient civilizations (Grobman et al., 2012), and selective breeding by open pollination assures Andean accessions with minimal changes (Salvador-Reyes & Clerici, 2020). Based on floury maize

accessions, the breeding programs of Ecuador, Peru, and Bolivia have generated at least 18 improved floury maize-type varieties with more uniform kernels in the last 20 years (Zambrano et al., 2021). Floury maize is a staple crop in the Andean highland but remains underutilized worldwide due to low performance in traditional dry milling (Serna-Saldivar et al., 2001). Regarding native sweet maize (*Zea mays* var. *saccharata*), known all over the Andean region under names such as *Chullpi* (Peru, Chile, and Argentina), *Chuspillo* (Bolivia), and *Chulpi* (Ecuador), believes is related to Maiz Dulce (Mexico) through mutation from *Chullpi* (Tracy, 2001). The literature reports the Peruvian highland as the ancient center of dispersal of native sweet maize in South America (Grobman et al., 2012; Tracy, 2001). However, information on improved varieties of sweet maize in the Andean region is very limited (Narváez-González et al., 2006; Ortiz et al., 2008; Pagán-Jiménez et al., 2016), and is unclear the relation with the existing wild type and its mutants with a common genetic background *dull1* (Zhu et al., 2013).

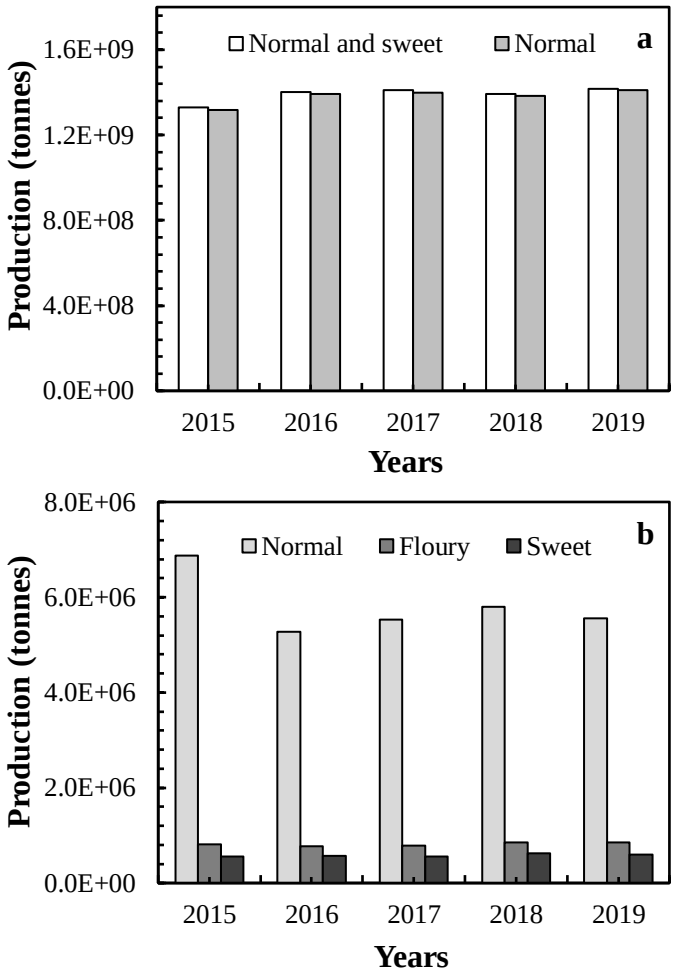

Figure. 1. Maize production comparison. Normal and sweet maize production worldwide (**a**). Normal, floury, and sweet maize production in the Andean region (**b**). Data from the FAOSTAT website and the official agricultural information websites from Peru and Ecuador.

The Andean population cultivates normal maize for animal feed and a minimum quantity for precooked flour. In the case of floury maize, the production is to prepare local food dishes such as cooked kernels on the immature cob in the milk stage ("*choclo*"); cooked kernel ("*mote*"), previously

boiled in calcium alkali, washed to remove the pericarp, and cooked until soft texture; whole dry kernel subjected to toasting ("*tostado*" or "*cancha*") and kernel preheating for whole maize flour. In contrast, native sweet maize is used in the mature state to toast whole kernels. In the Andean region, "*tostado*" or "*cancha*" and "*chulpi*" are the names of these floury and sweet ready-to-eat maize, respectively. Therefore, specialty floury and sweet maize kernels are the raw material to prepare homemade Andean whole ready-to-eat maize, using a pan and the perspective of microwave toasting (Lara & Ruales, 2021). However, using the data reported on the FAOSTAT website, the current trend in maize production at the world (Fig. 1a) and Andean level (Fig.1b) reflects the predominance of normal maize and the underutilization of the floury and sweet types.

3. Kernel characterization

Information on maize types with specialty kernels for toasting is very limited. The microstructural, physical, and chemical specifications of 71 accessions representing races of maize from Latin America (International Maize and Wheat Improvement Center, CIMMYT, Mexico) suggest that microstructure is responsible for the physical characteristics and chemical composition of maize kernels (Narváez-González et al., 2006), without indicating maize types used for toasting. In addition, recent studies address the importance (Salvador-Reyes & Clerici, 2020) and characteristics (Salvador-Reyes et al., 2021) of five main Peruvian varieties for different uses. Therefore, this review used unpublished information from a previous study (Lara, N.) to compare raw kernel properties between normal, floury, and sweet maize types cultivated in the Andean region. Thus, Table 1 summarizes typical uses and specifications according to the maize endosperm texture (hard, semi-hard, semi-soft, soft, and shrunken). In addition, the supplementary information in Table S1contains the chemical composition among normal, floury, and sweet with more variability in protein, fat, nitrogen-free extract, starch, amylose, magnesium, iron, and zinc, suggesting low protein contents for floury maize types. Table S2 shows the flour pasting and thermal behavior with a major difference in pasting properties between floury and sweet maize kernels compared to normal maize. Fig. S1(a-c) displays the viscosity profiles (Pa s) according to the endosperm texture in normal, floury, and sweet maize, with a clear difference between floury and sweet types (Fig. S1c) due to a high starch content in floury kernels and an important sugar-vitreous fraction in sweet kernels. Therefore, floury and sweet maize types are highly opposite in starch content and endosperm structure; however, both floury and sweet maize types have specialty kernels to make ready-to-eat maize by toasting in a pan and microwave oven (Lara & Ruales, 2021; Lara et al., 2021).

3.1. Floury maize for toasting

Floury maize used for toasting has kernels with completely soft endosperm, without vitreous fraction, and a thin pericarp (Salvador-Reyes et al., 2021). The kernel size presents a tendency to shrink uniformly upon drying. The kernels elongated in shape and large. The surface color varies from pale yellow to matte yellow, and the endosperm color is white. The toasted kernels are easy to chew, and the surface color changes to golden brown with significant shifts in physical, chemical, structural, and texture properties between raw and toasted kernels (Lara & Ruales, 2021; Lara et al., 2021). Fig. 2(a and c) illustrates that elongated kernels, yellow pericarp, white, and entirely soft endosperm are the main characteristics of floury maize to make "*tostado*," while Fig. 2(b and d) shows the cross-section of maize kernel after toasting (ready-to-eat maize) with a soft appearance and easy to chew. The completely floury endosperm appears as a simple starch-based material compared to starch-protein and lipid composites from other starchy sources. Therefore, Fig. 2(b and d) suggests that these toasted whole kernels can be the first insight into future challenges to modifying starch at the whole kernel endosperm level. Thus, the microwave-treated starch within the whole kernel can acquire desirable properties as those discussed in currents reviews (Bello-Pérez et al., 2021; Tao et al., 2020; Torbica et al., 2021) and research articles on different dextrins (Lee et al., 2021; Mao et al., 2021; Xie et al., 2021).

3.2. Sweet maize for toasting

After drying, mature sweet maize kernels shrunken and vitreous have a thick pericarp (Salvador-Reyes et al., 2021). The vitreous fraction is translucent, and the color can vary between beige and yellow. The shrunken endosperm has a sugary-vitreous fraction more significant than the floury endosperm, with high total sugars and water-soluble index (Lara et al., 2021) attributed to the accumulation of a nanoparticulated polysaccharide called phytoglycogen (Xue et al., 2019). The high water-soluble solids non-converted in starch contribute to developing a crispy texture and more intense golden brown color in sweet maize than floury maize during toasting (Lara & Ruales, 2021). Fig. 2e exhibits a shrunken yellow kernel and cross-section with the sugary-vitreous fraction greater than floury endosperm. There are significant structural changes between raw (Fig. 2e) and toasted sweet kernels (Fig. 2f) that suggest a crispy texture in the toasted kernel called "*chulpi*." Furthermore, the brown color throughout the toasted kernel suggests the chemical changes related to the Maillard reactions that usually occur in toasted starchy-rich foods. However, the hypothesis of reduced starch digestibility at low water activity due to Maillard reactions (Pellegrini et al., 2020) and the performing of phytoglycogen are unclear issues in sweet maize.

Table 1. Summary of physical specification of normal, floury, and sweet maize types cultivated in the Andean region.

Maize types	Kernel characteristics		Kernel color		Kernel proportions (g/100 g)			Kernel dimensions (mm)			Density (g/mL)	
	Texture	Typical use*	Aleurone	Endosperm	Endosperm	Germ	Pericarp	Length	Width	Thickness	Bulk	True
Normal 1	hard	cooked grits	white	white	82.8	13.1	4.0	11.7	11.2	6.8	0.70	1.22
Normal 2	hard	animal feed	intense yellow	yellow	82.2	13.7	4.1	9.6	9.3	5.0	0.72	1.28
Normal 3	semi-hard	grits	pale yellow	yellow	79.3	16.5	4.1	11.2	10.2	4.6	0.80	1.31
Floury 1	semi-soft	cooked kernel	white	white	86.3	9.9	3.8	16.9	15.1	7.1	0.60	1.04
Floury 2	semi-soft	cooked kernel	white	white	82.3	13.8	3.9	13.5	11.4	6.9	0.61	1.03
Floury 3	semi-soft	cooked kernel	white	white	81.4	14.6	4.0	12.9	11.2	7.9	0.61	0.99
Floury 4	soft	toasted kernel	white	white	84.6	11.8	3.6	12.6	10.0	5.8	0.58	1.01
Floury 5	soft	toasted kernel	yellow	white	83.2	12.8	4.0	14.0	10.7	6.4	0.64	1.06
Floury 6	soft	toasted kernel	pale yellow	white	83.2	12.8	4.1	12.5	10.9	7.9	0.63	1.11
Sweet 1	hard	toasted kernel	yellow	yellow**	78.3	16.8	4.9	13.2	8.9	5.1	0.59	1.17

* Local names related to the following typical uses: "*morocho*" (cooked grits with milk); "*mote*" (cooked kernel without pericarp); "*tostado*" or "*cancha*" (toasted floury kernels); "*chulpi*" (toasted sweet kernel). **Sugary-vitreous fraction in mayor kernel proportion.

The standard deviation values are available in the unpublished supplementary information from the previous study (Lara, N.) supported by the project "Investigación y desarrollo de nuevas alternativas alimenticias para consumo humano, basadas en maíz, banano, plátano y quinua" INIAP-PROMSA AQ-CV-012 (PROMSA, 2005).

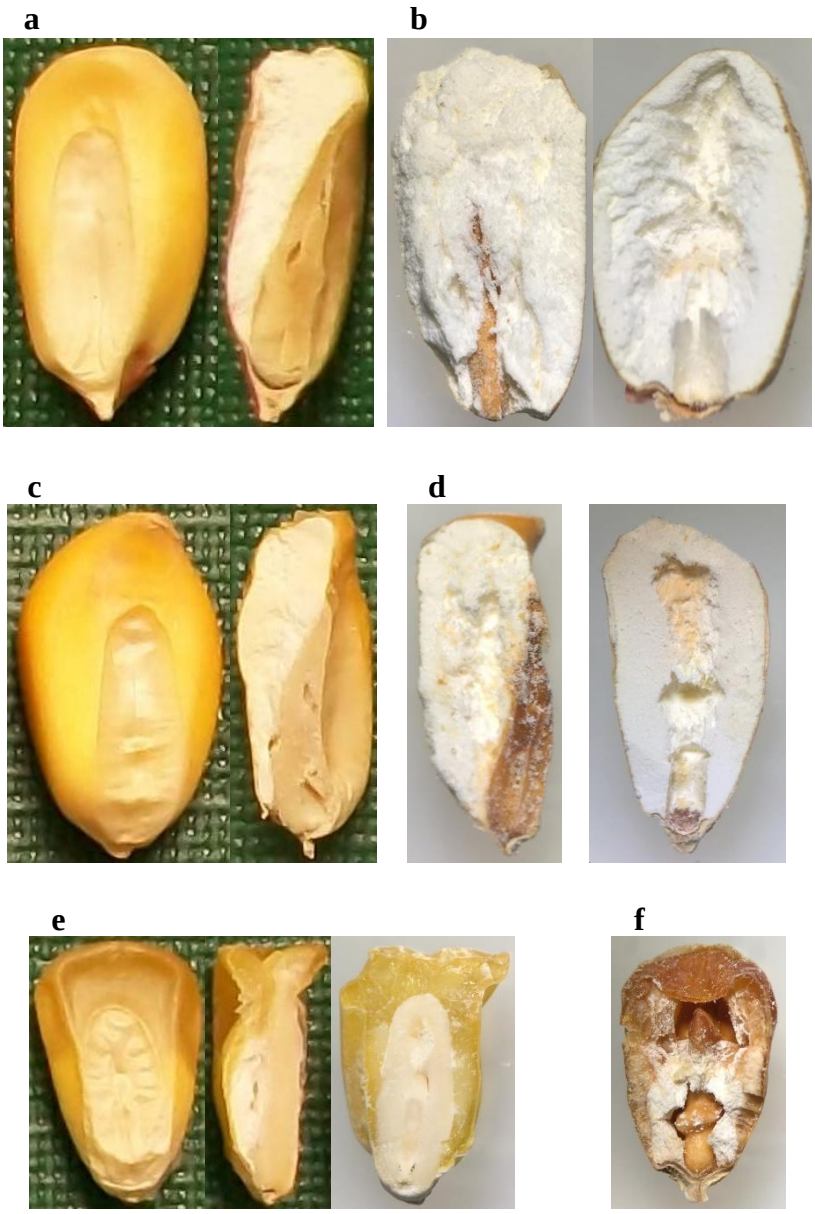

Figure. 2. Whole kernels, longitudinal sections, and cross-sections of maize types with specialty kernel for ready-to-eat whole maize by pan toasting. Floury Peruvian maize kernel before (**a**) and after (**b**) toasting. Floury Ecuadorian maize kernel before (**c**) and after (**d**) toasting. Sweet Peruvian maize kernel before (**e**) and after (**f**) toasting.

4. Andean traditional toasting

In the Andean region, toasting in a pan is an ancient method to transform the raw maize kernel into whole ready-to-eat maize on household and handcrafted scales. Maize toasting is an art of Aboriginal civilizations, with very little knowledge about its science and the emerging thermal technologies for innovation (Jermann et al., 2015; Moreno-Vilet et al., 2018). The toasting of whole kernels on a hot surface is a dry heat technique and has remained for generations, with some variations in fat or oil added. Today, the old fat-free toasting is a custom used by the population of marginal rural areas with no influence from deep-fried snacks. It may agree with the toasting stage of breakfast cereal processing to enhance color, flavor, and texture attributes (Breslin & Knott, 2020; Sumithra & Bhattacharya, 2008). The current studies on toasting in a pan using tempered floury and sweet maize

kernel at 14 g/100 g water content display the structural changes that occur in size kernel, true density, surface color, kernel texture, milling average partible size, swelling power, water-soluble index, endosperm microstructure, starch granule size, relative crystallinity, crystallite size, Raman bands, FTIR carbohydrate fingerprints, starch content, blue value, number average of molecular weight, intrinsic viscosity, total sugars and reducing sugars of fat-free ready-to-eat maize (Lara & Ruales, 2021; Lara et al., 2021). The information indicates no starch gelatinization by toasting in a pan using dry heating because the granular starch structure in floury endosperm fractions remains after toasting. This result is consistent with the remaining granular integrity in native maize starch by dry heating with and without acid (Lei et al., 2020; Li et al., 2020). In general, toasting is a traditional method to attain some starch functionalities in the endosperm matrix (Carrera et al., 2015), extend storage stability (Fukui et al., 2022; Sruthi & Rao, 2021), and develop sensorial attributes (Breslin & Knott, 2020; Sruthi et al., 2021; Sumithra & Bhattacharya, 2008). It implies that toasting maintains current interest among cereal and pseudocereal researchers (Dhua et al., 2021; Sharma et al., 2022) and represents a technological innovation challenge to develop new toasted kernel-based foods (Ajatta et al., 2021; van Rooyen et al., 2022).

5. Raw microwave maize

The maize kernel toasting using a pan is a slow process that can take 20 min to reach a uniform golden brown color with small kernel sizes (Lara & Ruales, 2021). Therefore, microwave toasting may be an innovative application to prepare soft and crispy maize kernels in short heating-toasting times, based on the increasing interest in microwave popping and its capacity to produce low-fat and healthy food ready-to-eat products (Rakesh & Datta, 2011). For example, raw microwave popcorn is the primary homemade snack compared to raw kernels for conventional popping (Gökmen, 2004). Furthermore, comparative studies with microwave heating show current popularity over conventional techniques (Sharma et al., 2022; Solaesa et al., 2021; Suhag et al., 2021) with a positive impact confronted with existing research (Guzik et al., 2022). Likewise, the new advances in uniform microwave heating aim to improve the volumetric heating of solid samples with rotary motion devices adaptable to all kinds of microwave cavities irrespective of geometric shapes (Ye et al., 2021). Therefore, microwave drying and toasting suggest developing theoretical or empirical models related to these processes (Ekezie et al., 2017; Ries de Carvalho et al., 2021; Shirkole et al., 2020). However, the assumptions required to apply Fick's second law of diffusion do not satisfactorily describe the maize kernel drying by microwave heating (Shivhare et al., 1994), and the toasting kinetics in raw microwave maize are challenges for future understanding. In addition, microwave toasting with intermittent manual shaking causes an increase in maize kernel volume ascribed to

internal expansion generated by water migration (Lara & Ruales, 2021) in contrast to the shrinkage effect in conventional drying processes (Azmir et al., 2019, 2020).

6. Heating-toasting time effect on raw microwave maize and kernel properties

Based on the referred studies on Andean maize background (Salvador-Reyes & Clerici, 2020), raw kernel characterization (Salvador-Reyes et al., 2021), structural changes (Lara et al., 2021), cold hydration, and physical properties (Lara & Ruales, 2021) before and after microwave toasting, a current study explores the behavior of a broad scope of variables in Andean maize types for toasting. Maize kernels, packed in sealed paper envelopes and subjected to six microwave heating-toasting times from 0 to 390, display the physical properties that can perform as time-related variables in raw microwave maize. Thus, in addition to WC, WR, and WL, the surface area S, volume V, and geometric mean diameter GMD behave like time-related variables with high correlation depending on maize types and kernel dimensions, revealing the importance of kernel size on water migration during heating-toasting of raw microwave maize (Lara et al., 2022). Furthermore, the ongoing study aims to model the curves of surface color difference (ΔE^*), internal porosity, milling average particle size, and flour cold hydration properties using empirical kinetics mathematical models derived from simple, polynomial, and nonlinear regressions. This basic information can be the first insight into more physical-based models of water diffusion during the heating-toasting of raw microwave maize to make low-fat and healthy whole ready-to-eat maize kernels. Thus, the application of microwave toasting can be an interesting opportunity to spread worldwide the Andean maize utilization. In addition, the elastic/viscous modulus ratio unveils rheological differences associated with microwave heating-toasting time effect on the contrasting structure of floury and sweet specialty Andean maize kernels used for toasting. This fact suggests that the rheological properties as a function of temperature (moduli and viscosities profiles) can contribute to developing new toasted kernel-based products.

7. Viewpoints and future frontier for the Andean maize

The dry heat application using a pan and microwave toasting implies specific viewpoints non-elucidated in whole ready-to-eat maize. One of them is acrylamide formation, ascribed to the Maillard reactions, widely discussed in comprehensive reviews of toasted foods using conventional and emerging technologies (Michalak et al., 2020; Sruthi et al., 2021). Acrylamide is harmful to human health, and the European Food Safety Authority recommends controlling its content in food items like maize-based breakfast cereals with values below the benchmark level indicated by the EU Regulation 2017/2158 (Brocca & Bocca, 2022). Therefore, in Andean ready-to-eat maize urges the

study of acrylamide formation. In addition, the toasting effect on phytoglycogen in sweet maize is unclear and requires further research. Another viewpoint is that toasting can increase the resistant starch content in kernel-based products like whole chestnut flour subjected to roasted and compared with drying systems (Yang et al., 2022). In addition, according to the available literature, microwave, with some modifications, is better than other novel technologies for increasing the resistant starch content in millet flour (Kaimal et al., 2021; Kanagaraj et al., 2019). Likewise, the resistant starch content of wheat starch fortified with lipids augments by the microwave effect (Kang et al., 2022).

On the other hand, the future perspective on starchy products indicates the tendency toward whole starchy-based foods with health-related compounds, novel properties, and wide homemade and industrial applications (Bello-Pérez et al., 2021; Chieregato Maniglia et al., 2021; Liu et al., 2022). Hence, the starch modification as complex matrixes of multi-components using physical and innovative technologies like microwave heating and toasting can represent interesting opportunities to extend the Andean floury maize frontiers. However, a future challenge is a milling emergent technology adapted to the floury specialty in Andean maize with completely soft endosperm and low protein content.

8. Conclusions

Maize is an important cereal worldwide, with a predominance of genetically generated dent and flint cultivars known as common, normal, or regular maize. However, among Andean maize, there are genotypes with specialty kernels to obtain whole ready-to-eat maize by toasting called "*tostado*" or "*cancha*" and "*chulpi*," which are easy to chew and crispy, respectively. About toasting, several aspects such as acrylamide formation, phytoglycogen, digestibility, and resistant starch are unknown topics in these ready-to-eat products. The up-to-date scientific literature regarding conventional and novel toasting techniques reflects the scientific community's attention to dry heating and toasting (roasting) as ways to modify starch in whole kernel and flour to get new functionalities using physical methods such as microwave heating and toasting.

Declarations

Author contribution statement

The author worked on the development and the writing of this article.

Funding statement

The author carried out this work within the DOCT-DI-2019-49 Project framework with the institutional sponsor of the Universidad Central del Ecuador.

Data availability statement

Data is available on request.

.

Declaration of interests statement

The author declares no conflict of interest.

Additional information

Supplementary information is available for this paper.

Acknowledgments

The author would like to thank to the Programa de Modernización de los Servicios Agropecuarios-PROMSA-MAG and the Instituto Nacional de Investigaciones Agropecuarias-INIAP, Ecuador for supporting previous studies.

References

Aceituno, F. J., & Loaiza, N. (2018). The origins and early development of plant food production and farming in Colombian tropical forests. *Journal of Anthropological Archaeology*, *49*, 161-172. https://doi.org/10.1016/j.jaa.2017.12.007

Achten, E., Schütz, D., Fischer, M., Fauhl-Hassek, C., Riedl, J., & Horn, B. (2019). Classification of grain maize (*Zea mays* L.) from different geographical origins with FTIR spectroscopy - A suitable analytical tool for feed authentication? *Food Analytical Methods*, *12*(10), 2172-2184. https://doi.org/10.1007/s12161-019-01558-9

Ajatta, M. A., Akinola, S. A., Osundahunsi, O. F., & Omoba, O. S. (2021). Effect of roasting on the chemical composition, functional characterisation and antioxidant activities of three varieties of marble vine (*Dioclea reflexa*): An underutilised plant. *Heliyon*, *7*(5), e07107. https://doi.org/10.1016/j.heliyon.2021.e07107

Alfonso-Durruty, M., Troncoso, A., Larach, P., Becker, C., & Misarti, N. (2017). Maize (*Zea mays*) consumption in the southern andes (30 degrees -31 degrees S. Lat): Stable isotope evidence (2000 BCE-1540 CE). *American Journal of Physical Anthropology*, *164*(1), 148-162. https://doi.org/10.1002/ajpa.23263

Athens, J. S., Ward, J. V., Pearsall, D. M., Chandler-Ezell, K., Blinn, D. W., & Morrison, A. E. (2017). Early prehistoric maize in northern highland Ecuador. *Latin American Antiquity*, *27*(1), 3-21. https://doi.org/10.7183/1045-6635.27.1.3

Azmir, J., Hou, Q., & Yu, A. (2019). CFD-DEM simulation of drying of food grains with particle shrinkage. *Powder Technology*, *343*, 792-802. https://doi.org/https://doi.org/10.1016/j.powtec.2018.11.097

Azmir, J., Hou, Q., & Yu, A. (2020). CFD-DEM study of the effects of food grain properties on drying and shrinkage in a fluidised bed. *Powder Technology*, *360*, 33-42. https://doi.org/https://doi.org/10.1016/j.powtec.2019.10.021

Bello-Pérez, L. A., Flores-Silva, P. C., Sifuentes-Nieves, I., & Agama-Acevedo, E. (2021). Controlling starch digestibility and glycaemic response in maize-based foods. *Journal of Cereal Science*, *99*, 103222. https://doi.org/10.1016/j.jcs.2021.103222

Boyer, C. D., & Hannah, L. C. (2001). Kernel mutants of corn. In A. R. Hallauer (Ed.), *Specialty Corns (Second Edition)*. CRC Press LLC. https://doi.org/https://doi.org/10.1201/9781420038569

Breslin, J. C., & Knott, K. (2020). 15 - Toasting. In A. A. Perdon, S. L. Schonauer, & K. S. Poutanen (Eds.), *Breakfast Cereals and How They Are Made (Third Edition)* (pp. 299-321). AACC International Press. https://doi.org/https://doi.org/10.1016/B978-0-12-812043-9.00015-1

Brocca, D., & Bocca, V. (2022). Chemical monitoring reporting guidance: 2022 data collection. *EFSA Supporting Publications*, *19*(1). https://doi.org/10.2903/sp.efsa.2022.EN-7132

Carrera, Y., Utrilla-Coello, R., Bello-Pérez, A., Alvarez-Ramirez, J., & Vernon-Carter, E. J. (2015). In vitro digestibility, crystallinity, rheological, thermal, particle size and morphological characteristics of pinole, a traditional energy food obtained from toasted ground maize. *Carbohydrate Polymers*, *123*, 246-255. https://doi.org/10.1016/j.carbpol.2015.01.044

Chieregato Maniglia, B., Carregari Polachini, T., Norwood, E.-A., Le-Bail, P., & Le-Bail, A. (2021). Thermal technologies to enhance starch performance and starchy products. *Current Opinion in Food Science*, *40*, 72-80. https://doi.org/10.1016/j.cofs.2021.01.005

Dhua, S., Kheto, A., Singh Sharanagat, V., Singh, L., Kumar, K., & Nema, P. K. (2021). Quality characteristics of sand, pan and microwave roasted pigmented wheat (*Triticum aestivum*). *Food Chemistry*, *365*, 130372. https://doi.org/10.1016/j.foodchem.2021.130372

Domínguez-Hernández, E., Gaytán-Martínez, M., Gutiérrez-Uribe, J. A., & Domínguez-Hernández, M. E. (2022). The nutraceutical value of maize (*Zea mays* L.) landraces and the determinants of its variability: A review. *Journal of Cereal Science*, *103*, 103399. https://doi.org/https://doi.org/10.1016/j.jcs.2021.103399

Ekezie, F.-G. C., Sun, D.-W., Han, Z., & Cheng, J.-H. (2017). Microwave-assisted food processing technologies for enhancing product quality and process efficiency: A review of recent developments. *Trends in Food Science & Technology*, *67*, 58-69. https://doi.org/10.1016/j.tifs.2017.05.014

Fukui, M., Islam, M. Z., Lai, H.-M., Kitamura, Y., & Kokawa, M. (2022). Effects of roasting on storage degradability and processing suitability of brown rice powder. *LWT - Food Science and Technology*, 113277. https://doi.org/10.1016/j.lwt.2022.113277

García-Lara, S., & Serna-Saldivar, S. O. (2019). Chapter 1 - Corn History and Culture. In S. O. Serna-Saldivar (Ed.), *Corn (Third Edition)* (pp. 1-18). AACC International Press. https://doi.org/https://doi.org/10.1016/B978-0-12-811971-6.00001-2

Gökmen, S. (2004). Effects of moisture content and popping method on popping characteristics of popcorn. *Journal of Food Engineering*, *65*(3), 357-362. https://doi.org/10.1016/j.jfoodeng.2004.01.034

Grobman, A., Bonavia, D., Dillehay, T. D., Piperno, D. R., Iriarte, J., & Holst, I. (2012). Preceramic maize from Paredones and Huaca Prieta, Peru. *Proceedings of the National Academy of Sciences of the United States of America*, *109*(5), 1755-1759. https://doi.org/10.1073/pnas.1120270109

Guzik, P., Szymkowiak, A., Kulawik, P., Zając, M., & Migdał, W. (2022). The confrontation of consumer beliefs about the impact of microwave-processing on food and human health with existing research. *Trends in Food Science & Technology*, *119*, 110-121. https://doi.org/https://doi.org/10.1016/j.tifs.2021.11.011

Hamaker, B. R. (2021). Current and future challenges in starch research. *Current Opinion in Food Science*, *40*, 46-50. https://doi.org/10.1016/j.cofs.2021.01.003

Jermann, C., Koutchma, T., Margas, E., Leadley, C., & Ros-Polski, V. (2015). Mapping trends in novel and emerging food processing technologies around the world. *Innovative Food Science & Emerging Technologies*, *31*, 14-27. https://doi.org/10.1016/j.ifset.2015.06.007

Kaimal, A. M., Mujumdar, A. S., & Thorat, B. N. (2021). Resistant starch from millets: Recent developments and applications in food industries. *Trends in Food Science & Technology*, *111*, 563-580. https://doi.org/10.1016/j.tifs.2021.02.074

Kanagaraj, S. P., Ponnambalam, D., & Antony, U. (2019). Effect of dry heat treatment on the development of resistant starch in rice (*Oryza sativa*) and barnyard millet (*Echinochloa furmantacea*). *Journal of Food Processing and Preservation*, *43*(7), 13965. https://doi.org/10.1111/jfpp.13965

Kang, X., Jia, S., Gao, W., Wang, B., Zhang, X., Tian, Y., Sun, Q., Atef, M., Cui, B., & Abd El-Aty, A. M. (2022). The formation of starch-lipid complexes by microwave heating. *Food Chemistry*, *382*, 132319. https://doi.org/https://doi.org/10.1016/j.foodchem.2022.132319

Lara, N., Osorio, F., & Ruales, J. (2022). Variables related to microwave heating-toasting time and water migration assessment with kernel size approaches of specialty maize types. *Journal of the Science of Food and Agriculture*. https://doi.org/10.1002/jsfa.11961

Lara, N., & Ruales, J. (2021). Physical and hydration properties of specialty floury and sweet maize kernels subjected to pan and microwave toasting. *Journal of Cereal Science*, *101*, 103298. https://doi.org/10.1016/j.jcs.2021.103298

Lara, N., Vizuete, K., Debut, A., Chango, I., Campaña, O., Villacrés, E., Bonilla, P., & Ruales, J. (2021). Underutilized maize kernels (*Zea mays* L. var. *amylacea* and var. *saccharata*) subjected to pan and microwave toasting: A comparative structure study in the whole kernel. *Journal Cereal Science*, *100*, 103249. https://doi.org/10.1016/j.jcs.2021.103249

Lee, D.-J., Kim, J.-M., & Lim, S.-T. (2021). Characterization of resistant waxy maize dextrins prepared by simultaneous debranching and crystallization. *Food Hydrocolloids*, *112*, 106315. https://doi.org/https://doi.org/10.1016/j.foodhyd.2020.106315

Lei, N., Chai, S., Xu, M., Ji, J., Mao, H., Yan, S., Gao, Y., Li, H., Wang, J., & Sun, B. (2020). Effect of dry heating treatment on multi-levels of structure and physicochemical properties of maize starch: A thermodynamic study. *International Journal of Biological Macromolecules*, *147*, 109-116. https://doi.org/10.1016/j.ijbiomac.2020.01.060

Li, H., Ji, J., Yang, L., Lei, N., Wang, J., & Sun, B. (2020). Structural and physicochemical property changes during pyroconversion of native maize starch. *Carbohydrate Polymers*, *245*, 116560. https://doi.org/10.1016/j.carbpol.2020.116560

Liu, X., Huang, S., Chao, C., Yu, J., Copeland, L., & Wang, S. (2022). Changes of starch during thermal processing of foods: Current status and future directions. *Trends in Food Science & Technology*, *119*, 320-337. https://doi.org/https://doi.org/10.1016/j.tifs.2021.12.011

Mao, H., Li, J., Chen, Z., Yan, S., Li, H., Wen, Y., & Wang, J. (2021). Molecular structure of different prepared pyrodextrins and the inhibitory effects on starch retrogradation. *Food Research International*, *143*, 110305. https://doi.org/10.1016/j.foodres.2021.110305

McMichael, C. N. H., Witteveen, N. H., Scholz, S., Zwier, M., Prins, M. A., Lougheed, B. C., Mothes, P., & Gosling, W. D. (2021). 30,000 years of landscape and vegetation dynamics in a mid-elevation Andean valley. *Quaternary Science Reviews*, *258*, 106866. https://doi.org/10.1016/j.quascirev.2021.106866

Michalak, J., Czarnowska-Kujawska, M., Klepacka, J., & Gujska, E. (2020). Effect of microwave heating on the acrylamide formation in foods. *Molecules*, *25*(18). https://doi.org/10.3390/molecules25184140

Moreno-Vilet, L., Hernández-Hernández, H. M., & Villanueva-Rodríguez, S. J. (2018). Current status of emerging food processing technologies in Latin America: Novel thermal processing. *Innovative Food Science & Emerging Technologies*, *50*, 196-206. https://doi.org/https://doi.org/10.1016/j.ifset.2018.06.013

Narváez-González, E. D., Figueroa-Cárdenas, J. d. D., Taba, S., Tostado, E. C., Martínez Peniche, R. Á., & Rincon Sánchez, F. (2006). Relationships between the microstructure, physical features, and chemical composition of different maize accessions from Latin America. *Cereal Chemistry*, *83*(6), 595-604. https://doi.org/10.1094/cc-83-0595

Ortiz, R., Crossa, J., Franco, J., Sevilla, R., & Burgueño, J. (2008). Classification of Peruvian highland maize races using plant traits. *Genetic Resources and Crop Evolution*, *55*(1), 151-162. https://doi.org/10.1007/s10722-007-9224-7

Pagán-Jiménez, J. R., Guachamín-Tello, A. M., Romero-Bastidas, M. E., & Constantine-Castro, A. R. (2016). Late ninth millennium B.P. use of *Zea mays* L. at Cubilán area, highland Ecuador, revealed by ancient starches. *Quaternary International*, *404*, 137-155. https://doi.org/10.1016/j.quaint.2015.08.025

Pellegrini, N., Vittadini, E., & Fogliano, V. (2020). Designing food structure to slow down digestion in starch-rich products. *Current Opinion in Food Science*, *32*, 50-57. https://doi.org/10.1016/j.cofs.2020.01.010

PROMSA. (2005). *Oferta tecnologica para cadenas agroalimentarias* (J. Chang, Ed.). PROMSA. https://fdocuments.ec/document/oferta-tecnologica-para-cadenas-agroalimentarias-documento.html

Rakesh, V., & Datta, A. K. (2011). Microwave puffing: Determination of optimal conditions using a coupled multiphase porous media – Large deformation model. *Journal of Food Engineering*, *107*(2), 152-163. https://doi.org/10.1016/j.jfoodeng.2011.06.031

Ries de Carvalho, G., Lemos Monteiro, R., Lauriano, J. B., & Augusto, P. E. D. (2021). Microwave and microwave-vacuum drying as alternatives to convective drying in barley malt processing. *Innovative Food Science & Emerging Technologies*, *73*, 102770. https://doi.org/https://doi.org/10.1016/j.ifset.2021.102770

Salvador-Reyes, R., & Clerici, M. T. P. S. (2020). Peruvian Andean maize: General characteristics, nutritional properties, bioactive compounds, and culinary uses. *Food Research International*, *130*, 108934. https://doi.org/10.1016/j.foodres.2019.108934

Salvador-Reyes, R., Rebellato, A. P., Lima Pallone, J. A., Ferrari, R. A., & Clerici, M. T. P. S. (2021). Kernel characterization and starch morphology in five varieties of Peruvian Andean maize. *Food Research International*, *140*, 110044. https://doi.org/10.1016/j.foodres.2020.110044

Santos Vecino, G., Monsalve Marín, C. A., & Correa Salas, L. V. (2015). Alteration of tropical forest vegetation from the Pleistocene–Holocene transition and plant cultivation from the end of early Holocene through middle Holocene in Northwest Colombia. *Quaternary International*, *363*, 28-42. https://doi.org/10.1016/j.quaint.2014.09.018

Serna-Saldivar, S. O., Gomez, M. H., & Rooney, L. W. (2001). Food uses of regular and specialty corns and their dry-milled fractions. In A. R. Hallauer (Ed.), *Sprecialty Corns (Second Edition)*. CRC Pess LLC. https://doi.org/https://doi.org/10.1201/9781420038569

Serna-Saldivar, S. O., & Perez Carrillo, E. (2019). Chapter 16 - Food uses of whole corn and dry-milled fractions. In S. O. Serna-Saldivar (Ed.), *Corn (Third Edition)* (pp. 435-467). AACC International Press. https://doi.org/https://doi.org/10.1016/B978-0-12-811971-6.00016-4

Sharma, S., Kataria, A., & Singh, B. (2022). Effect of thermal processing on the bioactive compounds, antioxidative, antinutritional and functional characteristics of quinoa (*Chenopodium quinoa*). *LWT - Food Science and Technology*, 113256. https://doi.org/10.1016/j.lwt.2022.113256

Shirkole, S. S., Jayabalan, R., & Sutar, P. P. (2020). Dry sterilization of paprika (*Capsicum annuum* L.) by short time-intensive microwave-infrared radiation: Establishment of process using glass transition, sorption, and quality degradation kinetic parameters. *Innovative Food Science & Emerging Technologies*, *62*, 102345. https://doi.org/https://doi.org/10.1016/j.ifset.2020.102345

Shivhare, U. S., Raghavan, G. S. U., & Biosisio, R. G. (1994). Modelling of drying kinetics of maize in a microwave environment. *Journal of Agricultural Engineering Research*, *57*, 199-205.

Singh, N., Singh, S., & Shevkani, K. (2019). Chapter 9 - Maize: composition, bioactive constituents, and unleavened bread. In V. R. Preedy & R. R. Watson (Eds.), *Flour and Breads and their Fortification in Health and Disease Prevention (Second Edition)* (pp. 111-121). Academic Press. https://doi.org/https://doi.org/10.1016/B978-0-12-814639-2.00009-5

Solaesa, Á. G., Villanueva, M., Muñoz, J. M., & Ronda, F. (2021). Dry-heat treatment vs. heat-moisture treatment assisted by microwave radiation: Techno-functional and rheological modifications of rice flour. *LWT - Food Science and Technology*, *141*, 110851. https://doi.org/10.1016/j.lwt.2021.110851

Sruthi, N. U., Premjit, Y., Pandiselvam, R., Kothakota, A., & Ramesh, S. V. (2021). An overview of conventional and emerging techniques of roasting: Effect on food bioactive signatures. *Food Chemistry*, *348*, 129088. https://doi.org/10.1016/j.foodchem.2021.129088

Sruthi, N. U., & Rao, P. S. (2021). Effect of processing on storage stability of millet flour: A review. *Trends in Food Science & Technology*, *112*, 58-74. https://doi.org/10.1016/j.tifs.2021.03.043

Suhag, R., Dhiman, A., Deswal, G., Thakur, D., Sharanagat, V. S., Kumar, K., & Kumar, V. (2021). Microwave processing: A way to reduce the anti-nutritional factors (ANFs) in food grains. *LWT - Food Science and Technology*, *150*, 111960. https://doi.org/10.1016/j.lwt.2021.111960

Sumithra, B., & Bhattacharya, S. (2008). Toasting of corn flakes: Product characteristics as a function of processing conditions. *Journal of Food Engineering*, *88*(3), 419-428. https://doi.org/10.1016/j.jfoodeng.2008.03.001

Tao, Y., Yan, B., Fan, D., Zhang, N., Ma, S., Wang, L., Wu, Y., Wang, M., Zhao, J., & Zhang, H. (2020). Structural changes of starch subjected to microwave heating: A review from the perspective of dielectric properties. *Trends in Food Science & Technology*, *99*, 593-607. https://doi.org/10.1016/j.tifs.2020.02.020

Torbica, A., Belovic, M., Popovic, L., & Cakarevic, J. (2021). Heat and hydrothermal treatments of non-wheat flours. *Food Chemistry*, *334*, 127523. https://doi.org/10.1016/j.foodchem.2020.127523

Tracy, W. F. (2001). Sweet corn. In A. R. Hallauer (Ed.), *Specialty Corns (Second Edition)*. CRC Pess LLC. https://doi.org/https://doi.org/10.1201/9781420038569

van Rooyen, J., Simsek, S., Oyeyinka, S. A., & Manley, M. (2022). Holistic view of starch chemistry, structure and functionality in dry heat-treated whole wheat kernels and flour. *Foods*, *11*(2). https://doi.org/10.3390/foods11020207

Wang, L., Josephs, E. B., Lee, K. M., Roberts, L. M., Rellan-Alvarez, R., Ross-Ibarra, J., & Hufford, M. B. (2021). Molecular parallelism underlies convergent highland adaptation of maize landraces. *Molecular Biology and Evolution*, *38*(9), 3567-3580. https://doi.org/10.1093/molbev/msab119

Washburn, E., Nesbitt, J., Burger, R., Tomasto-Cagigao, E., Oelze, V. M., & Fehren-Schmitz, L. (2020). Maize and dietary change in early Peruvian civilization: Isotopic evidence from the Late Preceramic Period/Initial Period site of La Galgada, Peru. *Journal of Archaeological Science: Reports*, *31*, 102309. https://doi.org/10.1016/j.jasrep.2020.102309

Xie, A.-J., Lee, D.-J., & Lim, S.-T. (2021). Characterization of resistant waxy maize dextrins prepared by simultaneous debranching and crystallization followed by acidic or enzymatic hydrolysis. *Food Hydrocolloids*, *121*, 106942. https://doi.org/https://doi.org/10.1016/j.foodhyd.2021.106942

Xue, J., Inzero, J., Hu, Q., Wang, T., & Wusigale, Y. L. (2019). Development of easy, simple and low-cost preparation of highly purified phytoglycogen nanoparticles from corn. *Food Hydrocolloids*, *95*, 256-261. https://doi.org/10.1016/j.foodhyd.2019.04.041

Yang, Z., Zhang, Y., Wu, Y., & Ouyang, J. (2022). The role of drying methods in determining the in vitro digestibility of starch in whole chestnut flour. *LWT - Food Science and Technology*, *153*, 112583. https://doi.org/10.1016/j.lwt.2021.112583

Ye, J., Xia, Y., Yi, Q., Zhu, H., Yang, Y., Huang, K., & Shi, K. (2021). Multiphysics modeling of microwave heating of solid samples in rotary lifting motion in a rectangular multi-mode cavity. *Innovative Food Science & Emerging Technologies*, *73*, 102767. https://doi.org/https://doi.org/10.1016/j.ifset.2021.102767

Zambrano, J. L., Yánez, C. F., & Sangoquiza, C. A. (2021). Maize breeding in the highlands of Ecuador, Peru, and Bolivia: A review. *Agronomy*, *11*(2), 212. https://doi.org/10.3390/agronomy11020212

Zhu, F., Bertoft, E., Kallman, A., Myers, A. M., & Seetharaman, K. (2013). Molecular structure of starches from maize mutants deficient in starch synthase III. *Journal of Agricultural and Food Chemistry*, *61*(41), 9899-9907. https://doi.org/10.1021/jf402090f

Supplementary information

Table S1. Chemical characterization of normal, floury, and sweet maize types cultivated in the Andean region.

Maize types*	Macro components (g/100 g)							Macro elements (mg/100 g)				Microelements (µg/g)			
	Protein	**Fat**	**Fiber**	**Ash**	**NFE**	**Starch**	**Amylose**	**Ca**	**Mg**	**K**	**P**	**Cu**	**Fe**	Mn	Zn
Normal 1	6.28	5.29	2.79	1.53	84.11	68.31	32.90	10	100	320	340	6	32	4	21
Normal 2	8.16	4.92	3.62	1.21	82.09	67.58	28.07	10	70	280	260	6	37	4	40
Normal 3	10.28	4.75	4.40	1.47	79.11	64.91	30.53	10	80	320	360	4	46	4	28
Floury 1	4.49	4.09	3.49	1.48	86.46	60.67	38.73	10	100	440	280	2	18	4	36
Floury 2	6.77	5.19	3.27	1.56	83.20	73.62	30.32	10	110	450	310	3	23	5	18
Floury 3	6.49	4.17	3.23	1.40	84.71	73.18	27.75	10	90	420	280	4	19	5	18
Floury 4	6.44	4.81	2.69	1.51	84.55	69.56	30.21	10	20	340	390	4	29	3	17
Floury 5	6.81	5.77	2.94	1.50	82.98	73.28	29.04	10	110	410	310	3	16	4	17
Floury 6	7.31	5.24	3.16	1.54	82.76	71.32	30.18	10	100	430	310	3	23	5	21
Sweet 1	9.59	6.50	2.77	1.93	79.21	40.98	42.34	10	120	560	330	3	16	4	19

* Averages of two replications. NFE (nitrogen-free extract).

The standard deviation values are available in the unpublished supplementary information from the previous study (Lara, N.) supported by the project "Investigación y desarrollo de nuevas alternativas alimenticias para consumo humano, basadas en maíz, banano, plátano y quinua" INIAP-PROMSA AQ-CV-012 (PROMSA, 2005).

Table S2. Summary of pasting and thermal properties of normal, floury, and sweet maize types cultivated in the Andean region (raw maize kernels reduced to flour).

Maize types	Pasting viscosities (Pa s)					Peak time	Pasting T (°C)	DSC heating cycle (°C)			(J/g)	DSC cooling cycle (°C)			(J/g)
	Peak	Trough	B	Final	Setback			Onset	Peak	Final	ΔH	Onset	Peak	Final	ΔH
Normal 1	1.10	0.78	0.32	2.28	1.50	8.5	72.2	53.0	64.4	76.5	6.6	78.1	81.9	84.0	-6.2
Normal 2	1.08	0.82	0.27	2.63	1.81	8.7	74.3	61.7	70.2	81.3	5.0	76.7	80.6	82.6	-5.2
Normal 3	0.47	0.46	0.00	1.30	0.84	12.8	78.5	61.8	69.9	78.5	7.1	77.5	81.5	83.4	-5.4
Floury 1	3.08	1.00	2.08	2.55	1.55	6.7	72.2	58.5	66.2	75.2	10.9	79.2	82.7	84.6	-6.5
Floury 2	1.54	0.81	0.73	2.45	1.64	8.2	74.3	57.5	65.7	74.6	10.0	78.1	81.9	83.9	-6.1
Floury 3	0.93	0.38	0.55	1.20	0.82	8.1	73.2	56.5	65.4	73.9	7.5	77.9	81.4	83.4	-5.6
Floury 4	1.93	0.96	0.97	2.42	1.45	8.4	74.0	55.0	63.6	74.1	7.1	77.0	81.0	83.4	-5.8
Floury 5	1.50	0.81	0.69	2.19	1.39	8.0	74.3	57.5	65.8	74.3	9.0	78.2	81.8	83.8	-5.8
Floury 6	1.52	0.75	0.78	2.08	1.33	8.0	75.6	57.5	65.3	73.8	10.6	78.0	81.6	83.6	-5.9
Sweet 1	0.13	0.12	0.01	0.15	0.03	10.7	89.7	52.4	60.3	69.7	6.4	76.1	80.2	82.2	-4.8

* Averages of two replications. B (breakdown); T (temperature); Peak time in min; ΔH (enthalpy).

The standard deviation values are available in the unpublished supplementary information from the previous study (Lara, N.) supported by the project "Investigación y desarrollo de nuevas alternativas alimenticias para consumo humano, basadas en maíz, banano, plátano y quinua" INIAP-PROMSA AQ-CV-012 (PROMSA, 2005).

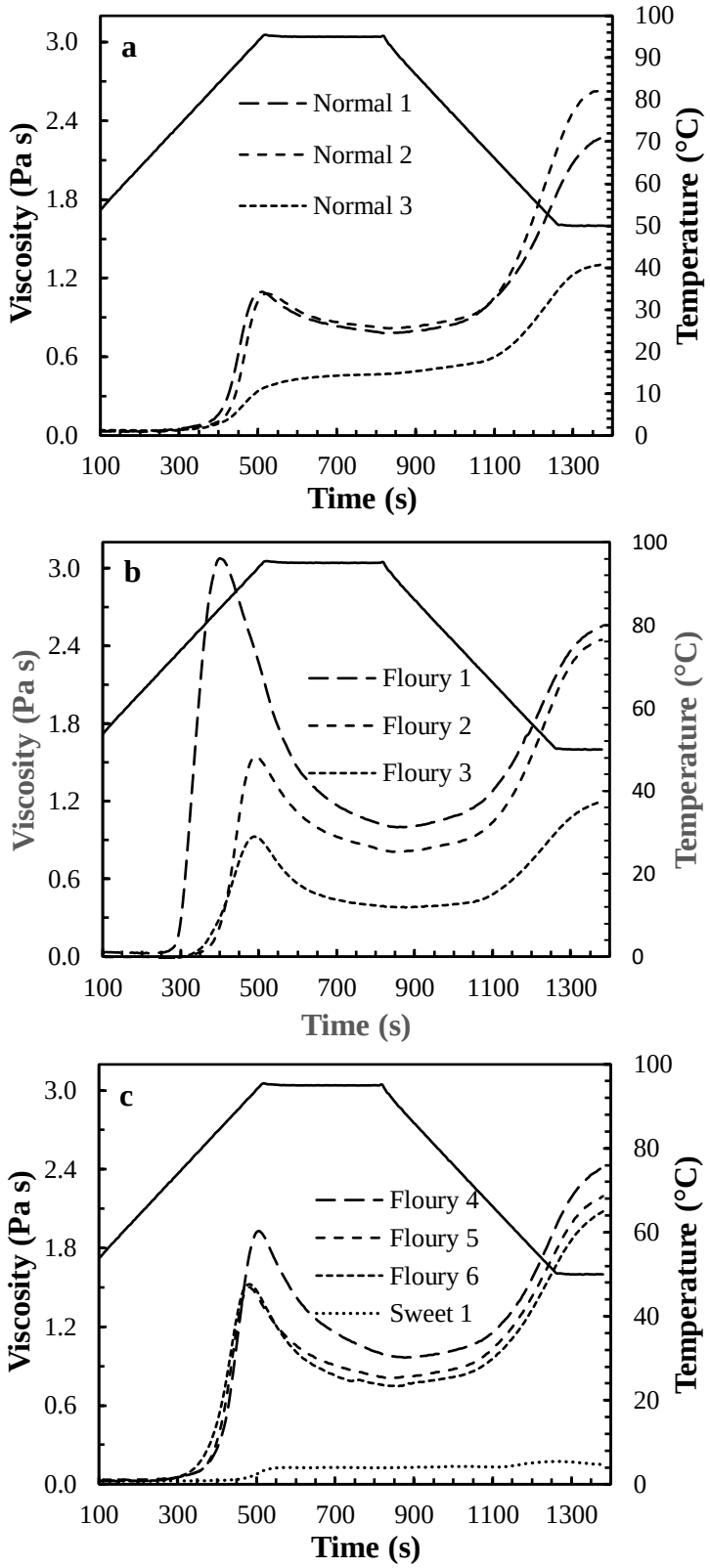

Figure S1. Whole flour viscosity profiles in Pa s for normal, floury, and sweet maize types cultivated in the Andean region. Hard and semi-hard endosperm (**a**), Semi-soft endosperm (**b**), and soft endosperm (**c**). Data from unpublished information (Lara, N) obtained within the framework of the project "Investigación y desarrollo de nuevas alternativas alimenticias para consumo humano, basadas en maíz, banano, plátano y quinua" INIAP-PROMSA AQ-CV-012 (PROMSA, 2005).

Chapter 2

Underutilized maize kernels (*Zea mays* L. var. *amylacea* and var. *saccharata*) subjected to pan and microwave toasting: a comparative structure study in the whole kernel

Nelly Lara[a,b*], Karla Vizuete[c], Alexis Debut[c], Ivan Chango[d], Orlando Campaña[e], Elena Villacrés[f], Pablo Bonilla[g], Jenny Ruales[a]

[a] Departamento de Ciencia de Alimentos y Biotecnología, Escuela Politécnica Nacional, Av. Ladrón de Guevara E11-253 Edificio 19 Quito, Ecuador

[b] CADET, Facultad de Ciencias Agrícolas, Universidad Central del Ecuador, Calle Universitaria s/n, Tumbaco, Ecuador

[c] Centro de Nanociencia y Nanotecnología, Universidad de Las Fuerzas Armadas (ESPE), Sangolquí 171103, Ecuador

[d] Centro de Investigaciones Aplicadas a Polímeros, Escuela Politécnica Nacional, Av. Ladrón de Guevara E11-253 Edificio 11, Quito, Ecuador.

[e] Laboratorio de Nuevos Materiales, Escuela Politécnica Nacional, Av. Ladrón de Guevara E11-253 Edificio 14, Quito, Ecuador.

[f] Departamento de Nutrición y Calidad, Estación Experimental Santa Catalina, INIAP, Mejía, Pichincha, Ecuador.

[g] Facultad de Ciencias Químicas, Universidad Central del Ecuador, Av. Universitaria, Quito, Ecuador

ABSTRACT

Toasting in a pan is a household activity to make ready-to-eat maize using the whole kernels of underutilized maize types (*Zea mays* L. var. *amylacea* and var. *saccharata*) in the Andean region. Floury (a0 and a1) and sweet (a2) maize kernels with 14 g/100 g moisture content (T0) were subjected to a pan (T1) and microwave (T2) toasting. The comparative evaluation by maize types and kernel conditions (raw and toasted processes) revealed structural variations in starch granule size measured by scanning electron microscopy (SEM). In floury maize, blue value (BV), number average of molecular weight ($\overline{M}_n$) and intrinsic viscosity [η] evidenced consistent conformational variations. The FWHM ratio 865/941 allowed the differentiation between floury and sweet maize and between raw and toasted kernels. Floury maize displayed high ATR FTIR band intensities in the

* Corresponding author: CADET, Facultad de Ciencias Agrícolas, Universidad Central del Ecuador, Calle Universitaria s/n, Tumbaco, Ecuador. E-mail: nvlara@uce.edu.ec (N. Lara)

range of 994 to 1151 cm^{-1} and low from 1646 to 3298 cm^{-1} compared with sweet maize. Microwave toasting exhibited higher (1454 – 2924 cm^{-1}) and lower (3298 cm^{-1}) ATR FTIR band intensities than those for raw kernel and toasting in a pan. Microwave toasting had the same effect as toasted in a pan on carbohydrate structure and caused changes linked to the band intensity increases ascribed to protein and lipid structures.

Keywords: maize kernel, toasting; microwave, crystallite size; Raman, intrinsic viscosity

1. Introduction

Specialty floury and sweet maize types underutilized worldwide remain available minimally changed by selective breeding in the Andean region (Salvador-Reyes & Clerici, 2020). However, no published information about maize kernel structure studies focuses on traditional food processes such as toasting. For example, in floury maize kernels (*Zea mays* L. var. *amylacea*), the endosperm is entirely soft, with no vitreous fraction. On the other hand, in sweet maize kernels (*Zea mays* L. var. *saccharata*), the endosperm is relatively small and quite shrunken, with a sugary-vitreous fraction that is more significant than the floury endosperm. Although these maize types are two highly contrasted in starch and endosperm structure, both are specialty kernels to make ready-to-eat maize by toasting in a pan, widely consumed from southern Colombia to northern Chile.

Toasting technology, also called roasting, has been traditionally applied to prepare toasted maize kernels for beverage processing and ingredients in various food processes (Woo et al., 2018; Youn & Chung, 2012). Commercial maize kernels toasted in a pan and reduced to flour is a traditional energy food widely consumed by different ethnic groups of Northern Mexico and Southwest USA (Carrera et al., 2015). Palatable maize flour from toasted semi-dent kernels is an integral ingredient for many food processing applications (Raigar & Mishra, 2018). On the other hand, toasting in a pan of floury and sweet maize kernels is a household activity, and information on the kernel structure before and after toasting is not available in previous studies. Furthermore, toast in a pan weights equivalent to raw microwave popcorn is a slow process that can take 20 to 25 minutes. Thus, the microwave technique is a potential innovation in maize kernel toasting to reduce processing time.

Toasting is a dry heating technique with many reports referring to starch dextrinization and limited information on whole kernels of flint, dent, and semi dent maize types to understand its effect on physicochemical properties (Carrera et al., 2015; Raigar & Mishra, 2018), bioactive compounds (Woo et al., 2018), and nutritional and sensorial attributes (Youn & Chung, 2012). The latest studies by repeated dry heating using a muffle furnace and several techniques for analysis have improved

the understanding of structural changes and physicochemical properties of food-grade native maize starch. However, the effect of toasting (dry heating) initiated from a pan and microwave on the whole maize kernels is still unexplored. Therefore, it is of great interest to understand the toasting impact on floury and sweet maize kernels used after toasting like ready-to-eat maize. This work aims to investigate three specialty maize kernels (a0, a1, and a2) before (T0) and after toasting (T1 and T2) conditions. Therefore, floury (a0 and a1) and sweet (a2) maize kernels were subjected to a pan (T1 antique way) and microwave (T2 innovative way) toasting. The size distribution of starch granules, diffraction patterns, average crystallite size, Raman and ATR-FTIR bands ascribed to functional groups, intrinsic viscosity, and other properties were measured.

2. Materials and methods

2.1. Materials

Commercial kernel batches of the three main specialty maize used for toasting in a pan were acquired from a local market in Quito. Two (floury a0 and sweet a2) from Perú and the other (floury a1) from Ecuador. Floury maize types a0 and a1 were *Zea mays* L. var. *amylacea* with completely soft endosperm, and it is more representative in the kernel. Sweet maize type a2 was *Zea mays* L var *saccharata,* with the sugary-vitreous fraction more significant than the floury endosperm.

Samples (1.2 kg) of each maize type were taken in polypropylene airtight containers (2.3 L), adjusted to 14 g/100 g moisture content by adding the required amount of water, and stored for two weeks at room temperature (15 – 20 ℃). Three trials conducted on different dates assured the application of rigorous statistical analyses. The chemicals and reagents used were analytical grades, purchased from Merck and Sigma Aldrich Chemical Co. supplier for Quito, Ecuador.

2.2. Toasting process

Samples with 14 g/100 g moisture content (150 g) were used for the toasting (T1 and T2) and raw (T0) kernel treatments. Toasting in a pan (T1) was done by placing the maize kernels (150 g) in a multipurpose electric pan set at 175 ℃ with a rheostat (Atlantic Promotion INC., Longueuil, Canada) and an accessory for manual stirring, carrying out the toasting for 1500 s. For microwave toasting (T2), preliminary studies allowed the definition of the experimental method. Maize kernels (150 g) contained in a sealed paper bag (17.5 cm wide and 24 cm long) were put on a flat plate and placed at the center of the microwave oven (Panasonic, Shanghai, China), and toasted at 492 W for 390 s (floury maize) and 312 s (sweet maize). All treatments were packed in foil gusseted bags for further

measurements on kernel endosperm and then reduced to flour using an ultra-centrifugal mill (Retsch GmbH, Haan, Germany). Before and after pan and microwave toasting treatments were evaluated using different techniques.

2.3. Scanning electron microscopy (SEM)

Whole maize kernels cut widthwise allowed the obtaining of endosperm matrix fragments from each treatment. The endosperm matrix fragment mounted on a stub with a double-sided carbon adhesive tape was coated with gold (20 nm) and imaged using a field emission gun (FEG) coupled to the scanning electron microscope (TESCAN, S. A. Brno, Czech Republic). The accelerating voltage was 10 kV with a magnification of 2.67 kx and an IR camera in the depth mode. The ImageJ analysis software facilitated the manual measurement of more than 1000 entire starch granule diameters from six to eight micrographs acquired from the endosperm matrix fragments. FEG-SEM micrograph sections obtained with a magnification of 5.33 kx and selected from endosperm matrix fragment micrographs are included in this paper by treatment. The Kernel density, also called density trace, was estimated with the starch granule diameter data using the OriginPro software, option distribution fitting (Version 2020, Microcal Inc., Northampton, MA, USA).

2.4. X-ray diffraction (XRD)

Kernel samples reduced to flour using an ultra-centrifugal mill and passed through a 40-micron opening sieve that allowed the extraction of flour samples with fine and uniform granulometry for floury maize (a0 and a1) and sweet maize (a2) treatments. X-ray diffraction patterns (XRD) of the maize flour samples were acquired with an Empyrean diffractometer (Malvern Panalytical, Almelo, The Netherlands), using a Cu Kα radiation wavelength of 1.5406 Å. The measurement of each treatment was by triplicate. Relative crystallinity was calculated from the relationship between the crystalline area (sum all peaks) and the total area within the range at 2θ of 5 to 30° (Minakawa et al., 2019). The OriginPro software (Version 2020 Microcal Inc., Northampton, MA, USA) permitted estimating the relative crystallinity (Peng & Yao, 2018), the crystallite size (Scherrer equation), and diffraction spacing (d-spacing, Bragg law).

2.5. Vibrational measurements by Raman spectroscopy

The flour treatment spectra were acquired on a Raman spectrometer (Horiba France SAS, Palaiseau, France) with a 785 nm laser source, a motor-powered microscope, and a cooled charge-coupled device (CCD) detector. The spectral data were collected in the range of 4000-400 cm^{-1} at a resolution

of 1 cm^{-1} with constant measurement parameters (acquisition time: 60 s). The OriginPro software (Version 2020, Microcal Inc., Northampton, MA, USA) was used to calculate the full width at the half maximum of the band at 480 cm^{-1}.

2.6. Vibrational measurements by Fourier transform infrared (FTIR) spectroscopy.

Dry sample spectra were collected for each treatment using an FTIR spectrophotometer (JASCO International Co., Ltd., Tokyo, Japan) coupled to a single attenuated total reflectance accessory (ATR ProOne). The absorbance was recorded in the wavenumber range of 4000-400 cm^{-1} with a resolution of 0.07 cm^{-1}. In addition, the OriginPro software (Version 2020, Microcal Inc., Northampton, MA, USA) permitted finding hidden band intensities at 1047 and 1017 cm^{-1}.

2.7. Starch content and Blue value (BV)

Soluble compounds of flour were removed along with the initial rinsing water, so starch and the blue value were determined from the free samples of water-soluble solids (Samotus et al., 1993). Starch content was precipitated as iodine-iodide complex, purified, and measured against a blank by the anthrone method at 625 nm. The BV was defined as 100 mg of sample starch-iodine complex absorbance in 100 mL of aqueous solution at 620 nm (Thermo Scientific, Madison, Wisconsin, EE. UU).

2.8. Number average of molecular weight ($\bar{M}_n$)

The number average molecular weight was estimated by the expressions related to maltose equivalent, reducing power, and the average molecular weight (Singh & Ali, 2008). Maltose equivalent of the free maize flour water-soluble solids was determined using alkaline potassium ferricyanide [$K_3Fe(CN)_6$], with some modification. Ceric sulfate solution 0.005M was used for the redox titration of reduced alkaline potassium ferricyanide, and ferroin solution 0.025 M was added as a redox indicator.

2.9. Intrinsic viscosity [η]

Samples of maize flour free of soluble solids were treated following the method to determine [η] in some starches (Leach, 1963; Singh & Ali, 2008). A measured volume of 5M potassium hydroxide solution was used to dissolve the sample and give a final alkali concentration of 1.00M. Accurate

dilutions were made between 0.1-0.4 g/100g, using l M potassium hydroxide solution. Relative viscosity η_{rel} (efflux *t* solution/efflux t_0 solvent) was determined at each concentration using a Cannon-Fenske capillary viscometer No.100 at 25 °C. The η_{rel} results allowed the calculation of the specific viscosity ($\eta_{sp} = (t - t_0)/t_0$) and reduced viscosity ($\eta_{red} = \eta_{sp}/c$ solution concentration). Plotting η_{red} on the y-axis versus *c* and versus η_{sp} on the x-axis, the extrapolating back to zero *c* and η_{sp} showed the same y-intercept, called [η] (Kowalski et al., 2018; Leach, 1963; Singh & Ali, 2008). All measurements were performed in triplicates.

2.10. Water-soluble index

The water-soluble index (WSI) was measured in raw and toasted maize flour using the suspension-centrifugation procedure to recuperate the supernatant liquid and dry it in an oven set at 104 °C (Lara & Ruales, 2002) with slight modifications. First, an equivalent weight of 1 g (dry base) was placed in a pre-weighed centrifugal tube, completely dispersed with 5 mL of distilled water, and stored at room temperature (18-21 °C) for 20 h. Next, the suspension was mixed, completed to 7 mL with distilled water, and centrifuged (2683xg) for 20 min at 3 °C.

2.11. Total soluble sugar and reducing sugar

Total soluble sugar was determined by the sulfuric phenol method (Dubois et al., 1956), and reducing sugar was determined by the Somogyi-Nelson test with a slight modification.

2.12. Statistical analysis

Considering maize types as a known source of variation in the experiment, blocking in the experimental design provides a more valid measure of this variation source due to maize types. Thereby, applying a two-way analysis of variance (ANOVA) by blocks and treatments without interactions, maize types were blocks, and kernel conditions were treatments. According to the normal data distribution, the response variables (two-way matrix) were analyzed, including or excluding sweet maize as the primary source of variability. The means were compared using Tukey´s multiple range test ($P \leq 0.05$). Statistical analyses were performed with Statgraphics software (Statgraphics centurion 18, USA). The OriginPro software (Version 2020, Microcal Inc., Northampton, MA, USA) was used to analyze starch granule size distribution (Kernel density), X-ray diffraction, Raman, and ATR FTIR spectra.

3. Result and discussion

3.1. Scanning electron microscopy

Floury endosperm FEG-SEM micrographs displayed round starch granules for all treatments (Fig.1a0T0-a2T2). The round shape indicated the lack of protein bodies surrounding these granules compared with those reported in normal and waxy maize (Yu et al., 2015). Fig. 1a1T1 exhibited a thin membrane, revealing the protein structure in floury maize. Fig. 1a0T2 and a1T1 unveiled starch granules with many pores at the surface. Fig. 1a0T0 presented a few starch granules with some pores, and the others (a0T1, a1T0, a2T0, a2T1, and a2T2) appeared to have none. These pores could correspond to internal channels inherent to maize types (Gayral et al., 2016) and appear during toasting conditions (Zou et al., 2020). Except for a0T1 in swelling and a1T0 in raw condition, floury maize treatments contained starch granules with a few and many pores. These results demonstrated open pores at the surface of untoasted starch granules and pores exposed in floury maize types during toasting conditions. Fig. 1a0T2 and a1T2 evidenced starch granules connected and reduced in size attributed to some grade of melting caused by dry heat at the low moisture content (14 g/100 g). In sweet maize, starch granules did not present surface pores (a2T0, a2T1, and a2T2). However, the main feature was a central cavity or "donut-shaped starch" in Fig. 1a2T1 that could occur or enlarge due to the collapse of internal channels around the hilum by water vapor realized during toasting in a pan. Fig. 1a0T1, a2T0, a2T1, and a2T2 showed starch granules with an unsmoothed surface, in agreement with the SEM micrographs reported for semi-dented vitreous maize flour (Carrera et al., 2015). Toasting in a pan (T1) displayed more heterogeneous surfaces than microwave toasting (T2); swollen starch granules in a0T1, starch surface with pores in a1T1, and a central cavity surrounding the hilum in a2T1. It may indicate that the toasting effect in a pan varied with large (a0) and small (a1 and a2) maize kernel sizes.

Multimodal and unimodal particle size distributions display structural differences ascribed to starch granule size variation in flint and dent maize types (Gayral et al., 2016). In this study, the size distributions of starch granules predicted as Kernel density (R-squares from 92.16 to 98.74%) showed variation in maize types and changes in toasted kernels compared to the raw kernel condition (Fig. 2a-c). Raw and toasted treatments exhibited distribution curves with unimodal (one peak) shape, differentiated by the shift positions on the granule size axis due to the pan and microwave toasting. In Fig. 2a, the curves showed the changes that occurred in the starch granule size distribution, varying from a wide range (6 to 23 µm) for the floury maize a0T0, a0T1 treatments and a narrow range (4 to 14 µm) for a0T2 with a reduction in the granule size. All curves in Fig. 2b ranged between 6 to 19 µm with a decreasing granule size for a1T1 and a1T2. In Fig. 2c, the

distribution curves of sweet maize had the same trend observed for floury maize, but the range varied between 3 to 23 µm for a2T0 and a2T1 and 3 to 16 µm for a2T2. The shift positions by toasting effect were consistent with the weight distribution of pyrodextrin samples related to native starch (Li et al., 2020). The granule size distribution characterized as geometric mean diameter (GMD) also exhibited size variation associated with the study factors (Table 1). The GMD of the starch granules was statistically different ($P \leq 0.05$) between floury and sweet maize kernels and decreased due to the kernel microwave toasting effect. The GMD by treatment agreed with the x-axis intercept on the maximum value of Kernel density. The size reduction observed in the FEG-SEM micrographs a0T2, a1T2, and a2T2 was consistent with the significant decrease in starch granule GMD and the shift to the Kernel density curve toward smaller sizes. These findings implied a size reduction credited to the carbohydrates solubilized from starch granule during the whole kernel toasting (dry heat) and inherent to maize types with 14 g/100 g moisture content.

3.2. Crystalline structure

In Fig. 3a, the X-ray diffraction patterns of floury and sweet maize starches displayed the A-type crystalline structure for all maize flour treatments in agreement with those reported for normal maize starch treated by dry heating (Lei et al., 2020; Li et al., 2020; Zou et al., 2020). The diffractograms exhibited peaks positions at 2θ of 15°, 17°, 18°, 20°, and 23°, which were consistent with those described for normal, waxy, and super-sweet maize starch (Yu et al., 2015) in the native state. For all raw and toasted flour treatments, the peak positions at 2θ of 15°, 17°, 18°, 20°, and 23° corresponded to 5.9 ± 0.2, 5.2 ± 0.1, 4.9 ± 0.0, 4.4 ± 0.1, and 3.9 ± 0.1 Å diffraction spacings (d-spacing of the Bragg law), respectively. The peak intensity at 2θ of 20° (4.4 Å), detected in amylose standard (Vega-Rojas et al., 2016) and high amylose maize starch (Chen et al., 2019), augmented in sweet maize toasting treatments (a2T1 and a2T2) (Fig. 3a) and almost no varied in floury maize a0T1, a0T2, a1T1 and a1T2 (Fig. 3a and b). A broad peak at 2θ of 23° (3.9 Å), identified in amylopectin standard (Vega-Rojas et al., 2016) and waxy maize starch (Yu et al., 2015), was found in all maize treatments (Fig 3a) with reduced intensity peaks due to the toasting conditions induced by dry heat on maize kernels at the low moisture content (14 g/100 g). These findings evidenced that the peak of the amylose-lipid complex (4.4 Å) was a structural trait intrinsic to sweet maize kernels, subjected to pan and microwave toasting. On the other hand, the relationship between peak intensity and diffraction spacing indicated a partial loss of crystallite in starch granules, mainly ascribed to the double helices disaggregated from the amylopectin chains (Lei et al., 2020; Zou et al., 2020). Fig. 3b shows the diffraction intensities before and after toasting for the floury maize (a1) treatments with an initial moisture content of 14 g/100 g. The results revealed changes in diffraction intensity and a

remaining semicrystalline structure with crystallite sizes of 7.4 ± 0.1, 8.1 ± 0.3, and 7.8 ±0.1 nm, respectively, for the maize kernel treatments a1T0, a1T1, and a1T2.

Table 1. Mean comparison (Tukey's HSD test) by maize types and kernel conditions: responses of SEM, X-ray diffraction, Raman, ATR FTIR, and physicochemical properties in whole kernels reduced to flour

	Maize types (T0, T1, T2)			Kernel conditions (a0, a1, a2)		
Properties	**a0**	**a1**	**a2**	**T0**	**T1**	**T2**
SEM						
GMD (μm)	12.5 ± 2.1 b	12.5 ± 0.8 b	11.5 ± 1.4 a	13.2 ± 1.3 b	12.5 ± 2.1 b	10.7 ± 1.7 a
X-ray						
Ac	3959 ± 430 b	3577 ± 366 a	1295 ± 407 ⊄	4199 ± 327 b	3572 ± 427 a	3532 ± 130 a
Aa	5723 ± 593 a	6003±655 ab	6354 ± 782 b	5325 ± 463 a	6610 ± 561 b	6145 ± 394 b
RC (%)	40.9 ± 4.8 b	37.5 ± 4.8 a	17.2 ± 6.1 ⊄	44.7 ± 3.3 b	35.8 ± 4.3 a	37.1 ± 1.1 a
Cs (nm)	8.2 ± 0.5 a	7.8 ± 0.4 a	8.0 ± 0.7 a	7.8 ± 0.7 a	8.4 ± 0.4 b	7.7 ± 0.3 a
RAMAN						
FWHM480	21.0 ± 4.0 a	22.2 ± 5.8 a	20.0 ± 5.0 a	16.0 ± 1.0 a	19.9 ± 2.4 b	27.2 ± 1.0 c
RF-865/941	1.03 ± 0.12 b	0.96 ± 0.14 b	0.77 ± 0.21 a	1.07 ± 0.10 b	0.87 ± 0.08 a	0.83 ± 0.24 a
FTIR						
BI 994	0.70 ± 0.14 b	0.79 ± 0.12 b	0.50 ± 0.03 a	0.68 ± 0.20 a	0.62 ± 0.08 a	0.69 ± 0.20 a
BI 1017	0.62 ± 0.12 b	0.70 ± 0.11 b	0.46 ± 0.03 a	0.60 ± 0.16 a	0.55 ± 0.05 a	0.63 ± 0.18 a
BI 1151	0.24 ± 0.05 b	0.25 ± 0.04 b	0.19 ± 0.02 a	0.23 ± 0.06 a	0.21 ± 0.02 a	0.24 ± 0.05 a
BI 1454	0.18 ± 0.03 a	0.18 ± 0.03 a	0.20 ± 0.01 a	0.18 ± 0.03 a	0.17 ± 0.02 a	0.21 ± 0.02 b
BI 1646	0.28 ± 0.04 a	0.29 ± 0.05 a	0.23 ± 0.02 b	0.25 ± 0.03 a	0.26 ± 0.02 a	0.29 ± 0.02 b
BI 1745	0.25 ± 0.11 a	0.27 ± 0.09 a	0.35 ± 0.05 b	0.23 ± 0.05 a	0.25 ± 0.12 a	0.39 ± 0.05 b
BI 2854	0.48 ± 0.15 a	0.48 ± 0.17 a	0.64 ± 0.01 b	0.49 ± 0.13 a	0.45 ± 0.15 a	0.66 ± 0.03 b
BI 2923	0.76 ± 0.19 a	0.76 ± 0.21 a	1.00 ± 0.00 b	0.78 ± 0.18 a	0.73 ± 0.21 a	1.00 ± 0.00 b
BI 3298	0.99 ± 0.02 a	0.98 ± 0.03 a	0.85 ± 0.08 b	0.97 ± 0.07 b	0.95± 0.08 b	0.90 ± 0.10 a
R-1017/994	0.91 ± 0.02 a	0.91 ± 0.02 a	0.95 ± 0.02 b	0.92 ± 0.02 a	0.92 ± 0.02 a	0.94 ± 0.03 b
Physicochemical						
BV	11.8 ± 0.3 a	11.7 ± 1.3 a	12.3 ± 0.5 b	12.5 ± 0.4 c	12.1 ± 0.7 b	11.2 ± 0.8 a
$\bar{M}_n$ x 10^3	169 ± 16 a	174 ± 6 b	80 ± 22 ∉	181 ± 1 c	175 ± 4 b	158 ± 11 a
IV (mL/g)	250 ± 11 a	256 ± 9 b	214 ± 39 ∉	265 ± 5 c	252 ± 3 b	242 ± 6 a

Mean ± SD related to three replications for maize types n = (9) and kernel conditions n = (9). Floury maize a0 and a1. Sweet maize a2. Raw kernels T0. Toasted kernels in a pan T1. Microwave toasted kernels T2.
GMD: geometric mean diameter; **Ac**: crystalline pick area; **Aa**: amorphous pick area; **RC**: relative crystallinity; **Cs**: crystallite size; **FWHM**: full width at a half maximum of a Raman band; **RF**: the ratio between FWHM; R: the ratio between band intensities; **BI**: band intensity; **BV**: blue value; $\bar{M}_n$**:** Number average molecular weight (g/mol); **IV**: intrinsic viscosity.

By study factor, means with different letters in the same row indicated significant variation ($P \leq 0.05$). ⊄: level data no included because they cause no normal distribution. ∉ level data excluded; they do not follow the Mark-Houwink equation.

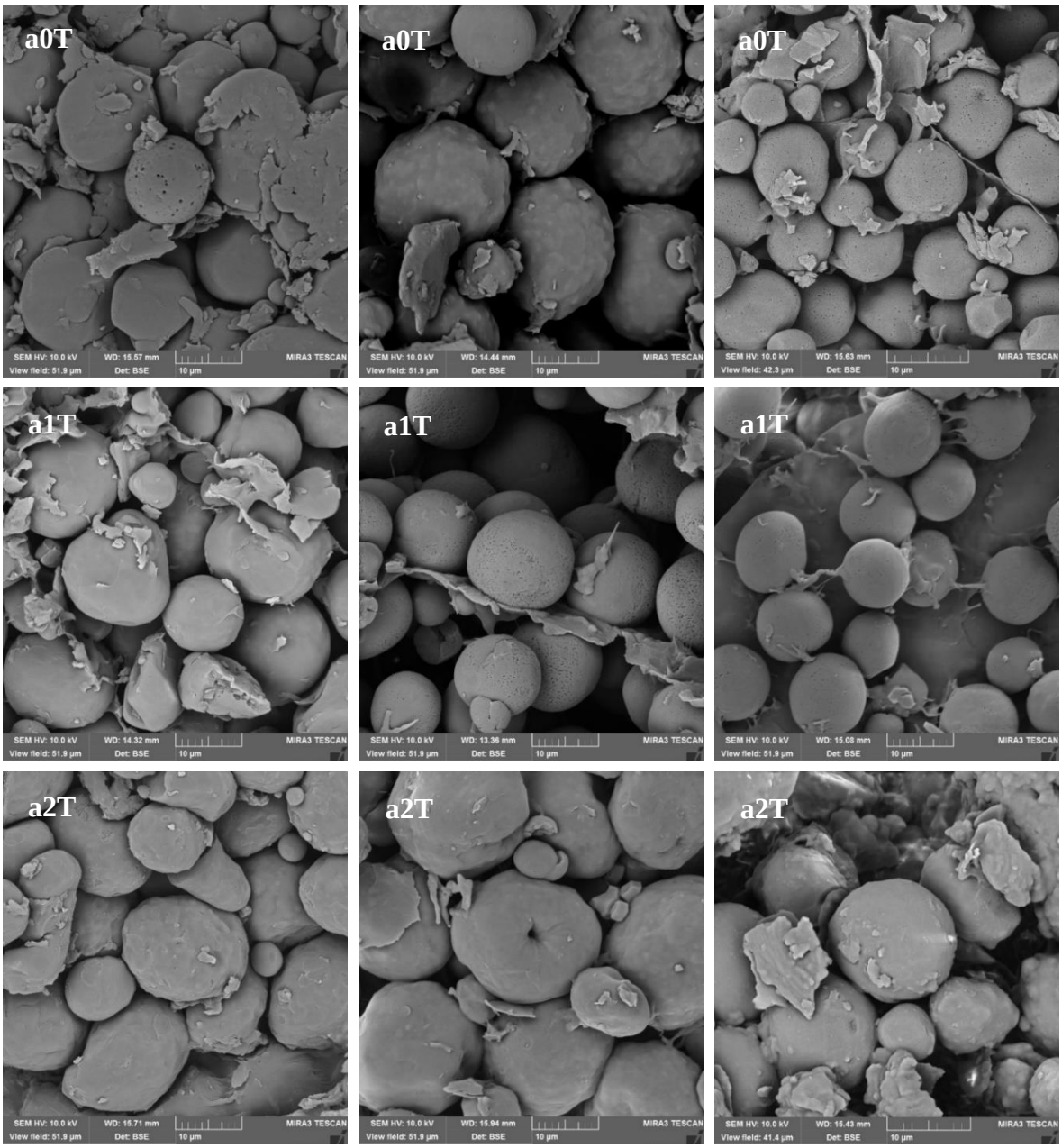

Figure 1. Endosperm fraction FEG SEM micrographs (10 µm) of floury (a0 and a1) and sweet (a2) maize kernels: raw (**a0T0, a1T0, a2T0**), toasted kernels in a pan (**a0T1, a1T1, a2T1**) and microwave toasted kernels (**a0T2, a1T2, and a2T2**).

According to the study factors (Table 1) and their treatments (Fig.3a), crystalline area (Ac), amorphous area (Mousaviraad & Tekeste), relative crystallinity (RC), and average crystallite size (Cs) exhibited significant variation ($P \leq 0.05$) by maize types (a0, a1, a2) and kernel conditions (T0, T1, T2). Ac and RC were different between floury maize (a0 and a1), and compared with sweet maize (a2), it had low values. Compared with the raw kernels (T0), an equal decreasing significance had Ac and RC by the effect of the pan (T1) and microwave (T2) toasting with variation coefficients

slightly higher than 10%. Aa was almost similar for maize types; however, there was a significant reduction due to pan (T1) and microwave (T2) toasting compared to the raw kernel condition (T0).

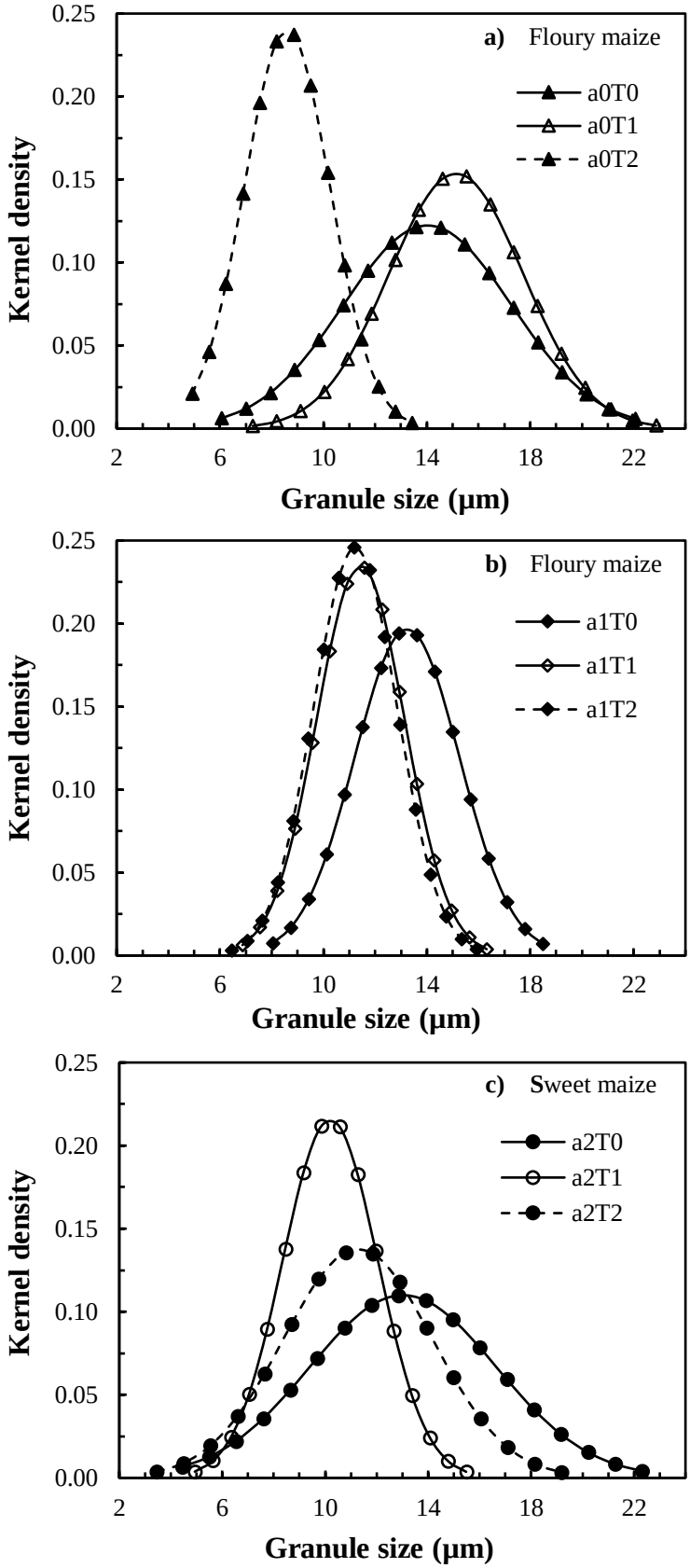

Figure 2. Size distribution of starch granules contained in floury endosperm fraction under conditions T0 (raw kernels), T1 (toasted kernels in a pan), and T2 (microwave toasted kernels). Kernel density distribution is also called density trace.

All floury maize treatments had higher relative crystallinity (Fig. 3a) than that determined for normal maize starches (Peng & Yao, 2018). The average crystallite size was similar for maize types, and its behavior against toasting processes indicated statistical significance by the effect of toasting in a pan (Table 1). It may be related to the Kernel density distribution reported in Fig 2a for floury maize treatment a0T1 in the swelling phase with GMD 14.91 ± 1.19 μm and Cs 8.4 ± 0.3 nm. The peak intensity, diffraction spacing, average Cs, and starch granule size distribution are still open for further research.

3.3. Vibrational measurements by Raman spectroscopy

Raman spectroscopy was a suitable technique for structural characterization of the floury (a0 and a1) and sweet (a2) maize kernels under the conditions: raw (T0), toasted in a pan (T1), and microwave toasting (T2). Samples of maize kernel treatment, all reduced to flour, were used to collect Raman signals in a full spectral range. According to the literature, the four spectral demarcated regions showed specific bands that correspond to the maize flour functional groups (i.e., Fig. 3c). Regions I (200 to 800 cm^{-1}) and III (1200 to 1500 cm^{-1}) are characterized by deformational vibrations of the CCO and CH / CH2 groups, respectively. Regions II (800 to 1200 cm^{-1}) and IV (2800 to 3050 cm^{-1}) are assigned to the stretching vibrations of molecular bonds of the C-O / C-C and CH / CH2 groups, respectively (Wiercigroch et al., 2017). In all spectra of maize treatments (a0T0, a0T1, a0T2, a1T0, a1T1, a1T2, a2T0, a2T1 and a2T2), the relevant bands were in the ranges of 477-484 cm^{-1}, 864-865 cm^{-1}, 941-942 cm^{-1}, 1082-1090 cm^{-1}, 1338-1340 cm^{-1}, 1462-1465 cm^{-1}, and 2902-2909 cm^{-1}. The band between 477-484 cm^{-1} attributed to the glucopyranose ring skeletal vibration is an intense marker in the glycogen, amylose, and amylopectin Raman spectra (Wiercigroch et al., 2017). The full width at half maximum (FWHM) of this band (477-484 cm^{-1}) is often used to characterize the short-range order of starch (Chen et al., 2019). The FWHM480 values obtained from maize treatment spectra showed non-significant ($P \geq 0.05$) variation among maize types and agreed with crystallite size determined by X-ray diffraction. However, the FWHM480 values for raw kernels and toasted using a pan and microwave varied significantly ($P \leq 0.05$) (Table 1), reflecting the toasting effect on the crystalline structure of starch granules. The band at 864-865 cm^{-1} is assigned to symmetric C-O-C stretching/ring breathing and is sensitive to molecular starch structure orientation. The band at 941-942 cm^{-1} is assigned to symmetric C-O-C stretching of α-1-6 linkages related to amylopectin (Gayral et al., 2016). Raman intensity varies directly with the crystalline region size (Liu et al., 2015), and the band intensity ratio (865/941) is a marker of starch crystallinity sensitive to its molecular orientation (Gayral et al., 2016). In this study, the band intensity ratio 865/941 presented a non-significant difference among maize types and kernel conditions, suggesting a non-significant change in the orientation of crystallites within the starch granules. However, the FWHM ratio 865/941

revealed differences ($P \leq 0.05$) between floury and sweet maize, as well as between raw and toasted kernels in agreeing with the results of GMD, crystalline area, relative crystallinity, and ATR FTIR band intensities at 994, 1017 and 1151 cm^{-1} (Table 1). The FWHM ratio 865/941 was more sensitive than the band intensity ratio (865/941) to detect the molecular orientation at nanocrystal levels (7.4 ± 0.1 – 8.6 ± 0.4 nm) within the starch granules.

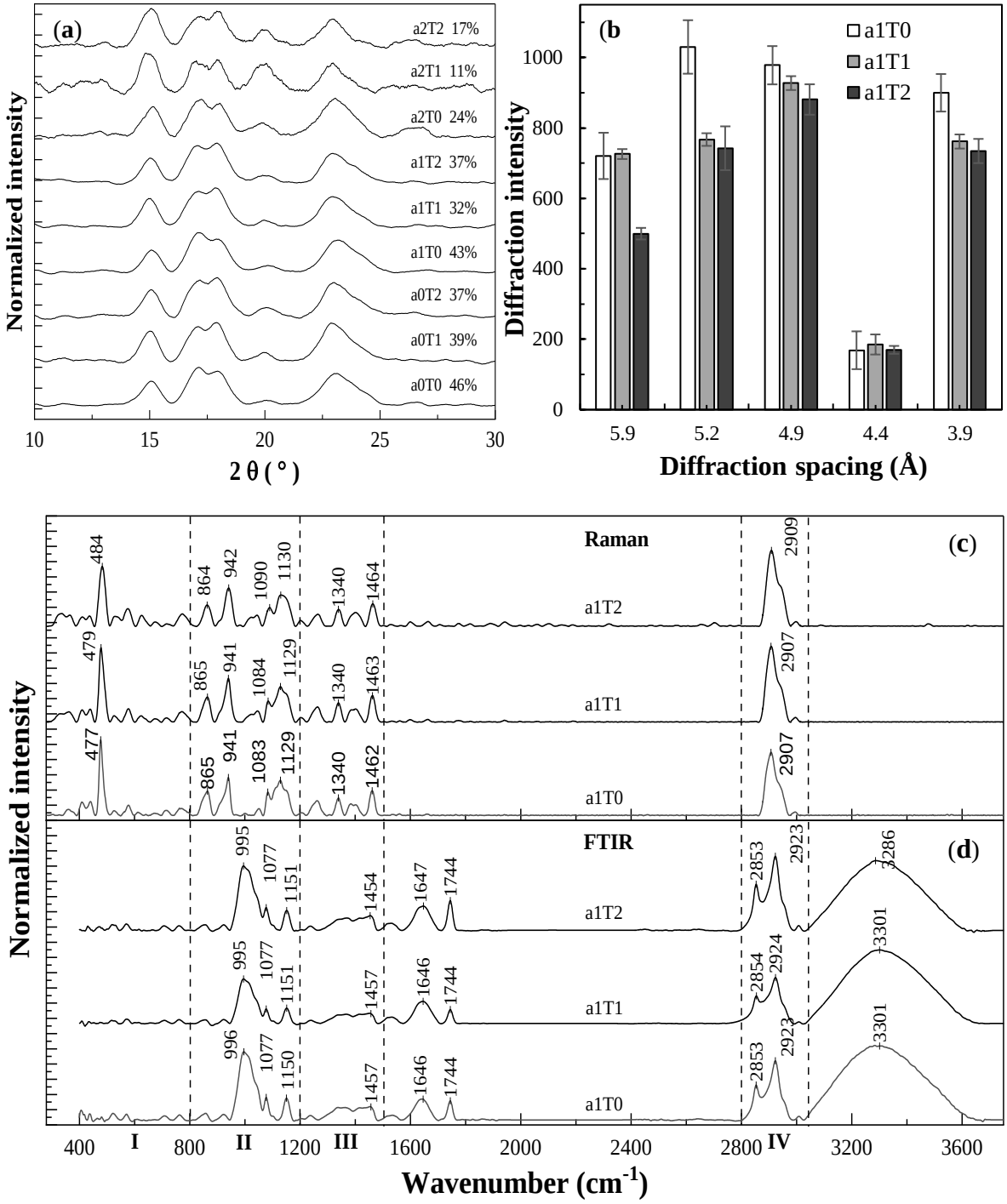

Figure 3. X-ray diffraction patterns of all treatments (**a**), an example of the effect of kernel conditions on X-ray diffraction intensity related to intermolecular spacing in floury maize (**b**), and an example of kernel conditions on Raman (**c**), and ATR FTIR (**d**) spectra of floury maize.

3.4. Vibrational measurements by Fourier transform infrared (FTIR) spectroscopy

FTIR and Raman are complementary techniques. Hence spectral bands obtained by attenuation total reflection Fourier transform infrared (ATR FTIR) were demarcated within four functional group regions (Wiercigroch et al., 2017). According to recent studies (Achten et al., 2019), the ATR-FTIR spectra of maize flour displayed different regions for carbohydrates, proteins, and lipids. Fig. 3d exhibits the spectra of the a1T0, a1T1, and a1T2 maize treatments with bands related to a specific molecular vibration acquired in the 400 to 3750 cm^{-1} range. ATR FTIR spectra of all maize treatments showed bands in the 990-996, 1074-1077, 1150-1152, 1450-1458, 1640-1648, 1744-1745, 2853-2855, 2923-2924 and 3288-3319 cm^{-1} ranges. The fingerprint region from 990 to 1152 cm^{-1} had hidden bands related to carbohydrate structures (Chen et al., 2019). The bands around 1643 cm^{-1} indicated the secondary structure of proteins (Achten et al., 2019). The bands at 1744-1745 cm^{-1} corresponded to vibration signals assigned to the C=O stretching of fatty acid esters (Achten et al., 2019). Raw sweet maize spectra exhibited an additional minimum band at 1709 cm^{-1} associated with free fatty acids that disappeared by the toasting effect. This band is distinctive in the maize oil extract spectrum (Achten et al., 2019), and the band at 1709 cm^{-1} is undetectable in floury maize treatments. The bands from 2853 to 2924 cm^{-1} attributed to C–H stretching vibrations were generated by asymmetric and symmetric stretching vibrations of methylene and methyl groups (Achten et al., 2019). The bands from 3288 to 3319 cm^{-1} showed a broad vibrational signal related to hydroxylic groups from carbohydrates, amide structures, or moisture in the sample (Achten et al., 2019). A band at 3295 cm^{-1} detected in sweet maize spectra agreed with a similar O-H band in the FT-IR spectra of phytoglycogen nanoparticles from sugary-1 maize (Xue et al., 2019).

Figs 4a-c showed some primary band intensities for all maize flour treatments, and Table 1 indicates most of them with significant combined effect ($P \leq 0.05$) by study factors. Floury maize displayed high ATR FTIR band intensities in 994 to 1151 cm^{-1} and low from 1646 to 3298 cm^{-1} compared with sweet maize. Microwave toasting exhibited higher (1454 – 2924 cm^{-1}) and lower (3298 cm^{-1}) ATR FTIR band intensities than those for raw kernel and toasted in a pan. The band intensity at 994, 1017, and 1047 cm^{-1} is sensitive to changes in starch conformation, so the band intensity ratio 1047/1017 reflects the grade of order, and the band intensity ratio 1017/994 indicates the ratio of amorphous to an ordered structure of the starch (Cai et al., 2014; Chen et al., 2019). In this study, the band intensity ratio at 1047/1017 showed a non-significant ($P \geq 0.05$) variation among all maize treatments with a mean value of 0.56 ± 0.05, like those estimated for normal and waxy maize starches (Sui et al., 2015). The band intensity ratio at 1017/994 significantly ranged from 0.91 ± 0.02 to 0.95 ±0.02 (Table 1). The results of both rates were consistent with those reported for native starch of normal maize (Cai

et al., 2014), super-sweet maize (Yu et al., 2015) and were slightly different from those corresponding to native starch of waxy, normal, and high amylose maize (Chen et al., 2019).

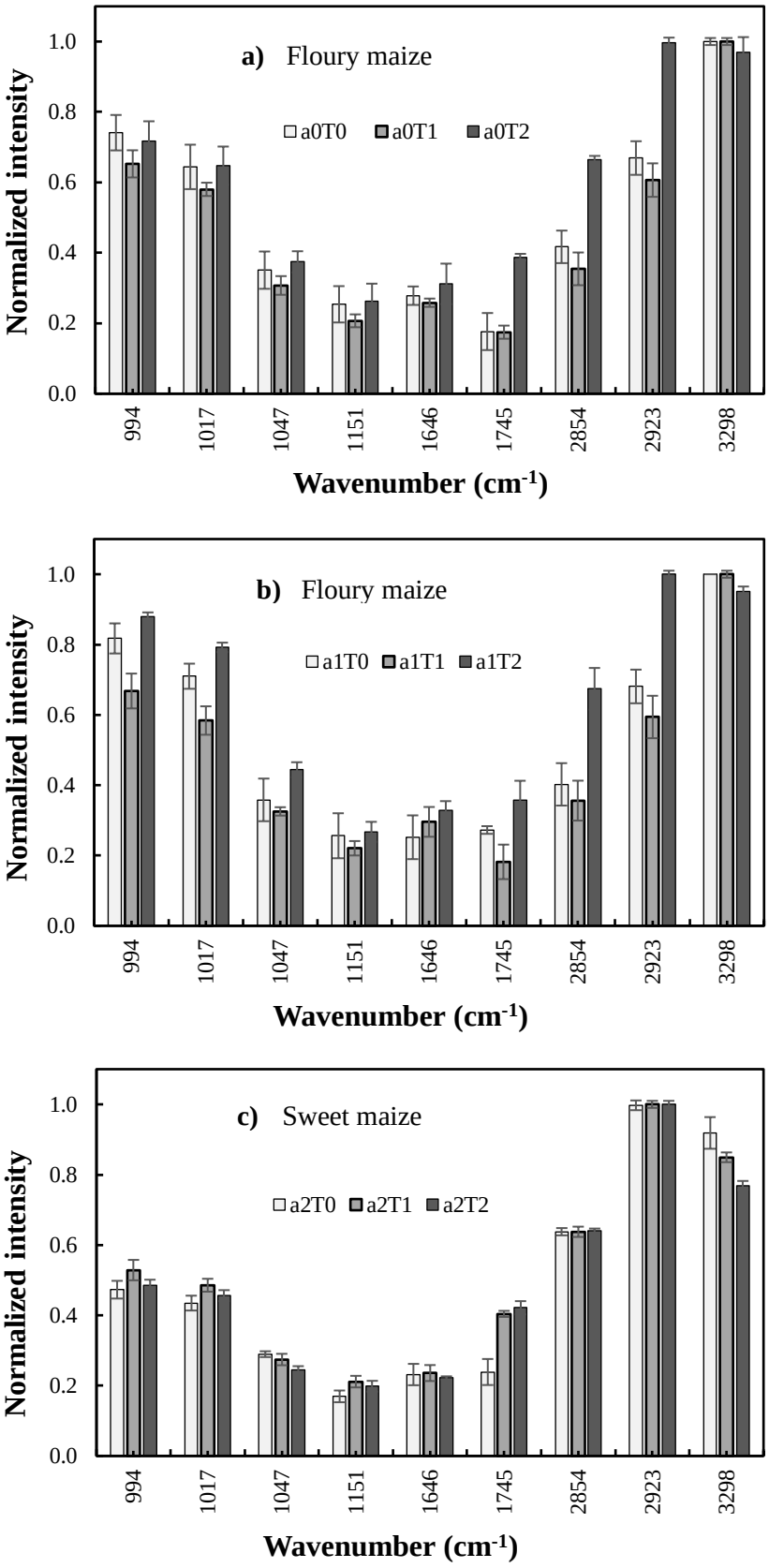

Figure 4. ATR FTIR band intensities of maize treatment spectra. Raw kernels (T0), the toasted kernel in a pan (T1), and microwave toasting kernels (T2).

3.5. Starch content and Blue value (BV)

The starch content in floury maize was higher than that in sweet maize. This variation was consistent with that reported between normal and super-sweet maize (Yu et al., 2015). The starch content in floury toasted kernels was lower than that initial content in raw maize kernels, i.e., it varied from 65 ± 1 g/100 g in raw (a0T0) to 56 ± 3 g/100 g in toasted in a pan (a0T1) and 55 ± 1 g/100 in toasted with microwaves (a0T2). Therefore, the starch content of each treatment was used to determine the corresponding BV for mean comparison (Table 1), the number average molecular weight $\bar{M}_n$ and intrinsic viscosity [η] (Fig. 4a).

The blue color developed and measured as the absorbance at 620 nm generated readings ranged from 0.376 ± 0.005 to 0.556 ± 0.003. These readings related to the sample starch content free of soluble solids gave a BV range from 10.21 ± 0.21 to 13.03 ± 0.07. The BVs reported by the effect of the study factors in Table 1 allowed the differentiation between floury and sweet maize. This behavior was consistent with those presented for the geometric mean diameter (GMD) of starch granules, crystalline area (Ac), relative crystallinity (RC), Raman FWMH ratio (RF-865/941), ATR FTIR band intensities, and ATR FTIR intensity ratio (R-1017/994), all of them with significantly lower or higher means for floury maize compared to sweet maize. According to kernel conditions, raw kernels (T0) had the highest BV, toasted in a pan (T1) an intermediate, and microwave toasting kernels (T2) the lowest. This decreasing influence of the kernel conditions on the BV agreed with the increasing effect on the FWHM 480 cm^{-1} (Table 1). The BVs obtained for raw kernels, considering absorbance readings, agreed with those reported for floury endosperm flours from different maize types (Zhang & Xu, 2019). A significant difference in the BV implied that the blue-colored complex varied with amylose and amylopectin chain length (Minakawa et al., 2019; Zhang & Xu, 2019).

3.6. Number average of molecular weight ($\bar{M}_n$)

Raw kernel treatments a0T0 and a1T0 showed a $\bar{M}_n$ of 180 ± 1 x 10^3 g/mol, while a2T0 had an $\bar{M}_n$ of 52 ± 1 x 10^3 g/mol. The $\bar{M}_n$ obtained for floury maize raw kernels was higher than that (120 x 10^3 g/mol) reported for normal maize native starch (Singh & Ali, 2008). The toasted kernels with microwave (a0T2, a1T2, and a2T2) showed $\bar{M}_n$ of 148 ± 1 x 10^3, 168 ± 1 x 10^3 and 92 ± 2 x 10^3 g/mol compared to toasted kernels in a pan (a0T1, a1T1, a2T1) with $\bar{M}_n$ of 177 ± 4 x 10^3, 173 ± 4 x 10^3 and 96 ± 1 x 10^3 g/mol, respectively. These results determined for a0T1 and a1T1 were slightly lower than the molecular size maximum (180 x 10^3 g/mol) reported for pyrodextrins prepared by heating waxy maize starch (Han et al., 2018). In floury maize (a0 and a2) treatments, the decreasing $\bar{M}_n$ due to kernel toasting revealed conformational changes according to the Mark-Houwink equation

(Kowalski et al., 2018) used to characterize polymer structure. In sweet maize (a2) toasted treatments, the increase in $\bar{M}_n$ inferred an increase mass of chain segments, increase in molecular density, and decrease in viscosity. This hypothesis agreed with the unique structural properties associated with phytoglycogen contained in sugary-1 mutants from native sweet maize; a nanoparticulated natural carbohydrate with 2% more α-1,6- glucosidic linkage than amylopectin, with high water retention, low viscosity and high stability in water (Xue et al., 2019). However, further investigation is needed to understand the results in sweet maize kernels subjected to pan and microwave toasting. Therefore, Fig. 5a shows the $\bar{M}_n$ changes in floury maize kernels, following Mark-Houwink polymeric conformation. Table 1 displays the statistical mean comparisons for floury maize types and the average value between raw and toasted conditions (T0, T1, T2) for sweet maize in the blocking column a2, excluding sweet maize results of statistical analyses. Consequently, under the significant effect ($P \leq 0.05$) of the study factors, floury maize types (a0 and a1) were different in the $\bar{M}_n$. Relative to kernel conditions (T0, T1 and T2), the $\bar{M}_n$ highest mean value was for raw kernels and the lowest for microwave toasted.

3.7. Intrinsic viscosity [η]

The [η] decreased from 263 ± 1 (a0T0), 267 ± 7 (a1T0) and 264 ± 1 (T2T0) mL/g in raw maize kernels to 251 ± 4 (a0T1), 253 ± 1 (a1T1) and 173 ± 2 (a2T1) mL/g in toasted kernel in a pan and to 238 ± 2 (a0T2), 247 ± 1 (a1T2) and 205 ± 4 (a2T2) mL/g in maize kernel subjected to microwave toasting. The rheological variation revealed structural or conformational changes by the toasting conditions effect. The results in floury maize were consistent with the $\bar{M}_n$ (Fig. 5a). The [η] determined for raw maize kernels (Fig. 5a), based on the starch concentration, was higher than that (175 ± 5 mL/g) for untreated waxy wheat integral flour (Kowalski et al., 2018), that (178 mL/g) obtained for normal maize native starch (Singh & Ali, 2008) and those reported for maize amylose (123.94 ± 0.62 mL/g), and amylopectin (162.56 ± 1.20) standards (Yu et al., 2014). In sweet maize, intrinsic viscosity decreased while the $\bar{M}_n$ increased. These results do not follow the Mark-Houwink equation because floury and sweet maize are two highly contrasted in starch and endosperm structure. Sweet maize also showed a water-soluble index very high in agreement with its total and reducing sugar content in Fig 5b. It may be associated with phytoglycogen nanoparticles with unusual natural properties related to high water retention, low viscosity, and high stability in water (Xue et al., 2019). Excluding sweet maize data, the statistical comparison for floury maize (a0 and a1) and kernel conditions displayed equivalents significant differences for $\bar{M}_n$ and [η] (Table 1). On the other hand, the average datum for sweet maize (a2) was the lowest value in agreement with those of GMD, Ac, RC, RF-865/941, BI-994, BI-1017, BI-1151 and $\bar{M}_n$.

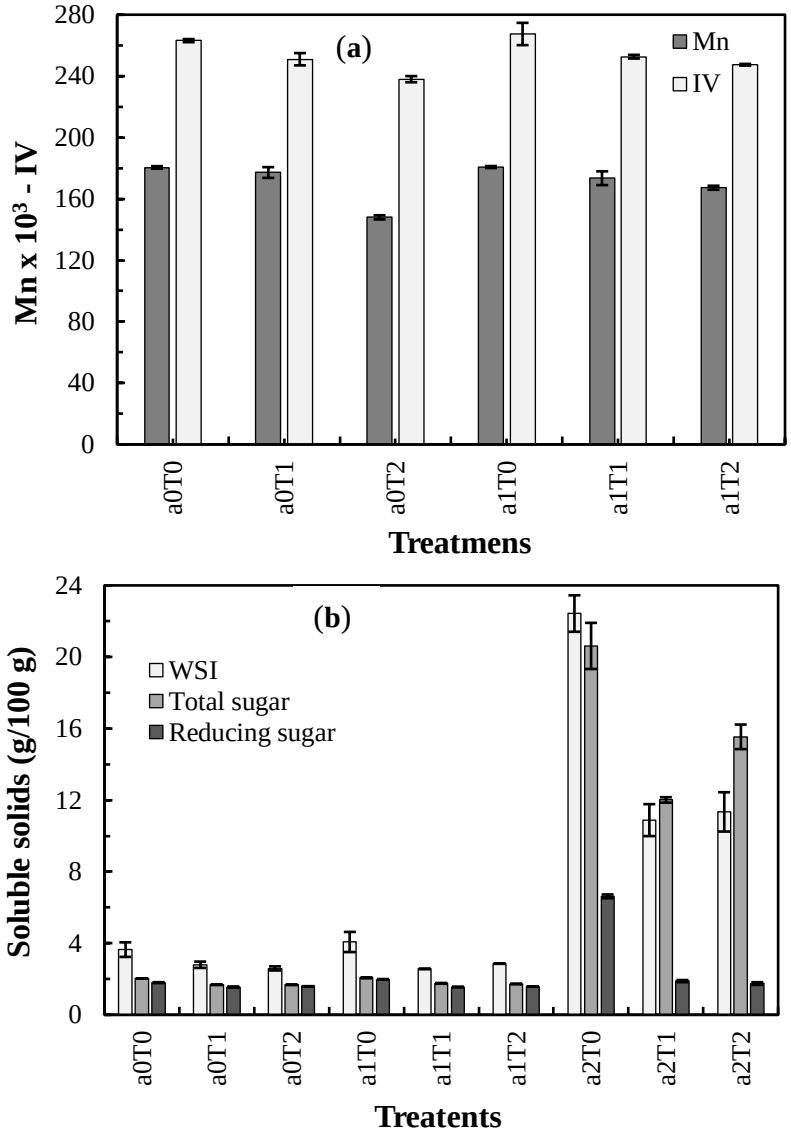

Fig. 5. Number average molecular weight ($\bar{M}_n$, g/mol) and intrinsic viscosity (IV, mL/g) (**a**) of floury maize types (a0 and a1), water-soluble index (WSI), total and reducing sugars (**b**) of floury (a0 and a1), and sweet (a2) maize types under the kernel conditions: raw (T0), toasted in a pan (T1) and microwave toasting (T2).

3.8. Water-soluble index, total soluble sugar, and reducing sugar

WSI, expressed as soluble solids, is presented together with the total and reducing sugars in Fig. 5b. The WSI and total sugar displayed a considerable difference between sweet and floury maize with decreasing ranges from 22.43 ± 1.02 to 11.34 ± 1.1 g/100 g and from 4.07 ± 0.56 to 1.67 ± 0.01 g/100 g, respectively, reflecting the action of toasting processes as compared to raw kernels. The finding on floury maize WSI was equivalent to that determined at 25 °C for maize flour obtained from whole kernel samples treated with NIR lamp heating (Deepa & Hebbar, 2017). Moreover, WSI and total sugar reduction may depend on the free sugar drop ascribed to Maillard metabolite formations in toasted maize kernels at high temperatures (Woo et al., 2018; Youn & Chung, 2012). The high WSI in sweet maize may be associated with the accumulation of phytoglycogen detected in sugary-1 mutants (Xue et al., 2019). Reducing sugar was high for a2T0, and there was also a decreasing variation by the effect of the toasting methods. These findings could demonstrate that the vitreous

fraction in sweet maize mainly contained water-soluble carbohydrates, and a reduced fraction of floury endosperm consisted of starch.

4. Conclusion

The findings of this study, obtained by different techniques, disclosed structural variations in floury and sweet maize kernels inherent to their specialty maize types (*Zea mays* var *amylacea* and var *saccharate*). The whole maize kernels subjected to pan a microwave toasting presented partially modified crystalline structures, remaining nanocrystals with average size from 7 to 9 nm, and vibrational functional groups ascribed to carbohydrates, proteins, and lipids. Microwave treatments showed the lowest values for starch granule size, BV, number average molecular weight, intrinsic viscosity, and less ordered crystalline structures. After toasting treatments by pan and microwave toasting (dry heating at 14 g/100 g moisture content), floury maize displayed endosperm with starch granules partially modified, whereas sweet maize mainly implied a sugary-vitreous fraction. Both ready-to-eat Andean maize.

Funding statement

The author carried out this work within the DOCT-DI-2019-49 Project framework with the institutional sponsor of the Universidad Central del Ecuador.

Data availability statement

Data is available on request.

Conflict of interest

The authors declare no conflict of interest.

Acknowledgments

This work was supported by the Research Program of the Universidad Central del Ecuador. The authors would like to thank the Research Laboratories of the Escuela Politécnica Nacional, Universidad Central del Ecuador, Universidad de las Fuerzas Armadas, and Estación Experimental Santa Catalina for supporting this study.

References

Achten, E., Schütz, D., Fischer, M., Fauhl-Hassek, C., Riedl, J., & Horn, B. (2019). Classification of grain maize (*Zea mays* L.) from different geographical origins with FTIR spectroscopy - A suitable analytical tool for feed authentication? *Food Analytical Methods*, *12*(10), 2172-2184. https://doi.org/10.1007/s12161-019-01558-9

Cai, C., Lin, L., Man, J., Zhao, L., Wang, Z., & Wei, C. (2014). Different structural properties of high-amylose maize starch fractions varying in granule size. *Journal of Agricultural and Food Chemistry*, *62*(48), 11711-11721. https://doi.org/10.1021/jf503865e

Carrera, Y., Utrilla-Coello, R., Bello-Pérez, A., Alvarez-Ramirez, J., & Vernon-Carter, E. J. (2015). In vitro digestibility, crystallinity, rheological, thermal, particle size and morphological characteristics of pinole, a traditional energy food obtained from toasted ground maize. *Carbohydrate Polymers*, *123*, 246-255. https://doi.org/10.1016/j.carbpol.2015.01.044

Chen, L., McClements, D. J., Zhang, H., Zhang, Z., Jin, Z., & Tian, Y. (2019). Impact of amylose content on structural changes and oil absorption of fried maize starches. *Food Chemistry*, *287*, 28-37. https://doi.org/10.1016/j.foodchem.2019.02.083

Deepa, C., & Hebbar, H. U. (2017). Influence of micronization on physicochemical properties of maize grains. *Starch - Stärke*, *69*(3-4), 1600060. https://doi.org/10.1002/star.201600060

Dubois, M., Gilles, K. A., Hamilton, J. K., Rebers, P. A., & Smith, F. (1956). Colorimetric method for determination of sugars and related substances. *Analytical Chemistry*, *28*(3), 350-356.

Gayral, M., Gaillard, C., Bakan, B., Dalgalarrondo, M., Elmorjani, K., Delluc, C., Brunet, S., Linossier, L., Morel, M. H., & Marion, D. (2016). Transition from vitreous to floury endosperm in maize (*Zea mays* L.) kernels is related to protein and starch gradients. *Journal of Cereal Science*, *68*, 148-154. https://doi.org/10.1016/j.jcs.2016.01.013

Han, X., Kang, J., Bai, Y., Xue, M., & Shi, Y.-C. (2018). Structure of pyrodextrin in relation to its retrogradation properties. *Food Chemistry*, *242*, 169-173. https://doi.org/10.1016/j.foodchem.2017.09.015

Kowalski, R. J., Hause, J. P., Joyner, H., & Ganjyal, G. M. (2018). Waxy flour degradation - Impact of screw geometry and specific mechanical energy in a co-rotating twin screw extruder. *Food Chemistry*, *239*, 688-696. https://doi.org/10.1016/j.foodchem.2017.06.120

Lara, N., & Ruales, J. (2002). Popping of amaranth grain (*Amaranthus caudatus*) and its effect on the functional, nutritional and sensory properties. *Journal of the Science of Food and Agriculture*, *82*(8), 797-805.

Leach, H. W. (1963). Determination of intrinsic viscosity of starches. *Cereal Chemistry*, *40*(6), 593-600.

Lei, N., Chai, S., Xu, M., Ji, J., Mao, H., Yan, S., Gao, Y., Li, H., Wang, J., & Sun, B. (2020). Effect of dry heating treatment on multi-levels of structure and physicochemical properties of maize starch: A thermodynamic study. *International Journal of Biological Macromolecules*, *147*, 109-116. https://doi.org/10.1016/j.ijbiomac.2020.01.060

Li, H., Ji, J., Yang, L., Lei, N., Wang, J., & Sun, B. (2020). Structural and physicochemical property changes during pyroconversion of native maize starch. *Carbohydrate Polymers*, *245*, 116560. https://doi.org/10.1016/j.carbpol.2020.116560

Liu, Y., Xu, Y., Yan, Y., Hu, D., Yang, L., & Shen, R. (2015). Application of Raman spectroscopy in structure analysis and crystallinity calculation of corn starch. *Starch - Stärke*, *67*(7-8), 612-619. https://doi.org/10.1002/star.201400246

Minakawa, A. F. K., Faria-Tischer, P. C. S., & Mali, S. (2019). Simple ultrasound method to obtain starch micro-and nanoparticles from cassava, corn and yam starches. *Food Chemistry*, *283*, 11-18. https://doi.org/10.1016/j.foodchem.2019.01.015

Mousaviraad, M., & Tekeste, M. Z. (2020). Effect of grain moisture content on physical, mechanical, and bulk dynamic behaviour of maize. *Biosystems Engineering*, *195*, 186-197. https://doi.org/10.1016/j.biosystemseng.2020.04.012

Peng, X., & Yao, Y. (2018). Small-granule starches from sweet corn and cow cockle: Physical properties and amylopectin branching pattern. *Food Hydrocolloids*, *74*, 349-357. https://doi.org/10.1016/j.foodhyd.2017.08.025

Raigar, R. K., & Mishra, H. N. (2018). Study on the effect of pilot scale roasting conditions on the physicochemical and functional properties of maize flour (Cv. *Bio 22027*). *Journal of Food Processing and Preservation*, *42*(5), e13602. https://doi.org/10.1111/jfpp.13602

Salvador-Reyes, R., & Clerici, M. T. P. S. (2020). Peruvian Andean maize: General characteristics, nutritional properties, bioactive compounds, and culinary uses. *Food Research International*, *130*, 108934. https://doi.org/10.1016/j.foodres.2019.108934

Samotus, B., Tuz, J., & Doerre, E. (1993). Evaluation of blue value in different plant materials as a tool for rapid starch determination. *Acta Societatis Botanicorum Poloniae*, *62*(3-4), 137-141.

Singh, V., & Ali, S. Z. (2008). Properties of starches modified by different acids. *International Journal of Food Properties*, *11*(3), 495-507. https://doi.org/10.1080/10942910802083774

Sui, Z., Yao, T., Zhao, Y., Ye, X., Kong, X., & Ai, L. (2015). Effects of heat-moisture treatment reaction conditions on the physicochemical and structural properties of maize starch: Moisture and length of heating. *Food Chemistry*, *173*, 1125-1132. https://doi.org/10.1016/j.foodchem.2014.11.021

Vega-Rojas, L. J., Contreras-Padilla, M., Rincon-Londoño, N., Del Real-López, A., Lima-Garcia, R. M., Palacios-Rojas, N., & Rodriguez-Garcia, M. E. (2016). The effect of maize grain size on the physicochemical properties of isolated starch, crude maize flour and nixtamalized maize flours. *Agricultural Sciences*, *07*(02), 114-125. https://doi.org/10.4236/as.2016.72011

Wiercigroch, E., Szafraniec, E., Czamara, K., Pacia, M. Z., Majzner, K., Kochan, K., Kaczor, A., Baranska, M., & Malek, K. (2017). Raman and infrared spectroscopy of carbohydrates: A review. *Spectrochimica Acta A: Molecular and Biomolecular Spectroscopy*, *185*, 317-335. https://doi.org/10.1016/j.saa.2017.05.045

Woo, K. S., Kim, M. J., Kim, H.-J., Lee, J. H., Lee, B. W., Jung, G. H., Lee, B. K., & Kim, S. L. (2018). Changes in the functional components and radical scavenging activity of maize under various roasting conditions. *Food Science and Biotechnology*, *27*(3), 837-845. https://doi.org/10.1007/s10068-017-0294-9

Xue, J., Inzero, J., Hu, Q., Wang, T., & Wusigale, Y. L. (2019). Development of easy, simple and low-cost preparation of highly purified phytoglycogen nanoparticles from corn. *Food Hydrocolloids*, *95*, 256-261. https://doi.org/10.1016/j.foodhyd.2019.04.041

Youn, K.-S., & Chung, H.-S. (2012). Optimization of the roasting temperature and time for preparation of coffee-like maize beverage using the response surface methodology. *LWT - Food Science and Technology*, *46*(1), 305-310. https://doi.org/10.1016/j.lwt.2011.09.014

Yu, S., Xu, J., Zhang, Y., & Kopparapu, N. K. (2014). Relationship between intrinsic viscosity, thermal, and retrogradation properties of amylose and amylopectin. *Czech Journal of Food Sciences*, *32*(5), 514–520.

Yu, X., Yu, H., Zhang, J., Shao, S., Xiong, F., & Wang, Z. (2015). Endosperm structure and physicochemical properties of starches from normal, waxy and super-sweet maize. *International Journal of Food Properties*, *18*(12), 2825-2839. https://doi.org/10.1080/10942912.2015.1015732

Zhang, H., & Xu, G. (2019). Physicochemical properties of vitreous and floury endosperm flours in maize. *Food Science & Nutrition*, *7*(8), 2605-2612. https://doi.org/10.1002/fsn3.1114

Zou, J., Xu, M., Tang, W., Wen, L., & Yang, B. (2020). Modification of structural, physicochemical and digestive properties of normal maize starch by thermal treatment. *Food Chemistry*, *309*, 125733. https://doi.org/10.1016/j.foodchem.2019.125733

Chapter 3

Physical and hydration properties of specialty floury and sweet maize kernels subjected to pan and microwave toasting.

Nelly Lara[a,b1], Jenny Ruales[a]

[a] Departamento de Ciencia de Alimentos y Biotecnología, Escuela Politécnica Nacional, Av. Ladrón de Guevara E11-253 Edificio 19 Quito, Ecuador

[b] CADET, Facultad de Ciencias Agrícolas, Universidad Central del Ecuador, Calle Universitaria s/n, Tumbaco, Ecuador

ABSTRACT

The three main underutilized maize types from the Andean region have specialty floury and sweet kernels to make entire ready-to-eat maize by toasting in a pan until a golden-brown surface color. The study aims to characterize these maize kernels before and after pan and microwave toasting. The initial moisture content for the raw kernel condition was the same (14.06 ± 0.13 g/100 g) to ensure data reliability by maize types and toasting conditions. The toasting conditions generated kernel expansions studied through the geometric, gravimetric, surface color, instrumental texture, milling average particle size, and hydration properties. Innate to maize types, the color properties (L*, a*, b*, C*, h*, and ΔE*) demonstrated that the toasted kernels developed a comparable range of surface color by the effect of pan and microwave toasting conditions ($P \geq 0.05$). Large kernel sizes, low kernel hardness, and small average particle size ascribed to the endosperm softness were the main properties that characterize floury maize. High color differences, high water-soluble index, low density, high kernel hardness, and large average particle size confirmed the sugary-vitreous fraction in sweet maize. Microwave toasting produced lower remaining moisture content and kernel density, larger kernel size associated with the internal porosity created during toasting, higher water absorption capacity, and swelling power than pan toasting.

Keywords: Floury maize, microwave toasting, kernel volume, internal porosity, color space, cutting force

[1] Corresponding author: Nelly Lara, CADET, Facultad de Ciencias Agrícolas, Universidad Central del Ecuador, Calle Universitaria s/n, Tumbaco, Ecuador. E-mail: nvlara@uce.edu.ec

1. Introduction

Around the world, toasting is a traditional technique that uses dry heating to develop acceptable attributes (Schoeman et al., 2017) and color (Chung et al., 2014) in maize kernels for food products. Yellow flint type (*Zea mays* var *indurate*) and Korean hybrids toasted by conventional techniques are the base for maize beverages with desired qualities of coffee-like drinks (Youn & Chung, 2012) and nutraceutical extracts (Woo et al., 2018). Popular semi-dent maize kernels (Cv. *Bio 22027*) submitted to electric toasters and reduced to flours are integral ingredients for many food processing applications (Raigar & Mishra, 2018) in India. Vitreous white and blue maize kernels toasted in a pan and ground is a traditional energy food usually consumed by different ethnic groups of Northern Mexico and Southwest USA (Carrera et al., 2015). While floury (*Zea mays* L. var. *amylacea*) and sweet maize types (*Zea mays* L. var. *saccharata*) highly contrasted in starch and endosperm structure have specialty kernels for toasting in a pan and making entire ready-to-eat maize that remain underutilized in the Andean region (Lara et al., 2021). Information on the physical and hydration properties relative to raw and toasted kernels for these floury and sweet maize types is limited. Recent studies reveal relevant properties in raw kernels of the five main Peruvian maize cultivars (Salvador-Reyes et al., 2021) and microstructural changes in floury and sweet maize kernels by pan and microwave toasting (Lara et al., 2021).

In contrast, geometric and gravimetric properties are potential indicators of wet-milling (Uriarte-Aceves et al., 2020; Uriarte-Aceves et al., 2019) and dry-milling quality (Guelpa et al., 2015; Guelpa et al., 2016) in common maize types. Also, maize types with low protein content would be suitable for wet-milling with high starch yields (Uriarte-Aceves et al., 2019). In toasted common maize types, the volumetric increase reveals an internal porosity attributed to cavities created during toasting (Schoeman et al., 2017) that produce changes in texture (Raigar & Mishra, 2018), color (Chung et al., 2014), and hydration properties (Deepa & Hebbar, 2017; Raigar & Mishra, 2018). In addition, based on the interest in super soft wheat (Delwiche et al., 2020), raw and toasted floury maize kernels can be promising intermediate products for future applications.

On the other hand, achieving toasted maize kernels with the characteristic golden brown surface color and easy to chew can take 20 to 25 minutes using pan toasting. At the same time, microwave heating seems to be a prospective innovation in maize kernel toasting with some advantages over a pan toaster (Lara et al., 2021). Furthermore, vitreous maize kernels dried by microwave improve the dry milling quality (Velu et al., 2006), sorghum kernel treated by microwave and reduced to flour can contribute to the functional bakery products (Sharanagat et al., 2019) and inhibits the lipases for stabilizing sorghum flour (Adebowale et al., 2020).

The behavior of floury and sweet maize types with specialty kernels for toasting (14 g/100g moisture content) involves water loss and changes in the floury and sweet kernel properties, making toasted kernels with a soft and crunchy texture and easy to chew. Floury maize type has no vitreous fraction, and its endosperm is entirely soft, whereas sweet maize has kernels quite shrunken with a sugary-vitreous fraction more significant than floury endosperm. However, information on kernel sizes, shapes, texture, and hydration properties associated with water losses and kernel expansions during toasting is not available for floury and sweet maize types. Therefore, this study aimed to characterize the properties related to the kernel expansion of the three main maize types with floury (a0 and a1) and sweet (a2) kernels at the raw kernel initial condition (T0) and the toasted conditions in a pan (T1) and microwave (T2).

2. Materials and methods

2.1. Materials

Floury (a0) and sweet (a2) maize from Perú and floury maize (a1) from Ecuador are the three main specialty kernels used for traditional toasting in a pan. Floury maize type (*Zea mays* L. var. *amylacea*) has no vitreous fraction, and its endosperm is entirely soft, whereas sweet maize (*Zea mays* L. var. *saccharata*) has shrunken kernels with a sugary-vitreous fraction more significant than the floury endosperm (Lara et al., 2021). These kernel types (1.2 kg) obtained from a local market in Quito were taken in polypropylene airtight containers (2.3 L), adjusted to 14 g/100 g moisture content by adding the required amount of water and stored for two weeks at room temperature (15 – 20 °C). Three trials conducted on different dates assured the application of rigorous statistical analyses.

2.2. Toasting process

The moisture content of maize kernels was verified by weight difference after forced air oven drying (Across International, New Jersey-EE.UU.) at 104 ± 1 °C for 48 h (Odjo et al., 2012). By replication, the equilibrated samples divided into 150 g experimental units were collected by packed in foil gusseted bags according to maize types: floury (a0 and a1) and sweet (a2) and kernel conditions: raw kernels (T0), toasted in a pan (T1) and microwave toasting (T2). Toasting in a pan (T1) was adjusted to achieve a uniform golden-brown color across the entire kernel surface. Therefore, using a multipurpose electric pan (Atlantic Promotion INC., Longueuil, Canada) adapted for manual mixing, maize kernels (150 g) were toasted on moderate heating (175 °C) for 1500 s until to obtain the characteristic color range for the three maize types. Under the same premise of color range for

microwave toasting, maize kernels (150 g) packed in a sealed paper bag (17.5 cm wide and 24 cm long) were put on a flat plate and placed at the center of the microwave oven (Panasonic, Shanghai, China), and toasted at 492 W for 390 s (floury maize) and 312 s (sweet maize) with manual shaking each 60 s. The toasted samples were cooled and weighed using a precision balance with a readability of 0.001 g (Boeco, Humburg, Germany). Finally, all samples (raw and toasted kernels) were packed in foil gusseted bags for further measurements on the whole kernel and reduced to flour.

2.3. Geometric properties

Random samples consisting of forty maize kernels for each replication were taken to measure the individual kernel length (L), width (W), and thickness (T) using a digital caliper with a resolution of 0.01 mm. Then, the geometric mean diameter (GMD), sphericity, surface area, and volume were determined using the individual kernel dimensions (L, W, T), and the equations reported to evaluate the maize kernel size and shape (Karababa, 2006; Karababa & Coşkuner, 2007).

$GMD = (LWT)^{1/3}$
Sphericity = GMD/L
Surface area = $\pi BL^2/2L\text{-}B$
Volume = $\pi B^2L^2/6(2L\text{-}B)$
Where: $B = (WT)^{1/2}$

2.4. Gravimetric properties

Cavities referred to as large air spaces created by water loss during toasting (Schoeman et al., 2017; Sumithra and Bhattacharya, 2008), are characterized as porosity. Therefore, in this study, the volume difference between toasted and raw kernels divided by toasted kernel volume was associated with the internal porosity created during maize kernel toasting. The expansion ratio was the fraction between kernel volume after and before toasting (Schoeman et al., 2017). The individual maize kernels used to measure dimensions also were weighed, and the ratio of weight/volume gave the individual kernel density (Erkinbaev et al., 2019). The average individual weight and forty kernels per replica allowed the extrapolation to thousand-kernel weight.

2.5. Color measurements

Color parameters (L*a*b*C*h*), the color difference (ΔE*) and cumulative color simulation patterns were measured on the maize kernel surface, employing a 3nh_NH310 colorimeter with

main light D65 and a ϕ 4 mm measuring aperture (Shenzhen 3NH Technology Co., LTD., Shenzhen, China). The CQCS3 software displays white and black calibration, standard measurements, sample measurements, the color difference (ΔE*), and color simulations. Three raw kernels of characteristic color were selected as color standards by maize type and replication. The CIEL L*, a*, b*, C*, and h* parameters were measured in the reflectance mode on the maize kernel surface, using the standard and samples of 30 to 40 maize kernels (90-120 maize kernels in three replicates). L* denotes the degree of darkness (0) to lightness (100), whereas a* indicates redness or greenness, b* means yellowness or blueness with positive and negative values, respectively, C* represents color intensity or chroma, and h* signifies the hue angle (Chung et al., 2014). By setting the CIE L *, a *, and b * standard values, the CQCS3 software generated the ΔE* values and the cumulative color simulation patterns. Thus, the analysis of individual kernel parameters under each standard displayed the individual ΔE* values. Comparing the mass sample data to a standard gave the color cumulative simulation patterns.

2.6. Instrumental texture measurement

The instrumental texture of raw and toasted maize kernels was determined in the compression test mode using a CT3-10kg texture analyzer (Brookfield Engineering Labs. Inc., Middleboro, MA, USA) outfitted with a TA-CKA adapter (craft knife) and entering the average dimensions of length, width, and thickness. Next, the probe cut the cross-sectional area with minimal deformation by placing a kernel between the TA-CKA adapter and the fixture base table. The resulting data collected using the TexturePro CT software, V1.2 Build 9, displayed the individual kernel hardness or cutting force (maximum pick load in N), deformation at target (distance value at the target in mm), and stress pick (stress at the hardness pick in kPa by dividing the load at a given pick for the kernel cross-sectional area). The average texture measurement consisted of ten replicates for each treatment.

2.7. Milling of whole maize kernels

The raw and toasted maize kernels were milled (Retsch GmbH, Haan, Germany), and the flours were stored in airtight bottles at 4 °C for further analysis. Flour particle size distribution was determined by sifting and weighing separated fractions through sieves with opening sizes of 630, 400, 315, 200, 90, 25, and 0 (pan) µm. The acquired data on adjacent sieves allowed the application of statistical equations reported for the particle size calculation (Kalivoda et al., 2017; Velu et al., 2006).

2.8. Hydration properties

The water absorption capacity (WAC), swelling power (SP), and water-soluble index (WSI) were measured in maize flour using the suspension-centrifugation procedure (Lara & Ruales, 2002) with some modifications. First, an equivalent weight of 1 g (dry base) was placed in a pre-weighed centrifugal tube, completely dispersed with 5 mL of distilled water, and stored at room temperature (18-21 °C) for 20 h. Next, the suspension was mixed with a thin rod, completed to 7 ml with distilled water, and centrifuged at 2683xg (3 °C) for 20 min. After weighing the sediment and supernatant fractions, a supernatant volume of known weight was dried overnight and weighed. All water absorption analyses were in triplicate.

2.9. Statistical analysis

The experiment designed by complete blocks and treatments (without interactions) provided a more valid measure of the known source of variation due to maize types. Therefore, applying a two-way ANOVA by blocks and treatments, maize types (a0, a1, and a2) were blocks, and kernel conditions (T0, T1, and T2) were treatments to characterize the toasted maize kernels. After checking the normal distribution of data, the response variables (two-way matrix) were analyzed, excluding sweet maize (a2) when it was the primary source of non-normal variability. Then, Tukey's multiple range test by blocks (a0, a1, a2) and treatments (T0, T1, T2) were applied to find the level(s) that created significant differences ($P \leq 0.05$) within each group. The statistical analyses were determined using the Statgraphics Software (Statgraphics centurion 18, USA). The OriginPro software (Version 2020, Microcal Inc., Northampton, MA, USA) was used to obtain the Kernel density or density trace distribution for volume and ΔE*.

3. Result and discussion

3.1. Toasting process and remaining moisture content

The two-way data matrix of moisture content exhibited normal distribution and varied according to two-way ANOVA influenced by the kernel conditions. Once the statistical variations were confirmed, the comparison of means by maize types presented in Table 1 indicated that moisture content variations between floury (a0 and a1) and sweet (a2) maize were statistically equivalent ($P \geq 0.05$) with high standard deviations ascribed to the water loss achieved between initial and remaining moisture contents during toasting conditions. In agreement with water loss, the moisture content was significantly different ($P \leq 0.05$) among initial (T0) and toasted kernel conditions (T1

and T2), with less moisture remaining content in microwave toasted kernels (T2), compared to toasted kernels in a pan (T1). The remaining moisture content attributed to toasting in a pan was 2.73 ± 0.01 g/100 g in a0T1, 2.34 ± 0.04 g/100 g in a1T1, and 3.45 ± 0.02 g/100 g in a2T1, whereas microwave toasting exhibited remaining moisture content of 2.10 ± 0.08 g/100 g in a0T2, 2.28 ± 0.16 g/100 g in a1T2 and 2.10 ± 0.09 g/100 g in a2T2. The results revealed a rapid water loss by microwave toasting using all maize types, with a remaining moisture content close to the moisture levels (less than 2 g/100 g) of toasted maize flakes (Sumithra & Bhattacharya, 2008). The maize kernels toasted in a pan (1500 s) had a lower moisture content than those (4-5 g/100 g) reported in the normal maize toasted for 1500 s at a pilot scale (Raigar & Mishra, 2018).

The initial fixed moisture content was 14.06 ± 0.13 g/100 g in the raw kernels of a0T0, a1T0, and a2T0. This fact ensured the reliability of the measurement results for the other response variables, mainly considering the relationship between physical properties and moisture content reported in raw kernels of popcorn (Karababa, 2006), sweet maize (Karababa & Coşkuner, 2007), and normal maize (Mousaviraad & Tekeste, 2020).

3.2. Geometric properties

The variability was the same for the three replications (120 individual maize kernels), with variation coefficients (Cv%) between 5 and 22%. With a normal distribution of the two-way data matrix, the geometric properties evaluated as length, width, thickness, GMD, sphericity, surface area, and volume exhibited the significant variability ($P \leq 0.05$) inherent to maize types and attributed to kernel conditions. Based on these significant results derived from two-way ANOVA, Table 1 contains the comparison of means by blocks (a0, a1, a2) and treatments (T0, T1, T2) to find the level(s) that created significant differences ($P \leq 0.05$) within each group. Most of the geometric properties revealed significant variation ($P \leq 0.05$) among maize types a0, a1, and a2 with big, medium, and small kernel dimensions. Table 1 also indicated that the length and width dimensions presented the same ($P \geq 0.05$) variation due to the toasting condition (T1 and T2) and between raw (T0) and toasted kernels in a pan (T1), respectively. Raw kernels (T0), toasted in a pan (T1), and microwave toasting (T2) had a significant influence ($P \leq 0.05$) on thickness, GMD, surface area, and volume, with the highest changes achieved in microwave toasting (T2) compared to the initial values in raw kernels (T0) and the increases attained during toasting in a pan (T1). These increasing kernel sizes agreed with the moisture content variations and demonstrated that the changes in size kernel depended on the moisture migration from the center to the kernel surface area.

Table 1. Comparison means (Tukey's test HSD test) by maize types and kernel conditions: physical and hydration properties

Kernel properties	Maize types (T0, T1, T2)			Kernel conditions (a0, a1, a2)		
	a0	a1	a2	T0	T1	T2
Toasting						
Moisture	6.82 ± 6.84 a	6.79 ± 6.94 a	6.91 ± 6.69 a	15.62 ± 0.15c	2.84 ± 0.56 b	2.06 ± 0.35 a
Geometric						
Length	16.8 ± 0.5 b	17.0 ± 0.4 b	14.5 ± 0.4 a	15.7 ± 1.3 a	16.2 ± 1.2 b	16.4 ± 1.2 b
Width	10.7 ± 0.2 c	9.4 ± 0.2 b	8.5 ± 0.1 a	9.5 ± 0.9 a	9.4 ± 1.0 a	9.7 ± 1.0 b
Thickness	7.7 ± 1.0 c	7.2 ± 0.8 b	6.8 ± 1.2 a	5.9 ± 0.5 a	7.8 ± 0.4 b	8.0 ± 0.4 c
GMD	11.1 ± 0.6 c	10.4 ± 0.5 b	9.4 ± 0.7 a	9.5 ± 0.8 a	10.5 ± 0.7 b	10.8 ± 0.7 c
Sphericity	0.66 ± 0.03 c	0.62 ± 0.02 a	0.65 ± 0.03 b	0.61 ± 0.02 a	0.66 ± 0.03 b	0.66 ± 0.02 b
Surface area	388 ± 42 c	343 ± 32 b	278 ± 40 a	288 ± 49 a	352 ± 47 b	369 ± 50 c
Volume	751± 102 c	618 ± 73 b	450 ± 82 a	500 ± 127 a	637 ± 132 b	683 ± 142 c
Gravimetric						
IKW	0.55 ± 0.03 c	0.43 ± 0.03 b	0.30 ± 0.02 a	0.46 ± 0.11 b	0.41 ± 0.11 a	0.41 ± 0.10 a
IKD	0.75 ± 0.14 c	0.72 ± 0.13 b	0.70 ± 0.20 a	0.93 ± 0.04 c	0.65 ± 0.05 b	0.60 ± 0.03 a
T-KW	548 ± 28 c	431 ± 29 b	299 ± 21 a	456 ± 110 b	4014 ± 110 a	408 ± 104 a
Colour space						
L*	62.3 ± 9.9 b	62.5 ± 7.5 b	50.6 ± 13.6 a	72.6 ± 2.9 b	51.7 ± 8.3 a	51.5 ± 7.0 a
a*	14.0 ± 5.6 b	15.7 ± 3.8 c	9.8 ± 1.8 a	8.4 ± 1.9 a	15.5 ± 3.9 b	15.7 ± 3.5 b
b*	34.2 ± 2.0 b	41.7 ± 9.1 c	26.5 ± 12.0 a	43.3 ± 8.0 b	29.6 ± 9.2 a	29.5 ± 8.6 a
C*	37.4 ± 2.1 b	45.0 ± 7.8 c	28.7 ± 11.0 a	44.2 ± 8.2 b	33.4 ± 9.9 a	33.5 ± 9.2 a
h*	67.7 ± 8.7 b	68.1 ± 7.8 b	66.4 ± 9.9 a	79.1 ± 0.9 b	61.7 ± 1.7 a	61.4 ± 1.8 a
ΔE*	18.0 ± 10.1 a	22.0 ± 11.2 b	26.3 ± 15.1 c	6.2 ± 2.3 a	30.0 ± 5.8 b	30.0 ± 5.5 b
Texture						
Hardness (N)	13.7 ± 4.2 a	15.2 ± 4.4 b	23.7 ± 6.8 ⊄	19.8 ± 2.2 b	12.2 ± 1.8 a	11.3 ± 1.8 a
Hydration						
WAC	2.39 ± 0.19 b	2.42 ± 0.22 b	2.19 ± 0.28 a	2.04 ± 0.16 a	2.44 ± 0.12 b	2.52 ± 0.07 c
SP	2.46 ± 0.19 a	2.49 ± 0.21 a	2.53 ± 0.20 b	2.24 ± 0.05 a	2.57 ± 0.04 b	2.66 ± 0.05 c
WSI	3.01 ± 0.54 a	3.16 ± 0.76 a	14.9 ± 6.0 ⊄	3.86 ±0.47 a	2.68 ± 0.17 a	2.72 ± 0.17 a

Mean ± SD related to three replications for maize types n = (9) and kernel conditions n = (9). Floury maize a0 and a1. Sweet maize a2. Raw kernels T0. Toasted kernels in a pan T1. Microwave toasted kernels T2.

Different letters in the same row by block and treatments indicated Tukey's test significant variations ($P \leq 0.05$). ⊄: level data excluded because they cause non-normal distribution.

Moisture content (g/100 g); kernel dimension (mm); GMD: geometric mean diameter (mm); surface area (mm^2); volume (mm^3); IKW: individual kernel weight (g); IKD: individual kernel density (g/mL); T-KW: thousand-kernel weight; ΔE*: colour difference; WAC: water absorption capacity (g/g sample); SP: swelling power (g/g insoluble solids); WSI: water solubility index (g/100 g total solids). ⊄: level data no included because they cause no normal distribution.

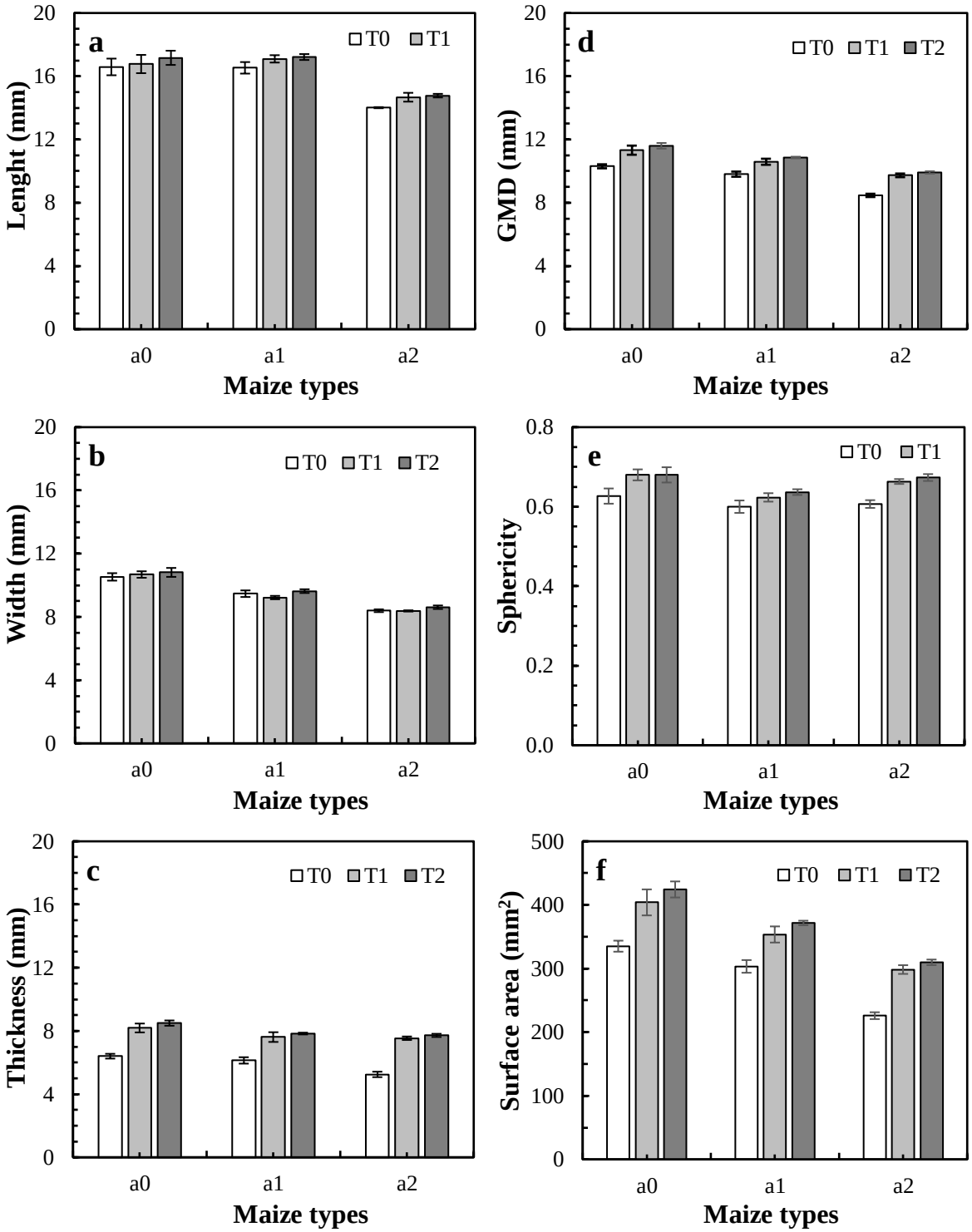

Figure 1. Average kernel dimension (**a, b, c**) and geometrical properties (**d, e, f**) by maize types and kernel conditions. Floury maize (a0 and a1), sweet maize (a2), raw kernels (T0), toasted kernels in a pan (T1), and toasted kernels in microwaves. Geometric mean diameter (GMD). Averages (n = 120) ± SD.

Fig. 1 (a-f) shows the clustered columns by maize types with the average (three replications) geometric properties to illustrate the effect of kernel conditions within each block. The clustered columns reflected the variations inherent to kernel size (Fig. 1 d) and shape (Fig. 1 e) by maize types

and the changes from raw to toasting kernel conditions ascribed to kernel expansion. The kernel expansion due to thickness variations (Fig. 1 c) was more evident than those caused for the other two kernel dimensions (Fig. 1 a and b), implying that the kernel thickness generated the GMD (Fig. 1 d), surface area (Fig. 1 f), and volume (Fig. 2 a-c) increases. Furthermore, the kernel volume distribution (Kernel density or density trace) by maize types (Fig. 2a-c) was consistent with the significant increases in kernel volume indicated in Table 1. The top of volume distribution curves projected on the X-axis gave average volume values of 628 ± 29, 784 ± 55, 842 ± 36, 529 ± 27, 637 ± 33, 688 ± 70, 343 ± 11, 489 ± 16 and 518 ± 11 mm^3 for a0T0, a0T1, a0T2, a1T0, a1T1, a1T2, a2T0, a2T1, and a2T2, respectively. The volumetric changes from raw to toasted indicated the kernel expansion associated with the internal porosity created during toasting conditions and discussed for toasted normal maize kernels (Schoeman et al., 2017) and coffee beans (Oliveros et al., 2017). Based on raw kernel geometric properties, floury maize had larger kernel sizes than those determined for yellow (Mousaviraad & Tekeste, 2020) and white (Guelpa et al., 2016; Uriarte-Aceves et al., 2019) normal maize at comparable moisture content. In sweet maize, the kernel dimensions were larger than that sweet maize hybrid (Karababa & Coşkuner, 2007) and slightly equivalent to the Peruvian sweet maize called *Chullpi* (Salvador-Reyes et al., 2021).

3.3. Gravimetric properties

The two-way data matrix of expansion ratio and internal porosity created during kernel toasting, weight per kernel, individual kernel density, and thousand-kernel weight presented normal distribution. Expansion ratio and internal porosity described the volume difference observed in Fig. 2 (a-c) between toasted and raw kernels, and the two-way ANOVA of these response variables reflected the statistical distinctions between pan (T1) and microwave (T2) toasting by maize type. For example, Fig. 2 (d) indicates the internal porosity differences between T1 and T2 illustrated by maize types. The expansion ratio with low (1.27 ± 0.3) and high (1.47 ± 0.01) values ($P \leq 0.05$) corresponded to floury and sweet maize kernels, respectively, as well as a lower expansion ratio (1.29 ± 0.02) in maize kernels toasted in a pan than that (1.38 ± 0.04) obtained from microwave toasting kernels. These results were higher than 1.11 ± 0.17 in normal white maize toasted in a conventional oven (Schoeman et al., 2017). Fig. 2 (d) demonstrated that the average internal porosity significantly segregated ($P \leq 0.05$) floury (0.21 ± 0.02) and sweet (0.32 ± 0.01) maize, as well as toasting in a pan (0.22 ± 0.01) and microwave (0.27 ± 0.02). The expansion ratio and internal porosity generated during microwave toasting agreed with a rapid water loss deduced from the remaining moisture content in toasted kernels with microwaves, proving that the toasting process increases the porosity of maize kernels by water loss effect (Schoeman et al., 2017).

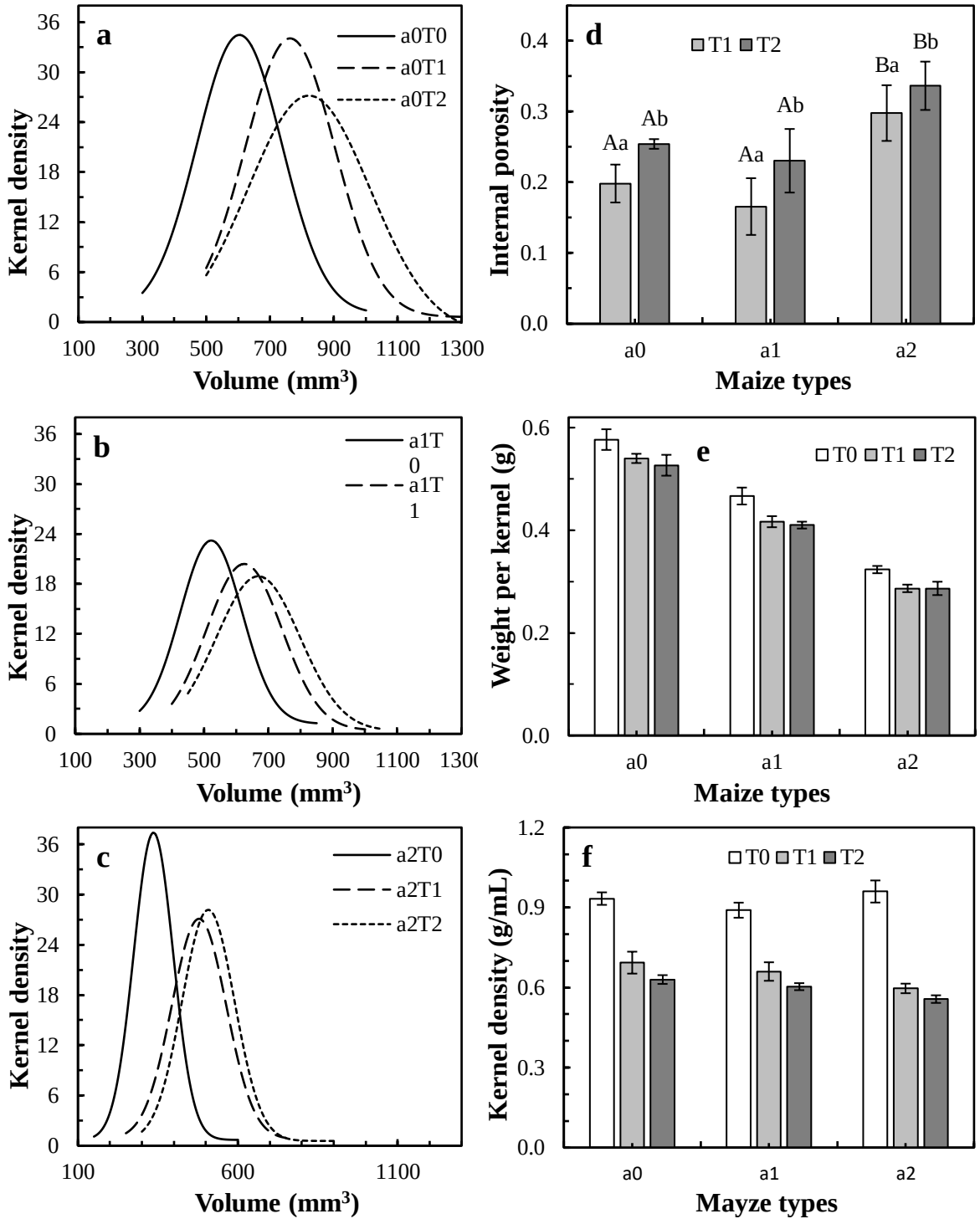

Figure 2. Kernel volume distribution (**a, b, c**), average internal porosity by maize types and toasting conditions (**d**), average individual weight (**e**), and individual kernel density (**f**) by maize types and kernel conditions. Floury maize (a0 and a1), sweet maize (a2), raw kernels (T0), toasted kernels in a pan (T1), and toasted kernels in microwaves (T2). Averages (n = 120) ± SD.

The two-way ANOVA and the comparison of means shown in Table 1 indicated significant differences ($P \leq 0.05$) among maize types (a0, a1, and a2) for weight per kernel, individual kernel density, and thousand-kernel weight, in agreement with their main geometric properties. Relative to

treatments, the individual kernel density exhibited significant variation from raw kernels (T0) to toasted in a pan and microwave toasting (T2), which were consistent with moisture content, thickness, GMD, surface area, and volume variations by the toasting effect (Table 1). However, the decrease from raw (T0) to toasting conditions (T1 and T2) was statistically equivalent to weight per kernel and thousand-kernel weight.

The clustered columns of weight per kernel (Fig. 2e) and individual kernel density (Fig. 2f) implied variations inherent to maize types (a0, a1, and a2) and decreased with the toasting conditions (T1, T2) compared to raw kernels (T0). Floury (a0 and a1) and sweet maize (a2) had the lowest raw individual kernel density when compared to those values for raw kernel reported in sweet maize (Karababa & Coşkuner, 2007) and normal maize (Guelpa et al., 2016; Mousaviraad & Tekeste, 2020; Uriarte-Aceves et al., 2020; Uriarte-Aceves et al., 2019). Moreover, pan and microwave toasting presented a higher reduction in kernel density than that determined for normal maize toasted using a conventional oven (Schoeman et al., 2017). These results explain why floury maize types like a0 and a1 have remained underutilized in the traditional milling processes. However, innovation in milling can help to take advantage of floury maize with completely soft endosperm and low protein content, mainly intended for starch extraction.

3.4. Colour space

The two-way data matrix of the CIE L *, a *, b *, C *, and h * parameters and the color difference (ΔE*) presented normal distribution and varied according to the two-way ANOVA by maize types (a0, a1, a2) and kernel conditions (T0, T1, T2). Table 1 summarizes the comparison means for each color response variable by blocks (a0, a1, a2) and treatments (T0, T1, T2). Where L* and h* parameters only showed significant differences between floury (a0 and a1) and sweet (a2) types, whereas a*, b*, C*, and ΔE* were significantly different ($P \leq 0.05$) among a0, a1, and a2 maize types. On the other way, all color response variables (L*, a*, b*, C*, h*, and ΔE*) statistically demonstrated differences ($P \leq 0.05$) between raw (T0) and toasted kernels (T1, T2), indicating that the maize kernel subjected to a pan (T1) and microwave (T2) toasting developed a comparable surface color towards golden brown.

Fig. 3 (a, b, and c) displays the average L*, a*, and b* values for floury maize a0 (a0T0, a0T1, a0T2), floury maize a1 (a1T0, a1T1, a1T2), and sweet maize a2 (a2T0, a2T1, and a2T3), respectively. Raw floury maize kernels a0 and a1 with an opaque surface gave L* values from 72.38 ± 0.57 to 75.41 ± 0.31 (Fig. 3a-b), whereas the L* value was 68.77 ± 0.76 in raw sweet maize kernels (Fig. 3c) with a crystalline appearance. The sweet maize CIE L*, a*, and b* parameters presented in Fig. 3 (c) agreed

with the color parameters reported for the Peruvian sweet maize called *Chullpi* (Salvador-Reyes et al., 2021).

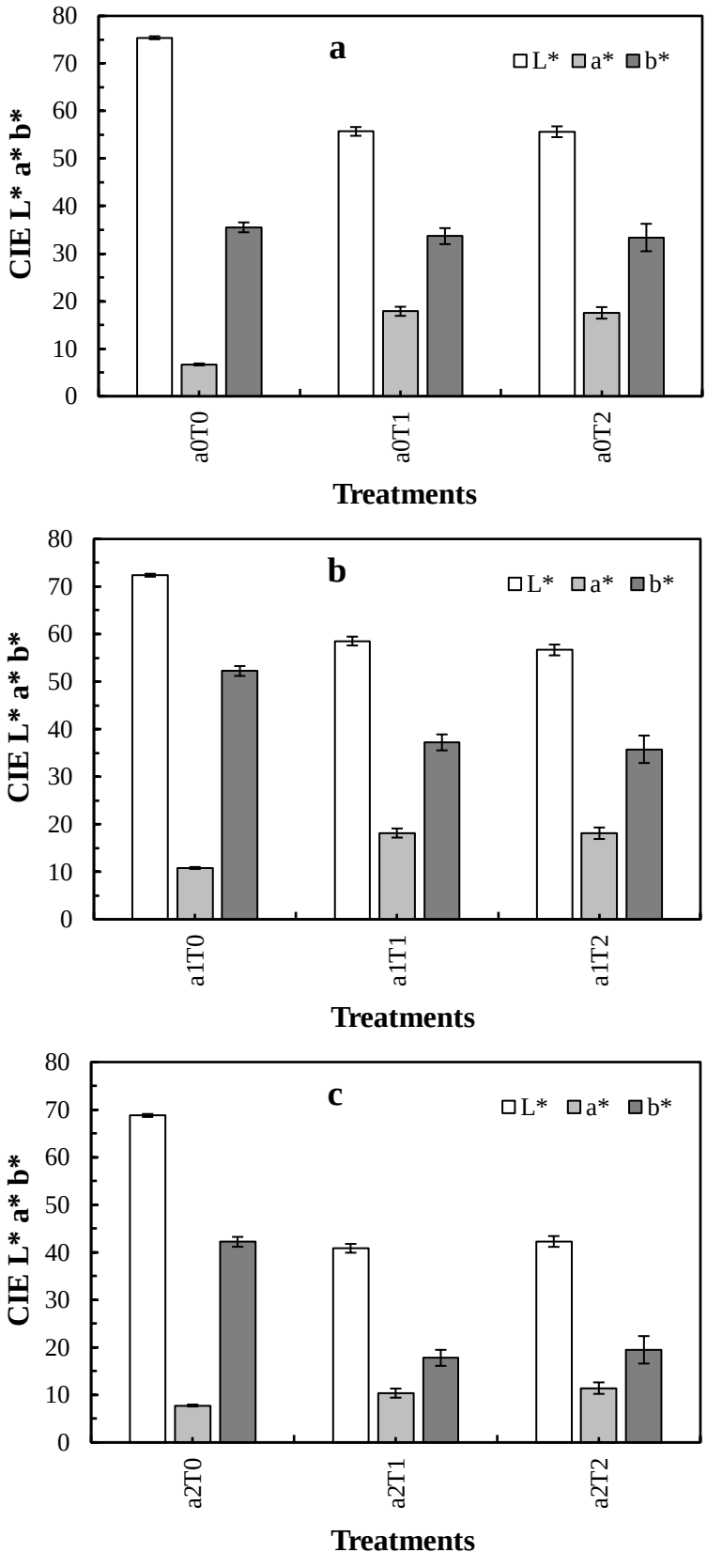

Figure 3. Average CIE L*, a*, and b* parameters clustered by kernel conditions: floury maize a0 (a), floury maize a1 (b), and sweet maize a2 (c). Raw kernels (T0), toasted kernels in a pan (T1), and toasted kernels in microwaves (T2). Averages (n = 90 – 120) ± SD.

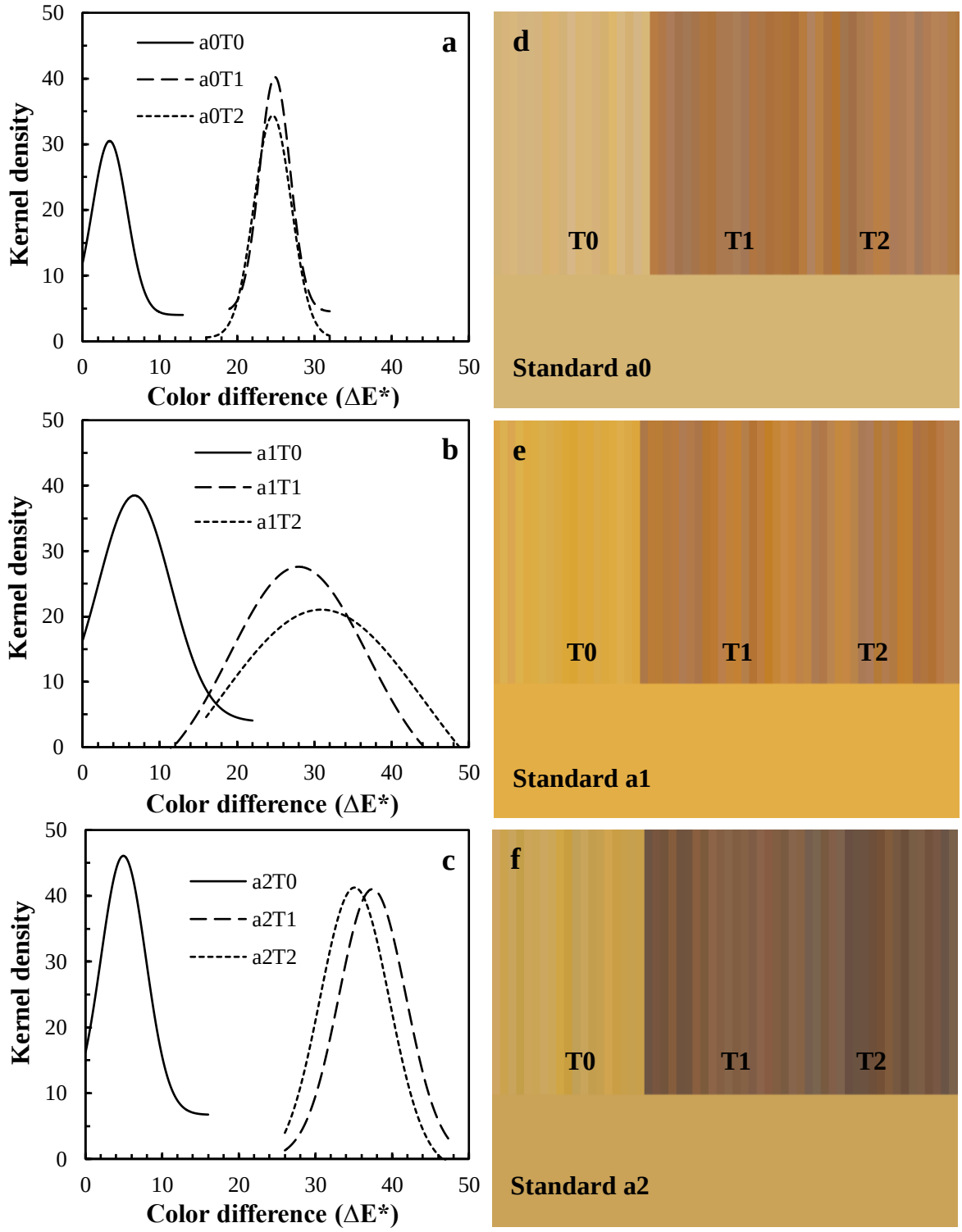

Color standards	L*	a*	b*	C*	h*
a0; n = 9	75.6 ± 0.3	5.9 ± 0.4	37.5 ± 1.2	37.9 ± 1.2	81.1 ± 0.5
a1; n = 9	74.4 ± 0.7	12.1 ± 0.8	58.4 ± 0.6	59.7 ± 0.7	78.4 ± 0.8
a2; n = 9	69.3 ± 0.5	7.5 ± 0.7	41.3 ± 3.0	41.9 ± 2.8	79.7 ± 0.7

Figure 4. Color difference (ΔE*) distribution (**a,b,c**), cumulative colour simulation patterns (**d, e, f**) and standard color (CIE L*, a*, b*, C*and h* values). Floury maize (a0 and a1), sweet maize (a2), raw kernels (T0), toasted kernels in a pan (T1), and toasted kernels in microwaves (T2). ΔE* data, n = 270 – 360.

The L* and b* parameters decreased while a* augmented during pan and microwave toasting. These decreases in L*, b*, and increase in a* parameters were consistent with the trend changes in the same color parameters during the electrical rotary toasting of *Zea mays* var. *indurate* for 50 min (Chung et al., 2014). The L*, a*, and b* values per individual kernels and standard color kernels generated the ΔE* distributions expressed as Kernel density in Fig. 4 (a, b, and c), where the differences inherent to maize types, the changes in color from raw to toasted kernels and the similarities between toasting conditions were consistent with the results of the Tukey's test displayed in Table 1. Indeed, Fig. 4 (a-c) graphically describes the cumulative color simulation patterns exhibited in Fig. 4 (d-f). Furthermore, the changes toward brown surface color were more marked in sweet maize (Fig. 4 f) than in floury maize (Fig. 4 d-e). This finding is mainly attributed to its sugary-vitreous fraction, rich in reducing sugars (Lara et al., 2021) and ascribed to nonenzymatic browning reactions, known as the Maillard reaction and sugar caramelization (Chung et al., 2014; Youn & Chung, 2012). However, the sweet maize kernels also had smaller kernel dimensions, and lower weights than floury maize types (Table 1 and Figs. 1 and 2) contributed to changes in the surface color. Fig. 4 includes the average L *, a *, b *, C *, and h * values and standard deviation in selected maize kernels (a0, a1, and a2) used as standards. The standard color spaces revealed high values for h* (yellowness) and L* (lightness), equivalent values for b* (yellowness) and C* (chroma), and low values for a* (redness), implying reduced participation assigned to a* parameter in the expression to estimate C*, defined as purity or intensity of the color (Chung et al., 2014).

3.5. Instrumental texture measurements

The two-way data matrix of kernel hardness or cutting force, deformation at target, and stress pick did not present normal distributions, invalidating any parametrical analysis; however, the variation coefficients ranged from 9.61 to 16.55%, 0.13 to 1.28 %, and 9.61 to 16.55%, respectively. Excluding sweet maize as the primary source of unnormal variation in the two-way ANOVA of kernel hardness data, the floury maize types (a0 and a1) showed a significant difference ($P \leq 0.05$), as is indicated in Table 1. For kernel conditions, the significant difference ($P \leq 0.05$) found was between raw (T0) and toasted (T1 and T2) kernel hardness, with a decreasing kernel hardness attributed to the cavities created during toasting conditions (Schoeman et al., 2017). Furthermore, the clustered columns by maize types exhibited in Fig. 5 (a) demonstrated that the average kernel hardness values in floury maize with entirely soft endosperm were lower than that obtained in sweet maize a2, characterized by a sugary-vitreous kernel fraction with more than 20% of total sugar (Lara et al., 2021). The kernel hardness results agreed with low and high hardness reported for soft and vitreous maize endosperm in normal white maize (Guelpa et al., 2015; Schoeman et al., 2017). Thus, the hardness values obtained for raw kernels a0, a1, and a2 reflected the difference in maize types associated with the

kernel structure. The clustered columns in floury maize a0 and a1showed a decrease in raw kernel hardness (T0) from 19.06 ± 1.86 and 20.61 ± 2.37 N to 11.55 ± 1.76 (T1) and 12.89 ± 1.73 N in toasted kernels in a pan (T1), and to 10.50 ± 1.23, and 12.15 ± 2.01 N in microwave toasting (T2), respectively. In the issue of sweet maize (a2), the raw kernel hardness (T0) diminished from 31.80 ± 3.64 N to 18.73 ± 3.0 N in T1 and 20.55 ± 2.35 N in T2.

The clustered columns in Fig. 5 (b) exhibited minimal deformation at target results related to the cutting force of the compression cycle. The influence of T1 and T2 conditions on the deformation appeared equivalent, but this effect was higher than that for the raw kernel condition (T0). In Fig. 5 (c), the clustered columns by maize types indicated the stress pick results calculated as the kernel hardness divided by the kernel cross-section. The same behavior described for kernel hardness showed the response variable stress pick with a clear difference between raw (T0) and toasted (T1 and T2) conditions, as well as between floury and sweet maize, which inferred that the softness and crispness, respectively in toasted floury and sweet maize could be the main attributes of entire ready-to-eat maize.

3.6. Milling of whole maize kernels

Raw and toasted kernels reduced to flour implied the behavior by maize type and indicated the effect of the kernel conditions on the average particle size after milling. The average particle size measured by sieving varied from 113.42 ± 2.35 µm to 114.13 ± 2.62 µm in raw floury maize, was 181.48 ± 2.10 µm in raw sweet maize, ranged from 85.25 ± 2.46 µm to 76.91 ± 2.51 µm in toasted floury maize, and was 135.82 ± 2.25 µm in toasted sweet maize. These results reflected different structural properties between floury and sweet maize and the structural changes in the kernel endosperm during the toasting conditions, with a considerable reduction in the average particle size associated with the decreasing hardness in the raw maize kernel (T0) subjected to the pan (T1) and microwave (T2) toasting (Table 1 and Fig. 5 a). Compared to floury maize, sweet maize's largest average particle sizes confirmed the kernel hardness ascribed to its sugary-vitreous fraction with more than 20 % total sugars (Lara et al., 2021).

3.7. Hydration properties of maize kernels reduced to flour

Except for WSI, the two-way data matrix of hydration properties (WAC and SP) presented normal distribution, and the two-way ANOVA showed the variations in WAC and SP by maize types (a0, a1, and a2) and kernel conditions (T0, T1, and T2). In Table 1, the WAC comparison means by maize types evidenced the significant change ($P \leq 0.05$) between floury (a0 and a1) and sweet (a2) maize,

and this statistical variation was consistent with kernel length and the color L* and h* parameters. Depending on the WAC and WSI, the SP behaved as WAC with a significant increase ($P \leq 0.05$) in sweet maize due to its high WSI compared to floury maize (Table 1).

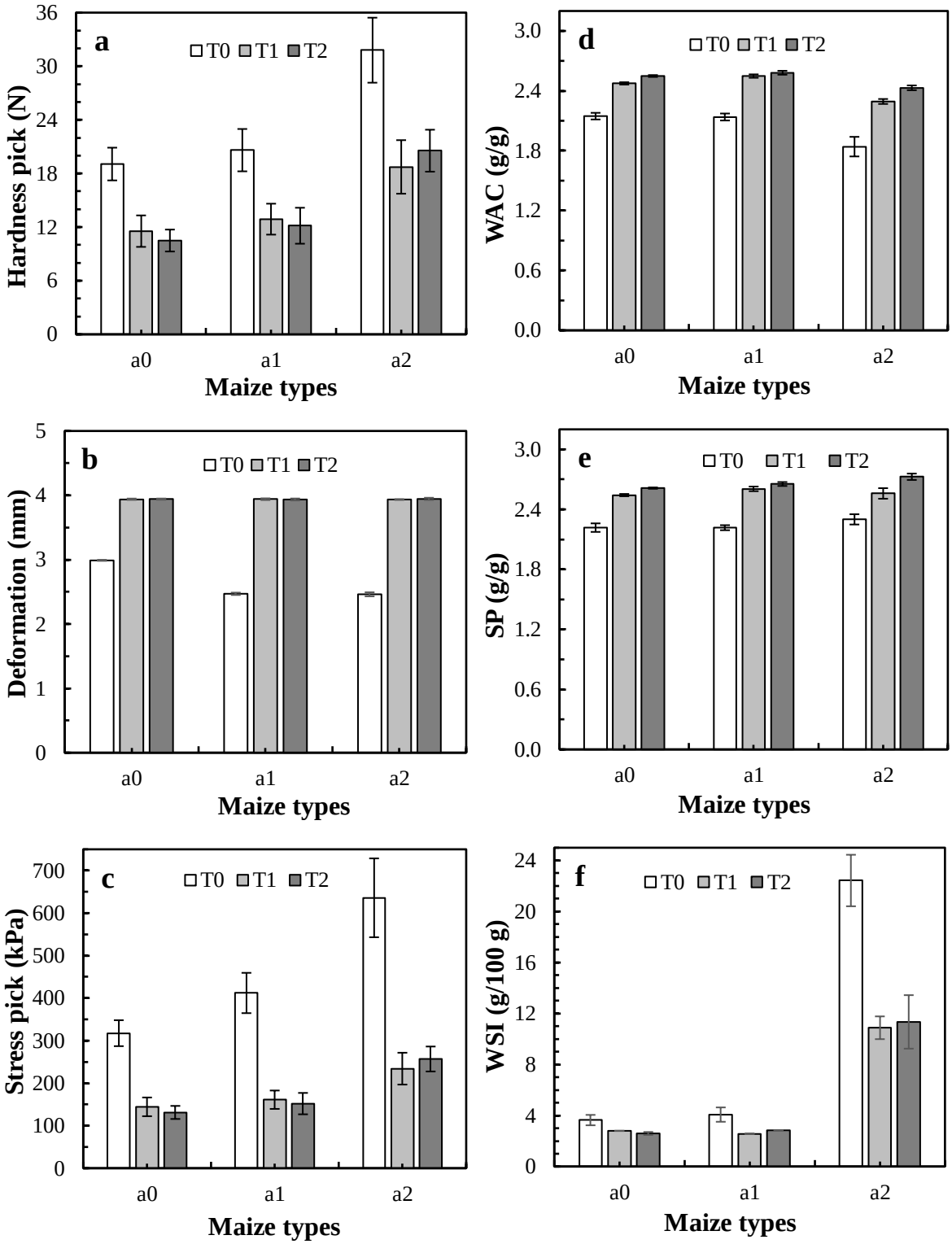

Figure 5. Average texture parameters (**a, b, c**) and hydration properties (**d, e, f**) by maize types and kernel conditions. Floury maize (a0 and a1), sweet maize (a2), raw kernels (T0), toasted kernels in a pan (T1), and toasted kernels in microwaves (T2). Water absorption capacity (WAC), swelling power (SP), and water-soluble index (WSI). Average texture (n = 10) ± SD, average hydration properties (n = 6) ± SD.

The comparison of means among raw kernel, toasted in a pan, and microwave toasting exhibited significant increases ($P \leq 0.05$) in WAC and SP caused by pan (T1) and microwave toasting (T2) compared to their raw counterparts (T0). These significant variations in WAC and SP by kernel conditions agreed with moisture content, thickness, GMD, surface area, volume, and kernel density (Table 1). On the other hand, the clustered columns by maize types (a0, a1, and a2) illustrated the rise of WAC (Fig. 5 a) and SP (Fig. 5 e) occurred in raw kernels (T0) subjected to the pan (T1) and microwave (T2) toasting. In floury maize, the WAC rose on average from 2.14 ± 0.03 g/g (T0) to 2.54 ± 0.01 g/g (T1 and T2), while in sweet maize increased from 1.84 ± 0.10 g/g (T0) to 2.43 ± 0.02 g/g (T1 and T2). These results in WAC and SP agreed with the increasing hydration properties of arrowhead tubers subjected to pan and microwave toasting (Wani et al., 2016). Moreover, the WAC of raw and toasted maize types were consistent with those reported in raw (Paesani et al., 2020; Wang et al., 2019) and normal toasted maize at the pilot-scale (Raigar & Mishra, 2018), while the SP value in raw kernels was lower than that reported for raw conventional maize flour at 25 °C (Deepa & Hebbar, 2017). In contrast to WAC and SP, the clustered columns by maize types (Fig. 5 f) revealed the decrease of WSI by the toasting effect, and similar behavior in WSI occurred in whole maize kernels treated by NIR lamp heating (Deepa & Hebbar, 2017). In floury maize, the average reduction in WSI was from 3.86 ± 0.49 (T0) to 2.70 ± 0.06 g/100 g, whereas in sweet maize decreased from 22.43 ± 1.02 (T0) to 11.11 ± 1.49 g/100 g, suggesting that the WSI reduction reflected the decreasing free sugar during maize kernel toasting (Lara et al., 2021; Woo et al., 2018; Youn & Chung, 2012). Finally, the main feature of the high WSI in sweet maize compared to floury maize is the natural accumulation of phytoglycogen nanoparticles, an α-D-glucan highly water-dispersible (Xue et al., 2019).

4. Conclusion

Underutilized maize kernels subjected to pan and microwave toasting displayed changes in geometric, gravimetric, surface color, instrumental texture, milling average particle size, and hydration properties inherent to the maize types and the water loss that governed the kernel expansion and its internal porosity. Pan and microwave toasting developed a comparable surface color. The remaining moisture content between pan and microwave toasting agreed with kernel size, density, WAC, and SP variations. With the recent interest in super soft cereals, flour maize with large kernel sizes and low hardness could be a potential crop to develop unconventional milling processes. Internal porosity ascribed to geometric properties, hardness, stress pick, and the average particle size implied that the softness and crispness in toasted floury and sweet maize might be the main attributes of the entire ready-to-eat kernels of these specialty maize types, respectively.

Funding statement

The author carried out this work within the DOCT-DI-2019-49 Project framework with the institutional sponsor of the Universidad Central del Ecuador.

Data availability statement

Data is available on request.

Conflict of interest

The authors declare no conflict of interest.

Acknowledgments

The Research Program of the Universidad Central del Ecuador supported this work, and the authors would like to thank the research laboratories of the Escuela Politécnica Nacional, Universidad Central del Ecuador, and Universidad Técnica de Ambato for the instrumental facilities.

References

Adebowale, O. J., Taylor, J. R. N., & de Kock, H. L. (2020). Stabilization of wholegrain sorghum flour and consequent potential improvement of food product sensory quality by microwave treatment of the kernels. *LWT - Food Science and Technology*, *132*, 109827. https://doi.org/10.1016/j.lwt.2020.109827

Carrera, Y., Utrilla-Coello, R., Bello-Pérez, A., Alvarez-Ramirez, J., & Vernon-Carter, E. J. (2015). In vitro digestibility, crystallinity, rheological, thermal, particle size and morphological characteristics of pinole, a traditional energy food obtained from toasted ground maize. *Carbohydrate Polymers*, *123*, 246-255. https://doi.org/10.1016/j.carbpol.2015.01.044

Chung, H.-S., Kim, J.-K., Moon, K.-D., & Youn, K.-S. (2014). Changes in color parameters of corn kernels during roasting. *Food Science and Biotechnology*, *23*(6), 1829-1835. https://doi.org/10.1007/s10068-014-0250-x

Deepa, C., & Hebbar, H. U. (2017). Influence of micronization on physicochemical properties of maize grains. *Starch - Stärke*, *69*(3-4), 1600060. https://doi.org/10.1002/star.201600060

Delwiche, S. R., Morris, C. F., & Kiszonas, A. M. (2020). Compressive strength of super soft wheat endosperm. *Journal of Cereal Science*, *91*, 102894. https://doi.org/10.1016/j.jcs.2019.102894

Erkinbaev, C., Ramachandran, R. P., Cenkowski, S., & Paliwal, J. (2019). A comparative study on the effect of superheated steam and hot air drying on microstructure of distillers' spent grain pellets using X-ray micro-computed tomography. *Journal of Food Engineering*, *241*, 127-135. https://doi.org/10.1016/j.jfoodeng.2018.08.004

Guelpa, A., du Plessis, A., Kidd, M., & Manley, M. (2015). Non-destructive estimation of maize (*Zea mays* L.) kernel hardness by means of an X-ray micro-computed tomography (µCT) density calibration. *Food and Bioprocess Technology*, *8*(7), 1419-1429. https://doi.org/10.1007/s11947-015-1502-3

Guelpa, A., du Plessis, A., & Manley, M. (2016). A high-throughput X-ray micro-computed tomography (µCT) approach for measuring single kernel maize (*Zea mays* L.) volumes and densities. *Journal of Cereal Science*, *69*, 321-328. https://doi.org/10.1016/j.jcs.2016.04.009

Kalivoda, J. R., Jones, C. K., & Stark, C. R. (2017). Impact of varying analytical methodologies on grain particle size determination. *Journal of Animal Science*, *95*(1), 113. https://doi.org/10.2527/jas.2016.0966

Karababa, E. (2006). Physical properties of popcorn kernels. *Journal of Food Engineering*, *72*(1), 100-107. https://doi.org/10.1016/j.jfoodeng.2004.11.028

Karababa, E., & Coşkuner, Y. (2007). Moisture dependent physical properties of dry sweet corn kernels. *International Journal of Food Properties*, *10*(3), 549-560. https://doi.org/10.1080/10942910601003981

Lara, N., & Ruales, J. (2002). Popping of amaranth grain (*Amaranthus caudatus*) and its effect on the functional, nutritional and sensory properties. *Journal of the Science of Food and Agriculture*, *82*(8), 797-805.

Lara, N., Vizuete, K., Debut, A., Chango, I., Campaña, O., Villacrés, E., Bonilla, P., & Ruales, J. (2021). Underutilized maize kernels (*Zea mays* L. var. *amylacea* and var. *saccharata*) subjected to pan and microwave toasting: A comparative structure study in the whole kernel. *Journal Cereal Science*, *100*, 103249. https://doi.org/10.1016/j.jcs.2021.103249

Mousaviraad, M., & Tekeste, M. Z. (2020). Effect of grain moisture content on physical, mechanical, and bulk dynamic behaviour of maize. *Biosystems Engineering*, *195*, 186-197. https://doi.org/10.1016/j.biosystemseng.2020.04.012

Odjo, S., Malumba, P., Dossou, J., Janas, S., & Béra, F. (2012). Influence of drying and hydrothermal treatment of corn on the denaturation of salt-soluble proteins and color parameters. *Journal of Food Engineering*, *109*(3), 561-570. https://doi.org/10.1016/j.jfoodeng.2011.10.023

Oliveros, N. O., Hernández, J. A., Sierra-Espinosa, F. Z., Guardián-Tapia, R., & Pliego-Solórzano, R. (2017). Experimental study of dynamic porosity and its effects on simulation of the coffee beans roasting. *Journal of Food Engineering*, *199*, 100-112. https://doi.org/10.1016/j.jfoodeng.2016.12.012

Paesani, C., Bravo-Núñez, Á., & Gómez, M. (2020). Effect of extrusion of whole-grain maize flour on the characteristics of gluten-free cookies. *LWT - Food Science and Technology*, *132*, 109931. https://doi.org/10.1016/j.lwt.2020.109931

Raigar, R. K., & Mishra, H. N. (2018). Study on the effect of pilot scale roasting conditions on the physicochemical and functional properties of maize flour (Cv. *Bio 22027*). *Journal of Food Processing and Preservation*, *42*(5), e13602. https://doi.org/10.1111/jfpp.13602

Salvador-Reyes, R., Rebellato, A. P., Lima Pallone, J. A., Ferrari, R. A., & Clerici, M. T. P. S. (2021). Kernel characterization and starch morphology in five varieties of Peruvian Andean maize. *Food Research International*, *140*, 110044. https://doi.org/10.1016/j.foodres.2020.110044

Schoeman, L., du Plessis, A., Verboven, P., Nicolaï, B. M., Cantre, D., & Manley, M. (2017). Effect of oven and forced convection continuous tumble (FCCT) roasting on the microstructure and dry milling properties of white maize. *Innovative Food Science & Emerging Technologies*, *44*, 54-66. https://doi.org/10.1016/j.ifset.2017.07.021

Sharanagat, V. S., Suhag, R., Anand, P., Deswal, G., Kumar, R., Chaudhary, A., Singh, L., Singh Kushwah, O., Mani, S., Kumar, Y., & Nema, P. K. (2019). Physico-functional, thermo-pasting and antioxidant properties of microwave roasted sorghum [*Sorghum bicolor* (L.) Moench]. *Journal of Cereal Science*, *85*, 111-119. https://doi.org/10.1016/j.jcs.2018.11.013

Sumithra, B., & Bhattacharya, S. (2008). Toasting of corn flakes: Product characteristics as a function of processing conditions. *Journal of Food Engineering*, *88*(3), 419-428. https://doi.org/10.1016/j.jfoodeng.2008.03.001

Uriarte-Aceves, P. M., Rangel-Peraza, J. G., & Sopade, P. A. (2020). Kinetics of water absorption and relation with physical, chemical, and wet-milling properties of commercial yellow maize (*Zea mays* L.) hybrids. *Journal of Food Processing and Preservation*, *44*(7), e14509. https://doi.org/10.1111/jfpp.14509

Uriarte-Aceves, P. M., Sopade, P. A., & Rangel-Peraza, J. G. (2019). Physical, chemical and wet-milling properties of commercial white maize hybrids cultivated in México. *Journal of Food Processing and Preservation*, *43*(7), e13998. https://doi.org/10.1111/jfpp.13998

Velu, V., Nagender, A., Prabhakara Rao, P. G., & Rao, D. G. (2006). Dry milling characteristics of microwave dried maize grains (*Zea mays* L.). *Journal of Food Engineering*, *74*(1), 30-36. https://doi.org/10.1016/j.jfoodeng.2005.02.014

Wang, S., Ai, Y., Hood-Niefer, S., & Nickerson, M. T. (2019). Effect of barrel temperature and feed moisture on the physical properties of chickpea, sorghum, and maize extrudates and the

functionality of their resultant flours - Part 1. *Cereal Chemistry*, *96*(4), 609-620. https://doi.org/10.1002/cche.10149

Wani, I. A., Gani, A., Tariq, A., Sharma, P., Masoodi, F. A., & Wani, H. M. (2016). Effect of roasting on physicochemical, functional and antioxidant properties of arrowhead (*Sagittaria sagittifolia* L.) flour. *Food Chemistry*, *197*(Pt A), 345-352. https://doi.org/10.1016/j.foodchem.2015.10.125

Woo, K. S., Kim, M. J., Kim, H.-J., Lee, J. H., Lee, B. W., Jung, G. H., Lee, B. K., & Kim, S. L. (2018). Changes in the functional components and radical scavenging activity of maize under various roasting conditions. *Food Science and Biotechnology*, *27*(3), 837-845. https://doi.org/10.1007/s10068-017-0294-9

Xue, J., Inzero, J., Hu, Q., Wang, T., & Wusigale, Y. L. (2019). Development of easy, simple and low-cost preparation of highly purified phytoglycogen nanoparticles from corn. *Food Hydrocolloids*, *95*, 256-261. https://doi.org/10.1016/j.foodhyd.2019.04.041

Youn, K.-S., & Chung, H.-S. (2012). Optimization of the roasting temperature and time for preparation of coffee-like maize beverage using the response surface methodology. *LWT - Food Science and Technology*, *46*(1), 305-310. https://doi.org/10.1016/j.lwt.2011.09.014

Chapter 4

Variables related to microwave heating-toasting time and water migration assessment with kernel size approaches of specialty maize types

Nelly Lara[a,b*], Fernando Osorio[c], Jenny Ruales[a]

[a] Departamento de Ciencia de Alimentos y Biotecnología, Escuela Politécnica Nacional, Av. Ladrón de Guevara E11-253 Edificio 19 Quito, Ecuador

[b] CADET, Facultad de Ciencias Agrícolas, Universidad Central del Ecuador, Calle Universitaria s/n, Tumbaco, Ecuador

[c] Departamento de Ciencia y Tecnología de Alimentos, Universidad de Santiago de Chile, Santiago, Chile

ABSTRACT

Three main maize types with specialty kernels to make ready-to-eat maize by traditional toasting can innovate toward raw microwave maize. However, the toasting process of these Andean maize has remained with little knowledge about its science. Therefore, this study aimed to explore the behavior of a broad scope of variables in these maize types. The kernels were packed in sealed paper envelopes and subjected to six microwave heating-toasting times from 0 to 390 s. After, with actual kernel size approaches, water content WC, water ratio WR, and water loss WL were analyzed. In addition to WC, WR, and WL, the surface area S, volume V, and geometric mean diameter GMD behaved like time-related variables with high correlation depending on maize types and kernel dimensions. Thus, the WC, WR, and WL third-order polynomial regression curves computed with the spatial $(S/V)^2$ and distance $(GMD/2)^2$ approaches evidenced the water variation at each microwave heating-toasting time with a clear difference among maize types a0, a1, and a2. Regarding their exchange profiles without and with the spatial $(S/V)^2$ approach, the maximum rates showed significant differences between maize types and WC and WL. Likewise, the maximum rates displayed significant differences between the spatial $(S/V)^2$ and distance $(GMD/2)^2$ approaches, revealing a notable lack of consistency with the distance $(GMD/2)^2$ approach. Kernel size approaches reflected that water migration rates depended on differences in maize types. The basic information represents the first insight into more physical-based models of water diffusion during the raw microwave maize heating-toasting.

Keywords: floury maize; sweet maize; microwave; kernel dimensions; toasted kernel; water loss

* Corresponding author: CADET, Facultad de Ciencias Agrícolas, Universidad Central del Ecuador, Calle Universitaria s/n, Tumbaco, Ecuador. E-mail: nvlara@uce.edu.ec (N. Lara)

1. Introduction

In a commercial dry state, the three main underutilized maize types from the Andean region have specialty floury and sweet kernels to make entire ready-to-eat maize by toasting (Lara & Ruales, 2021). The two types of floury maize (*Zea maize* L. var. *amylacea*) have elongated kernels with a thin layer of matte yellow aleurone, thin pericarp, and entirely soft endosperm. In these maize types, endosperm softness is the key characteristic that guarantees easy-to-chew kernels. In contrast, the shrunken elongated kernels of sweet maize (*Zea maize* L. var. *saccharata*) have a translucent and more significant sugary-vitreous fraction than floury endosperm that becomes crispy after toasting (Lara & Ruales, 2021). According to unpublished results (Lara N), endosperm, germ, and pericarp represent 82, 13, and 6% in floury maize and 78, 17, and 5% in sweet maize types, respectively.

Toasting is an appropriate and peculiar technique that improves attributes such as flavor, color, texture, and appearance of kernel-based products (Ekezie et al., 2017). For this reason, toasting is one of the important final steps in ready-to-eat corn flakes that contributes to lowering the water content (0.01 – 0.03 g/g) and improving the crispness of this breakfast cereal (Sumithra & Bhattacharya, 2008). However, the maize traditional toasting process has remained in the Andean region with very little knowledge of its science. In addition, the kernel toasting in a pan is a slow process, and it can take 1200 to 1500 seconds compared to 390 seconds for floury maize and 320 seconds for sweet maize using microwave toasting (Lara & Ruales, 2021; Lara et al., 2021), where the remaining water contents are the lowest (0.021 to 0.023 g/g) (Lara & Ruales, 2021) and comparable to those in corn flakes levels (Sumithra & Bhattacharya, 2008). Microwave toasting may be an innovative application to prepare these soft and crispy kernels in short heating-toasting times, based on the increasing interest in microwave popping and its capacity to produce low-fat and healthy ready-to-eat food products (Rakesh & Datta, 2011). For example, microwave popcorn is the primary homemade snack compared to conventional popped corn (Gökmen, 2004). Furthermore, microwave technology, recognized as volumetric heating, can reach fast drying rates and enhance the food quality attributes (Chandrasekaran et al., 2013). Advances in microwave heating imply current popularity over conventional techniques, such as drying and toasting (Ekezie et al., 2017), suggesting the pertinence of developing science-supported and physics-based models related to microwave volumetric heating, minimizing the empirical assumptions (Pham et al., 2020; Welsh et al., 2021).

Several assumptions are required to model the microwave thin-layer drying using Fick's second law of diffusion for conventional geometry samples and long-time drying (Jahanbakhshi et al., 2020;

Shirkole & Sutar, 2018). The latest reviews summarize microwave convective drying developments, including modeling advances derived from the Fickcian law, physics-based simulations (Kumar & Karim, 2019), and the main challenges for developing multiscale models in food drying (Welsh et al., 2018). In addition, moisture-dependent effective diffusivity appears as an objective approach in convective drying food materials; a 3D simulation based on the thickness ratio from zero to a time (t) is critical to visualize the spatial water distribution inside the sample (Khan et al., 2016). On the other hand, considering the arbitrary shape of cereal kernels seems reasonable to adopt different volume-to-surface ratios (V/S), i.e., for the sphere ($V/S = r_0/3$), cylinder ($V/S = r_0/2$), and the half-thickness of the slab ($V/S = r_0$) to determine the moisture-dependent effective diffusivity. Thus, for cereal kernels with complex shapes, the squared surface-to-volume ratio $(S/V)^2$ replaces the center of symmetry to surface distance (X^2) in general solutions in the neighborhood of time zero and time greater than zero (Becker, 1959), implying that the ratio $(S/V)^2$ ascribed to maize kernel geometric properties (Lara & Ruales, 2021) contribute to explain the water diffusion variation at times zero to infinity. However, the assumptions required to apply Fick's second law of diffusion do not satisfactorily describe the maize kernel drying by microwave heating (Shivhare et al., 1994), suggesting that microwave drying depends on a broad range of time-related variables, e.g., the drying rate differs from kernel sizes (Becker, 1959). Thus, the modeling kinetics of maize kernel drying in microwave chambers implies a more complex interpretation of water ratio (Shivhare et al., 1994). Even more, in microwave toasting, where, e.g., the maize kernel expansion increases the surface area and volume by the heating-toasting effect (Lara & Ruales, 2021), the mathematical interpretation may involve more physics-based approaches depending on a broad scope of time-related variables to minimize the empirical hypotheses. However, there is a lack of basic information on these specialty maize types to hypothesize the water migration mechanism in maize kernels subjected to microwave heating intervals until complete toasting.

Conventional (Schoeman et al., 2017) and microwave (Lara & Ruales, 2021) toasting cause an increase in maize kernel volume ascribed to internal expansion generated by water migration. As a function of water content, the volume, surface area variations, and true density provide empirical rates for mass transfer modeling in coffee beans (Bustos-Vanegas et al., 2018). However, no earlier microwave toasting studies used the floury and sweet specialty maize types to predict the toasting kinetics associated with kernel size approaches. Therefore, based on previous studies to evaluate structural changes (Lara et al., 2021) and physical properties (Lara & Ruales, 2021) before and after microwave toasting, the objectives of this study by maize type aimed to generate basic information on three main aspects. First, to explore correlations between a broad scope of variables (water content, water ratio, water loss, kernel sizes, true density, kernel surface color, milling

average particle size, and flour hydration properties) obtained at six microwave heating-toasting times. Second, to fit the curves of the time-related variables (water content, ratio, and loss) without and with two kernel size approaches. Third, to evaluate the water content, ratio, and loss exchange profiles with two kernel size approaches.

2. Materials and methods

2.1. Maize types

Commercial batches of the primary three maize types with specialty kernels for toasting were obtained from a local market (Quito, Ecuador), and the water content was adjusted to 0.16 ± 0.1 g/g on a dry basis according to previous studies (Lara & Ruales, 2021; Lara et al., 2021). Table 1 contains raw kernel physical specifications determined for these maize types during preliminary trials. In addition, floury maize (*Zea mays* L. var. *amylacea*) has completely soft endosperm (a0 and a1) and sweet maize (*Zea mays* L. var. *saccharata*) shrunken kernels and a significant sugary-vitreous fraction (a2) (Lara & Ruales, 2021).

Table 1. Geometric, gravimetric, and color parameters of commercial raw maize kernels for toasting

Physical specifications	Floury maize a0	Floury maize a1	Sweet maize a2
Thickness (mm)	6.4 ± 0.2	6.1 ± 0.2	5.2 ± 0.2
GMD (mm)	10.3 ± 0.1	9.8 ± 0.2	8.5 ± 0.1
Surface area (mm^2)	335 ± 9	303 ± 10	226 ± 5
Volume (mm^3)	628 ± 29	529 ± 27	343 ± 11
Weight (g)	0.58 ± 0.02	0.47 ± 0.02	0.33 ± 0.01
Density (g ml^{-1})	0.93 ± 0.02	0.89 ± 0.03	0.94 ± 0.04
L* (lightness)	75.4 ± 0.3	72.4 ± 0.6	68.8 ± 0.8
h* (hue angle)	79.3 ± 0.6	78.3 ± 1.0	79.6 ± 0.6
a* (redness)	6.7 ± 0.2	10.8 ± 0.8	7.8 ± 0.5
b* (yellowness)	35.5 ± 1.0	52.2 ± 4.6	42.2 ± 4.4
C* (chroma)	36.2 ± 1.0	53.4 ± 4.5	42.9 ± 4.4

GMD: geometric mean diameter. Averaging values of 30-40 individual kernels.

2.2. Sample preparation

The equilibrated kernel samples of the three maize types (a0, a1, and a2) were randomly partitioned in 150 g for the microwave heating-toasting treatment at six times with equal intervals (0; 78; 156; 234; 312 and 390 s). Zero (t = 0 s) represented untreated kernel samples with known initial water content in all experimental units packed in foil gusseted bags by maize type. All experimental units and measurements were performed in triplicates following 3 blocks (a0, a1, and a2) x 6 treatments (0; 78; 156; 234; 312 and 390 s) arrangement.

2.3. Microwave heating-toasting

According to the experimental method used in previous studies (Lara & Ruales, 2021; Lara et al., 2021), the equilibrated kernel samples (150 g) contained in a sealed paper envelope (17.5 cm wide and 24 cm long) were subjected to a microwave oven (Panasonic, Shanghai, China) operated at 492 W and six heating-toasting times (0, 78, 156, 234, 312 and 390 s) with manual agitation intervals every 60 s. At the end of each heating-toasting time, the envelope was opened to release the generated water vapor, cooled, and weighed using a precision balance with a readability of 0.001 g (Boeco, Humburg, Germany). Next, all treated samples were packed in foil gusseted bags and stored at 4 °C for later measurements in whole and milled kernels.

2.4. Average geometric properties

Based on kernel dimensions (length, width, and thickness), the geometric mean diameter (GMD), sphericity, surface area (S), and volume (V) of individual kernels were obtained using the geometric expression previously reported and applied for these maize types (Lara & Ruales, 2021), popcorn (Karababa, 2006) and sweet maize (Karababa & Coşkuner, 2007). Each random sample consisted of 40 kernels per microwave heating-toasting time and replicate.

2.5. Average gravimetric properties

The individual maize kernels used to measure dimensions were also weighed (Lara & Ruales, 2021), and the weight to volume ratio gave the individual kernel density (Bustos-Vanegas et al., 2018; Erkinbaev et al., 2019). The volume difference between treated (V_t) and raw (V_0) individual kernel divided by treated (V_t) kernel volume (Schoeman et al., 2017; Sumithra & Bhattacharya, 2008) was associated with the internal porosity (IP) created by the effect of each heating-toasting time (Lara & Ruales, 2021) as in Eq. [1]. After (V_t) and before (V_0) being treated, the fraction between kernel volume was the expansion ratio (Schoeman et al., 2017) as in Eq. [2] at each microwave heating-toasting time, with three replications.

$$IPt = (V_t - V_0) / V_t \quad [1]$$

$$ERt = V_t / V_0 \quad [2]$$

Where V_t is the volume at time t, and V_0 is the volume at t = 0 in raw maize kernels.

2.6. Color measurements

Color parameters L*, a*, b*, C*, h*, and color difference (ΔE*) were determined on the surface of maize kernels at each microwave heating-toasting time following the method described for these maize types in a previous study (Lara & Ruales, 2021). All color data (L*, a*, b*, C*, h*, and ΔE*) were acquired using a 3nh_NH310 colorimeter, software CQCS3, main light D65, and a ϕ 4 mm measuring aperture device (Shenzhen 3NH Technology Co., LTD., China).

2.7. Particle size distribution

The kernel samples collected at each microwave heating-toasting time were reduced separately into flour using an ultra-centrifugal mill (Retsch ZM 200 Ultra centrifugal mill, Germany). Flour samples were equilibrated at 35 °C in a forced-air oven for 16 hours. Flour particle size distribution was determined by sifting and weighing the separated fractions through sieves (Prüfsiieb, Western Germany) with opening sizes of 630, 400, 315, 200, 90, 25, and 0 (pan) μm (Lara & Ruales, 2021), selected from a standard sieve stack used for quality testing of entire wheat flour (Doblado-Maldonado et al., 2013). The acquired weights in the adjacent sieves were the data to apply the statistical equations reported for the particle size analysis (Kalivoda et al., 2017; Velu et al., 2006).

2.8. Hydration properties

The water absorption capacity (WAC), swelling power (SP), and water-soluble index (WSI) were measured in maize flour using the suspension-centrifugation procedure (Lara & Ruales, 2002) with some modifications for weighing the sediment and supernatant fractions. Afterward, a supernatant volume of known weight was dried overnight and weighed (Lara & Ruales, 2021).

2.9. Water content, dimensionless water ratio, and water loss curves

By replication, the water amount determined by weight difference using oven drying at 104 ± 1 °C (Odjo et al., 2012) was the initial water content expressed on a dry basis (WC_0) in raw kernel equilibrated samples (t = 0). Then, for the rest of the heating-toasting times (78, 156, 234, 312, and 390 s), the water content was calculated, applying material balance relative to the water released at each time t according to Eq. [3] (Jiang et al., 2020).

$$WC_t = (m_0 \times WC_0 - m_0 + m_t) / m_t \text{ on dry basis} \quad [3]$$

Where WC_t is the water content at time t, m_0 is the maize kernel weight at t = 0, and m_t is the maize kernel weight at time t.

The equilibrium water content of several materials is comparatively smaller than water content (Jiang et al., 2020), and many researchers assume it is negligible in dimensionless water ratio expression (Jahanbakhshi et al., 2020; Kipcak & Doymaz, 2020). Hence, the water ratio (WR) appears in Eq. [4] as the water content at time t (WC_t) standardized to water content at time t = 0 (WC_0).

$$WR_t = WC_t / WC_0 \quad [4]$$

The weight difference determined by the sample before and after toasting gives the water amount released each time (Bustos-Vanegas et al., 2018). Therefore, the water loss at time t = 0 was zero, and Eq. [5] gave the water loss at time t (WL_t).

$$WL_t = (m_0 - m_t) / m_0 \quad [5]$$

2.10. Kernel size approaches

Considering the water migration in solids of arbitrary shape for wheat kernel drying (Becker, 1959) and the challenges to overcome in modeling maize kernel drying kinetics using microwaves (Shivhare et al., 1994), this study aimed to introduce two kernel size approaches into WC, WR, and WL curves. Hence, the two comparative kernel size approaches were the square of the surface-to-volume ratio $(S/V)^2$ as a spatial kernel size approach and the square of the half-geometric mean diameter $(GMD/2)^2$ equivalent to X^2 using actual geometric results. Then, multiplying $(S/V)^2$ and dividing $(GMD/2)^2$ in Eqs. [3, 4, and 5], the results display the water variation by mm^2 at time t as follows in Eqs. [6a, 6b, 7a, 7b, 8a, and 8b]:

Eq. [3] x $(S_t/V_t)^2$;	$WC_t = \{(m_0 \times WC_0 - m_0 + m_t) / m_t\} \times (S_t/V_t)^2$	[6a]
Eq. [3] / $(GMD_t/2)^2$;	$WC_t = \{(m_0 \times WC_0 - m_0 + m_t) / m_t\}/(GMD_t/2)^2$	[6b]
Eq. [4] x $(S_t/V_t)^2$;	$WR_t = \{WC_t / WC_0\} \times (S_t/V_t)^2$	[7a]
Eq. [4] / $(GMD_t/2)^2$;	$WR_t = \{WC_t / WC_0\} / (GMD_t/2)^2$	[7b]
Eq. [5] x $(S_t/V_t)^2$;	$WL_t = \{(m_0 - m_t) / m_0\} \times (S_t/V_t)^2$	[8a]
Eq. [5] / $(GMD_t/2)^2$;	$WL_t = \{(m_0 - m_t) / m_0\} / (GMD_t/2)^2$	[8b]

2.11. WC, WR, and WL regression curves without and with kernel size approaches

The models reported in the literature for microwave drying (Jahanbakhshi et al., 2020; Kipcak & Doymaz, 2020; Shirkole & Sutar, 2018) were applied using the three replications of the WC, WR, and WL experimental data to check the lack-of-fit. After that, a third-order polynomial regression was applied to describe the relationship between the dependent (WC, WR, and WL) and independent (heating-toasting time) variables according to Eqs. [9, 10, and 11], without and with kernel size approaches.

$$WC_t = a + bt + ct^2 + dt^3 \quad [9]$$

$$WR_t = a + bt + ct^2 + dt^3 \quad [10]$$

$$WL_t = a + bt + ct^2 + dt^3 \quad [11]$$

2.12. WC, WR, and WL exchange profiles without and with kernel size approaches

Finally, as a close reference to water migration or water diffusion, the first derivative indicated the exchange profiles relative to water migration evaluated as WC, WR, and WL. Thus, the mathematical differential was applied to obtain the first derivative from the average third-order polynomial regression curves without and with kernel size approaches using the OriginPro software (Version 2020, Microcal Inc., Northampton, MA, USA).

2.13. Statistical analysis

Under randomized experimental work, the maize types (a0, a1, a2) were treated separately at the six heating-toasting times (0, 78, 156, 234, 312, and 390 s). First, the experimental data of each measured variable, obtained at the six-time levels and their replicas, were organized in matrices by maize type to verify the normal distribution of the data using the Statgraphics Centurion XII software (Statgraphics centurion 18, USA). Second, Pearson's correlation was the statistical method to explore the relationship between physical properties, including heating-toasting time to determine the time-related variables. Third, considering the heating-toasting time as the independent variable, the simple and polynomial regressions performed by comparison models with the lack-of-fit test and three replication was used to establish whether linearized or more complex models describe the experimental data of WC, WR, and WL. Forth, the OriginPro software (Version 2020, Microcal Inc., Northampton, MA, USA) allowed obtaining the first derivative profiles from the average third-order polynomial regression curves by mathematical differential. In addition, two-way ANOVA and Tukey's test (means comparison) were performed in

separated matrixes to compare the influence of maize types against WC and WL and against two kernel size approaches.

3. Results and discussion

3.1. Microwave heating-toasting time-related variables

The experimental data presented a normal distribution, making the proposed statistical analysis feasible. All measured variables (WC, WR, WL, geometric characteristics, gravimetric properties, internal porosity, expansion ratio, space color parameters, milling average particle size, and flour hydration properties) were by maize type at six heating-toasting times (0, 78, 156, 234, 312, and 390 s) and three replications. In fact, including the microwave heating-toasting time, the relationship between measurement variables was explored by applying Pearson's correlation ($P \leq 0.05$), and the result displayed high, moderate, and low correlation coefficients by maize type. Thus, in Tables S1, S2, and S3, the gray color indicates low and moderate correlations with coefficients less than 0.7 (absolute value) for a0, a1, and a2, respectively. On the other hand, the correlation coefficient of more than 0.7 (absolute value) showed that physical properties could be generalized as time-related variables with positive and negative relationships. Therefore, in addition to WC, WR, and WL, most of the physical properties correlated with the microwave heating-toasting time when the initial water content (time t = 0) was 0.16 ± 01 g/g on a dry basis. Sweet maize, a2 showed more good correlations (Table S3) than the floury maize types a1 (Table S2) and a0 (Table S1). Moreover, floury maize a0 displayed fewer good correlations than floury maize a1. These results were consistent with the significant differences in GMD, surface area (S), volume (V), kernel density, color parameters (a*, b*, and C*), and color difference ΔE* by the same maize types (a0, a1, and a2) and kernel conditions (raw and toasted kernels) reported in a previous study (Lara & Ruales, 2021). This fact demonstrated that the number of time-related variables with good correlations depended on the maize types.

WC, WR, bulk density, kernel density, kernel weight, C* (in a1 and a2), L*, b*, h* and parameters, milling average particle size, and water-soluble index negatively correlated with the microwave heating-toasting time, whereas WL, kernel dimensions (length, width, thickness, GMD, sphericity, surface area, and volume), internal porosity, expansion ratio, C* (in a0), a* and color difference (ΔE*), and flour hydration properties (water absorption capacity and swelling power) positively correlated with the microwave heating-toasting time (Table 2). On the other hand, kernel thickness (KT) correlated with the microwave heating-toasting time with 0.866 ± 0.006 in all maize types (Table 2). This kernel dimension was consistent in correlations coefficients with the kernel density,

GMD, volume, and surface area. In addition to the kernel size relevance, the experimental (unfilled markers) and fit (drawn curves) relationships between density and volume (Fig. 1) efficiently illustrated the significant difference attributed to kernel sizes by maize types (Lara & Ruales, 2021).

Table 2. Positive and negative correlations (n = 18, $P \leq 0.05$) between physical properties and microwave heating-toasting time (0, 78, 156, 234, 312, and 390 s) illustrate the time-related variables by maize types.

	Correlation coefficients by maize types		
Time-related variables⸸	**a0**	**a1**	**a2**
WC: water content (g/g)	-0.9838	-0.9871	-0.9829
WR: water ratio	-0.9877	-0.9919	-0.9889
WL: water loss (g/g)	0.9801	0.9796	0.9684
APS: milling average particle size (µm)	-0.9564	-0.9744	-0.9415
WAC: water absorption capacity (g/g total solids)	0.9682	0.9791	0.8629
SP: swelling power (g/g insoluble solids)	0.9665	0.9788	0.8679
L*: color parameter	-0.9302	-0.9327	-0.9970
a*: color parameter	0.9499	0.9456	0.3412
h*: color parameter	-0.9210	-0.9312	-0.9257
ΔE*: color difference	0.9168	0.8766	0.9899
BD: bulk density (g/mL)	-0.9154	-0.9093	-0.9029
KD: individual kernel density (g/mL)	-0.9199	-0.9034	-0.8960
KT: kernel thickness (mm)	0.8695	0.8715	0.8576
GMD: geometric mean diameter (mm)	0.8687	0.8840	0.8778
KSA: kernel surface area (mm^2)	0.8669	0.8843	0.8803
KV: kernel volume (mm^3)	0.8553	0.8869	0.8857
IP: internal porosity	0.8669	0.8726	0.8631
KW: individual kernel weight (g)	-0.7787	-0.8753	-0.9537
WSI: water-soluble index (g/100 g total solids)	-0.7765	-0.7086	-0.8568
KS: kernel sphericity	0.6552	0.8092	0.7995
ER: expansion ratio	0.5184	0.8630	0.8678
KWth: kernel width (mm)	0.4243	0.4863	0.7663
KL: kernel length (mm)	0.4586	0.7680	0.8964
C*: color parameter	0.4137	-0.7143	-0.9446
b*: color parameter	-0.0792	-0.7732	-0.9555

⸸ Gray color indicates low and moderate correlations between physical properties and microwave heating toasting time.

Density decreased when kernel volume increased by the effect of the microwave heating-toasting process. This result agreed with the density reduction in toasted coffee beans (Bustos-Vanegas et al., 2018). Simple regression evidenced that the squared-Y logarithmic-X model adequately described the relationship between this pair of time-related variables, calculated from geometric properties and the weight of individual kernels. Likewise, adjusted R-squared (determination coefficient), standard error, and Durbin-Watson statistics indicated a good fit of density to volume (Table 3). Therefore, the kernel dimension differences by maize types validated the reliability of the kernel size approaches tried in this study. Additionally, the relationship of individual kernel

density to volume can represent a quick and easy way of estimating apparent density in toasted maize kernels.

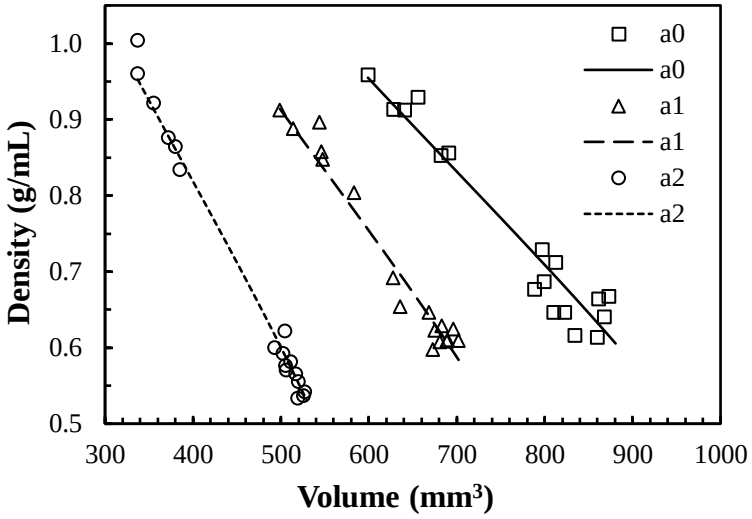

Figure 1. Experimental data and regression curves between density and volume of individual kernels by floury (a0 and a1) and sweet (a2) maize types subjected to microwave heating-toasting time from 0 to 390 s.

Table 3. Regression model and statistical parameters ($P \leq 0.05$) for the relationship between density (KD) and volume (KV) of individual maize kernels at six microwave heating-toasting times (0, 78, 156, 234, 312, and 390 s)

Statistics and parameters⁜	**a0**	**a1**	**a2**
Model for KD versus KV	$Y = (a + b \times \ln X)^{0.5}$		
Correlation coefficient (*r*)	-0.97	-0.98	-1.00
Intercept	10.25 ± 0.55	10.00 ± 0.38	9.05 ± 0.16
Slope	-1.46 ± 0.08	-1.47 ± 0.06	-1.40 ± 0.03
Adj. R-squared	94.77	97.49	99.42
Standard Error	0.044	0.027	0.017
Durbin-Watson ($P > 0.05$)	0.507	0.501	0.963

⁜ Simple regression with three replications for floury maize (a0 and a1) and sweet (a2) maize types. Durbin-Watson's values indicated non-serial autocorrelation in the residuals.

3.2. WC, WR, and WL regression curves without and with kernel size approaches

The models used for microwave drying (Jahanbakhshi et al., 2020; Kipcak & Doymaz, 2020; Shirkole & Sutar, 2018) generated kinetic curves of WC, WR, and WL with a highly significant lack-of-fit ($P \leq 0.01$), possibly due to the difference between drying a thin layer on an open tray and toasting inside a closed package. However, simple regression performed by comparison models with the lack-of-fit test and three replication evidenced more complex models describing the WC, WR, and WL experimental data for the three maize types. Therefore, third-order polynomial models appeared adequate to describe the relationship of WC, WR, and WL with the heating-toasting time. Consequently, in Figs. 2a, 3a, and 4a, the drawn average curves showed the third-

order polynomial regression results and described the experimental data (unfilled markers) measured at each microwave heating-toasting time without kernel size approaches. In Figs. 2c. 3c and 4c, the curves displayed the spatial kernel size $(S/V)^2$ approach and in Figs. 2e, 3e, and 4e, the curves indicated the center of the symmetry to surface distance assumed as $(GMD/2)^2$ approach. Table S4 includes the intercepts (a) and constants (b, c, d) of the average third-order polynomial regression models according to Eqs. [9, 10, and 11] by maize types without kernel size approach compared to the spatial $(S/V)^2$ and distance $(GMD/2)^2$ approaches. In addition, the main statistical parameters related to WC, WR, and WL regression curves clustered by maize types (Table 4) demonstrated the high (no color) and low (gray color) reliability of third-order polynomial regression models without and with kernel size approach.

Water contents of 0.16 ± 0.01 g/g on a dry basis were the initial experimental values in WC regression curves (Fig. 2a) and exhibited almost similar relationships between the decreasing water content and increasing microwave heating-toasting time for the three maize types. These results implied that the remaining water contents in toasted maize kernels were between those (0.01 – 0.03 g/g) reported for toasted corn flakes (Sumithra & Bhattacharya, 2008) and were consistent with the non-significant levels of the remaining water in the microwave toasted kernels of these maize types (Lara & Ruales, 2021). However, the calculated initial water contents were slightly higher than their experimental counterparts, while the estimated final water contents were close to zero with a high coincidence to the measured values. This fact indicated that the equilibrium water content could tend to zero. In addition, fixing the average value of initial water content in the regression models could enhance the statistical parameters that reflect high reliability.

The WC regression curves (Fig. 2c) computed with the actual $(S/V)^2$ approach (g/g mm^2) reflected the spatial water distribution at each microwave heating-toasting time with a clear difference among maize types a0, a1, and a2 due to the variation in kernel surface area (S) and volume (V) inherent to each maize type. Also, by maize types, the WC regression curves (Fig. 2e) with the actual $(GMD/2)^2$ (g/g mm^2) approach appeared well set apart as the result of the water migration from the center of the symmetry to the surface distance, reflecting the differences in geometric mean diameter (GMD) ascribed to maize types. These results agreed with the significant differences in GMD, S, and V demonstrated by maize types and between raw and toasted kernels (Lara & Ruales, 2021) and suggested that it seems reasonable to consider the time-related kernel size approaches in water migration to the kernel surface and the surrounding medium within the package during heating-toasting of raw microwave maize.

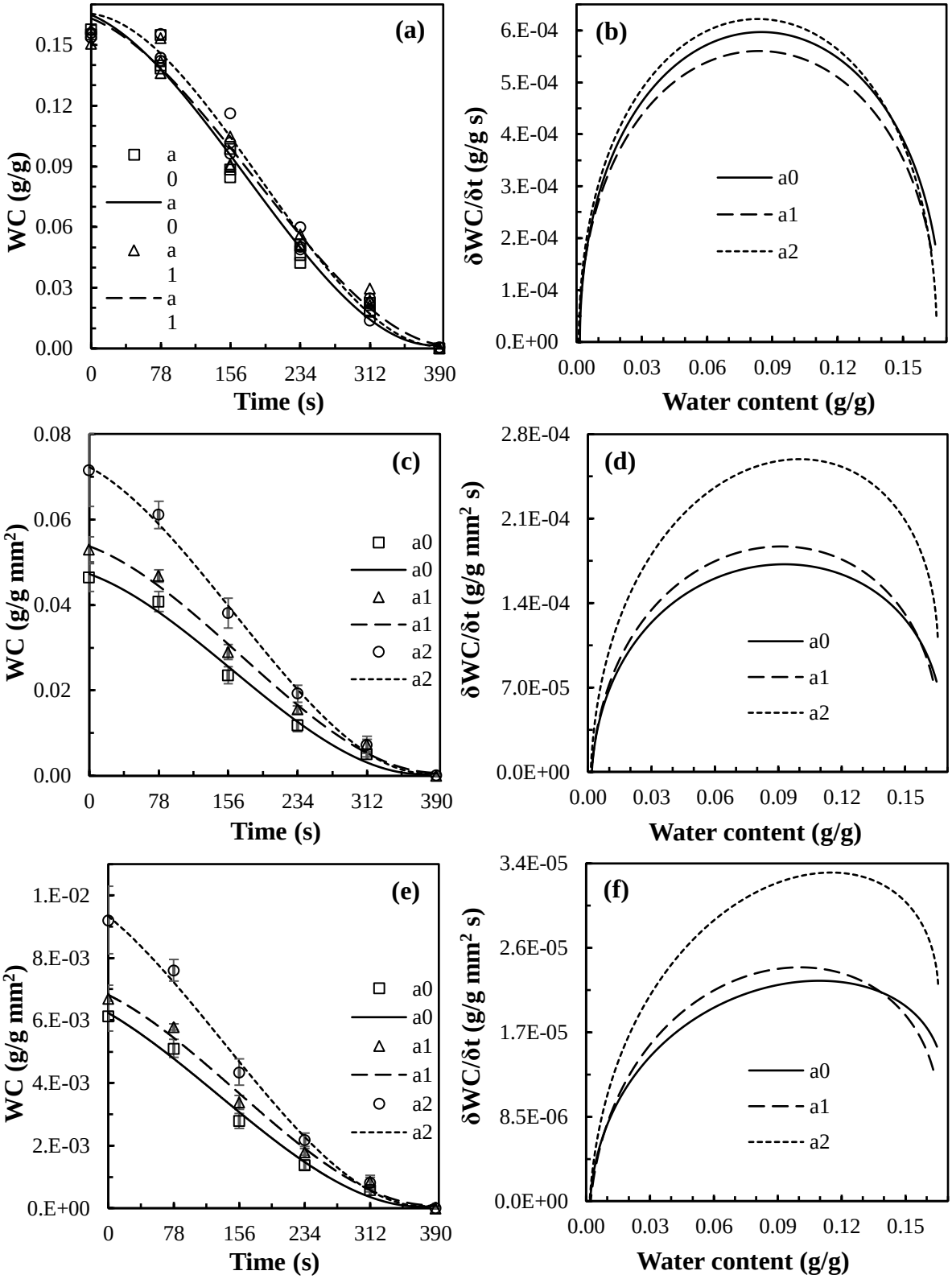

Figure 2. WC regression curves on a dry basis and their exchange profiles (δWC/δt in absolute value) of floury (a0 and a1) and sweet (a2) maize kernels. Without kernel size approaches (**a**) and (**b**). Spatial $(S/V)^2$ approach (**c**) and (**d**). Distance $(GMD/2)^2$ approach (**e**) and (**f**). WC: water content. S: surface area, V: volume, and GMD: geometric mean diameter of individual maize kernels.

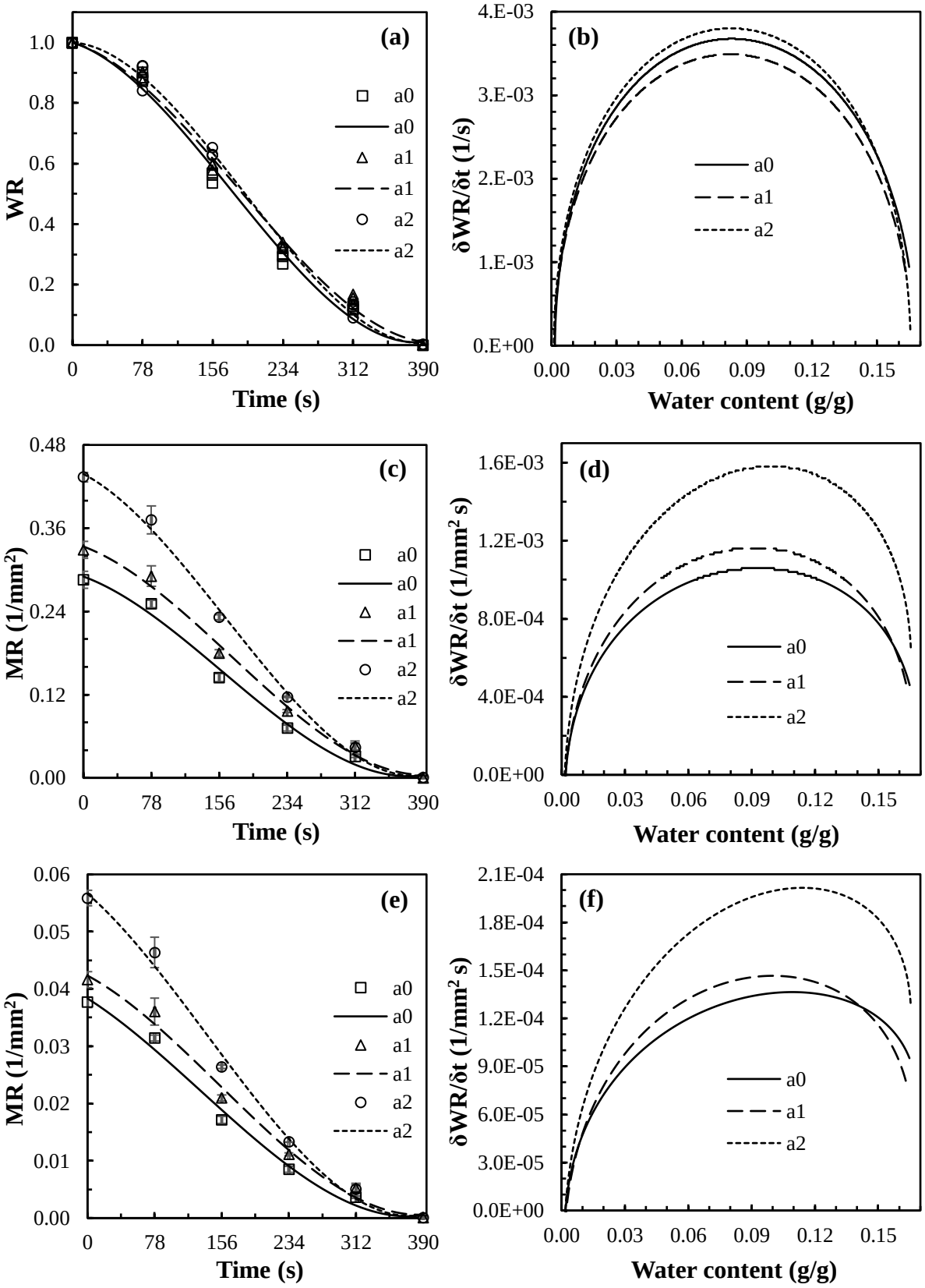

Figure 3. WR regression curves on a dry basis and their exchange profiles (δWR/δt in absolute value) of floury (a0 and a1) and sweet (a2) maize kernels. Without kernel size approaches (**a**) and (**b**). Spatial $(S/V)^2$ approach (**c**) and (**d**). Distance $(GMD/2)^2$ approach (**e**) and (**f**). WR: water ratio. S: surface area, V: volume, and GMD: geometric mean diameter of individual maize kernels.

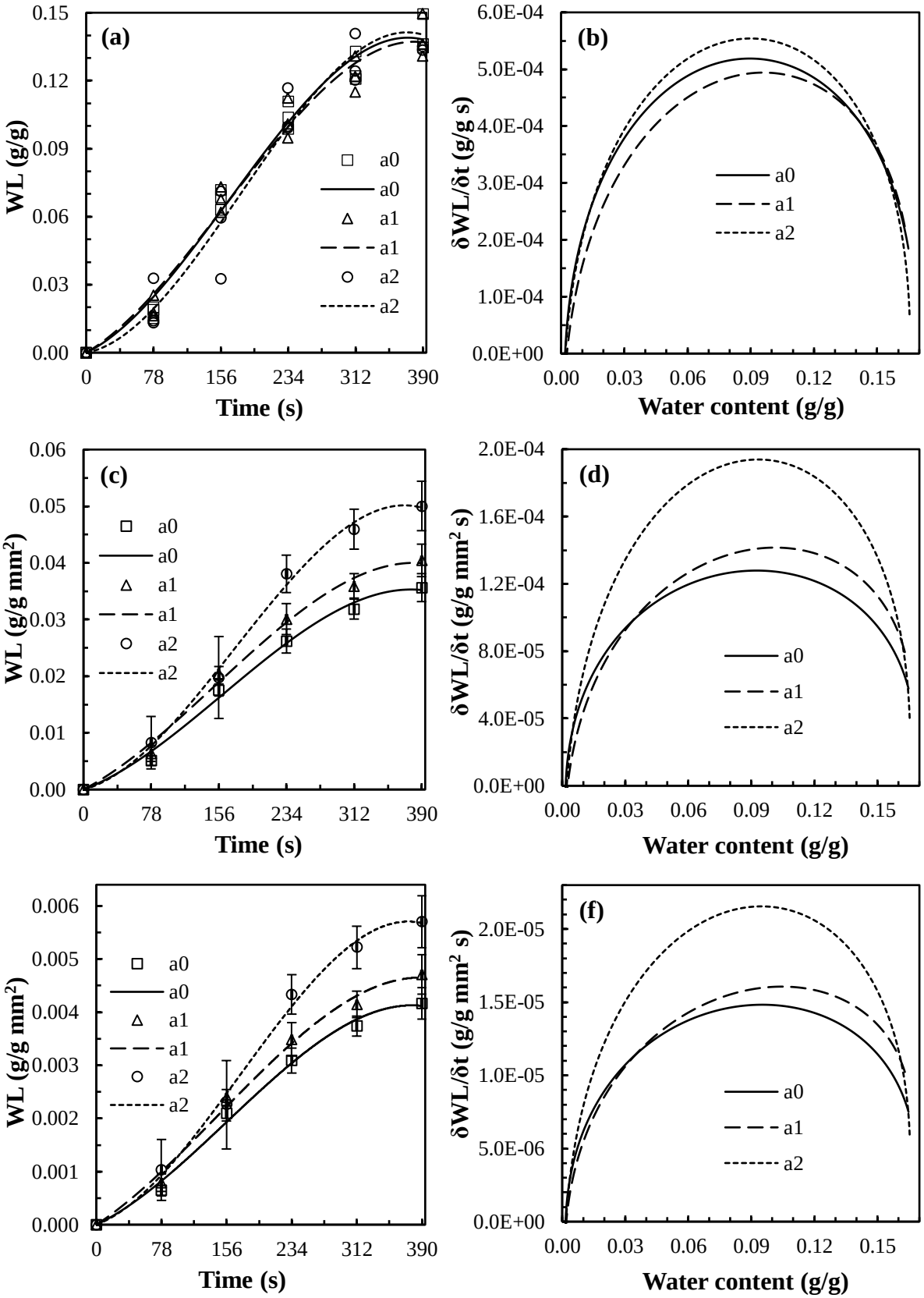

Figure 4. WL regression curves on a dry basis and their exchange profiles (δWL/δt) of floury (a0 and a1) and sweet (a2) maize kernels. Without kernel size approaches (**a**) and (b). Spatial $(S/V)^2$ approach (**c**) and (**d**). Distance $(GMD/2)^2$ approach (**e**) and (**f**). LW: water loss. S: surface area, V: volume, and GMD: geometric mean diameter of individual maize kernels.

WR or dimensionless moisture ratio in the drying process can be another generalized method to analyze the remaining water content in heating-toasting kernels standardized in initial water content. Therefore, WR regression curves (Fig. 3a) exhibited the same trends for floury (a0 and a1) and sweet maize (a2) types already discussed based on WC regression curves. However, significant ($P < 0.05$) serial autocorrelations and lack-to-fits observed in Table 4 are challenging to overcome with more complex solutions in the future. Fig. 3c displays the WR regression curves with the actual spatial $(S/V)^2$ approach ($1/mm^2$) relative to actual surface area and volume by maize type. Concerning the center of symmetry to surface distance $(GMD/2)^2$ approach, Fig. 3e shows variations ($1/mm^2$) ascribed to actual GMD differences inherent to maize types.

The WL regression curves with a negative relationship to WC curves exhibited similar trends for the three maize types (Fig. 4a). Thus, when WC decreased in Fig. 2a, WL rose with increasing microwave heating-toasting time in Fig. 4a. The WL regression curves in Fig. 4c also revealed the spatial water content distribution results associated with the $(S/V)^2$ approach, observed in WC (g/g mm^2) and WR (mm^2). Likewise, the WL regression curves in Fig. 4e exhibited variations between floury and sweet maize types due to the $(GMD/2)^2$ approach. In addition, the statistical parameters of the third-order polynomial WL regression model indicated a good fit with non-significant autocorrelation and lack-of-fit ($P > 0.05$) without and with kernel size approaches (Table 4). These findings proved that the WL depended on the maize kernel S, V, and GMD and was consistent with the cavities created in individual maize kernels during toasting, measured as standardized volume increases (Schoeman et al., 2017), internal porosity (Lara & Ruales, 2021), and the expansion in toasted coffee beans (Bustos-Vanegas et al., 2018). On the other hand, the WC (Fig 2e), WL (Fig. 4e), and WR (Fig. 3e), with the $(GMD/2)^2$ approach, were lower than those in Fig. 2c, Fig. 4c, and Fig. 3c with the $(S/V)^2$ approach, respectively.

3.3. WC, WR, and WL exchange profiles without and with kernel size approaches

The first derivative obtained from the average third-order polynomial regression curves indicated the exchange profiles of water distributed in maize kernels without and with kernel size approaches. Thus, Figs. 2b, 3b, and 4b revealed the WC, WR, and WL shift profiles without kernel size approach plotted against the water content. In Figs. 2d. 3d and 4d, the exchange profiles displayed the spatial $(S/V)^2$ approach and Figs. 2f, 3f, and 4f indicated the exchange profiles from the center of the symmetry to surface distance approach assumed as $(GMD/2)^2$. In Table 4, the last three rows show the WC, WR, and WL maximum rates and the time-related water content values on the X-axis at those top rates without and with kernel size approaches. Regarding these last

results, Tukey's comparison means revealed the significant differences clustered by maize types with WC and WL in Table 5a and with kernel size approaches in Table 5b.

Table 4. Statistical parameters of the third-order polynomial regression models ($P \leq 0.05$) and variables linked to maximum rates without and with kernel size approaches for floury (a0 and a1) and sweet (a2) maize kernels.

Statistical and kinetic parameters	WC curves			WR curves			WL curves		
	a0	a1	a2	a0	a1	a2	a0	a1	a2
Average values without maize kernel size approaches									
Adj. R-square (%)	98.38	98.21	98.05	99.31	99.43	99.56	98.37	97.78	95.59
Standard Error	0.008	0.008	0.009	0.032	0.029	0.026	0.007	0.008	0.012
Durbin-Watson	0.247	0.282	0.535	0.002	0.001	0.447	0.206	0.328	0.871
Lack-of-fit	0.059	0.148	0.656	0.000	0.000	0.105	0.051	0.083	0.587
MR⇟	$5.97\ 10^{-4}$	$5.60\ 10^{-4}$	$6.22\ 10^{-4}$	$3.68\ 10^{-3}$	$3.49\ 10^{-3}$	$3.80\ 10^{-3}$	$5.19\ 10^{-4}$	$4.94\ 1^{-4}$	$5.54\ 10^{-4}$
Water content (g/g)	0.085	0.084	0.083	0.083	0.082	0.083	0.089	0.096	0.090
Time (s)	173	183	190	177	186	191	166	162	180
Average values with spatial maize kernel $(S/V)^2$ approach									
Adj. R-square (%)	98.05	98.72	97.85	98.66	98.80	99.32	97.87	97.55	97.12
Standard Error	0.003	0.002	0.004	0.013	0.014	0.014	0.002	0.002	0.003
Durbin-Watson	0.135	0.075	0.316	0.009	0.015	0.069	0.270	0.284	0.815
Lack-of-fit	0.008	0.005	0.302	0.000	0.001	0.053	0.064	0.065	0.671
MR⇟⇟	$1.72\ 10^{-4}$	$1.87\ 10^{-4}$	$2.59\ 10^{-4}$	$1.06\ 10^{-3}$	$1.16\ 10^{-3}$	$1.58\ 10^{-3}$	$1.28\ 10^{-4}$	$1.42\ 10^{-4}$	$1.94\ 10^{-4}$
Water content (g/g)	0.093	0.091	0.100	0.093	0.091	0.099	0.093	0.101	0.093
Time (s)	160	170	163	160	170	164	160	152	174
Average values with the center of symmetry to surface distance $(GMD/2)^2$ approach									
Adj. R-square (%)	96.86	96.62	97.24	98.76	99.52	99.02	98.20	97.81	96.90
Standard Error	0.000	0.000	0.001	0.002	0.001	0.002	0.000	0.000	0.000
Durbin-Watson	0.069	0.006	0.223	0.001	0.039	0.028	0.384	0.299	0.764
Lack-of-fit	0.051	0.007	0.159	0.000	0.002	0.002	0.082	0.116	0.737
MR⇟⇟	$2.22\ 10^{-5}$	$2.35\ 10^{-5}$	$3.31\ 10^{-5}$	$1.36\ 10^{-4}$	$1.47\ 10^{-4}$	$2.02\ 10^{-4}$	$1.48\ 10^{-5}$	$1.61\ 10^{-5}$	$2.15\ 10^{-5}$
Water content (g/g)	0.110	0.101	0.115	0.109	0.100	0.114	0.095	0.105	0.095
Time (s)	132	153	138	132	154	139	156	146	172

WC: water content, WR: water ratio, WL: water loss, MR: maximum rate, S: surface area, V: volume, and GMD: geometric mean diameter. The gray color indicates significant serial autocorrelation in the residual (Durbin-Watson statistic) and significant lack-of-fit ($P < 0.05$). Water content and time at the maximum rate.

⇟ MR: (g/g s) in WC and WL curves, and (1/s) in WR.

⇟⇟ MR: (g/g mm^2 s) in WC and WL curves, and ($1/mm^2$ s) in WR curves.

In Fig. 2b, 3b, and 4b without kernel size approaches, the exchange profiles in WC, WR, and WL, respectively, reached the maximum values during the falling rate period with a rapid migration of vapor water from the center to the kernel surface area by maize types. Thus, sweet maize a2 had the highest, floury maize a0 an intermediate, and floury maize a1 had the lowest maximum rates in the WC (Fig 2b), WR (Fig. 3b), and WL (Fig. 4b) shift profiles. A high internal porosity in sweet maize reflected a high volumetric expansion (Lara & Ruales, 2021) ascribed to water migration and thermal exchanges by the toasting effect (Bustos-Vanegas et al., 2018). Relative to this finding, the internal porosity could improve water migration because the molecular diffusion is faster in pores than in compact solids (Chen et al., 2009). Afterward, the decrease of maximum rates depended on the decreasing water content in the maize kernels. Therefore, these WC, WR, and WL exchange profiles almost did not have a constant rate, agreeing with that reported for maize microwave drying (Shivhare et al., 1994). On the other hand, the evaporation rate from the surface area to the surrounding medium caused a maximum swelling of the paper package directly related to the top rate associated with the microwave volumetric heating capacity (Kipcak & Doymaz, 2020).

The WC (Fig. 2d), WR (Fig. 3d), and WL (Fig.4d) exchange profiles mainly reflected the variation between floury and sweet maize types due to the spatial kernel size $(S/V)^2$ approach. Also, with differences between floury and sweet maize types, the WC (Fig. 2f), WR (Fig. 3f), and WL (Fig.4f) exchange profiles displayed maximum rates within an early and non-constant period ascribed to the center of symmetry to surface distance applied as $(GMD/2)^2$ approach. As a result, for both $(S/V)^2$ and $(GMD/2)^2$ approaches, the exchange profiles rapidly reached maximum rates with position shifts on the X-axis water content. Furthermore, the X-axis water content linked to the top rates and the corresponding time also indicated the highest rates achieved in shorter times (Table 4) attributed to kernel size influence on water migration. However, reaching the top values was more delayed in sweet maize than floury maize with and without kernel size influence ascribed to compact structure in its sugary-vitreous fraction (Lara et al., 2021). This fact may agree with the results in the coffee bean WL due to delayed porosity created in a conventional toasting process up to 400 s (Oliveros et al., 2017).

On the other hand, the significant differences in maximum rates in Table 5a agreed with the arrangement of exchange profiles by maize types in Figs 2b and 4b without kernel size approaches; in Figs. 2d and 4d with spatial $(S/V)^2$ influence, and these results were consistent with the average value variants reported in Table 4. In contrast, the differences in maximum rates with the $(GMD/2)^2$ approach were non-significant and non-consistent with the shift profiles in Figs. 2f and 4f, implying a lack of reliability with very low values generated by the $(GMD/2)^2$ approach.

Table 5. Tukey comparison means ($P \leq 0.05$) of the maximum values from the first derivative profiles clustered according to maize types and by the influence of water migration viewpoints and kernel size approaches.

(a) Without and with KSA	**Maize types (WC + WL)**			**Expressing methods (a0 + a1 + a2)**	
	a0	**a1**	**a2**	**WC**	**WL**
Without KSA					
MR (g/g s)	5.58 10^{-4} b	5.27 10^{-4} a	5.88 10^{-4} c	5.93 10^{-4} b	5.22 10^{-4} a
Water content (g/g)	0.087 a	0.090 a	0.087 a	0.084 a	0.092 b
Time (s)	170 a	173 a	185 a	182 a	169 a
$(S/V)^2$ (mm^2)					
MR (g/g mm^2 s)	1.50 10^{-4} a	1.65 10^{-4} a	2.27 10^{-4} b	2.06 10^{-4} b	1.55 10^{-4} a
Water content (g/g)	0.093 a	0.096 a	0.097 a	0.095 a	0.096 a
Time (s)	160 a	161 a	169 a	164 a	162 a
$(GMD/2)^2$ (mm^2)					
MR (g/g mm^2 s)	1.85 10^{-5} a	1.98 10^{-5} a	2.73 10^{-5} a	2.63 10^{-5} a	1.75 10^{-5} a
Water content (g/g)	0.103 a	0.103 a	0.105 a	0.109 a	0.098 a
Time (s)	144 a	150 a	155 a	141 a	158 a
(b) Expressing methods	**Maize types [$(S/V)^2$ + $(GMD/2)^2$]**			**KSA (a0 + a1 + a2)**	
	a0	**a1**	**a2**	**$(S/V)^2$**	**$(GMD/2)^2$**
WC (g/g mm^2)					
MR (g/g mm^2 s)	9.71 10^{-5} a	1.05 10^{-4} a	1.46 10^{-4} a	2.06 10^{-4} b	2.63 10^{-5} a
Water content (g/g)	0.102 a	0.096 a	0.108 a	0.095 a	0.109 b
Time (s)	146 a	162 a	151 a	164 b	141 a
WR (1/mm^2)					
MR (1/mm^2 s)	5.98 10^{-4} a	6.54 10^{-4} a	8.91 10^{-4} a	1.27 10^{-3} b	1.62 10^{-4} a
Water content (g/g)	0.101 a	0.096 a	0.107 a	0.094 a	0.108 b
Time (s)	146 a	162 a	152 a	165 b	142 a
WL (g/g mm^2)					
MR (g/g mm^2 s)	7.14 10^{-5} a	7.91 10^{-5} a	1.08 10^{-4} a	1.55 10^{-4} b	1.75 10^{-5} a
Water content (g/g)	0.094 a	0.103 b	0.094 a	0.096 a	0.098 a
Time (s)	158 b	149 a	173 c	162 a	158 a

KSA: kernel size approach, WC: water content, WR: water ratio, WL: water loss, MR: maximum rate, S: surface area, V: volume, and GMD: geometric mean diameter. Water content and time at the maximum rate.

Different letters in each row indicate significant variation ($P \leq 0.05$) by maize types, expressing methods, and kernel size approach.

Likewise, statistical differences were significant between WC and WL without kernel size approaches and with the spatial $(S/V)^2$ approach, whereas they were similar with the $(GMD/2)^2$ approach (Table 5a), reflecting the last approach a significant lack of influence on the results by maize types, as well as in WC and WL. Concerning the WC, WR, and WL comparison by maize types and kernel size approaches, reported in Table 5b, the maximum rates mainly revealed

significantly higher effects with the $(S/V)^2$ approach than those with the $(GMD/2)^2$ approach. By maize types, the maximum rates were similar and non-consistent with the exchange profile differences between floury and sweet maize types observed in Figs 2d, 2f, 3d, 3f, 4d, and 4f. These differences disappeared due to an overlapping effect associated with the high variation between the two kernel size approaches. In addition, significant differences caused by the kernel size approaches were evident in the water content and time at the maximum rates for WC and WR, while for WL, these parameters were similar. However, a greater influence due to sweet maize than floury maize was detectable on the microwave heating-toasting time at the maximum rates for WL. This finding could indicate that WL better interpreted the water migration in these maize types, agreeing with the non-significant lack-of-fit of the third-order polynomial regression model. These results, evaluated as WC, WR, and WL, revealed that the actual spatial $(S/V)^2$ approach better explained the exchange profiles derived from the water variations in maize kernels by the microwave heating-toasting effect. Also, WL could properly explain the heating-toasting of raw microwave maize governed by volumetric heating with water migration to the surface and the surrounding medium inside a package.

4. Conclusions

The three maize types with specialty kernels for toasting presented a broad scope of physical properties with good correlations for the microwave heating-toasting time intervals from 0 to 390 s, and the initial water content in raw microwave maize standardized to 0.16 ± 01 g/g on a dry basis. Thus, the geometric properties inherent to maize types validated the kernel size approaches applied to evaluate WC, WR, and WL. The third-order polynomial regression model appeared suitable to describe WC, WR, and WL without and with actual spatial $(S/V)^2$ and distance $(GMD/2)^2$ approaches. The regression curves with the actual $(S/V)^2$ and $(GMD/2)^2$ approaches reflected the water distribution at each microwave heating-toasting time with clear differences among maize types, whereas these curves looked almost overlapping without the kernel size approaches. The remaining water content in all toasted microwave maize was equivalent to those reported for toasted corn flakes. The WC, WR, and WL exchange profiles, without and with these kernel size approaches, rapidly reached maximum rates within early and non-constant rates. At the maximum rates, the X-axis water content slightly varied, and the time was shorter with the actual $(S/V)^2$ and $(GMD/2)^2$ approaches than without kernel size approaches. WC and WL showed significant differences regarding regression curves and exchange profiles, and WL could better explain the water migration in raw microwave maize than WC. Finally, the actual $(S/V)^2$ and $(GMD/2)^2$ approaches were significantly different, and the $(S/V)^2$ approach was consistent with regression curves and exchange profiles of these maize types with specialty kernels for raw microwave maize.

Funding statement

The author carried out this work within the DOCT-DI-2019-49 Project framework with the institutional sponsor of the Universidad Central del Ecuador.

Data availability statement

Data is available on request.

Conflict of interest

The authors declare no conflict of interest.

Acknowledgments

This work was supported by the Research Program of the Universidad Central del Ecuador. In addition, the authors would like to thank the Universidad Central del Ecuador, Escuela Politécnica Nacional, and Universidad de Santiago de Chile research laboratories.

References

Becker, H. A. (1959). A study of diffusion in solids of arbitrary shape, with application to the drying of the wheat kernel. *Journal of Applied Polymer Science*, *1*(2), 212-226.

Bustos-Vanegas, J. D., Corrêa, P. C., Martins, M. A., Machado Baptestini, F. M., Campos, R. C., Horta de Oliveira, G. H., & Martins Nunes, E. H. (2018). Developing predictive models for determining physical properties of coffee beans during the roasting process. *Industrial Crops and Products, 112*, 839-845. https://doi.org/10.1016/j.indcrop.2017.12.015

Chandrasekaran, S., Ramanathan, S., & Basak, T. (2013). Microwave food processing—A review. *Food Research International, 52*(1), 243-261. https://doi.org/10.1016/j.foodres.2013.02.033

Chen, G., Maier, D. E., Campanella, O. H., & Takhar, P. S. (2009). Modeling of moisture diffusivities for components of yellow-dent corn kernels. *Journal of Cereal Science*, *50*(1), 82-90. https://doi.org/10.1016/j.jcs.2009.03.003

Doblado-Maldonado, A. F., Flores, R. A., & Rose, D. J. (2013). Low moisture milling of wheat for quality testing of wholegrain flour. *Journal of Cereal Science*, *58*(3), 420-423. https://doi.org/10.1016/j.jcs.2013.08.006

Ekezie, F.-G. C., Sun, D.-W., Han, Z., & Cheng, J.-H. (2017). Microwave-assisted food processing technologies for enhancing product quality and process efficiency: A review of recent developments. *Trends in Food Science & Technology*, *67*, 58-69. https://doi.org/10.1016/j.tifs.2017.05.014

Erkinbaev, C., Ramachandran, R. P., Cenkowski, S., & Paliwal, J. (2019). A comparative study on the effect of superheated steam and hot air drying on microstructure of distillers' spent grain pellets using X-ray micro-computed tomography. *Journal of Food Engineering*, *241*, 127-135. https://doi.org/10.1016/j.jfoodeng.2018.08.004

Gökmen, S. (2004). Effects of moisture content and popping method on popping characteristics of popcorn. *Journal of Food Engineering*, *65*(3), 357-362. https://doi.org/10.1016/j.jfoodeng.2004.01.034

Jahanbakhshi, A., Kaveh, M., Taghinezhad, E., & S.V., R. (2020). Assessment of kinetics, effective moisture diffusivity, specific energy consumption, shrinkage, and color in the pistachio kernel drying process in microwave drying with ultrasonic pretreatment. *Journal of Food Processing and Preservation, 44*(6). https://doi.org/10.1111/jfpp.14449

Jiang, M., Wu, P., Xing, H., Li, L., Jia, C., Chen, S., Zhang, S., & Wang, L. (2020). Water migration and diffusion mechanism in the wheat drying. *Drying Technology*, *39*(6), 738-751. https://doi.org/10.1080/07373937.2020.1716001

Kalivoda, J. R., Jones, C. K., & Stark, C. R. (2017). Impact of varying analytical methodologies on grain particle size determination. *Journal of Animal Science*, *95*(1), 113. https://doi.org/10.2527/jas.2016.0966

Karababa, E. (2006). Physical properties of popcorn kernels. *Journal of Food Engineering*, *72*(1), 100-107. https://doi.org/10.1016/j.jfoodeng.2004.11.028

Karababa, E., & Coşkuner, Y. (2007). Moisture dependent physical properties of dry sweet corn kernels. *International Journal of Food Properties*, *10*(3), 549-560. https://doi.org/10.1080/10942910601003981

Khan, M. I. H., Kumar, C., Joardder, M. U. H., & Karim, M. A. (2016). Determination of appropriate effective diffusivity for different food materials. *Drying Technology*, *35*(3), 335-346. https://doi.org/10.1080/07373937.2016.1170700

Kipcak, A. S., & Doymaz, I. (2020). Mathematical modeling and drying characteristics investigation of black mulberry dried by microwave method. *International Journal of Fruit Science*, *20*(sup3), S1222-S1233. https://doi.org/10.1080/15538362.2020.1782805

Kumar, C., & Karim, M. A. (2019). Microwave-convective drying of food materials: A critical review. *Critical Reviews in Food Science and Nutrition*, *59*(3), 379-394. https://doi.org/10.1080/10408398.2017.1373269

Lara, N., & Ruales, J. (2002). Popping of amaranth grain (*Amaranthus caudatus*) and its effect on the functional, nutritional and sensory properties. *Journal of the Science of Food and Agriculture*, *82*(8), 797-805.

Lara, N., & Ruales, J. (2021). Physical and hydration properties of specialty floury and sweet maize kernels subjected to pan and microwave toasting. *Journal of Cereal Science*, *101*, 103298. https://doi.org/10.1016/j.jcs.2021.103298

Lara, N., Vizuete, K., Debut, A., Chango, I., Campaña, O., Villacrés, E., Bonilla, P., & Ruales, J. (2021). Underutilized maize kernels (*Zea mays* L. var. *amylacea* and var. *saccharata*) subjected to pan and microwave toasting: A comparative structure study in the whole kernel. *Journal Cereal Science*, *100*, 103249. https://doi.org/10.1016/j.jcs.2021.103249

Odjo, S., Malumba, P., Dossou, J., Janas, S., & Béra, F. (2012). Influence of drying and hydrothermal treatment of corn on the denaturation of salt-soluble proteins and color parameters. *Journal of Food Engineering*, *109*(3), 561-570. https://doi.org/10.1016/j.jfoodeng.2011.10.023

Oliveros, N. O., Hernández, J. A., Sierra-Espinosa, F. Z., Guardián-Tapia, R., & Pliego-Solórzano, R. (2017). Experimental study of dynamic porosity and its effects on simulation of the coffee beans roasting. *Journal of Food Engineering*, *199*, 100-112. https://doi.org/10.1016/j.jfoodeng.2016.12.012

Pham, N. D., Khan, M. I. H., & Karim, M. A. (2020). A mathematical model for predicting the transport process and quality changes during intermittent microwave convective drying. *Food Chem*, *325*, 126932. https://doi.org/10.1016/j.foodchem.2020.126932

Rakesh, V., & Datta, A. K. (2011). Microwave puffing: Determination of optimal conditions using a coupled multiphase porous media – Large deformation model. *Journal of Food Engineering*, *107*(2), 152-163. https://doi.org/10.1016/j.jfoodeng.2011.06.031

Schoeman, L., du Plessis, A., Verboven, P., Nicolaï, B. M., Cantre, D., & Manley, M. (2017). Effect of oven and forced convection continuous tumble (FCCT) roasting on the microstructure and dry milling properties of white maize. *Innovative Food Science & Emerging Technologies*, *44*, 54-66. https://doi.org/10.1016/j.ifset.2017.07.021

Shirkole, S. S., & Sutar, P. P. (2018). High power short time microwave finish drying of paprika (*Capsicum annuum* L.): Development of models for moisture diffusion and color degradation. *Drying Technology*, *37*(2), 253-267. https://doi.org/10.1080/07373937.2018.1454941

Shivhare, U. S., Raghavan, G. S. U., & Biosisio, R. G. (1994). Modelling of drying kinetics of maize in a microwave environment. *Journal of Agricultural Engineering Research*, *57*, 199-205.

Sumithra, B., & Bhattacharya, S. (2008). Toasting of corn flakes: Product characteristics as a function of processing conditions. *Journal of Food Engineering*, *88*(3), 419-428. https://doi.org/10.1016/j.jfoodeng.2008.03.001

Velu, V., Nagender, A., Prabhakara Rao, P. G., & Rao, D. G. (2006). Dry milling characteristics of microwave dried maize grains (*Zea mays* L.). *Journal of Food Engineering*, *74*(1), 30-36. https://doi.org/10.1016/j.jfoodeng.2005.02.014

Welsh, Z., Simpson, M. J., Khan, M. I. H., & Karim, M. A. (2018). Multiscale Modeling for Food Drying: State of the Art. *Compr Rev Food Sci Food Saf*, *17*(5), 1293-1308. https://doi.org/10.1111/1541-4337.12380

Welsh, Z. G., Khan, M. I. H., & Karim, M. A. (2021). Multiscale modeling for food drying: A homogenized diffusion approach. *Journal of Food Engineering*, *292*, 110252. https://doi.org/10.1016/j.jfoodeng.2020.110252

Appendices

Supplementary results are in Tables: S1, S2, S3, and S4.

Table S1. Pearson's correlation coefficients (-1 to +1) of a broad range of physical properties, determined for floury maize **a0** at microwave heating-toasting times from 0 to 390 s (n = 18, P ≤ 0.05).

	Time	MC	MR	WL	APS	WAC	SP	L*	a*	h*	ΔE*	BD	KD	KT	GMD	KSA	KV	IP	KW	WSI	KS	ER	KWth	KL	C*	b*
Time		-0.98	-0.99	0.98	-0.96	0.97	0.97	-0.93	0.95	-0.92	0.92	-0.92	-0.92	0.87	0.87	0.87	0.86	0.87	-0.78	-0.78	0.66	0.52	0.42	0.46	0.41	-0.08
WC, water content			1.00	-0.99	0.97	-0.95	-0.95	0.89	-0.92	0.88	-0.87	0.94	0.94	-0.91	-0.91	-0.90	-0.90	-0.91	0.73	0.80	-0.73	-0.55	-0.51	-0.40	-0.48	-0.01
WR, water ratio				-1.00	0.96	-0.96	-0.96	0.89	-0.93	0.88	-0.87	0.94	0.95	-0.91	-0.91	-0.91	-0.90	-0.91	0.77	0.79	-0.70	-0.56	-0.47	-0.46	-0.49	-0.01
WL, water loss					-0.95	0.95	0.95	-0.87	0.90	-0.85	0.85	-0.97	-0.96	0.92	0.92	0.92	0.91	0.92	-0.80	-0.75	0.67	0.60	0.43	0.51	0.53	0.06
APS, milling average particle size						-0.94	-0.94	0.85	-0.91	0.86	-0.84	0.89	0.89	-0.88	-0.86	-0.86	-0.85	-0.85	0.69	0.81	-0.73	-0.44	-0.49	-0.34	-0.49	-0.02
WAC, water absorption capacity							1.00	0.85	-0.91	0.86	-0.84	0.89	0.89	-0.88	-0.86	-0.86	-0.85	-0.85	0.69	-0.70	-0.73	-0.44	-0.49	-0.34	-0.49	-0.02
SP, swelling power								-0.91	0.92	-0.90	0.89	-0.90	-0.91	0.87	0.87	0.87	0.87	0.85	-0.73	-0.69	0.64	0.42	0.43	0.49	0.38	-0.10
L*, color parameter									-0.94	0.98	-1.00	0.75	0.76	-0.68	-0.69	-0.69	-0.68	-0.68	0.74	0.72	-0.50	-0.35	-0.33	-0.39	-0.11	0.39
a*, color parameter										-0.98	0.96	-0.79	-0.79	0.72	0.72	0.72	0.71	0.73	-0.77	-0.79	0.54	0.42	0.36	0.38	0.30	-0.22
h*, color parameter											-0.99	0.71	0.73	-0.66	-0.67	-0.67	-0.66	-0.66	0.71	0.76	-0.50	-0.30	-0.37	-0.36	-0.11	0.41
ΔE*, color difference												-0.72	-0.73	0.64	0.65	0.65	0.64	0.64	-0.74	-0.72	0.47	0.32	0.32	0.38	0.09	-0.42
BD, bulk density													0.99	-0.95	-0.95	-0.95	-0.94	-0.95	0.77	0.63	-0.66	-0.67	-0.41	-0.57	-0.63	-0.23
KD, individual kernel density														-0.96	-0.98	-0.98	-0.97	-0.96	0.72	0.65	-0.70	-0.63	-0.49	-0.57	-0.57	-0.17
KT, kernel thickness															0.99	0.99	0.98	0.97	-0.55	-0.70	0.84	0.60	0.61	0.38	0.58	0.22
GMD, geometric mean diameter																1.00	1.00	0.97	-0.57	-0.64	0.79	0.57	0.62	0.47	0.54	0.18
KSA, kernel surface area																	1.00	0.97	-0.57	-0.64	0.79	0.56	0.62	0.47	0.54	0.18
KV, kernel volume																		0.96	-0.55	-0.63	0.78	0.54	0.65	0.48	0.51	0.15
IP, internal porosity																			-0.62	-0.71	0.80	0.72	0.56	0.41	0.63	0.26
KW, individual kernel weight																				0.47	-0.14	-0.57	0.14	-0.70	-0.47	-0.07
WSI, water-soluble index																					-0.74	-0.41	-0.50	0.04	-0.33	0.07
KS, kernel sphericity																						0.43	0.83	-0.17	0.40	0.14
ER, expansion ratio																							0.13	0.30	0.68	0.47
KWth, kernel width																								-0.19	0.03	-0.13
KL, kernel length																									0.27	0.07
C*, color parameter																										0.86
b*, color parameter																										

Gray color means correlation coefficients less than 0.7 (absolute number).

Table S2. Pearson's correlation coefficients (-1 to +1) of a broad range of physical properties, determined for floury maize **a1** at microwave heating-toasting times from 0 to 390 s (n = 18, P ≤ 0.05).

Time	MC	MR	WL	APS	WAC	SP	L*	a*	h*	ΔE*	BD	KD	KT	GMD	KSA	KV	IP	KW	WSI	KS	ER	KWth	KL	C*	b*
Time	-0.99	-0.99	0.98	-0.97	0.98	0.98	-0.93	0.95	-0.93	0.88	-0.91	-0.90	0.87	0.88	0.88	0.89	0.87	-0.88	-0.71	0.81	0.86	0.49	0.77	-0.71	-0.77
WC, water content		0.99	-0.98	0.96	-0.97	-0.97	0.91	-0.92	0.92	-0.88	0.92	0.91	-0.89	-0.89	-0.89	-0.89	-0.90	0.89	0.74	-0.84	-0.89	-0.46	-0.74	0.74	0.80
WR, water ratio			-0.99	0.97	-0.97	-0.97	0.91	-0.94	0.91	-0.86	0.92	0.93	-0.91	-0.92	-0.92	-0.92	-0.90	0.89	0.73	-0.85	-0.89	-0.51	-0.77	0.70	0.76
WL, water loss				-0.97	0.95	0.95	-0.88	0.94	-0.86	0.80	-0.94	-0.95	0.93	0.94	0.94	0.94	0.90	-0.90	-0.69	0.88	0.89	0.51	0.77	-0.62	-0.68
APS, milling average particle size					-0.96	-0.95	0.88	-0.90	0.88	-0.82	0.93	0.94	-0.91	-0.92	-0.92	-0.92	-0.92	0.90	0.71	-0.81	-0.90	-0.43	-0.84	0.67	0.72
WAC, water absorption capacity						1.00	-0.93	0.90	-0.94	0.90	-0.88	-0.90	0.85	0.87	0.87	0.87	0.87	-0.90	-0.72	0.80	0.86	0.46	0.75	-0.77	-0.82
SP, swelling power							-0.93	0.90	-0.93	0.89	-0.88	-0.90	0.85	0.87	0.87	0.87	0.87	-0.90	-0.70	0.80	0.86	0.47	0.75	-0.76	-0.81
L*, color parameter								-0.92	0.98	-0.94	0.77	0.76	-0.72	-0.74	-0.74	-0.75	-0.73	0.75	0.71	-0.71	-0.73	-0.53	-0.59	0.76	0.83
a*, color parameter									-0.89	0.80	-0.83	-0.81	0.77	0.79	0.79	0.80	0.74	-0.79	-0.69	0.75	0.73	0.53	0.66	-0.56	-0.64
h*, color parameter										-0.98	0.76	0.75	-0.71	-0.73	-0.73	-0.73	-0.77	0.77	0.77	-0.66	-0.78	-0.45	-0.64	0.85	0.90
ΔE*, color difference											-0.72	-0.69	0.66	0.67	0.67	0.67	0.75	-0.72	-0.77	0.62	0.77	0.38	0.56	-0.94	-0.97
BD, bulk density												0.93	-0.91	-0.90	-0.90	-0.89	-0.91	0.91	0.67	-0.81	-0.88	-0.33	-0.80	0.59	0.64
KD, individual kernel density													-0.98	-0.99	-0.99	-0.98	-0.96	0.92	0.66	-0.91	-0.94	-0.47	-0.83	0.56	0.61
KT, kernel thickness														0.99	0.99	0.98	0.95	-0.87	-0.64	0.95	0.93	0.45	0.76	-0.53	-0.58
GMD, geometric mean diameter															1.00	1.00	0.95	-0.85	-0.63	0.94	0.93	0.54	0.81	-0.53	-0.58
KSA, kernel surface area																1.00	0.95	-0.85	-0.63	0.94	0.93	0.54	0.81	-0.53	-0.58
KV, kernel volume																	0.95	-0.84	-0.62	0.94	0.93	0.57	0.81	-0.53	-0.58
IP, internal porosity																		-0.88	-0.77	0.86	1.00	0.37	0.83	-0.69	-0.72
KW, individual kernel weight																			0.71	-0.75	-0.86	-0.21	-0.78	0.63	0.67
WSI, water-soluble index																				-0.58	-0.78	-0.18	-0.55	0.72	0.75
KS, kernel sphericity																					0.83	0.59	0.56	-0.48	-0.52
ER, expansion ratio																						0.37	0.82	-0.72	-0.75
KWth, kernel width																							0.30	-0.19	-0.25
KL, kernel length																								-0.45	-0.49
C*, color parameter																									0.99
b*, color parameter																									

Gray color means correlation coefficients less than 0.7 (absolute number).

Table S3. Pearson's correlation coefficients (-1 to +1) of a broad range of physical properties, determined for floury maize **a2** at microwave heating-toasting times from 0 to 390 s (n = 18, P ≤ 0.05).

	Time	MC	MR	WL	APS	WAC	SP	L*	a*	h*	ΔE*	BD	KD	KT	GMD	KSA	KV	IP	KW	WSI	KS	ER	KWth	KL	C*	b*
Time		-0.98	-0.99	0.97	-0.94	0.86	0.87	-1.00	0.34	-0.93	0.99	-0.90	-0.90	0.86	0.88	0.88	0.89	0.86	-0.95	-0.86	0.80	0.87	0.77	0.90	-0.94	-0.96
WC, water content			0.99	-0.96	0.95	-0.82	-0.82	0.99	-0.42	0.96	-0.98	0.91	0.90	-0.85	-0.88	-0.88	-0.88	-0.85	0.96	0.82	-0.79	-0.86	-0.76	-0.91	0.95	0.97
WR, water ratio				-0.98	0.94	-0.83	-0.83	0.99	-0.43	0.96	-0.98	0.92	0.90	-0.86	-0.88	-0.88	-0.89	-0.86	0.95	0.83	-0.80	-0.87	-0.76	-0.89	0.93	0.95
WL, water loss					-0.92	0.78	0.79	-0.97	0.48	-0.95	0.95	-0.91	-0.89	0.86	0.88	0.88	0.88	0.87	-0.93	-0.79	0.83	0.87	0.79	0.84	-0.89	-0.91
APS, milling average particle size						-0.67	-0.68	0.94	-0.45	0.92	-0.93	0.95	0.95	-0.92	-0.93	-0.93	-0.94	-0.92	0.97	0.67	-0.86	-0.91	-0.77	-0.94	0.94	0.95
WAC, water absorption capacity							1.00	-0.86	0.05	-0.73	0.86	-0.61	-0.61	0.55	0.59	0.59	0.60	0.56	-0.73	-0.99	0.49	0.59	0.58	0.67	-0.78	-0.78
SP, swelling power								-0.87	0.06	-0.74	0.86	-0.62	-0.62	0.57	0.60	0.60	0.61	0.58	-0.74	-0.99	0.50	0.60	0.59	0.68	-0.79	-0.79
L*, color parameter									-0.34	0.93	-1.00	0.91	0.90	-0.86	-0.88	-0.89	-0.89	-0.86	0.96	0.86	-0.80	-0.87	-0.77	-0.90	0.96	0.97
a*, color parameter										-0.64	0.30	-0.40	-0.37	0.36	0.37	0.37	0.37	0.39	-0.36	-0.13	0.32	0.39	0.30	0.41	-0.19	-0.26
h*, color parameter											-0.92	0.86	0.84	-0.80	-0.82	-0.82	-0.83	-0.80	0.90	0.76	-0.73	-0.82	-0.71	-0.88	0.85	0.88
ΔE*, color difference												-0.90	-0.89	0.85	0.87	0.87	0.88	0.85	-0.95	-0.86	0.79	0.85	0.75	0.90	-0.96	-0.97
BD, bulk density													0.99	-0.99	-0.99	-0.99	-0.99	-0.98	0.94	0.61	-0.96	-0.97	-0.82	-0.91	0.93	0.94
KD, individual kernel density														-0.99	-1.00	-1.00	-1.00	-0.98	0.95	0.59	-0.96	-0.98	-0.84	-0.92	0.94	0.94
KT, kernel thickness															1.00	1.00	1.00	0.99	-0.91	-0.55	0.98	0.98	0.81	0.89	-0.90	-0.91
GMD, geometric mean diameter																1.00	1.00	0.99	-0.92	-0.57	0.97	0.99	0.83	0.91	-0.92	-0.92
KSA, kernel surface area																	1.00	0.99	-0.92	-0.58	0.97	0.99	0.83	0.91	-0.92	-0.92
KV, kernel volume																		0.99	-0.93	-0.59	0.97	0.99	0.84	0.92	-0.92	-0.93
IP, internal porosity																			-0.91	-0.55	0.96	1.00	0.83	0.90	-0.88	-0.89
KW, individual kernel weight																				0.72	-0.86	-0.91	-0.81	-0.91	0.96	0.97
WSI, water-soluble index																					-0.48	-0.58	-0.55	-0.66	0.75	0.76
KS, kernel sphericity																						0.95	0.84	0.79	-0.85	-0.86
ER, expansion ratio																							0.84	0.91	-0.88	-0.89
KWth, kernel width																								0.70	-0.79	-0.79
KL, kernel length																									-0.91	-0.92
C*, color parameter																										1.00
b*, color parameter																										

Gray color means correlation coefficients less than 0.7 (absolute number).

Table S4. Constant of the third-order polynomial regression model ($Y = a + bX + cX^2 + dX^3$) between water migration (WC, WR, and WL) and microwave heating-toasting time from 0 to 390 s by floury (a0 and a1) and sweet (a2) maize types without and with kernel size approaches.

Polynomial	Without kernel size approach			Spatial $(S/V)^2$ approach			Distance $(GMD/2)^2$ approach		
constants	a0	a1	a2	a0	a1	a2	a0	a1	a2
WC: water content									
a	1.65E-01	1.63E-01	1.65E-01	4.72E-02	5.37E-02	7.22E-02	6.24E-03	6.82E-03	9.33E-03
b	-1.88E-04	-1.76E-04	-5.02E-05	-7.48E-05	-7.63E-05	-1.12E-04	-1.55E-05	-1.32E-05	-2.19E-05
c	-2.36E-06	-2.10E-06	-3.01E-06	-6.08E-07	-6.52E-07	-9.04E-07	-5.04E-08	-6.72E-08	-8.13E-08
d	4.53E-09	3.82E-09	5.27E-09	1.26E-09	1.28E-09	1.85E-09	1.28E-10	1.46E-10	1.97E-10
WR: water ratio									
a	1.00E+00	1.00E+00	1.00E+00	2.90E-01	3.34E-01	4.38E-01	3.83E-02	4.23E-02	5.66E-02
b	-9.42E-04	-8.95E-04	-1.94E-04	-4.60E-04	-4.69E-04	-6.53E-04	-9.52E-05	-8.10E-05	-1.30E-04
c	-1.55E-05	-1.39E-05	-1.89E-05	-3.74E-06	-4.09E-06	-5.65E-06	-3.13E-07	-4.25E-07	-5.14E-07
d	2.92E-08	2.49E-08	3.29E-08	7.79E-09	8.01E-09	1.15E-08	7.89E-10	9.20E-10	1.23E-09
WL: water loss									
a	0.00E+00	0.00E+00	0.00E+00	0.00E+00	0.00E+00	0.00E+00	0.00E+00	0.00E+00	0.00E+00
b	1.85E-04	2.24E-04	6.89E-05	5.78E-05	7.94E-05	4.03E-05	7.50E-06	1.02E-05	5.95E-06
c	2.02E-06	1.67E-06	2.70E-06	4.36E-07	4.09E-07	8.82E-07	4.69E-08	4.00E-08	9.08E-08
d	-4.05E-09	-3.45E-09	-5.02E-09	-9.05E-10	-8.97E-10	-1.69E-09	-1.00E-10	-9.14E-11	-1.76E-10

Chapter 5

Modeling of the microwave heating-toasting time-related variables and characterization of non-isothermal rheological properties of floury and sweet specialty maize kernels

Nelly Lara[a,b*], Arnulfo Portilla[b], Fernando Osorio[c], Jenny Ruales[a]

[a] Departamento de Ciencia de Alimentos y Biotecnología, Escuela Politécnica Nacional, Av. Ladrón de Guevara E11-253 Edificio 19 Quito, Ecuador

[b] CADET, Facultad de Ciencias Agrícolas, Universidad Central del Ecuador, Calle Universitaria s/n, Tumbaco, Ecuador

[c] Departamento de Ciencia y Tecnología de Alimentos, Universidad de Santiago de Chile, Santiago, Chile

ABSTRACT

The three primary floury and sweet maize types, with specialty kernels to make entire ready-to-eat maize, and packed in sealable paper envelopes, were the experimental units (150 g of raw kernels) to model the effect of the microwave heating-toasting (2450 MHz microwave oven, 492 W, times 0, 78, 156, 234, 312, and 390 s) on time-related variables and characterize the non-isothermal rheological properties. Pauses every 60 s for a rapid manual shaking compensated for non-uniformity of microwave volumetric heating. Surface color difference (ΔE*), internal porosity, milling average particle size, and flour hydration properties displayed curves adequately described by simple and nonlinear regression models. The milling particle size, hydration properties, and rheological parameters illustrated floury and sweet kernel differences ascribed to their proximal composition. Onset and peak temperatures depended on maize types and showed a little variation attributed to microwave heating-toasting times. The elastic/viscous modulus ratio increased in floury maize. It decreased in sweet maize, unveiling rheological differences associated with microwave heating-toasting time effect on the contrasting structure of floury and sweet specialty Andean maize kernels used for toasting.

Keywords: maize kernels; microwave toasting; water-soluble index; temperature ramp; elastic/viscous ratio

* Corresponding author: CADET, Facultad de Ciencias Agrícolas, Universidad Central del Ecuador, Calle Universitaria s/n, Tumbaco, Ecuador. E-mail: nvlara@uce.edu.ec (N. Lara)

1. Introduction

Floury and sweet maize types with specialty kernels to make ready-to-eat maize by dry heat (toasting) are stapled cultivars in the Andean region and remain underutilized worldwide. According to personal information, the three kernel fractions (endosperm, germ, and pericarp) are 83, 13, and 4% and 78, 17, and 5% in these floury and sweet maize types, respectively. Floury maize kernels (*Zea maize* L. var. *amylacea*) have completely soft endosperm and are easy to chew when toasted. In contrast, the shrunken kernels of sweet maize (*Zea maize* L. var. *saccharata*) have a sugary-vitreous fraction more significantly than floury endosperm, which becomes crunchy after toasting. Although these floury and sweet maize kernels have specialty attributes to make ready-to-eat maize called *Tostado* and *Chulpi*, respectively in Ecuador and *Cancha* in Peru (Salvador-Reyes & Clerici, 2020), this traditional process has remained in the Andean region with very little knowledge on the science behind them. Limited studies present an overview of Peruvian maize varieties and based on raw kernel characterization, explain that these maize types can be ingredients of greater importance in the food industry (Salvador-Reyes & Clerici, 2020; Salvador-Reyes et al., 2021). Recent comparative studies using a pan and microwave toasting reveal structural changes in floury and sweet maize toasted kernels and imply the application of microwave ovens instead of pans to reduce the toasting time, e.g., from 1500 s to 390 s in floury maize and 312 s in sweet maize (Lara & Ruales, 2021; Lara et al., 2021).

In whole kernels, microwave hydrothermal studies (30 g/100 g water content, annealing) have more extensive coverage in the scientific literature than microwave dry heat treatments with low water content (e.g., 14 g/100 g, toasting). Therefore, the knowledge of the kinetics of time-related variables in whole kernel matrices subjected to microwave is limited. The first insight on kernel water migration kinetics shows the physical properties defined as time-related variables in maize kernel toasting (Lara et al., 2022). In addition, the main microwave parameters used in most studies are power and time (Tao et al., 2020) because volumetric heating relies on the absorption of microwave radiation, and its conversion into heat reflects the response of a food matrix to microwave treatment (van Rooyen et al., 2022). Electromagnetic energy in microwave heating propagates by time-varying electric and magnetic fields to the water spaces contained in the maize kernels. The friction and collision of polar molecules and ions throughout the material convert electromagnetic energy into volumetric heating. This volumetric heating allows higher diffusion rates and pressure gradients to remove water from the maize kernels, reducing the time process by approximately 80% (Pham et al., 2020). This electromagnetic theory suggests that microwave heating achieves high heating rates with a short start-up time and indicates that managing these characteristics could allow controlled structural changes in starch-based kernel toasting, considering that toasted maize kernel (ready-to-

eat maize) is traditional human food in the Andean region. However, the microwave heating-toasting kinetic curves of time-related variables are not studied. In addition, the rheological properties of these maize kernels with specialty attributes for toasting are still unknown. In contrast, current hypotheses aim to develop rheological maps based on starch concentration and swelling volume to understand the texture changes in starchy foods (Joyner et al., 2021) and imply possible relationships of rheological properties with the dynamic oral chewing of foods in the mouth (Ahmed, 2018). According to these facts, some rheological parameters can explain softness in floury maize and crunchiness in sweet maize kernels.

On the other hand, continuous research reflects the effect of dry heating treatments on normal maize native starch and its rheological properties to improve the dynamics of starch-based food systems (Mao et al., 2021; Qu et al., 2021). Using steady shear analyses and frequency sweep measurements, the rheological properties in terms of elastic and viscous moduli, loss tangent, complex and apparent viscosities display the physicochemical shifts ascribed to modified maize native starches (Lee et al., 2021; Lei et al., 2020; Li et al., 2020; Mao et al., 2021). However, a few rheological references show temperature ramp measurements (non-isothermal rheology) in maize starch (Singh et al., 2006; Zhu et al., 2016) and compared to other starches (Dong et al., 2021; Li & Zhu, 2018; J. Zhang et al., 2021). Likewise, the rheological changes during a heating period ascribed to the onset and peak temperatures (B. Zhang, D. Qiao, et al., 2021) suggest consistency with thermal and pasting analysis when a cooling period is registered to define conclusion temperatures (Singh et al., 2006; Wen et al., 2020). Therefore, the objective of this study was to model the effect of microwave heating-toasting times (0, 78, 156, 234, 312, and 390 s) on time-related variables such as surface color difference and internal porosity in maize kernels, average particle size by milling, hydration properties (water absorption capacity, swelling power, water-soluble index in flour maize) and characterize the non-isothermal rheological properties (onset and peak temperatures, elastic and viscous moduli, and complex and dynamic viscosities at peak temperatures) using for toasting floury and sweet specialty maize kernels with 0.16 g/g water content on a dry basis.

2. Materials and methods

2.1. Maize types

Commercial lots of the primary three maize types (*Zea mays* L. var. *amylacea* and var. *saccharata*) with specialty kernels for pan and microwave toasting were obtained from a local market (Quito, Ecuador) and adjusted to 0.16 g/g (on a dry basis) water content according to previous studies with three replications (Lara & Ruales, 2021; Lara et al., 2021).

2.2. Sample preparation

Following a 3 (maize types) x 6 (microwave heating-toasting times) arrangement, the equilibrated kernel samples of the three maize types (blocks a0, a1, and a2) were randomly partitioned in 150 g for microwave heating-toasting at six different times (times: 0, 78, 156, 234, 312 and 390 s), where zero (0 s) is the raw kernels at the initial water content for a total of 18 maize kernel experimental units packed in foil gusseted bags by replication (Lara et al., 2022).

2.3. Microwave heating-toasting

According to the experimental method used in previous studies (Lara et al., 2022; Lara & Ruales, 2021), the equilibrated kernel samples (150 g) contained in a sealed paper envelope (17.5 cm wide and 24 cm long) were separately exposed to microwave heating-toasting times (0, 78, 156, 234, 312 and 390 s) using a microwave oven at 492 W (2450 MHz, 60.30 L, 10 power levels, Panasonic, Shanghai, China). Pauses every 60 s for a rapid manual shaking compensated for non-uniformity of microwave volumetric heating. The envelope was opened at the end of each heating-toasting time to release the generated water vapor. Afterward, all treated kernels of three replications were packed in foil gusseted bags and stored at 4 °C for further measurements on whole kernels and reduced to flour.

2.4. Color measurements

Color differences (ΔE*) based on color space (CIEL L*a*b*) at each microwave heating-toasting time, with three replications, were measured using a 3nh_NH310 colorimeter, main light D65, and a ϕ 4 mm measuring aperture device (Shenzhen 3NH Technology Co., LTD., Shenzhen, China), according to the method described for these maize types in a previous study (Lara & Ruales, 2021).

2.5. Internal porosity

Volume (V) of individual kernels was obtained according to the geometrical expression previously reported for popcorn (Karababa, 2006), sweet maize (Karababa & Coşkuner, 2007), and used for floury and sweet maize kernels (Lara & Ruales, 2021). The volume difference between treated (V_t) and raw (V_0) individual kernel divided by treated (V_t) kernel volume (Schoeman et al., 2017; Sumithra & Bhattacharya, 2008) was associated with the internal porosity (IP) created by the effect of each heating-toasting time (Lara & Ruales, 2021) as in Eq. [1].

$$IPt = (V_t - V_0)/V_t \quad [1]$$

2.6. Particle size distribution

The kernel samples collected at each microwave heating-toasting time with three replications were reduced separately into flour using an ultra-centrifugal mill ZM 200 (Retsch® Solution in milling & Sieving, Haan, Germany). Then, flour samples were equilibrated at 35 °C in a forced-air oven for 16 hours. Flour particle size distribution was determined by sifting through sieves (Prüfsiieb, Western Germany) with opening sizes of 630, 400, 315, 200, 90, 25, and 0 (pan) µm (Lara & Ruales, 2021), selected from a standard sieve stack used for quality testing of whole wheat flour (Doblado-Maldonado et al., 2013), and weighing of separated fractions. The acquired weights in the adjacent sieves were the data to apply the statistical equations reported for the particle size analysis (Kalivoda et al., 2017; Velu et al., 2006).

2.7. Hydration properties

The water absorption capacity (WAC), swelling power (SP), and water-soluble index (WSI) were measured in maize kernel samples into flour for each microwave heating-toasting time (0, 78, 156, 234, 312, and 390 s), using the suspension-centrifugation procedure indicated in previous studies (Lara & Ruales, 2002, 2021; Lara et al., 2021). The hydration of the flour-water dispersions was at room temperature (18–21 ◦C). All water absorption analyses were performed in triplicate.

2.8. Proximate composition and mineral content in raw and toasted maize kernels

The chemical composition of the maize kernel reduced to whole flour (at times 0 and 390 s) was analyzed according to AOAC methods to determine water, protein, total fat, crude fiber, and ash content (AOAC, 1995). The proximate composition recorded on a dry basis was used to calculate the nitrogen-free extract-NFE (Adeleye et al., 2020). The ash was digested in nitric acid to determine Ca, Mg, K, Fe, and Zn by flame atomic absorption spectrometry and P using spectrophotometry at 400 nm (Fick et al., 1976). All analyses were performed in triplicate.

2.9. Non-isothermal oscillatory measurement

Maize whole flour dispersions (particle sizes < 125 µm) prepared in distilled water at 15 g/100 g dry solids were maintained at room temperature (10-22 ° C) for 24 hours to ensure complete hydration of the dry solids. Then, 1 mL was placed onto the center of the fixed plate to operate the Carri-Med CSL2-100 rheometer (TA Instruments, Surrey, England) using a 40 mm parallel plate and a gap of 500 µm under non-isothermal oscillatory measurements (Zhu et al., 2016). The geometry perimeter

covered with a thin synthetic oil spray (code AD 205) minimized the water sample evaporation (Singh et al., 2006). Based on preliminary trials, the heating temperature ramp was recorded from 45 to 85 °C for floury maize samples and 45 to 95 °C for sweet maize samples at a linear heating rate of 2 °C/min with a frequency of 1 Hz and 0.5% strain. After two measurements (CSL^2 Rheology Solution Software, TA Instruments) by ample, all rheological parameters were obtained directly from the data analysis option (DATA Rheology Solution Software, TA Instruments) for each microwave heating-toasting time and replica. Graphically the onset temperature was fixed when the oscillatory stress suddenly changed from the constant value (0.05978 Pa) to a noticeable increase, pointing to the onset of starch swelling in the maize sample dispersions on the X-axis. The onset temperature was obtained graphically for the other rheological properties (G', G", η*, and η') using OriginPro software (Microcal Inc., Northampton, MA, USA). Likewise, using OriginPro software, the peak temperature was predicted by Gaussian fit from the height of the endpoint at 85 and 95 °C in floury and sweet maize, respectively, to the top at the full width of half maximum rheological peaks.

2.10. Statistical analysis

Under randomized experimental work, the maize types (a0, a1, a2) were treated separately at the six heating-toasting time levels (0, 78, 156, 234, 312, and 390 s). After checking the normal distribution of data, considering the heating-toasting time as the independent variable, the lack of fit test performed together with simple regression was used to establish whether linearized or nonlinear models adequately describe the time-related variables. On the other hand, for rheological responses, the experiment designed with complete blocks and treatments (without interactions) provided a more valid measure of the known source of variation due to maize types. Therefore, the rheological data organized in one-way and two-way arrays were the base to analyze differences in maize types (a0, a1, and a2) and microwave heating-roasting times. Then, Tukey's multiple range test was applied to find the level(s) that created significant differences ($P \leq 0.05$) within the blocks and treatments. The regression analyses were determined using the Statgraphics centurion 19 software (Statgraphics, USA), Minitab21.1. (Minitab, LLC., USA) and OriginPro 21 (Microcal Inc., Northampton, MA, USA).

3. Results and discussion

The response variables measured by maize types (a0, a1, and a2) and heating-toasting times (0, 78, 156, 234, 312, and 390 s) presented normal distribution, and one-way analyses indicated non-significant variances with a few exceptions, validating the statistical analyses applied in this work.

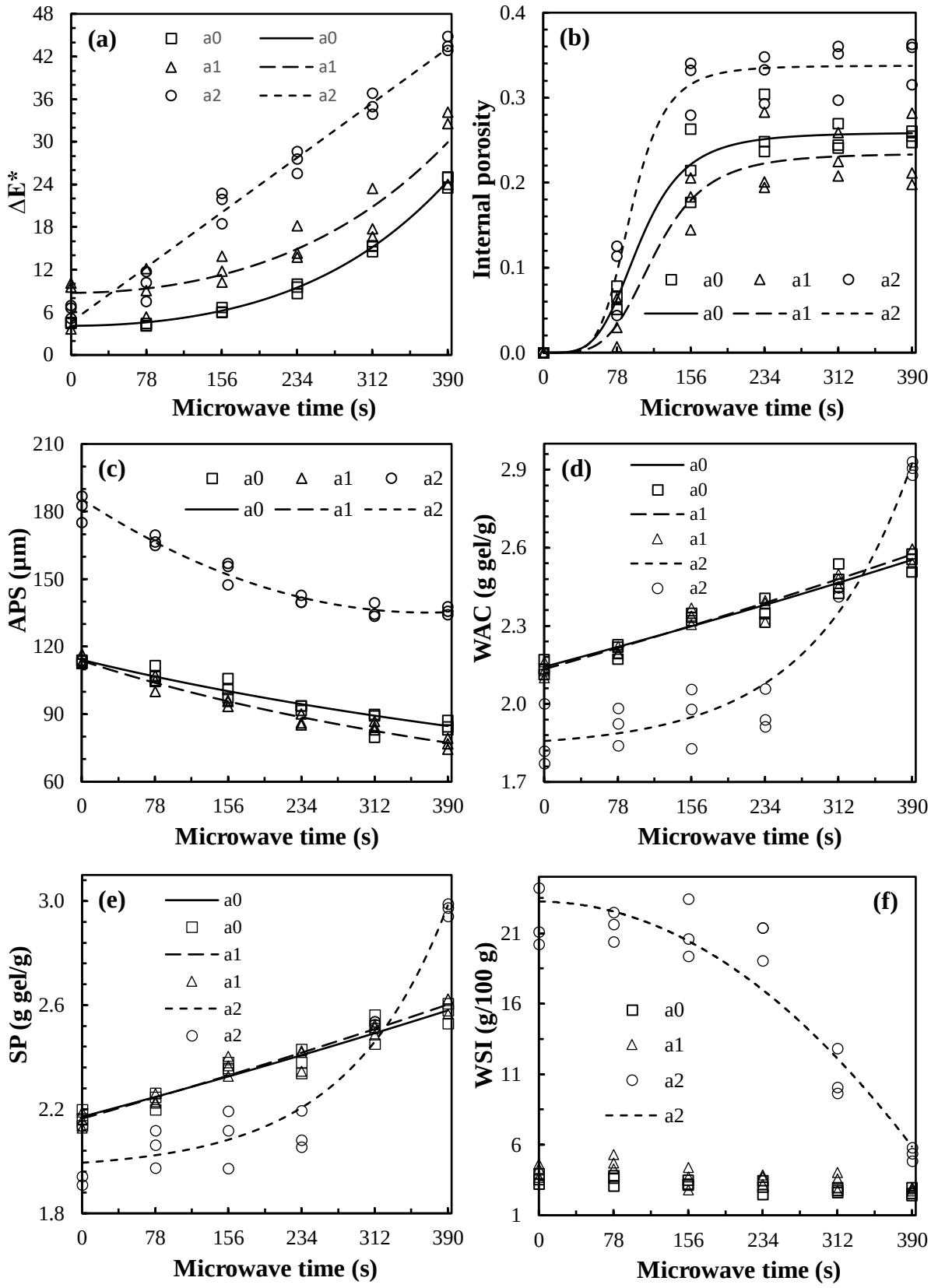

Figure 1. Effect of microwave heating-toasting times on experimental and fit kinetic curves: (**a**) Surface color difference (ΔE*); (**b**) internal porosity (IP); (**c**) average particle size (APS); (**d**) water absorption capacity (WAC); (**e**) swelling power (SP); and (**f**) water-soluble index (WSI) of floury (a0 and a1) and sweet (a2) maize kernels.

3.1. Maize kernel surface color

Fig. 1a shows the experimental (unfilled markers) and fit (drawn curves) relationships between ΔE* and microwave heating-toasting times. These color kinetic curves reflected a rising ΔE* with increasing heating-toasting time according to floury (a0 and a1) and sweet (a2) maize types and their large, medium, and small size kernels determined in a previous study for maize types a0, a1, and a2, respectively (Lara & Ruales, 2021). Simple regression analyses suggested that the complex model $Y^{1/2} = a + b \times X^2$ (square root-Y squared-X model) adequately described the floury (a0 and a1) maize surface color curves. In contrast, the linear model $Y = a + b \times X$ explained the sweet maize (a2) color curves with good fits (Table 1). The referred models presented Durbin-Watson statistics and lack-of-fit tests, with non-significant P-values ($P > 0.05$), and computing each model, a-values represent the intercept on Y-axis and b-values indicated the ratio of change between ΔE* and microwave heating-toasting times. Therefore, the color kinetic curves revealed a complex order increase in floury maize and an increasing linear trend in sweet maize (Fig 1a). Furthermore, the change toward brown color was greater in sweet maize than in floury maize due to the small kernel and its sugary-vitreous fraction with more than 20% of total sugars (Lara et al., 2021). In addition, the ΔE* curves inherent to maize types were consistent with the cumulative color simulation illustrated in Fig. 2 for the maize types a0, a1, and a2 at microwave heating-toasting times 0, 78, 156, 234, 312, and 390 s. Thus, two different models adequately describe the relationship between ΔE* and heating-toasting time in floury and sweet types, inferring that the color kinetics of microwave heating-toasting treatments depend on maize kernel types and the structure of their endosperm. In addition, according to the literature, the third-order polynomial provides good fits in toasting color kinetic of *Zea mays* var. *indurate* using an electric rotary toaster for 50 min (Chung et al., 2014).

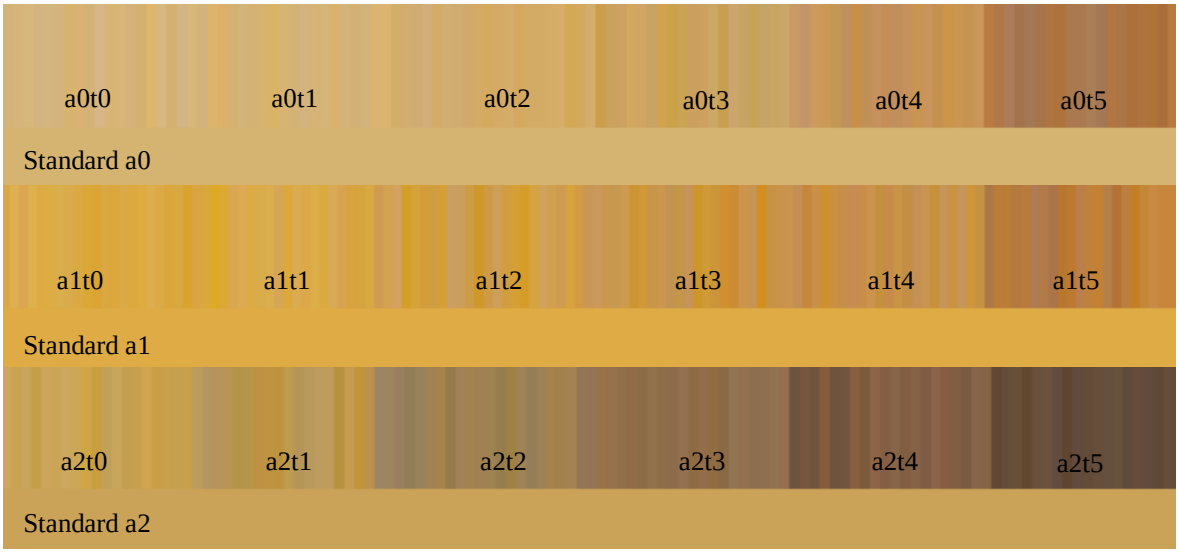

Figure 2. Cumulative color simulation based on its standard color for floury (a0 and a1) and sweet (a2) maize types at t0, t1, t2, t3, t4, and t5 equivalent to 0, 78, 156, 234, 312, and 390 s.

Table 1. Modeling and statistical parameters of time-related variables of specialty floury (a0 and a1) and sweet (a2) maize kernels with high correlations ($P \leq 0.05$) regarding microwave heating-toasting time (0, 78, 156, 234, 312, and 390 s)

Regression parameters⁜	**a0**	**a1**	**a2**
ΔE* versus time	**$Y^{1/2} = a + b \times X^2$**		**$Y = a + b \times X$**
Intercept-a	2.03 ± 0.03	2.90 ± 0.16	4.64 ± 0.84
Slope-b	$1.91\ 10^{-5} \pm 3.72\ 10^{-7}$	$1.70\ 10^{-5} \pm 2.09\ 10^{-6}$	0.10 ± 0.01
Adj. R-squared	99.36	79.31	97.86
Standard Error	0.085	0.479	2.001
Durbin-W. ($P > 0.05$)	0.266	0.587	0.533
Lack-of-fit ($P > 0.05$)	0.094	0.811	0.067
IP versus time	**$IP = IP_{max} \times X^n / (K^n + X^n)$ (Hill equation)**		
IP_{max}	0.26 ± 0.01	0.23 ± 0.01	0.34 ± 0.01
K	101.79 ± 6.77	118.65 ± 10.96	93.47 ± 5.87
n	4.17 ± 0.83	4.32 ± 1.14	5.20 ± 1.42
Adj. R-squared	95.55	91.30	96.11
Standard Error	0.023	0.030	0.028
Durbin-W. ($P > 0.05$)	0.571	0.714	0.809
Lack-of-fit ($P > 0.05$)	0.679	0.975	0.794
APS versus time	**$\ln Y = a + b \times X$**		**$\ln Y = a + b \times X^{1/2}$**
Intercept-a	4.72 ± 0.01	4.72 ± 0.01	5.24 ± 0.02
Slope-b	$-7.40\ 10^{-4} \pm 2.29\ 10^{-5}$	$-9.81\ 10^{-4} \pm 5.07\ 10^{-5}$	$-1.78\ 10^{-2} \pm 1.24\ 10^{-3}$
Adj. R-squared	97.30	95.64	93.23
Standard Error	0.018	0.029	0.029
Durbin-W. ($P > 0.05$)	0.345	0.276	0.085
Lack-of-fit ($P > 0.05$)	0.315	0.193	0.027
WAC versus time	**$\ln Y = a + b \times X$**		**$\ln (Y-Y_0) = \ln A_1 + (X/t_1)$**
Intercept-a (Y_0)	0.76 ± 0.01	0.76 ± 0.01	1.83 ± 0.05
Slope-b	$4.50\ 10^{-4} \pm 2.93\ 10^{-5}$	$4.82\ 10^{-4} \pm 2.51\ 10^{-5}$	
A_1			0.03 ± 0.02
t_1			105.09 ± 18.29
Adj. R-squared	93.45	95.57	93.96
Standard Error	0.016	0.014	0.091
Durbin-W. ($P > 0.05$)	0.509	0.343	0.339
Lack-of-fit ($P > 0.05$)	0.340	0.247	0.072
SP versus time	**$\ln Y = a + b \times X$**		**$\ln (Y-Y_0) = \ln A_1 + (X/t_1)$**
Intercept-a (Y_0)	0.78 ± 0.01	0.77 ± 0.01	1.97 ± 0.05
Slope-b	$4.42\ 10^{-4} \pm 2.98\ 10^{-5}$	$4.73\ 10^{-4} \pm 2.50\ 10^{-5}$	
A_1			0.03 ± 0.02
t_1			107.71 ± 19.17
Adj. R-squared	93.00	95.47	93.80
Standard Error	0.017	0.014	0.091
Durbin-W. ($P > 0.05$)	0.493	0.324	0.339
Lack-of-Fit ($P > 0.05$)	0.332	0.294	0.116

⁜ Mean values of three replications for color difference (ΔE*), internal porosity (IP), average particle size (APS), water absorption capacity (WAC), and swelling power (SP). P-values more than 0.05 indicate a non-significant lack-of-fit for the models and non-seral autocorrelation in the residuals (Durbin-Watson statistic).

3.2. Internal porosity

The internal porosity is time-dependent over the defined microwave heating-toasting duration. Fig. 1b displays the experimental (unfilled markers) and fit (drawn curves) relationships between internal porosity and microwave heating-toasting times. The internal porosity kinetic curves with sigmoidal shapes for all maize types revealed the rate of cavities created in the kernel endosperm during the microwave heating-toasting times due to the molecular water migration (Sumithra & Bhattacharya, 2008), implying that the formation of water vapor governed the kernel expansion (Schoeman et al., 2017) and gave rise to the internal porosity. Therefore, as a nonlinear dynamic system (Reeve & Turner, 2013), the Hill equation ($IP = IP_{max} \times X^n/(K^n + X^n)$**)** described the sigmoidal tendency of internal porosity with a good fit (Table 1). In this case, X was the microwave heating-toasting time variable used to describe the created cavities, K was the abscissa of the inflection point where the maximum internal porosity (IP_{max}) was half, and n was the Hill coefficient with values ascribed to the hills of the internal porosity curves created in floury and sweet maize kernels (Fig. 1b). Based on the Hill equation parameters reported in Table1, and the curves displayed in Fig. 1b, sweet maize exhibited greater internal porosity than floury maize. These results validated the use of the Hill equation to understand the internal porosity created in the specialty maize kernel for toasting. However, Hill equation application implies future challenges related to the law of mass action of starch granule structure, and the model parameters suggest a setting of physicochemical equilibrium principles that govern the starch modification. The increase in internal porosity was consistent with the porous media theory (Welsh et al., 2021; Yang & Chen, 2021; Zhu et al., 2015) that applies to toasted maize kernels in terms of the volume occupied by solids (on a dry basis), liquid (water), and gas (water vapor and air). Consequently, the current insight of porosity as a fraction of volume occupied by the water implies intrinsic expansions in the kernel matrix volume associated with high diffusion rates and pressure gradients to remove water from the maize kernels during microwave heating-toasting treatments.

3.3. Average particle size by milling of specialty maize kernels

Fig. 1c displays the decreasing milling average particle sizes (APS) by increasing heating-toasting times. The drawn curves in Fig. 1c correspond to fit values, and the unfilled markers are experimental data with clear differences between floury and sweet maize types, comparing only raw and toasted kernels (Lara & Ruales, 2021). Simple regression suggested that the $\ln Y = a + b \times X$ model (exponential model) appears adequate to describe the experimental data in floury maize, and the $\ln Y = a + b \times X^{1/2}$ (logarithmic-Y square root-X, an exponential model variation) explained the experimental data in sweet maize curves (Table 1). In Table 1, the parameters a and -b of each model

showed the hardness in raw kernels and the decreasing hardness rate due to increasing microwave heating-toasting times, respectively, expressed as average particle size. In addition, the lack-of-fit test and the Durbin-Watson statistic were non-significant, with P-values more than 0.05 for floury maize. The P-value less than 0.05 for the lack-of-fit test indicated that it might consider selecting a more complex model to evaluate the decreasing degree of hardness in sweet maize kernels by the microwave heating-toasting effect. Therefore, the time-related APS showed smaller and finer particles during the floury maize milling. These results imply that the milling of microwave-treated kernels consumes less energy and causes less damage to starch granules than untreated maize kernels. Furthermore, the milling behavior ascribed to the endosperm texture and kernel composition was consistent with the endosperm softness and kernel shrinkage of these specialty maize types used to make ready-to-eat maize easy to chew (floury maize) and crunchy (sweet maize).

3.4. Hydration properties

The water absorption capacity (WAC), swelling power (SP), and water-soluble index (WSI) curves evidenced the experimental and fit variation trends at the microwave heating-toasting times from 0 to 390 s (Fig. 1d, e and f). Simple regressions unveiled that the WAC and SP increasing rates (b-values) were exponential, ln Y = a + b x X model, for floury maize (Table 1), with Durbin-Watson statistic and lack of fit P-values non-significant ($P > 0.05$). On the other hand, for sweet maize using nonlinear regression, the grow exponential model appeared suitable ($P > 0.05$) for explaining the WAC and SP variations due to the high water-soluble solids compacted in the sugary-vitreous fraction. Therefore, concerning the model ln $(Y-Y_0)$ = ln $A_1 + (X/t_1)$ reported in Table 1, Y_0 represented the WAC and SP in sweet maize raw kernels, A_1 indicated the grow amplitude added to Y_0 and related to a time constant (t_1) with a growing rate of $1/t_1$. These time-related hydration properties also revealed the differences between floury and sweet maize types, suggesting that WAC and SP depended on the endosperm structure (e.g., soft, or hard) inherent to each kernel type and its average particle size in the flour. These results were consistent with kernel hardness decreased in the previous comparative study between raw and toasted maize kernels (Lara & Ruales, 2021), reflecting changes in the kernel matrix associated with increased accessibility to the hydrophilic groups in the starch and protein conformations (van Rooyen et al., 2022).

The WSI in Fig. 1f mainly reflected the decreasing curve of sweet maize (a2) ascribed to its kernel sugary-vitreous faction rich in highly dispersed compounds in water, while in floury maize (a0 and a1), due to low values of WSI, the correlation coefficients with the microwave heating-toasting time were non-relevant (-0.7766 and -0.7085) and the possible models presented significant lack-of-fit ($p \leq 0.5$). Simple regression demonstrated that a $Y = a + b \times X^2$ model could describe the WSI

diminution in sweet maize with a high correlation (-0.9076). The a-value or intercept represented the initial WSI in raw kernels, and the b-vale or slope-b was the decrease rate due to microwave heating-toasting times. Thus, the adjusted intercept (a-values) of 23.23 ± 0.78 g/100 g lessened to a decreasing rate of $-1.14\ 10^{-4} \pm 1.00\ 10^{-5}$ g/100 g s^2 and an adjusted R-squared of 88.29%. However, a significant ($P \leq 0.05$) lack-of-fit test and Durbin-Watson statistic suggested that a more complex model would better explain WSI reduction due to microwave heating-toasting times and the complex non-enzymatic formation ascribed to the Maillard reaction and sugar caramelization (Chung et al., 2014).

3.5. Proximate composition and mineral content

The normal distribution and variance comparison of the experimental data indicated that calcium and potassium were invalidated to statistical analysis by one-way or two-way matrix due to a great variation comparing the data in a2t0 and a2t390 s, ascribed to the endosperm structure and small kernel size (Lara & Ruales, 2021). With these exceptions, the average of proximate and mineral analyses summarized in Table 2, on a dry basis, revealed significant differences ($P \leq 0.05$) for floury and sweet maize types except for zinc content, whereas raw (t0 s) and microwave toasted kernels (t390 s) were not significant ($P > 0.05$). Consequently, the difference in the main macro and micro components was characteristic in floury and sweet maize types with specialty kernels to make ready-to-eat whole maize by toasting but contrasted in kernel fraction distribution, endosperm structure, and hardness properties expressed as average particle size variation.

Table 2. Proximal and mineral composition averages, differences among floury and sweet maize types, and similarities between raw and microwave toasted kernels⁜

Maize type - time	**a0t0**	**a0t390**	**a1t0**	**a1t390**	**a2t0**	**a2t390**
Macro components (g/100 g)						
Protein	7.6 ± 0.3 b	7.7 ± 0.1 b	6.7 ± 0.1 a	6.9 ± 0.2 a	9.5 ± 0.1 c	9.3 ± 0.2 c
Total fat	5.0 ± 0.1 a	5.1 ± 0.3 a	5.3 ± 0.1 a	5.2 ± 0.1 a	6.8 ± 0.4 b	7.0 ± 0.1 b
Crude fiber	1.6 ± 0.1 a	1.6 ± 0.1 a	1.6 ± 0.1 a	1.7 ± 0.2 a	2.6 ± 0.1 b	2.6 ± 0.1 b
Ash	1.5 ± 0.1 a	1.6 ± 0.1 a	1.6 ± 0.1 a	1.6 ± 0.1 a	1.9 ± 0.1 b	1.9 ± 0.1 b
Nitrogen-free extract	84.6 ± 0.2 b	84.2 ± 0.5 b	85.0 ± 0.1 b	85.0 ± 0.4 b	79.2 ± 0.2 a	79.1 ± 0.4 a
Micro components (mg/100 g)						
Calcium	54.5 ± 0.9	55.3 ± 0.6	56.1 ± 0.3	55.9 ± 0.2	52.9 ± 2.0	43.3 ± 0.1
Magnesium	159 ± 0 a	159 ± 0 a	167 ± 9 a	164 ± 3 a	192 ± 0 b	173 ± 4 b
Potassium	460 ± 4	449 ± 8	456 ± 8	460 ± 3	536 ± 8	458 ± 3
Phosphorous	278 ± 9 a	275 ± 3 a	300 ± 2 b	293 ± 5 b	344 ± 8 c	321 ± 2 c
Iron	3.7 ± 0.1 c	3.7 ± 0.1 c	3.2 ± 0.2 b	3.3 ± 0.1 b	2.5 ± 0.0 a	2.5 ± 0 a
Zinc	2.4 ± 0.2	2.4 ± 0.0	2.6 ± 0.0	2.6 ± 0.0	2.9 ± 0.2	2.6 ± 0.0

⁜ Floury (a0 and a1) and sweet (a2) maize types. The microwave heating-toasting effect at t0 s (raw kernels) and t390 s (toasted kernels) was non-significant. Values with different letters in the same row indicate significant differences in maize types ($P \leq 0.05$). Row without letters shows similar statistical levels in Zinc. Calcium and potassium values presented unnormal distribution.

The protein content of the floury and sweet raw kernel was consistent with the results obtained for *Piscorunto* (floury maize) and *Chullpi* (sweet maize) reported in the characterization of Andean maize (Salvador-Reyes et al., 2021). The NFE subtracted the non-digestible carbohydrates (Salvador-Reyes et al., 2021) agreed with the starch content in floury maize (Lara et al., 2021) and the composition in sweet maize that included water-soluble solids. On the other hand, the lower protein content in floury maize (Table 2) agreed with the floury endosperm microstructure (Lara et al., 2021), where the round shape of starch granules appeared packed between thin protein layers. The composition and structure in floury maize facilitated the milling and obtaining of fine particles.

3.6. Particle size distribution of specialty maize kernels

The relative distribution of milling particle size obtained according to geometric mean diameters (502, 355, 251, 47, and 13 µm), calculated for the stack of sieves used, and plotted against microwave heating-toasting time in Fig. 3(a, c, and e) exhibited the variation of the clustered columns for each time in the maize types a0, a1, and a2, respectively. The most noticeable difference was the particle size redistribution caused by the microwave heating-toasting effect, with the increased maximum proportion for the geometric mean diameter of 47 µm in floury (a0 and a1) and sweet (a2) maize kernels. Indeed, floury maize types a0 and a1 agreed in the clustered distribution pattern, with the maximum proportion in the geometric mean diameter of 47 µm (Fig. 3a and c) and an increasing redistribution from 0.30 ± 0.01 to 0.54 ± 0.01 g/g, associated with the microwave toasting time from 0 to 390 s. On the other hand, sweet maize, a2 showed a homogeneous particle size distribution in the range of geometric mean diameters from 251 µm (0.33 ± 0.01 g/g) to 134 µm (0.26 ± 0.01 g/g) ascribed to a sugary-vitreous fraction and a little floury endosperm. However, the proportion of floury endosperm with 47 µm rose by microwave heating-toasting time effect from 0.14 ± 0.02 to 0.29 ± 0.01 g/g (Fig. 3e). The increasing microwave heating-toasting times increased the fraction recovered with a geometric mean diameter of 47 µm. This finding was consistent with the maize kernel hardness reduction (Lara & Ruales, 2021), as well as the improvement in maize milling by the effect of microwave drying (Velu et al., 2006), the maize kernel hardness diminished by the toasting influence (Raigar & Mishra, 2018), and the reduction in the force required to cut toasted pistachios (Hojjati et al., 2015). Therefore, the particle size distribution evidenced the ease of milling floury maize and exhibited the microwave heating-toasting times with more than 50% of particles less than 50 microns, suggesting lower energy consumption during the milling of these maize types. This information reflects the potential of floury maize as a source of starch nanoparticles by size reduction, i.e., top-down.

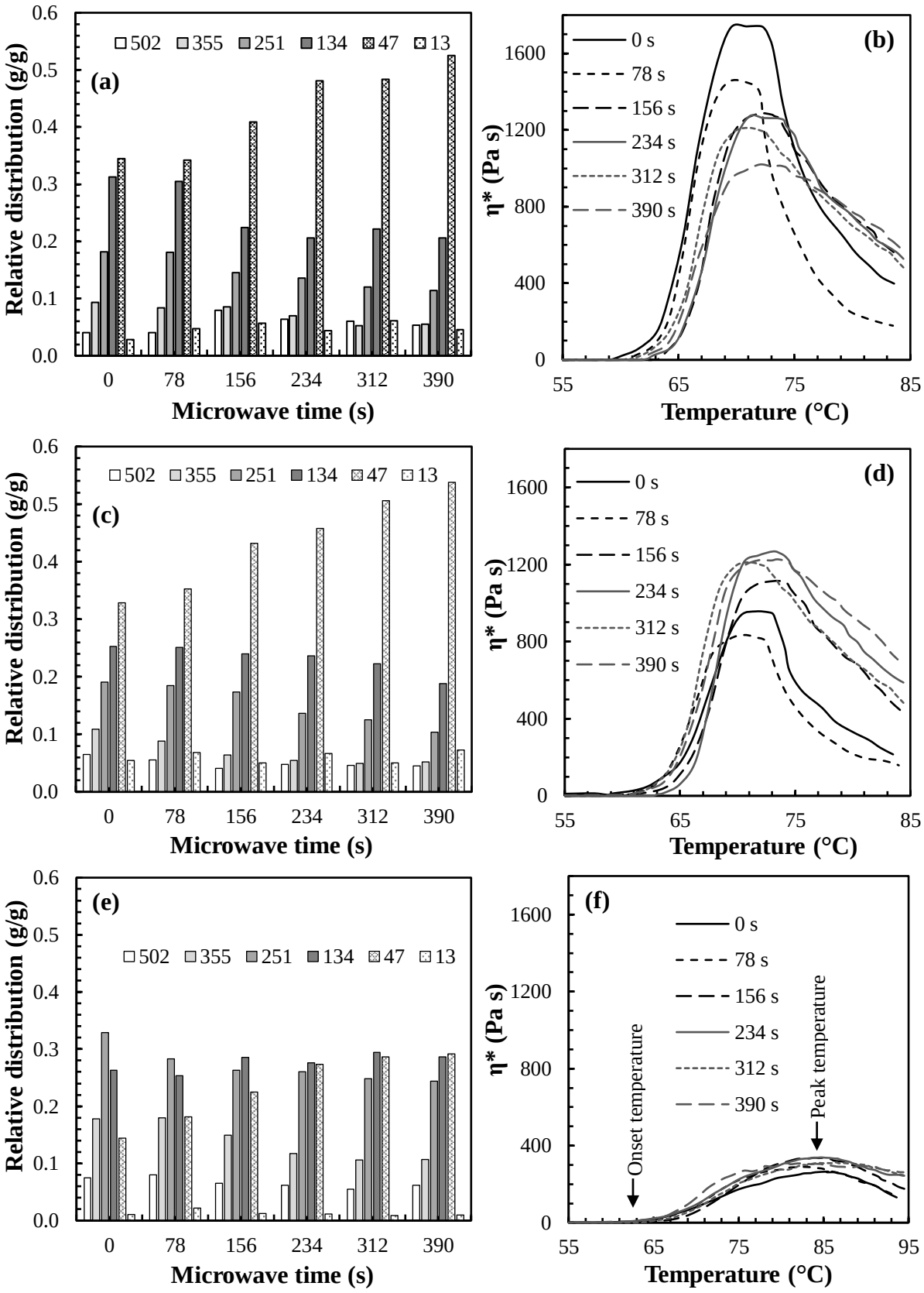

Figure 3. Milling particle size distributions from 13 to 502 µm by the microwave effect and complex viscosity (η*) profiles during non-isothermal oscillatory rheology of sample dispersions (15 g/100 g dry solid). Maize types: (**a** and **b**) floury a0; (**c** and **d**) floury a1; and (**e** and **f**) sweet a2 kernels subjected to microwave heating-toasting times from 0 to 390 s.

3.7. Non-isothermal oscillatory properties

In general, non-isothermal oscillatory measurements generated rheological profiles associated with elastic and viscous moduli of the sample dispersions in water. The complex viscosity rose slowly at onset temperature, achieved a maximum value at the peak temperature, evidenced by a 3-dimensional gel network of swollen starch granules and the leaching of amylose chains from the granules (Karunaratne & Zhu, 2016), and gradually decreased during the heating ramp due to a continuous loss of gel structure. Fig. 3(b, d, and f) shows the complex viscosity (η*) versus temperature of water dispersions (15 g/100 g dry solids) by maize types (a0, a1, and a2), respectively, illustrating the rheological curves at the microwave heating-toasting times (0., 78, 156, 234, 312, and 390 s). Floury maize samples displayed high jagged peaks (Fig. 3b and d), and sweet maize exhibited broad short peaks (Fig. 3f). After a maximum value, the complex viscosity reflected a continuous loss of gel structure in floury maize curves (Fig. 3b and d) associated with the differences in particle size distribution with a high floury proportion in floury maize types (Fig. 3a and c). In contrast, a slow gel disruption in Fig. 3f evidenced a little floury fraction in sweet maize particle size distribution (Fig. 3e). However, floury a1 (Fig. 3d) and sweet a2 (Fig. 3f) maize types displayed complex viscosity curves non-clearly affected by the microwave heating-toasting times from 0 to 390 s. This fact indicated that the rheological test was close to the parallel plate configuration limit (Ahmed, 2018; Li et al., 2020), restricting more sensitive differentiation associated with structural shifts in floury a1 and sweet a2 maize types.

The average onset and peak temperatures by maize type included the values obtained from oscillatory stress, storage (G') and loss (G") moduli, and complex (η*) and dynamic (η') viscosities which were plotted as a function of temperature (Table 3). The onset temperature represented the beginning of starch swelling ascribed to the non-isothermal oscillatory rheology, with non-detected shifts by maize type and heating-toasting treatments. In addition, the onset and peak temperatures were consistent with the temperature values found using differential scanning calorimetry (DSC) for normal and sweet native maize starches despite differences in analysis techniques. Onset temperatures reported by DSC ranged from 59.73 to 63.5 °C in normal maize (Chen et al., 2021; Singh et al., 2006; B. Zhang, Y. Xiao, et al., 2021) and from 60.5 to 64.5 °C in sweet maize (Singh et al., 2006; Zhu et al., 2016). The major peak temperature variation, also by maize types (Table 3), had higher values in sweet maize than those predicted in floury maize, agreeing with the peak temperature relative to maximum viscosity for normal (72.0-75.5 °C) and sweet maize native starches (83.8 °C) using a non-isothermal oscillatory test (Singh et al., 2006). The results also indicated that floury maize dispersions with more short-chain amylopectin fraction and less amylose content required a shorter time to achieve peak viscosity than sweet maize dispersions (Lara et al., 2021; Singh et al., 2006).

Likewise, independent of microwave heating-toasting times, the peak temperatures in floury maize agreed with the DSC peak temperatures (67.8 and 72.3 °C) in normal maize (Lei et al., 2020; Li & Zhu, 2018; Li et al., 2020; Singh et al., 2006; B. Zhang, Y. Xiao, et al., 2021). In contrast, the peak temperatures for sweet maize were lower (69.0-71.7 °C) by DSC (Singh et al., 2006; Zhu et al., 2016) than those (81.5-84.7 °C) predicted for Andean sweet maize a2 in this study. This comparison reflected differences between whole kernel rich in phytoglycogen (Xue et al., 2019) and native starch samples isolated from sweet maize, with floury endosperm as the main source of starch, but less significant than a sugary-vitreous fraction rich in water-soluble solids (Lara et al., 2021). In addition, onset and peak temperatures for floury maize types were consistent with DSC values of 59.28 ± 1.05 °C and 70.72 ± 0.85 °C, respectively, non-released for raw and toasted floury maize a0 and also agreed with those inferred on the X-axis of the normal maize native starch thermogram (Li & Hu, 2021).

Normally, the elastic or storage modulus (G') is greater than the viscous or loss modulus (G") in starch dispersions characterized by an elastic rheological behavior (Karunaratne & Zhu, 2016), and the change during a heating ramp depends on amylose content and internal structure of amylopectin (Wen et al., 2020). These rheological properties are associated with the complex (η*) and dynamic (η') viscosities, respectively, based on the fact that G' can satisfactorily describe the viscoelastic behavior of a starch gel (Li et al., 2021). The maximum elastic and viscous moduli predicted by Gaussian fit and linked to the peak temperature were higher (8125 ± 658 Pa and 1007 ± 289 Pa) in floury maize dispersions than those (1799 ± 124 Pa and 208 ± 23 Pa) in sweet maize. The maximum elastic and viscous moduli in floury maize were comparative to maximum elastic (6578 Pa at 75.2 °C) and viscous (1155 Pa at 72.5 °C) values listed for normal maize native starch (Li & Zhu, 2018), and the maximum G' was similar to that reported by waxy maize native starch at 71.30 °C (Wen et al., 2020). The sample results at time 0 s were consistent with the differences in the elastic modulus peak described between normal and sweet maize native starch dispersions at a heating ramp from 50 to 90 °C (Singh et al., 2006). The elastic to viscous modulus (G'/G") ratio indicated in Table 3 ranged between 5.96 and 11.52. The G'/G" modulus ratio significantly increased with increasing microwave heating-toasting times in floury maize dispersions and significantly decreased with sweet maize, suggesting that the G'/G" modulus ratio varied with the amylose content and amount of short-chain amylopectin fraction (Singh et al., 2006) and depended on the starch source (Dong et al., 2021). Relative to complex (η*) and dynamic viscosity (η'), it was possible to infer a non-relevant variation due to microwave heating-toasting times with decreasing trends from 0 to 156 s in complex viscosity (η*) for floury and sweet maize types, and from 0 to 390 s in dynamic viscosity (η') for floury maize (Table 3).

Table 3. Averages of non-isothermal oscillatory parameters obtained from 15 g/100 g (dry solids) dispersions of samples by maize types and microwave heating-toasting times⁜.

Maize types / Times (s)	Temperatures (°C)		Elastic/viscous ratio	Viscosities (Pa s)	
	Onset	Peak	G'/ G''	η*	η'
a0t0 (0)	58.4 ± 2.4	71.1 ± 0.6	6.60 ± 0.73 a	1402 ± 495	212 ± 78
a0t1 (78)	59.8 ± 0.5	70.7 ± 0.6	6.36 ± 0.14 a	1318 ± 128	205 ± 24
a0t2 (156)	62.5 ± 1.1	72.3 ± 0.5	8.41 ± 0.82 b	1207 ± 99	143 ± 2
a0t3 (234)	60.7 ± 1.3	72.0 ± 0.8	9.72 ± 0.99 bc	1403 ± 126	145 ± 19
a0t4 (312)	60.8 ± 1.5	71.9 ± 1.3	10.05 ± 0.45 bc	1203 ± 128	119 ± 12
a0t5 (390)	60.8 ± 1.6	72.2 ± 0.6	11.52 ± 0.44 c	1274 ± 330	110 ± 24
a1t0 (0)	59.0 ± 0.3	71.0 ± 0.5	6.43 ± 0.10 a	1562 ± 565	239 ± 84
a1t1 (78)	61.9 ± 0.6	70.7 ± 0.8	5.92 ± 0.10 a	1294 ± 578	217 ± 99
a1t2 (156)	58.4 ± 0.2	71.7 ± 1.2	7.71 ± 0.27 b	1250 ± 125	161 ± 10
a1t3 (234)	62.5 ± 0.2	71.8 ± 1.2	9.31 ± 0.57 c	1215 ± 47	130 ± 13
a1t4 (312)	60.5 ± 0.2	70.2 ± 0.8	9.74 ± 0.31 c	1213 ± 204	124 ± 17
a1t5 (390)	59.8 ± 0.6	72.9 ± 0.5	10.89 ± 0.24 d	1271 ± 244	116 ± 22
a2t0 (0)	59.9 ± 1.0	84.5 ± 1.3	9.60 ± 0.35 b	303 ± 94	31 ± 10
a2t1 (78)	60.4 ± 1.8	81.5 ± 1.0	9.50 ± 0.40 b	262 ± 26	27 ± 2
a2t2 (156)	64.2 ± 1.0	83.4 ± 2.1	8.02 ± 0.77 ab	266 ± 63	32 ± 5
a2t3 (234)	63.7 ± 2.5	83.8 ± 1.5	8.51 ± 0.79 ab	295 ± 62	35 ± 7
a2t4 (312)	63.6 ± 1.0	84.7 ± 1.7	9.00 ± 1.06 ab	308 ± 49	35 ± 8
a2t5 (390)	62.0 ± 2.5	84.1 ± 3.0	7.56 ± 0.21 a	293 ± 55	38 ± 6

⁜ Onset and peak temperatures (n = 15 values). Elastic/viscous modulus ratio and complex and dynamic viscosities, three replications (n = 3). Values with different lowercase letters in the same column by maize type indicate significant differences associated with the microwave heating-toasting time effect ($P \leq 0.05$). (η*) complex and (η') dynamic viscosities.

Tukey's test comparing means illustrated the significant variations determined by maize types (Fig. 4a, c, d, and e) and microwave heating-toasting times (Fig. 4f). However, due to evident contrasted trends in the (G'/G") ratio between floury and sweet maize, sweet maize data were excluded for two-way ANOVA (Fig. 4e and f). In Fig. 4a, onset and peak temperatures, Fig. 4c, G' and G" moduli and Fig 4d, and η*, η' viscosities exhibited significant variation ($P \leq 0.05$) between floury (a0 and a1) and sweet maize (a2) but similar levels ($P \geq 0.05$) relative to floury kernel types (a0 and a1). In Fig. 4b, the heating-toasting times applied to kernels appeared irrelevant ($P \geq 0.05$) because the temperature depended on the gelatinization phenomenon innate to each starch source during non-isothermal oscillatory measurements (Dong et al., 2021). However, excluding sweet maize data, the G'/G" modulus ratio also revealed significant variations ($P \leq 0.05$) inherent to specialty floury maize types (Fig 4e) and by the microwave heating-toasting time effect (Fig. 4f) at the peak temperatures agreeing with the one-way ANOVA results (Table 3).

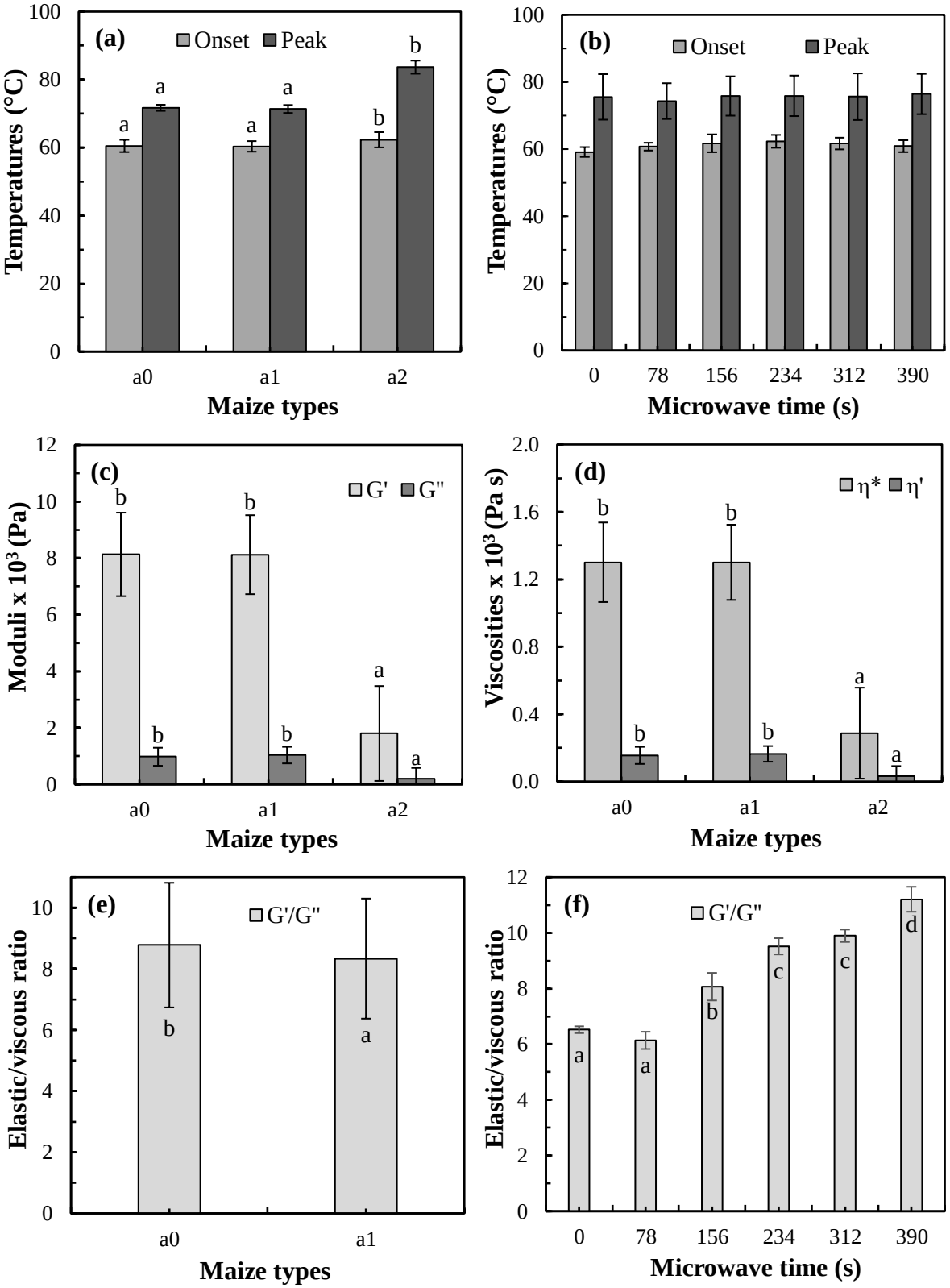

Figure 4. Tukey's comparing means ± standard deviation of non-isothermal oscillatory parameters clustered by maize types and microwave heating-toasting times: (**a**) Onset and peak temperatures for maize types (n = 18) and (**b**) microwave heating-toasting times (n = 9); (**c**) G' and G" and (**d**) η* and η' for maize types, (n = 18); (**e**) G'/G" for maize types (n = 18) and (**f**) microwave heating-toasting times (n = 6). Bars with different lowercase letters in the same graphic indicate significant differences in maize types or microwave heating-toasting time effect ($P \leq 0.05$). Maize types: floury (a0 and a1) and sweet (a2) kernels.

4. Conclusion

Modeling the kinetics of surface color difference (ΔE*), porosity, milling average particle size, and flour hydration properties showed that these physical properties were consistently time-related variables in floury and sweet maize kernels subjected to microwave heating-toasting treatments. Mainly linear (ΔE* in sweet maize), rational ((ΔE* in floury maize), exponential (APS, WAC, and SP in floury maize), and nonlinear (Internal porosity in all maize types and WAC and SP in sweet maize) models adequately appeared to describe these physical properties. In contrast, more complex models could be suitable for interpreting the average particle size and high soluble solids compacted in sweet maize. The physical, chemical, and rheological characterizations were inherent to these specialty maize kernels used to make whole ready-to-eat maize by toasting in the Andean region. The particle size distribution in floury and sweet maize varied with the increasing microwave heating-toasting time, and the highest proportion of fine particles and less than 50 μm was for floury maize, implying easier milling and less energy consumption for this maize type. Also, complex viscosity displayed jagged peaks in floury maize, and broad peaks in sweet maize ascribed average particle size, flour hydration properties, and proximal composition. The oscillatory stress parameter pointed to the onset of the starch granule swelling in the maize sample dispersions and agreed with the onset temperature. The G'/G" modulus ratio unveiled the microwave heating-toasting time effect on the rheological properties of these specialty Andean maize kernels. These results open new insight into physic-basic models for the design and quality control of microwave heating-toasting treatments focused on handling conditions to obtain whole grains with specialty matrices directed towards new frontiers of scientific study.

Funding statement

The author carried out this work within the DOCT-DI-2019-49 Project framework with the institutional sponsor of the Universidad Central del Ecuador.

Data availability statement

Data is available on request.

Conflict of interest

The authors declare no conflict of interest.

Acknowledgments

The Research Program of the Universidad Central del Ecuador supported this work. In addition, the authors would like to thank the research laboratories of the Universidad Central del Ecuador, Universidad de Santiago de Chile, and Escuela Politécnica Nacional for the instrumental facilities.

References

Adeleye, O. O., Awodiran, S. T., Ajayi, A. O., & Ogunmoyela, T. F. (2020). Effect of high-temperature, short-time cooking conditions on in vitro protein digestibility, enzyme inhibitor activity and amino acid profile of selected legume grains. *Heliyon*, *6*(11), e05419. https://doi.org/10.1016/j.heliyon.2020.e05419

Ahmed, J. (2018). Advances in rheological measurements of food products. *Current Opinion in Food Science*, *23*, 127-132. https://doi.org/10.1016/j.cofs.2018.10.007

AOAC. (1995). *Official methods of analysis of AOAC International* (P. Cunniff, Ed. 16th ed., Vol. 2). Gaitherburg, Maryland. https://searchworks.stanford.edu/view/4706329

Chen, P., Zhang, Y., Qiao, Q., Tao, X., Liu, P., & Xie, F. (2021). Comparison of the structure and properties of hydroxypropylated acid-hydrolysed maize starches with different amylose/amylopectin contents. *Food Hydrocolloids*, *110*, 106134. https://doi.org/10.1016/j.foodhyd.2020.106134

Chung, H.-S., Kim, J.-K., Moon, K.-D., & Youn, K.-S. (2014). Changes in color parameters of corn kernels during roasting. *Food Science and Biotechnology*, *23*(6), 1829-1835. https://doi.org/10.1007/s10068-014-0250-x

Doblado-Maldonado, A. F., Flores, R. A., & Rose, D. J. (2013). Low moisture milling of wheat for quality testing of wholegrain flour. *Journal of Cereal Science*, *58*(3), 420-423. https://doi.org/10.1016/j.jcs.2013.08.006

Dong, H., Zhang, Q., Gao, J., Chen, L., & Vasanthan, T. (2021). Comparison of morphology and rheology of starch nanoparticles prepared from pulse and cereal starches by rapid antisolvent nanoprecipitation. *Food Hydrocolloids*, *119*, 106828. https://doi.org/10.1016/j.foodhyd.2021.106828

Fick, K. R., Miller, S. M., Funk, J., Mcdowell, L. R., & Houser, R. H. (1976). Methods of mineral analysis for plant and animal tissues. *Plant Physiology*, *15*, 121-130.

Hojjati, M., Noguera-Artiaga, L., Wojdyło, A., & Carbonell-Barrachina, Á. A. (2015). Effects of microwave roasting on physicochemical properties of pistachios (*Pistaciavera* L.). *Food Science and Biotechnology*, *24*(6), 1995-2001. https://doi.org/10.1007/s10068-015-0263-0

Joyner, H. S., Wicklund, R. A., Templeton, C. M., Howarth, L. G., Wong, S.-S., Anvari, M., & Whaley, J. K. (2021). Development of starch texture rheological maps through empirical modeling of starch swelling behavior. *Food Hydrocolloids*, *120*, 106920. https://doi.org/10.1016/j.foodhyd.2021.106920

Kalivoda, J. R., Jones, C. K., & Stark, C. R. (2017). Impact of varying analytical methodologies on grain particle size determination. *Journal of Animal Science*, *95*(1), 113. https://doi.org/10.2527/jas.2016.0966

Karababa, E. (2006). Physical properties of popcorn kernels. *Journal of Food Engineering*, *72*(1), 100-107. https://doi.org/10.1016/j.jfoodeng.2004.11.028

Karababa, E., & Coşkuner, Y. (2007). Moisture dependent physical properties of dry sweet corn kernels. *International Journal of Food Properties*, *10*(3), 549-560. https://doi.org/10.1080/10942910601003981

Karunaratne, R., & Zhu, F. (2016). Physicochemical interactions of maize starch with ferulic acid. *Food Chemistry*, *199*, 372-379. https://doi.org/10.1016/j.foodchem.2015.12.033

Lara, N., Osorio, F., & Ruales, J. (2022). Variables related to microwave heating-toasting time and water migration assessment with kernel size approaches of specialty maize types. *Journal of the Science of Food and Agriculture*. https://doi.org/10.1002/jsfa.11961

Lara, N., & Ruales, J. (2002). Popping of amaranth grain (*Amaranthus caudatus*) and its effect on the functional, nutritional and sensory properties. *Journal of the Science of Food and Agriculture*, *82*(8), 797-805.

Lara, N., & Ruales, J. (2021). Physical and hydration properties of specialty floury and sweet maize kernels subjected to pan and microwave toasting. *Journal of Cereal Science*, *101*, 103298. https://doi.org/10.1016/j.jcs.2021.103298

Lara, N., Vizuete, K., Debut, A., Chango, I., Campaña, O., Villacrés, E., Bonilla, P., & Ruales, J. (2021). Underutilized maize kernels (*Zea mays* L. var. *amylacea* and var. *saccharata*) subjected

to pan and microwave toasting: A comparative structure study in the whole kernel. *Journal Cereal Science*, *100*, 103249. https://doi.org/10.1016/j.jcs.2021.103249

Lee, E. C., Lee, J. H., Chung, H.-J., & Park, E. Y. (2021). Impregnation of normal maize starch granules with ionic hydrocolloids by alkaline dry heating. *Food Hydrocolloids*, *113*, 106462. https://doi.org/10.1016/j.foodhyd.2020.106462

Lei, N., Chai, S., Xu, M., Ji, J., Mao, H., Yan, S., Gao, Y., Li, H., Wang, J., & Sun, B. (2020). Effect of dry heating treatment on multi-levels of structure and physicochemical properties of maize starch: A thermodynamic study. *International Journal of Biological Macromolecules*, *147*, 109-116. https://doi.org/10.1016/j.ijbiomac.2020.01.060

Li, C., & Hu, Y. (2021). A kinetics-based decomposition approach to reveal the nature of starch asymmetric gelatinization thermograms at non-isothermal conditions. *Food Chemistry*, *344*, 128697. https://doi.org/10.1016/j.foodchem.2020.128697

Li, G., & Zhu, F. (2018). Effect of high pressure on rheological and thermal properties of quinoa and maize starches. *Food Chemistry*, *241*, 380-386. https://doi.org/10.1016/j.foodchem.2017.08.088

Li, H., Ji, J., Yang, L., Lei, N., Wang, J., & Sun, B. (2020). Structural and physicochemical property changes during pyroconversion of native maize starch. *Carbohydrate Polymers*, *245*, 116560. https://doi.org/10.1016/j.carbpol.2020.116560

Li, J., Desam, G. P., Narsimhan, V., & Narsimhan, G. (2021). Methodology to predict the time-dependent storage modulus of starch suspensions during heating. *Food Hydrocolloids*, *113*, 106463. https://doi.org/10.1016/j.foodhyd.2020.106463

Mao, H., Li, J., Chen, Z., Yan, S., Li, H., Wen, Y., & Wang, J. (2021). Molecular structure of different prepared pyrodextrins and the inhibitory effects on starch retrogradation. *Food Research International*, *143*, 110305. https://doi.org/10.1016/j.foodres.2021.110305

Pham, N. D., Khan, M. I. H., & Karim, M. A. (2020). A mathematical model for predicting the transport process and quality changes during intermittent microwave convective drying. *Food Chem*, *325*, 126932. https://doi.org/10.1016/j.foodchem.2020.126932

Qu, J., Zhong, Y., Ding, L., Liu, X., Xu, S., Guo, D., Blennow, A., & Xue, J. (2021). Biosynthesis, structure and functionality of starch granules in maize inbred lines with different kernel dehydration rate. *Food Chemistry*, *368*, 130796. https://doi.org/10.1016/j.foodchem.2021.130796

Raigar, R. K., & Mishra, H. N. (2018). Study on the effect of pilot scale roasting conditions on the physicochemical and functional properties of maize flour (Cv. *Bio 22027*). *Journal of Food Processing and Preservation*, *42*(5), e13602. https://doi.org/10.1111/jfpp.13602

Reeve, R., & Turner, J. R. (2013). Pharmacodynamic models: parameterizing the hill equation, Michaelis-Menten, the logistic curve, and relationships among these models. *J Biopharm Stat*, *23*(3), 648-661. https://doi.org/10.1080/10543406.2012.756496

Salvador-Reyes, R., & Clerici, M. T. P. S. (2020). Peruvian Andean maize: General characteristics, nutritional properties, bioactive compounds, and culinary uses. *Food Research International*, *130*, 108934. https://doi.org/10.1016/j.foodres.2019.108934

Salvador-Reyes, R., Rebellato, A. P., Lima Pallone, J. A., Ferrari, R. A., & Clerici, M. T. P. S. (2021). Kernel characterization and starch morphology in five varieties of Peruvian Andean maize. *Food Research International*, *140*, 110044. https://doi.org/10.1016/j.foodres.2020.110044

Schoeman, L., du Plessis, A., Verboven, P., Nicolaï, B. M., Cantre, D., & Manley, M. (2017). Effect of oven and forced convection continuous tumble (FCCT) roasting on the microstructure and dry milling properties of white maize. *Innovative Food Science & Emerging Technologies*, *44*, 54-66. https://doi.org/10.1016/j.ifset.2017.07.021

Singh, N., Inouchi, N., & Nishinari, K. (2006). Structural, thermal and viscoelastic characteristics of starches separated from normal, sugary and waxy maize. *Food Hydrocolloids*, *20*(6), 923-935. https://doi.org/10.1016/j.foodhyd.2005.09.009

Sumithra, B., & Bhattacharya, S. (2008). Toasting of corn flakes: Product characteristics as a function of processing conditions. *Journal of Food Engineering*, *88*(3), 419-428. https://doi.org/10.1016/j.jfoodeng.2008.03.001

Tao, Y., Yan, B., Fan, D., Zhang, N., Ma, S., Wang, L., Wu, Y., Wang, M., Zhao, J., & Zhang, H. (2020). Structural changes of starch subjected to microwave heating: A review from the perspective of dielectric properties. *Trends in Food Science & Technology*, *99*, 593-607. https://doi.org/10.1016/j.tifs.2020.02.020

van Rooyen, J., Simsek, S., Oyeyinka, S. A., & Manley, M. (2022). Holistic view of starch chemistry, structure and functionality in dry heat-treated whole wheat kernels and flour. *Foods*, *11*(2). https://doi.org/10.3390/foods11020207

Velu, V., Nagender, A., Prabhakara Rao, P. G., & Rao, D. G. (2006). Dry milling characteristics of microwave dried maize grains (*Zea mays* L.). *Journal of Food Engineering*, *74*(1), 30-36. https://doi.org/10.1016/j.jfoodeng.2005.02.014

Welsh, Z. G., Khan, M. I. H., & Karim, M. A. (2021). Multiscale modeling for food drying: A homogenized diffusion approach. *Journal of Food Engineering*, *292*, 110252. https://doi.org/10.1016/j.jfoodeng.2020.110252

Wen, Y., Yao, T., Xu, Y., Corke, H., & Sui, Z. (2020). Pasting, thermal and rheological properties of octenylsuccinylate modified starches from diverse small granule starches differing in amylose content. *Journal of Cereal Science*, *95*, 103030. https://doi.org/10.1016/j.jcs.2020.103030

Xue, J., Inzero, J., Hu, Q., Wang, T., & Wusigale, Y. L. (2019). Development of easy, simple and low-cost preparation of highly purified phytoglycogen nanoparticles from corn. *Food Hydrocolloids*, *95*, 256-261. https://doi.org/10.1016/j.foodhyd.2019.04.041

Yang, R., & Chen, J. (2021). Mechanistic and machine learning modeling of microwave heating process in domestic ovens: A review. *Foods*, *10*(9). https://doi.org/10.3390/foods10092029

Zhang, B., Qiao, D., Zhao, S., Lin, Q., Wang, J., & Xie, F. (2021). Starch-based food matrices containing protein: Recent understanding of morphology, structure, and properties. *Trends in Food Science & Technology*, *114*, 212-231. https://doi.org/10.1016/j.tifs.2021.05.033

Zhang, B., Xiao, Y., Wu, X., Luo, F., Lin, Q., & Ding, Y. (2021). Changes in structural, digestive, and rheological properties of corn, potato, and pea starches as influenced by different ultrasonic treatments. *International Journal of Biological Macromolecules*, *185*, 206-218. https://doi.org/10.1016/j.ijbiomac.2021.06.127

Zhang, J., Ran, C., Jiang, X., & Dou, J. (2021). Impact of octenyl succinic anhydride (OSA) esterification on microstructure and physicochemical properties of sorghum starch. *LWT - Food Science and Technology*, *152*, 112320. https://doi.org/10.1016/j.lwt.2021.112320

Zhu, F., Bertoft, E., & Li, G. (2016). Morphological, thermal, and rheological properties of starches from maize mutants deficient in starch synthase III. *Journal of Agricultural and Food Chemistry*, *64*(34), 6539-6545. https://doi.org/10.1021/acs.jafc.6b01265

Zhu, H., Gulati, T., Datta, A. K., & Huang, K. (2015). Microwave drying of spheres: Coupled electromagnetics-multiphase transport modeling with experimentation. Part I: Model development and experimental methodology. *Food and Bioproducts Processing*, *96*, 314-325. https://doi.org/10.1016/j.fbp.2015.08.003

Chapter 6

Discussion and concluding remarks

Nelly Lara[a,b*]

[a] Campo Académico Docene Experimental la Tola, Facultad de Ciencias Agrícolas, Universidad Central del Ecuador, Calle Universitaria s/n, Tumbaco, Ecuador

[b] Departamento de Ciencia de Alimentos y Biotecnología, Escuela Politécnica Nacional, Av. Ladrón de Guevara E11-253 Edificio 19 Quito, Ecuador

1. Discussion

1.1. Floury and sweet Andean maize with specialty kernels for whole ready-to-eat maize by toasting

Floury and sweet maize with specialty kernels to make whole ready-to-eat maize by toasting remain underutilized worldwide. Consequently, a few scientific articles have been recently published on Andean maize kernel characterization (Salvador-Reyes & Clerici, 2020; Salvador-Reyes et al., 2021) and toasting (Lara & Ruales, 2021; Lara et al., 2021). Furthermore, a review that exhibits the existing literature on specialty Andean maize for toasting is unavailable. However, the toasting procedures that utilize dry heating have attracted the scientific community's attention with recent reviews related to current scientific literature about common and novel toasting techniques and their effect on the main properties of some foods (Sruthi et al., 2021). Likewise, the targeted treatments of whole kernels and multi-component mixtures to acquire desirable properties is a topic of current reviews (Bello-Pérez et al., 2021; Tao et al., 2020; Torbica et al., 2021).

1.2. Pan and microwave toasting effect on the whole maize kernel structure

Starch granule size distributions exhibited unimodal curves. Their fit as Kernel density (R-squares from 92.16 to 98.74%) displayed variations in floury and sweet maize types and structural changes from raw to toasted kernel conditions. These results were consistent with the statistical differences analyzed as starch granule geometric mean diameter (GMD), suggesting structural changes ascribed to starch granule size by type of maize endosperm and unimodal distributions associated with their

* Corresponding author: CADET, Facultad de Ciencias Agrícolas, Universidad Central del Ecuador, Calle Universitaria s/n, Tumbaco, Ecuador. E-mail: nvlara@uce.edu.ec (N. Lara)

spherical shape (Gayral et al., 2016). In addition, the spherical shape observed in the granule starch microphotographs reflected the lack of protein structures in the floury endosperm matrix.

All floury and sweet maize samples analyzed by X-ray diffraction presented starches with the A-type crystalline structure in agreement with those reported for normal maize starch treated by dry heating (Lei et al., 2020; Li et al., 2020; Zou et al., 2020) and peak positions at 2θ of 15°, 17°, 18°, 20°, and 23°, also consistent with those in native starch of normal, waxy, and super-sweet maize types (Yu et al., 2015). Thus, the peak intensity at 2θ of 20° (4.4 Å), a diffraction spacing marker in amylose standard (Vega-Rojas et al., 2016) and high amylose maize starch (Chen et al., 2019), was low in all treatments, but it augmented in sweet toasting treatments and almost no varied in floury maize. According to diffraction spacing, these findings evidenced that the peak of the amylose-lipid complex (4.4 Å) was a structural trait intrinsic to sweet maize kernels, subjected to pan and microwave toasting. In contrast, a broad peak intensity at 2θ of 23° (3.9 Å), a diffraction spacing marker in amylopectin standard (Vega-Rojas et al., 2016) and waxy maize starch (Yu et al., 2015), appeared in all maize treatments with reduced peak intensities due to the pan and microwave toasting effect. In this case, the peak intensity at diffraction spacing 3.9 Å indicated a partial loss of crystallite in starch granules by toasting effect, mainly ascribed to the double helices disaggregated from the amylopectin chains (Lei et al., 2020; Zou et al., 2020). These results support the differences in relative crystallinity by maize types and the decrease due to toasting treatments. In addition, raw floury and sweet maize treatments had high and low relative crystallinity compared to those reported for normal an sweet maize starches, respectively (Peng & Yao, 2018).

The band around 480 cm^{-1} is an intense marker in the glycogen, amylose, and amylopectin Raman spectra (Wiercigroch et al., 2017), and the full width at half maximum (FWHM) is an indicator related to the short-range order of starch (Chen et al., 2019). In this study, the FWHM480 values obtained from maize treatment spectra showed non-significant variation among maize types, whereas the FWHM480 values for raw kernels and toasted using a pan and microwave varied significantly. The band at 864-865 cm^{-1} is sensitive to molecular starch structure orientation, the band at 941-942 cm^{-1} is related to amylopectin (Gayral et al., 2016), and the band intensity ratio (865/941) is a marker of starch crystallinity sensitive to its molecular orientation (Gayral et al., 2016) because Raman intensity varies directly with the crystalline region size (Liu et al., 2015). In this study, the band intensity ratio 865/941 presented a non-significant difference among maize types and between raw and toasting conditions, suggesting a non-significant change in the orientation of crystallites within the starch granules. However, the FWHM ratio 865/941 revealed substantial differences between floury and sweet maize and between raw and toasted kernels, indicating that the FWHM ratio

865/941 was more sensitive than the band intensity ratio (865/941) to detect the molecular orientation at nanocrystal levels (7.4 ± 0.1 – 8.6 ± 0.4 nm) within the starch granules in floury and sweet maize.

The ATR-FTIR spectra of maize flour displayed different regions for carbohydrates, proteins, and lipids ascribed to the bands 990 to 1152 cm^{-1}, 1643 cm^{-1}, and 1744-1745 cm^{-1}, respectively (Achten et al., 2019). In the lipid region, raw sweet maize spectra exhibited an additional minimum band at 1709 cm^{-1} associated with free fatty acids that disappeared by the toasting effect. This band was undetected in whole floury maize treatments due to its low-fat content, and it is distinctive in the maize oil extract spectrum (Achten et al., 2019). In addition, a band at 3295 cm^{-1} detected in sweet maize spectra agreed with a similar O-H band in the FT-IR spectra of phytoglycogen nanoparticles from sugary-1 maize (Xue et al., 2019). In the carbohydrate structure region, the band intensities at 994, 1017, and 1047 cm^{-1}, separated by deconvolution, are sensitive to changes in starch conformation. Hence the band intensity ratio of 1047/1017 reflects the ordering level, and the band intensity ratio of 1017/994 indicates the ratio of amorphous to an ordered structure of the starch (Cai et al., 2014; Chen et al., 2019). In this study, the band intensity ratio at 1047/1017 was non-significant among all maize treatments with a mean value of 0.56 ± 0.05, and it was similar to those estimated for normal and waxy maize starches (Sui et al., 2015). In contrast, the band intensity ratio at 1017/994 reflected higher significant differences ascribed to sweet maize and the microwave toasting effect. However, the variation ranges of 1047/1017 and 1017/994 ratios were consistent with those reported for native starch of normal maize (Cai et al., 2014), super-sweet maize (Yu et al., 2015) and were slightly different from those corresponding to native starch of waxy, normal, and high amylose maize (Chen et al., 2019).

The starch content in floury maize was higher than that in sweet maize, and it was consistent with the variation between normal and super-sweet maize (Yu et al., 2015). The blue values determined in raw kernels agreed with those reported for the floury endosperm fraction extracted from different maize types (Zhang & Xu, 2019). A significant difference in the blue value implied variation of amylose and amylopectin chain length (Minakawa et al., 2019; Zhang & Xu, 2019). The number average of molecular weight ($\bar{M}_n$) was higher in floury maize kernel than that in sweet maize before and after toasting, and also higher than that reported for normal maize native starch (Singh & Ali, 2008). In floury maize treatments, the decreasing $\bar{M}_n$ revealed conformational changes according to the Mark-Houwink equation (Kowalski et al., 2018) with more effect due to microwave toasting than toasting in a pan. However, the values determined by toasting in a pan were slightly lower than that (180 x 10^3 g/mol) reported for pyrodextrins prepared by heating waxy maize starch (Han et al., 2018). In sweet maize toasted treatments, the increase in $\bar{M}_n$ inferred an increase mass of chain segments, increase in molecular density, and decrease in viscosity. This hypothesis agreed with the unique

structural properties associated with phytoglycogen in sugary-1 mutants from native sweet maize (Xue et al., 2019). However, further investigation is needed to understand the results in sweet maize kernels subjected to pan and microwave toasting. Consequently, for floury maize, the intrinsic viscosity [η] was consistent with the $\bar{M}_n$. The [η] determined for raw floury maize kernels was higher than that for untreated whole waxy wheat flour (Kowalski et al., 2018) than that obtained for normal maize native starch (Singh & Ali, 2008) and those reported for maize amylose, and amylopectin standards (Yu et al., 2014). In sweet maize, intrinsic viscosity decreased while the $\bar{M}_n$ increased. These results do not follow the Mark-Houwink equation because floury and sweet maize are two highly contrasted in starch and endosperm structure. Sweet maize also showed a water-soluble index very high in agreement with its total and reducing sugar content. The finding on floury maize water-soluble index was equivalent to that determined at 25 °C for maize flour obtained from whole kernel samples treated with NIR lamp heating (Deepa & Hebbar, 2017). Moreover, water-soluble index and total sugar reduction may depend on the free sugar drop ascribed to Maillard metabolite formations in toasted maize kernels at high temperatures (Woo et al., 2018; Youn & Chung, 2012).

1.3. Pan and microwave toasting effect on physical and hydration properties in whole maize kernels

Adjusting the initial water content in the raw maize kernels to 14 g/100 g on a wet basis avoided possible experimental errors ascribable to the influence of the water content on the physical properties reported in raw kernels of popcorn (Karababa, 2006), sweet maize (Karababa & Coşkuner, 2007), and normal maize (Mousaviraad & Tekeste, 2020). The results revealed a rapid water loss by microwave toasting (390 s) with remaining water contents closely comparable to water levels (less than 2 g/100 g) in breakfast cereal (Sumithra & Bhattacharya, 2008). Additionally, the maize kernels toasted in a pan (1500 s) had a lower water content than those (4-5 g/100 g) reported in the normal maize toasted for 1500 s at pilot trials (Raigar & Mishra, 2018). Kernel size was a specialty characteristic in floury and sweet maize types. Floury maize had larger kernel sizes than those determined for yellow (Mousaviraad & Tekeste, 2020) and white (Guelpa et al., 2016; Uriarte-Aceves et al., 2019) normal maize at comparable moisture content. In sweet maize, the kernel dimensions were larger than in sweet maize hybrid (Karababa & Coşkuner, 2007) and almost comparable to the Peruvian sweet maize called *Chullpi* (Salvador-Reyes et al., 2021). The volumetric variations from raw to toasted conditions suggested a kernel expansion linked to a large cavity or internal porosity created during pan and microwave toasting, likewise reported in toasted normal maize kernels (Schoeman et al., 2017) and coffee beans (Oliveros et al., 2017). However, the expansion ratios in floury and sweet maize kernels were higher by pan and microwave toasting than 1.11 ± 0.17 determined in normal white maize toasted in a conventional oven (Schoeman et al., 2017). In this study, maize types and toasting conditions significantly influenced volume expansion

expressed as expansion ratio and internal porosity. The expansion ratio was low and high in floury and sweet maize kernels, respectively, and directly associated with their contrasted endosperm structure. The expansion ratio and internal porosity generated during microwave toasting were consistent with the fast water loss inferred from the remaining water content in microwave toasting kernels, proving that the toasting process increased the porosity in maize kernels due to the water loss effect (Schoeman et al., 2017). Relative to the specialty characteristics, floury and sweet maize kernels had the lowest raw individual kernel density when compared to those values for raw kernel reported in sweet maize (Karababa & Coşkuner, 2007) and normal maize (Guelpa et al., 2016; Mousaviraad & Tekeste, 2020; Uriarte-Aceves et al., 2020; Uriarte-Aceves et al., 2019). In addition, pan and microwave toasting presented a higher reduction in kernel density than that determined for normal maize toasted in a conventional oven (Schoeman et al., 2017). These results reflected that floury and sweet maize had specialty kernels to make whole ready-to-eat maize by toasting. However, innovative technologies for industrial milling could enhance the floury maize properties with completely soft endosperm and low protein content, e.g., intended for starch extraction.

The changes toward golden surface color were more noticeable in sweet maize than in floury maize. This color behavior is due to its sugary-vitreous fraction and high reducing sugars (Lara et al., 2021), implying the Maillard reaction and sugar caramelization influence (Chung et al., 2014; Youn & Chung, 2012). The sweet maize L*, a*, and b* parameters agreed with the color parameters reported for the Peruvian sweet maize (Salvador-Reyes et al., 2021). During pan and microwave toasting, the L* and b* parameters decreased while a* augmented, and these variations were consistent with the trend changes in the same color parameters by electrical rotary toasting of *Zea mays* var. *indurate* for 50 min (Chung et al., 2014). The standard color parameters distribution in floury and sweet maize indicated high values for yellowness (h*) and lightness (L*), comparable values for yellowness (b*) and chroma (C*), and low values for redness (a*)(Chung et al., 2014).

In maize kernel texture, the main differences were between raw and toasted kernel hardness, with a decreasing kernel hardness associated with the internal porosity created or formation of cavities (Schoeman et al., 2017) by the pan and microwave toasting effect. The average kernel hardness values in floury maize with entirely soft endosperm were lower than that obtained in sweet maize with a sugary-vitreous kernel fraction more representative than floury endosperm (Lara et al., 2021). The kernel hardness results agreed with low and high hardness reported for soft and vitreous maize endosperm in normal white maize (Guelpa et al., 2015; Schoeman et al., 2017). The high hardness in sweet maize was consistent with the largest average particle sizes, also ascribed to its sugary-vitreous fraction with more than 20 % total sugars (Lara et al., 2021).

Water absorption capacity and swelling power reflected the water integration into non-soluble solids expressed by total sample and non-soluble solids. Water absorption capacity and swelling power varied according to the major differences in maize types before and after pan and microwave toasting. These results agreed with the increasing hydration properties of arrowhead tubers subjected to pan and microwave toasting (Wani et al., 2016), and the water absorption capacity, respectively, were consistent with the values reported in raw (Paesani et al., 2020; Wang et al., 2019) and normal toasted maize at pilot trials (Raigar & Mishra, 2018). In addition, the swelling power value in raw kernels was lower than that reported for raw normal maize flour at 25 °C (Deepa & Hebbar, 2017). In contrast to water absorption capacity and swelling power, the water-soluble index decreased by the toasting effect, and it was similar to that reported for whole maize kernels treated by NIR lamp heating (Deepa & Hebbar, 2017). The water-soluble index reduction reflected the decreasing free sugar during maize kernel toasting (Lara et al., 2021; Woo et al., 2018; Youn & Chung, 2012). The high water-soluble index in sweet maize compared to floury maize unveiled the natural accumulation of phytoglycogen nanoparticles, an α-D-glucan highly water-dispersible (Xue et al., 2019).

1.4. Microwave heating-toasting time-related variables and water migration in Andean specialty maize types

In addition to water content WC, water ratio WR, and water loss WL, most of the physical properties correlated with the microwave heating-toasting time when the initial water content (time t = 0) was 0.16 ± 01 g/g on a dry basis (14 ± 1 g/100 g on a wet basis). Sweet maize showed more good correlations than the floury maize types. Likewise, one of the floury maize types displayed fewer good correlations than the other. These results were consistent with the significant differences in geometric mean diameter (GMD), surface area (S), volume (V), kernel density, color parameters (a*, b*, and C*), and color difference ΔE* by the same maize types before and after toasting reported in a previous study (Lara & Ruales, 2021). This fact demonstrated that the number of time-related variables with good correlations depended on the maize types with their kernel properties. Kernel thickness appeared to have more influence on geometric properties than the other dimensions and was consistent in good correlation coefficients with the kernel density, GMD, volume, and surface area. e.g., density decreased when kernel volume increased by the microwave heating-toasting process, agreeing with the relationship density to volume in toasted coffee beans (Bustos-Vanegas et al., 2018). Consequently, the kernel dimension differences by maize types validated the reliability of the kernel size approaches tried in this study.

The models used in microwave drying to estimate water migration (Jahanbakhshi et al., 2020; Kipcak & Doymaz, 2020; Shirkole & Sutar, 2018) gave kinetic curves of WC, WR, and WL with a highly

significant lack-of-fit. It was due to the difference between drying a thin layer on an open tray and toasting inside a closed package like raw microwave maize. No previous studies have attempted to model the kernel microwave toasting. In this study, third-order polynomial models appeared adequate to describe the relationship of WC, WR, and WL with the heating-toasting time, including the kernel dimension influence in terms of spatial kernel size $(S/V)^2$ and center of the symmetry to surface distance $(GMD/2)^2$ approaches. Based on the lack-of-fit test, the main statistical parameters in WC, WR, and WL regression curves demonstrated intermedium, low and high reliability using the third-order polynomial regression model without and with the kernel size approach, respectively.

The WC regression curves computed with the actual $(S/V)^2$ approach (g/g mm^2) reflected the spatial water distribution at each microwave heating-toasting time with a clear difference among maize types due to the variation in their kernel surface area (S) and volume (V). Also, by maize types, the WC regression curves with the actual $(GMD/2)^2$ (g/g mm^2) approach appeared well set apart as the result of the water migration from the center of the symmetry to the surface distance, reflecting the differences in geometric mean diameter (GMD) ascribed to maize types. These results reflected GMD, S, and V differences in maize types and between raw and toasted kernels (Lara & Ruales, 2021).). In WR, the significant serial autocorrelations and lack-to-fits are challenging to overcome with more complex solutions in the future. On the other hand, WL depended on the maize kernel S, V, and GMD and was consistent with the cavities created in individual maize kernels during toasting, measured as standardized volume increases (Schoeman et al., 2017), internal porosity (Lara & Ruales, 2021), and the expansion in toasted coffee beans (Bustos-Vanegas et al., 2018). In addition, WC, WL, and WR with the $(GMD/2)^2$ approach were lower than those with the $(S/V)^2$ approach.

The first derivative obtained from the average third-order polynomial regression curves indicated the exchange profiles of water distributed in maize kernels without and with kernel size approaches. Thus, the exchange profiles in WC, WR, and WL without and with kernel size approaches reached the maximum values by maize types during the falling rate period. Afterward, the decrease of maximum rates depended on the decreasing water content in the maize kernels (Shivhare et al., 1994). Without kernel size approaches, sweet maize had the highest, and floury maize types had an intermediate to the lowest maximum rates in the WC, WR, and WL exchange profiles. With kernel size $(S/V)^2$ and $(GMD/2)^2$ approaches, the differences in maximum rates for the WC, WR, and WL exchange profiles were mainly between floury and sweet maize kernels, displaying the lowest values for floury maize types. For both $(S/V)^2$ and $(GMD/2)^2$ approaches, the exchange profiles rapidly reached maximum rates linked to position shifts on the X-axis water content and their corresponding shorter times attributed to kernel size influence on water migration. However, reaching the WL top values was more delayed in sweet maize than floury maize with and without kernel size influence

ascribed to compact structure in its sugary-vitreous fraction (Lara et al., 2021). This fact may agree with the results in the coffee bean WL due to delayed porosity created in a conventional toasting process up to 400 s (Oliveros et al., 2017). On the other hand, a high internal porosity in sweet maize reflected a high volumetric expansion (Lara & Ruales, 2021) ascribed to water migration and thermal exchanges by the toasting effect (Bustos-Vanegas et al., 2018). Therefore, the internal porosity could enhance water migration because the molecular diffusion is faster in porous media than in compact solids (Chen et al., 2009).

Finally, the specific experimental arrangement by maize types and 1) water migration comparing WC and WL, and 2) kernel size approaches (S/V)
^{2} and $(GMD/2)^2$ have effects on the maximum rate and the water content and time at the maximum rate as follows:

Maize types and water migration comparing WC and WL

- The significant differences in maximum rates by maize types agreed with the arrangement of exchange profiles without kernel size approaches and with spatial $(S/V)^2$ influence.
- The differences in maximum rates with the $(GMD/2)^2$ approach were non-significant and non-consistent with the exchange profiles, implying a lack of reliability with very low values generated by the $(GMD/2)^2$ approach.
- The maximum rates were significant between WC and WL without kernel size approaches and with the spatial $(S/V)^2$ approach, whereas they were similar with the $(GMD/2)^2$ approach.

Maize types and kernel size approaches $(S/V)^2$ and $(GMD/2)^2$

- The maximum rates mainly revealed significantly higher effects due to the $(S/V)^2$ approach than those with the $(GMD/2)^2$ approach effect.
- The maximum rates were similar and non-consistent with the exchange profile differences between floury and sweet maize types.
- The variations in maize types disappeared due to an overlapping effect associated with the high difference between the two kernel size approaches.
- Significant differences caused by the kernel size approaches were evident in the water content and time at the maximum rates for WC and WR, while for WL, these parameters were similar.
- For WL, the microwave heating-toasting time at the maximum rates reflected a greater influence due to sweet maize than floury maize.

1.5. Modeling of microwave heating-toasting time-related variables

The color kinetic curves reflected a rising color difference (ΔE*) with increasing heating-toasting time according to floury and sweet maize types and their large, medium, and small size kernels determined in a previous study by maize types (Lara & Ruales, 2021). With high reliability, simple regression analyses suggested that a complex model $Y^{1/2} = a + b \times X^2$ adequately described the floury maize surface color curves. In contrast, the linear model $Y = a + b \times X$ explained the sweet maize color curves. Consequently, two different linearized models adequately describe the relationship between ΔE* and heating-toasting time in floury and sweet types, inferring that the color kinetics of microwave heating-toasting treatments depend on maize kernel types and the structure of their endosperm. In addition, according to the literature, the third-order polynomial provides good fits in toasting color kinetic of *Zea mays* var. *indurate* using an electric rotary toaster for 50 min (Chung et al., 2014).

The internal porosity kinetic curves with sigmoidal shapes for all maize types revealed the rate of cavities created in the kernel endosperm during the microwave heating-toasting times. This structural change was due to the molecular water migration (Sumithra & Bhattacharya, 2008), implying that the formation of water vapor governed the kernel expansion (Schoeman et al., 2017) and gave rise to the internal porosity. Furthermore, for this time-related variable, a nonlinear dynamic system (Reeve & Turner, 2013) reported as the Hill equation ($IP = IP_{max} \times X^n/(K^n + X^n)$**)** described the sigmoidal tendency of internal porosity with high consistency. Based on the Hill equation parameters, sweet maize exhibited greater internal porosity than floury maize. These results were consistent with the highest water loss rate reported for sweet maize in a current study (Lara et al., 2022) and validated the use of the Hill equation to understand the internal porosity created in the specialty maize kernel for toasting. However, Hill equation application implies future challenges related to the law of mass action of starch granule structure, and the model parameters suggest a setting of physicochemical equilibrium principles that govern the starch modification. On the other hand, the increase in internal porosity agreed with the porous media theory (Welsh et al., 2021; Yang & Chen, 2021; Zhu et al., 2015). Consequently, the current insight of porosity as a fraction of volume occupied by the water indicated expansions in the kernel matrix volume associated with high diffusion rates and pressure gradients in the falling rate period to remove vapor water from the maize kernels during microwave heating-toasting short times.

The decreasing milling average particle sizes (APS) by increasing heating-toasting times agreed with the negative correlation of the time-related APS reported using Pearson's correlation (Lara et al., 2022). This time-related variable also displayed clear differences between floury and sweet maize

types, and it was consistent with the significant differences by maize type after and before pan and microwave toasting (Lara & Ruales, 2021). Simple regression suggested that the $\ln Y = a + b \times X$ model (exponential model) appears adequate to describe the experimental data in floury maize, and the $\ln Y = a + b \times X^{1/2}$ (logarithmic-Y square root-X, an exponential model variation) explained the experimental data in sweet maize curves. These relationships imply that the milling of microwave-treated kernels consumes less energy and causes less damage to starch granules than untreated maize kernels. Furthermore, the milling behavior ascribed to the endosperm texture and kernel composition was consistent with the endosperm softness and kernel shrinkage of these specialty maize types used to make ready-to-eat maize easy to chew (floury maize) and crunchy (sweet maize).

The water absorption capacity (WAC) and swelling power (SP) increased with microwave heating-toasting times. The increasing rate was exponential for floury maize ($\ln Y = a + b \times X$ model), while a growing exponential model [$\ln (Y-Y_0) = \ln A_{1+}(X/t_1)$] appeared adequate to explain the increasing rate for sweet maize with high water-soluble solids compacted in the sugary-vitreous fraction (Lara & Ruales, 2021). Therefore, these time-related hydration properties also revealed the differences between floury and sweet maize types, suggesting that WAC and SP depended on the endosperm structure (e.g., soft or hard) inherent to each kernel type and its average particle size in the flour. These results reflected the changes in the kernel matrix associated with increased accessibility to the hydrophilic groups in the starch and protein conformations (van Rooyen et al., 2022). Relative to the water-soluble index (WSI), it was high in sweet maize and decreased with the microwave heating-toasting time effect, while in floury maize with very low values, the WSI trend was undefined, agreeing with a moderate correlation against microwave heating-toasting time (-0.7766 and -0.7085), reported in a previous study ((Lara et al., 2022).

The difference in the main macro and micro components was characteristic in floury and sweet maize types with specialty kernels to make ready-to-eat whole maize by toasting but contrasted in kernel fraction distribution, endosperm structure, and hardness properties expressed as average particle size variation. Thus, the protein content of floury and sweet kernel structures was consistent with the results obtained for *Piscorunto* (floury maize) and *Chullpi* (sweet maize) reported in the characterization of Andean maize (Salvador-Reyes et al., 2021). On the other hand, the lower protein content in floury maize agreed with the floury endosperm microstructure (Lara et al., 2021), where the round shape of starch granules appeared packed between thin protein layers. The composition and structure in floury maize facilitated the milling and obtaining of fine particles.

In the relative distribution of milling particle size, the most noticeable difference was the particle size redistribution caused by the microwave heating-toasting effect, with the increased maximum

proportion for the geometric mean diameter of 47 μm for floury and sweet maize kernels. This finding was consistent with the decreasing APS by microwave heating-toasting effect, the maize kernel hardness reduction in microwave toasting kernels (Lara & Ruales, 2021), as well as the improvement in maize milling by the effect of microwave drying (Velu et al., 2006), and the normal maize hardness diminished by the toasting influence (Raigar & Mishra, 2018). Therefore, the particle size distribution evidenced the ease of milling floury maize and exhibited the microwave heating-toasting times with more than 50% of particles less than 50 microns, suggesting lower energy consumption during the milling of these maize types. This information reflects the potential of floury maize as a source of starch nanoparticles by size reduction, i.e., top-down.

1.6. Microwave heating-toasting time on maize kernels and its effect on non-isothermal rheological profiles

In complex viscosity, floury maize samples displayed high jagged peaks, and sweet maize exhibited broad short peaks, mainly ascribed to the differences found in starch content, blue value, relative crystallinity, hydration properties, and milling average particle size between floury and sweet maize types (Lara & Ruales, 2021; Lara et al., 2021). After a maximum value, the complex viscosity reflected a continuous loss of gel structure in floury maize profiles attributed to the particle size distribution with a high proportion of small particles in floury maize types. In contrast, a slow gel disruption evidenced a little floury fraction in sweet maize particle size distribution. The results were consistent with the differences in the elastic modulus peak described between normal and sweet maize native starch dispersions at a heating ramp from 50 to 90 °C (Singh et al., 2006).

Independent of microwave heating-toasting times, the average onset and peak temperatures by maize type included the values obtained from oscillatory stress, storage (G') and loss (G") moduli, and complex (η*) and dynamic (η') viscosities plotted as a function of temperature. Thus determined, the onset temperature was consistent with the temperature values generated using differential scanning calorimetry (DSC) for normal (Chen et al., 2021; Singh et al., 2006; Zhang et al., 2021) and sweet (Singh et al., 2006; Zhu et al., 2016) native maize starches. Likewise, the peak temperatures in floury maize agreed with the DSC peak temperatures in normal maize (Lei et al., 2020; Li & Zhu, 2018; Li et al., 2020; Singh et al., 2006; Zhang et al., 2021). In contrast, the peak temperatures for sweet maize were lower by DSC (Singh et al., 2006; Zhu et al., 2016) than those predicted for Andean sweet maize in this study. This last comparison reflected differences between whole kernel rich in phytoglycogen (Xue et al., 2019) and native starch samples isolated from sweet maize, with floury endosperm as the main souse of starch, but less significant than a sugary-vitreous fraction rich in water-soluble solids (Lara & Ruales, 2002).

At peak temperatures, the maximum elastic and viscous moduli were higher in floury maize dispersions than in sweet maize. The rheological differences between floury and sweet maize types were consistent with the corresponding water absorption capacity, swelling power, and water-soluble index for floury and sweet maize dispersions. In addition, these results were in harmony with previous findings on the physical (Lara & Ruales, 2021) and structural properties (Lara et al., 2021) of these specialty kernels used to make ready-to-eat maize by toasting. Furthermore, the maximum elastic and viscous moduli in floury maize were comparative to maximum elastic and viscous values listed for normal maize native starch (Li & Zhu, 2018), and the maximum G' was similar to that reported by waxy maize native starch at the same temperature (Wen et al., 2020).

On the other hand, the elastic to viscous modulus (G'/G") ratio varied by the microwave heating-toasting time effect according to floury and sweet maize endosperm structure (Lara et al., 2021). This relevant finding suggested that the G'/G" modulus ratio varied with the amylose content and short-chain amylopectin fraction (Singh et al., 2006) and depended on the starch source (Dong et al., 2021). Onset and peak temperatures exhibited significant variation between floury and sweet maize but similar levels relative to floury kernel types. The main reason for the significant variation was that the starchy endosperm was entirely soft in floury maize kernels than a sugary-vitreous fraction more significant than floury endosperm in sweet maize kernels (Lara et al., 2021). In contrast, the heating-toasting times applied to whole dry kernels appeared irrelevant at the onset and peak temperatures. Thus, the temperature depended on the gelatinization phenomenon innate to each starch source during non-isothermal oscillatory measurements (Dong et al., 2021). In addition, G' and G" moduli and η* and η' viscosities also revealed significant variations inherent to specialty floury and sweet maize kernels at the peak temperatures. These findings were consistent with the significant shifts reported in microstructure, X-ray diffraction, Raman and FTIR band intensities, physicochemical properties (Lara et al., 2021), hardness, and hydration properties compared to floury and sweet maize types (Lara & Ruales, 2021).

2. Conclusions and future perspective of the Andean maize toasting

The current scientific literature about conventional and novel toasting techniques indicates the scientific community's interest in dry heating and toasting (roasting) to adjust starch in whole kernel and flour to get new functionalities using physical methods such as microwave heating and toasting. The whole maize kernels subjected to pan a microwave toasting presented partially modified crystalline structures, remaining nanocrystals with average size from 7 to 9 nm, and vibrational functional groups ascribed to carbohydrates, proteins, and lipids. After pan and microwave toasting, floury maize displayed endosperm with starch granules partially modified, whereas sweet maize

mainly implied a sugary-vitreous fraction. Likewise, the toasting effect on physical and hydration properties displayed changes in geometric, gravimetric, internal porosity, surface color, instrumental hardness, milling average particle size, and hydration properties inherent to the maize types. Internal porosity, hardness, stress pick, and the average particle size implied that the softness in flory maize and crispness in sweet maize might be the main attributes of the whole ready-to-eat maize. The three maize types with specialty kernels for toasting presented a broad scope of physical properties with good correlations for the microwave heating-toasting time intervals from 0 to 390 s, and the initial water content in raw microwave maize standardized to 0.16 ± 01 g/g on a dry basis. Weter content and water loss showed significant differences regarding regression curves and exchange profiles, and the actual $(S/V)^2$ and $(GMD/2)^2$ approaches were significantly different. Therefore, water loss better explains the water migration in raw microwave maize, and the $(S/V)^2$ approach was consistent with regression curves and exchange profiles of these maize types with specialty kernels for raw microwave maize. Modeling the kinetics of surface color difference (ΔE*), porosity, milling average particle size, and flour hydration properties showed that these physical properties were consistently time-related variables in floury and sweet maize kernels subjected to microwave heating-toasting treatments. The particle size distribution in floury and sweet maize varied with the increasing microwave heating-toasting time, and the highest proportion of fine particles and less than 50 µm was for floury maize, implying easier milling and less energy consumption for this maize type. Also, complex viscosity displayed jagged peaks in floury maize, and broad peaks in sweet maize ascribed average particle size, flour hydration properties, and proximal composition. The G'/G" modulus ratio unveiled the microwave heating-toasting time effect on the rheological properties of these specialty Andean maize kernels.

With the recent interest in super soft cereals, flour maize with large kernel sizes, low hardness, and low protein could be a potential crop to develop unconventional milling processes and future challenges for native starch. According to current references cited and their prospective, essential aspects of Andean maize microwave toasting may be the resistant starch formation during dry heating treatments, maize flour modification for physical methods, Maillard reaction products, and acrylamide formation. In addition, phytoglycogen in sweet maize has a current interest. The thesis results open new insight into physic-basic models for the design and quality control of microwave heating-toasting treatments focused on handling conditions to obtain whole grains with specialty matrices directed towards new frontiers of scientific study.

References

Achten, E., Schütz, D., Fischer, M., Fauhl-Hassek, C., Riedl, J., & Horn, B. (2019). Classification of grain maize (*Zea mays* L.) from different geographical origins with FTIR spectroscopy - A

suitable analytical tool for feed authentication? *Food Analytical Methods*, *12*(10), 2172-2184. https://doi.org/10.1007/s12161-019-01558-9

Bello-Pérez, L. A., Flores-Silva, P. C., Sifuentes-Nieves, I., & Agama-Acevedo, E. (2021). Controlling starch digestibility and glycaemic response in maize-based foods. *Journal of Cereal Science*, *99*, 103222. https://doi.org/10.1016/j.jcs.2021.103222

Bustos-Vanegas, J. D., Corrêa, P. C., Martins, M. A., Machado Baptestini, F. M., Campos, R. C., Horta de Oliveira, G. H., & Martins Nunes, E. H. (2018). Developing predictive models for determining physical properties of coffee beans during the roasting process. *Industrial Crops and Products*, *112*, 839-845. https://doi.org/10.1016/j.indcrop.2017.12.015

Cai, C., Lin, L., Man, J., Zhao, L., Wang, Z., & Wei, C. (2014). Different structural properties of high-amylose maize starch fractions varying in granule size. *Journal of Agricultural and Food Chemistry*, *62*(48), 11711-11721. https://doi.org/10.1021/jf503865e

Chen, G., Maier, D. E., Campanella, O. H., & Takhar, P. S. (2009). Modeling of moisture diffusivities for components of yellow-dent corn kernels. *Journal of Cereal Science*, *50*(1), 82-90. https://doi.org/10.1016/j.jcs.2009.03.003

Chen, L., McClements, D. J., Zhang, H., Zhang, Z., Jin, Z., & Tian, Y. (2019). Impact of amylose content on structural changes and oil absorption of fried maize starches. *Food Chemistry*, *287*, 28-37. https://doi.org/10.1016/j.foodchem.2019.02.083

Chen, P., Zhang, Y., Qiao, Q., Tao, X., Liu, P., & Xie, F. (2021). Comparison of the structure and properties of hydroxypropylated acid-hydrolysed maize starches with different amylose/amylopectin contents. *Food Hydrocolloids*, *110*, 106134. https://doi.org/10.1016/j.foodhyd.2020.106134

Chung, H.-S., Kim, J.-K., Moon, K.-D., & Youn, K.-S. (2014). Changes in color parameters of corn kernels during roasting. *Food Science and Biotechnology*, *23*(6), 1829-1835. https://doi.org/10.1007/s10068-014-0250-x

Deepa, C., & Hebbar, H. U. (2017). Influence of micronization on physicochemical properties of maize grains. *Starch - Stärke*, *69*(3-4), 1600060. https://doi.org/10.1002/star.201600060

Dong, H., Zhang, Q., Gao, J., Chen, L., & Vasanthan, T. (2021). Comparison of morphology and rheology of starch nanoparticles prepared from pulse and cereal starches by rapid antisolvent nanoprecipitation. *Food Hydrocolloids*, *119*, 106828. https://doi.org/10.1016/j.foodhyd.2021.106828

Gayral, M., Gaillard, C., Bakan, B., Dalgalarrondo, M., Elmorjani, K., Delluc, C., Brunet, S., Linossier, L., Morel, M. H., & Marion, D. (2016). Transition from vitreous to floury endosperm in maize (*Zea mays* L.) kernels is related to protein and starch gradients. *Journal of Cereal Science*, *68*, 148-154. https://doi.org/10.1016/j.jcs.2016.01.013

Guelpa, A., du Plessis, A., Kidd, M., & Manley, M. (2015). Non-destructive estimation of maize (*Zea mays* L.) kernel hardness by means of an X-ray micro-computed tomography (µCT) density calibration. *Food and Bioprocess Technology*, *8*(7), 1419-1429. https://doi.org/10.1007/s11947-015-1502-3

Guelpa, A., du Plessis, A., & Manley, M. (2016). A high-throughput X-ray micro-computed tomography (µCT) approach for measuring single kernel maize (*Zea mays* L.) volumes and densities. *Journal of Cereal Science*, *69*, 321-328. https://doi.org/10.1016/j.jcs.2016.04.009

Han, X., Kang, J., Bai, Y., Xue, M., & Shi, Y.-C. (2018). Structure of pyrodextrin in relation to its retrogradation properties. *Food Chemistry*, *242*, 169-173. https://doi.org/10.1016/j.foodchem.2017.09.015

Jahanbakhshi, A., Kaveh, M., Taghinezhad, E., & S.V., R. (2020). Assessment of kinetics, effective moisture diffusivity, specific energy consumption, shrinkage, and color in the pistachio kernel drying process in microwave drying with ultrasonic pretreatment. *Journal of Food Processing and Preservation*, *44*(6). https://doi.org/10.1111/jfpp.14449

Karababa, E. (2006). Physical properties of popcorn kernels. *Journal of Food Engineering*, *72*(1), 100-107. https://doi.org/10.1016/j.jfoodeng.2004.11.028

Karababa, E., & Coşkuner, Y. (2007). Moisture dependent physical properties of dry sweet corn kernels. *International Journal of Food Properties*, *10*(3), 549-560. https://doi.org/10.1080/10942910601003981

Kipcak, A. S., & Doymaz, I. (2020). Mathematical modeling and drying characteristics investigation of black mulberry dried by microwave method. *International Journal of Fruit Science*, *20*(sup3), S1222-S1233. https://doi.org/10.1080/15538362.2020.1782805

Kowalski, R. J., Hause, J. P., Joyner, H., & Ganjyal, G. M. (2018). Waxy flour degradation - Impact of screw geometry and specific mechanical energy in a co-rotating twin screw extruder. *Food Chemistry*, *239*, 688-696. https://doi.org/10.1016/j.foodchem.2017.06.120

Lara, N., & Ruales, J. (2002). Popping of amaranth grain (*Amaranthus caudatus*) and its effect on the functional, nutritional and sensory properties. *Journal of the Science of Food and Agriculture*, *82*(8), 797-805.

Lara, N., & Ruales, J. (2021). Physical and hydration properties of specialty floury and sweet maize kernels subjected to pan and microwave toasting. *Journal of Cereal Science*, *101*, 103298. https://doi.org/10.1016/j.jcs.2021.103298

Lara, N., Vizuete, K., Debut, A., Chango, I., Campaña, O., Villacrés, E., Bonilla, P., & Ruales, J. (2021). Underutilized maize kernels (*Zea mays* L. var. *amylacea* and var. *saccharata*) subjected to pan and microwave toasting: A comparative structure study in the whole kernel. *Journal Cereal Science*, *100*, 103249. https://doi.org/10.1016/j.jcs.2021.103249

Lei, N., Chai, S., Xu, M., Ji, J., Mao, H., Yan, S., Gao, Y., Li, H., Wang, J., & Sun, B. (2020). Effect of dry heating treatment on multi-levels of structure and physicochemical properties of maize starch: A thermodynamic study. *International Journal of Biological Macromolecules*, *147*, 109-116. https://doi.org/10.1016/j.ijbiomac.2020.01.060

Li, G., & Zhu, F. (2018). Effect of high pressure on rheological and thermal properties of quinoa and maize starches. *Food Chemistry*, *241*, 380-386. https://doi.org/10.1016/j.foodchem.2017.08.088

Li, H., Ji, J., Yang, L., Lei, N., Wang, J., & Sun, B. (2020). Structural and physicochemical property changes during pyroconversion of native maize starch. *Carbohydrate Polymers*, *245*, 116560. https://doi.org/10.1016/j.carbpol.2020.116560

Liu, Y., Xu, Y., Yan, Y., Hu, D., Yang, L., & Shen, R. (2015). Application of Raman spectroscopy in structure analysis and crystallinity calculation of corn starch. *Starch - Stärke*, *67*(7-8), 612-619. https://doi.org/10.1002/star.201400246

Minakawa, A. F. K., Faria-Tischer, P. C. S., & Mali, S. (2019). Simple ultrasound method to obtain starch micro-and nanoparticles from cassava, corn and yam starches. *Food Chemistry*, *283*, 11-18. https://doi.org/10.1016/j.foodchem.2019.01.015

Mousaviraad, M., & Tekeste, M. Z. (2020). Effect of grain moisture content on physical, mechanical, and bulk dynamic behaviour of maize. *Biosystems Engineering*, *195*, 186-197. https://doi.org/10.1016/j.biosystemseng.2020.04.012

Oliveros, N. O., Hernández, J. A., Sierra-Espinosa, F. Z., Guardián-Tapia, R., & Pliego-Solórzano, R. (2017). Experimental study of dynamic porosity and its effects on simulation of the coffee beans roasting. *Journal of Food Engineering*, *199*, 100-112. https://doi.org/10.1016/j.jfoodeng.2016.12.012

Paesani, C., Bravo-Núñez, Á., & Gómez, M. (2020). Effect of extrusion of whole-grain maize flour on the characteristics of gluten-free cookies. *LWT - Food Science and Technology*, *132*, 109931. https://doi.org/10.1016/j.lwt.2020.109931

Peng, X., & Yao, Y. (2018). Small-granule starches from sweet corn and cow cockle: Physical properties and amylopectin branching pattern. *Food Hydrocolloids*, *74*, 349-357. https://doi.org/10.1016/j.foodhyd.2017.08.025

Raigar, R. K., & Mishra, H. N. (2018). Study on the effect of pilot scale roasting conditions on the physicochemical and functional properties of maize flour (Cv. *Bio 22027*). *Journal of Food Processing and Preservation*, *42*(5), e13602. https://doi.org/10.1111/jfpp.13602

Reeve, R., & Turner, J. R. (2013). Pharmacodynamic models: parameterizing the hill equation, Michaelis-Menten, the logistic curve, and relationships among these models. *J Biopharm Stat*, *23*(3), 648-661. https://doi.org/10.1080/10543406.2012.756496

Salvador-Reyes, R., & Clerici, M. T. P. S. (2020). Peruvian Andean maize: General characteristics, nutritional properties, bioactive compounds, and culinary uses. *Food Research International*, *130*, 108934. https://doi.org/10.1016/j.foodres.2019.108934

Salvador-Reyes, R., Rebellato, A. P., Lima Pallone, J. A., Ferrari, R. A., & Clerici, M. T. P. S. (2021). Kernel characterization and starch morphology in five varieties of Peruvian Andean maize. *Food Research International*, *140*, 110044. https://doi.org/10.1016/j.foodres.2020.110044

Schoeman, L., du Plessis, A., Verboven, P., Nicolaï, B. M., Cantre, D., & Manley, M. (2017). Effect of oven and forced convection continuous tumble (FCCT) roasting on the microstructure and dry milling properties of white maize. *Innovative Food Science & Emerging Technologies*, *44*, 54-66. https://doi.org/10.1016/j.ifset.2017.07.021

Shirkole, S. S., & Sutar, P. P. (2018). High power short time microwave finish drying of paprika (*Capsicum annuum* L.): Development of models for moisture diffusion and color degradation. *Drying Technology*, *37*(2), 253-267. https://doi.org/10.1080/07373937.2018.1454941

Shivhare, U. S., Raghavan, G. S. U., & Biosisio, R. G. (1994). Modelling of drying kinetics of maize in a microwave environment. *Journal of Agricultural Engineering Research*, *57*, 199-205.

Singh, N., Inouchi, N., & Nishinari, K. (2006). Structural, thermal and viscoelastic characteristics of starches separated from normal, sugary and waxy maize. *Food Hydrocolloids*, *20*(6), 923-935. https://doi.org/10.1016/j.foodhyd.2005.09.009

Singh, V., & Ali, S. Z. (2008). Properties of starches modified by different acids. *International Journal of Food Properties*, *11*(3), 495-507. https://doi.org/10.1080/10942910802083774

Sruthi, N. U., Premjit, Y., Pandiselvam, R., Kothakota, A., & Ramesh, S. V. (2021). An overview of conventional and emerging techniques of roasting: Effect on food bioactive signatures. *Food Chemistry*, *348*, 129088. https://doi.org/10.1016/j.foodchem.2021.129088

Sui, Z., Yao, T., Zhao, Y., Ye, X., Kong, X., & Ai, L. (2015). Effects of heat-moisture treatment reaction conditions on the physicochemical and structural properties of maize starch: Moisture and length of heating. *Food Chemistry*, *173*, 1125-1132. https://doi.org/10.1016/j.foodchem.2014.11.021

Sumithra, B., & Bhattacharya, S. (2008). Toasting of corn flakes: Product characteristics as a function of processing conditions. *Journal of Food Engineering*, *88*(3), 419-428. https://doi.org/10.1016/j.jfoodeng.2008.03.001

Tao, Y., Yan, B., Fan, D., Zhang, N., Ma, S., Wang, L., Wu, Y., Wang, M., Zhao, J., & Zhang, H. (2020). Structural changes of starch subjected to microwave heating: A review from the perspective of dielectric properties. *Trends in Food Science & Technology*, *99*, 593-607. https://doi.org/10.1016/j.tifs.2020.02.020

Torbica, A., Belovic, M., Popovic, L., & Cakarevic, J. (2021). Heat and hydrothermal treatments of non-wheat flours. *Food Chemistry*, *334*, 127523. https://doi.org/10.1016/j.foodchem.2020.127523

Uriarte-Aceves, P. M., Rangel-Peraza, J. G., & Sopade, P. A. (2020). Kinetics of water absorption and relation with physical, chemical, and wet-milling properties of commercial yellow maize (*Zea mays* L.) hybrids. *Journal of Food Processing and Preservation*, *44*(7), e14509. https://doi.org/10.1111/jfpp.14509

Uriarte-Aceves, P. M., Sopade, P. A., & Rangel-Peraza, J. G. (2019). Physical, chemical and wet-milling properties of commercial white maize hybrids cultivated in México. *Journal of Food Processing and Preservation*, *43*(7), e13998. https://doi.org/10.1111/jfpp.13998

van Rooyen, J., Simsek, S., Oyeyinka, S. A., & Manley, M. (2022). Holistic view of starch chemistry, structure and functionality in dry heat-treated whole wheat kernels and flour. *Foods*, *11*(2). https://doi.org/10.3390/foods11020207

Vega-Rojas, L. J., Contreras-Padilla, M., Rincon-Londoño, N., Del Real-López, A., Lima-Garcia, R. M., Palacios-Rojas, N., & Rodriguez-Garcia, M. E. (2016). The effect of maize grain size on the physicochemical properties of isolated starch, crude maize flour and nixtamalized maize flours. *Agricultural Sciences*, *07*(02), 114-125. https://doi.org/10.4236/as.2016.72011

Velu, V., Nagender, A., Prabhakara Rao, P. G., & Rao, D. G. (2006). Dry milling characteristics of microwave dried maize grains (*Zea mays* L.). *Journal of Food Engineering*, *74*(1), 30-36. https://doi.org/10.1016/j.jfoodeng.2005.02.014

Wang, S., Ai, Y., Hood-Niefer, S., & Nickerson, M. T. (2019). Effect of barrel temperature and feed moisture on the physical properties of chickpea, sorghum, and maize extrudates and the

functionality of their resultant flours - Part 1. *Cereal Chemistry*, *96*(4), 609-620. https://doi.org/10.1002/cche.10149

Wani, I. A., Gani, A., Tariq, A., Sharma, P., Masoodi, F. A., & Wani, H. M. (2016). Effect of roasting on physicochemical, functional and antioxidant properties of arrowhead (*Sagittaria sagittifolia* L.) flour. *Food Chemistry*, *197*(Pt A), 345-352. https://doi.org/10.1016/j.foodchem.2015.10.125

Welsh, Z. G., Khan, M. I. H., & Karim, M. A. (2021). Multiscale modeling for food drying: A homogenized diffusion approach. *Journal of Food Engineering*, *292*, 110252. https://doi.org/10.1016/j.jfoodeng.2020.110252

Wen, Y., Yao, T., Xu, Y., Corke, H., & Sui, Z. (2020). Pasting, thermal and rheological properties of octenylsuccinylate modified starches from diverse small granule starches differing in amylose content. *Journal of Cereal Science*, *95*, 103030. https://doi.org/10.1016/j.jcs.2020.103030

Wiercigroch, E., Szafraniec, E., Czamara, K., Pacia, M. Z., Majzner, K., Kochan, K., Kaczor, A., Baranska, M., & Malek, K. (2017). Raman and infrared spectroscopy of carbohydrates: A review. *Spectrochimica Acta A: Molecular and Biomolecular Spectroscopy*, *185*, 317-335. https://doi.org/10.1016/j.saa.2017.05.045

Woo, K. S., Kim, M. J., Kim, H.-J., Lee, J. H., Lee, B. W., Jung, G. H., Lee, B. K., & Kim, S. L. (2018). Changes in the functional components and radical scavenging activity of maize under various roasting conditions. *Food Science and Biotechnology*, *27*(3), 837-845. https://doi.org/10.1007/s10068-017-0294-9

Xue, J., Inzero, J., Hu, Q., Wang, T., & Wusigale, Y. L. (2019). Development of easy, simple and low-cost preparation of highly purified phytoglycogen nanoparticles from corn. *Food Hydrocolloids*, *95*, 256-261. https://doi.org/10.1016/j.foodhyd.2019.04.041

Yang, R., & Chen, J. (2021). Mechanistic and machine learning modeling of microwave heating process in domestic ovens: A review. *Foods*, *10*(9). https://doi.org/10.3390/foods10092029

Youn, K.-S., & Chung, H.-S. (2012). Optimization of the roasting temperature and time for preparation of coffee-like maize beverage using the response surface methodology. *LWT - Food Science and Technology*, *46*(1), 305-310. https://doi.org/10.1016/j.lwt.2011.09.014

Yu, S., Xu, J., Zhang, Y., & Kopparapu, N. K. (2014). Relationship between intrinsic viscosity, thermal, and retrogradation properties of amylose and amylopectin. *Czech Journal of Food Sciences*, *32*(5), 514–520.

Yu, X., Yu, H., Zhang, J., Shao, S., Xiong, F., & Wang, Z. (2015). Endosperm structure and physicochemical properties of starches from normal, waxy and super-sweet maize. *International Journal of Food Properties*, *18*(12), 2825-2839. https://doi.org/10.1080/10942912.2015.1015732

Zhang, B., Xiao, Y., Wu, X., Luo, F., Lin, Q., & Ding, Y. (2021). Changes in structural, digestive, and rheological properties of corn, potato, and pea starches as influenced by different ultrasonic treatments. *International Journal of Biological Macromolecules*, *185*, 206-218. https://doi.org/10.1016/j.ijbiomac.2021.06.127

Zhang, H., & Xu, G. (2019). Physicochemical properties of vitreous and floury endosperm flours in maize. *Food Science & Nutrition*, *7*(8), 2605-2612. https://doi.org/10.1002/fsn3.1114

Zhu, F., Bertoft, E., & Li, G. (2016). Morphological, thermal, and rheological properties of starches from maize mutants deficient in starch synthase III. *Journal of Agricultural and Food Chemistry*, *64*(34), 6539-6545. https://doi.org/10.1021/acs.jafc.6b01265

Zhu, H., Gulati, T., Datta, A. K., & Huang, K. (2015). Microwave drying of spheres: Coupled electromagnetics-multiphase transport modeling with experimentation. Part I: Model development and experimental methodology. *Food and Bioproducts Processing*, *96*, 314-325. https://doi.org/10.1016/j.fbp.2015.08.003

Zou, J., Xu, M., Tang, W., Wen, L., & Yang, B. (2020). Modification of structural, physicochemical and digestive properties of normal maize starch by thermal treatment. *Food Chemistry*, *309*, 125733. https://doi.org/10.1016/j.foodchem.2019.125733